Harnessing synthetic biology to target oncogenic pathogens in colon cancer

Kimberley A. Owen

A dissertation submitted in partial fulfillment

of the requirements for the degree of

Doctor of Philosophy

of

University College London.

Department of Cell & Developmental Biology

University College London

June 10, 2025

I, Kimberley A. Owen, confirm that the work presented in this thesis is my own. Where information has been derived from other sources, I confirm that this has been indicated in the work.

Abstract

Colorectal cancer is the 4th most common cancer in the UK. Patients with high levels of the bacteria *Fusobacterium nucleatum* (*F. nucleatum*) and *Bacteroides fragilis* (*B. fragilis*) within their tumours are associated with poorer survival outcomes. *F. nucleatum* promotes pro-inflammatory cytokines, tumour-immune cytokines, cancer stem cell-like states, genome instability/mutation, epithelial tight junction damage and supports chemotherapy component breakdown. Enterotoxigenic Bf (Ent. *B. fragilis*) strains produce a toxin, fragilysin, that forms biofilms, damages epithelial tight junctions, and induces inflammatory intestinal responses. We hypothesise that future therapies that remove pathogens such as *F. nucleatum* and Ent. *B. fragilis* from the tumour microenvironment could improve the success of chemotherapy and therefore patient outcomes. One approach is to remove these bacteria from the tumour environment by selectively killing them using an engineered live bacterial therapeutic product (eLBP). The eLBP would achieve this by using small, highly specific, antimicrobial peptides known as bacteriocins. Overall, this work had the following goals: 1) to identify bacteriocins that can target *F. nucleatum*/Ent. *B. fragilis* and 2) to build an eLBP that could deliver them. Bacteriocins that successfully kill *F. nucleatum*/*B. fragilis* were identified, and a number of delivery systems were explored, including secretion and lysis circuits. The bacteriocin, Aureocin A53 was successfully delivered, via a lysis circuit, but further work is required to express bacteriocin at high enough concentrations to kill the onco-pathogens. We investigated cancer patients' attitudes towards this technology through a charity associated survey, which we found to be positive. This work highlights some of the challenges involved in building bacteriocin secreting

eLBPs and can provide directions for building generic eLBPs to target the emerging pathobionts that interfere with chemotherapeutic treatment and drug-microbiome interactions more generally.

Impact Statement

Within academia this research confirms the feasibility of engineering *E. coli* to express bacteriocins that are not native to the species. The study demonstrated that *E. coli* can produce functional bacteriocins capable of effectively targeting pathogens, such as *Enterococcus faecalis*. Additionally, it was shown that *E. coli* can support a secretion system akin to colicin bacteriocins, allowing the release of functional bacteriocins without requiring a dedicated secretion mechanism. This work also highlights the complexity of engineering potent bacteriocins into uninducible platforms, as evidenced by the challenges encountered in developing expression plasmids for certain bacteriocins. These findings stress the importance of thoughtful design when working with antimicrobial peptides in synthetic biology. The benefit outside of academia is that this work represents a step forward in developing engineered live biotherapeutics that can selectively kill pathogens, with potential applications in fields like colon cancer treatment, where bacterial pathogens can reduce chemotherapy efficacy. It also contributes to addressing the urgent need for alternatives to antibiotics in combating antimicrobial resistance. Furthermore, the outreach efforts, such as the conducted survey, have raised awareness about innovative treatment options under development, creating a bridge between scientific advancements and public understanding. The overall impact of this work is that patients are now more aware of less invasive, innovative treatments that may emerge in the future, fostering hope and openness to new therapeutic approaches. Insights from the survey emphasize the critical role of clinicians in communicating these advancements to patients, underscoring the importance of their involvement in deploying new therapies. This research also serves as a cautionary tale for researchers:

not all antimicrobial peptides will function seamlessly in foreign hosts, urging careful consideration of the chassis used for engineering. For example, while *Bacillus subtilis* was initially considered as a chassis, it proved unsuitable due to its susceptibility to the peptides. These findings could guide future decisions to engineer alternative strains from the outset when *E. coli* is not the final intended host.

UCL Research Paper Declaration Form: referencing the doctoral candidate's own published work(s)

1. **For a research manuscript that has already been published** (if not yet published, please skip to Section 2):

1.1. **Title of the manuscript:** *Microbiome engineering: engineered live biotherapeutic products for treating human disease*

1.2. **Link or DOI:** https://doi.org/10.3389/fbioe.2022.1000873

1.3. **Where was the work published?** Frontiers Bioengineering & Biotechnology

1.4. **Who published the work?** Frontiers

1.5. **When was the work published?** 16th September 2022

1.6. **Authors:** Jack W. Rutter, Linda Dekker, Kimberley A. Owen, Chris P. Barnes

1.7. **Was the work peer-reviewed?** Yes

1.8. **Have you retained the copyright?**

1.9. **Was an earlier form uploaded to a preprint server (e.g., medRxiv)?** No

If 'No', please seek permission from the relevant publisher and check the box below:

☐ *I acknowledge permission of the publisher named under 1.4 to include in this thesis portions of the publication named in 1.3.*

1.10. **Title of the manuscript:** *A bacteriocin expression platform for targeting pathogenic bacterial species*

1.11. **Link or DOI:** https://doi.org/10.1038/s41467-024-50591-8

1.12. **Where was the work published?** Nature Communications

1.13. **Who published the work?** Nature Communications

1.14. **When was the work published?** 27th July 2024

1.15. **Authors:** Jack W. Rutter, Linda Dekker, Chania Clare, Zoe F. Slendebroek, Kimberley A. Owen, Julie A. K. McDonald, Sean P. Nair, Alex J. H. Fedorec, Chris P. Barnes

1.16. **Was the work peer-reviewed?** Yes

1.17. **Have you retained the copyright?**

1.18. **Was an earlier form uploaded to a preprint server (e.g., medRxiv)?** No

If 'No', please seek permission from the relevant publisher and check the box below:

□ *I acknowledge permission of the publisher named under 1.13 to include in this thesis portions of the publication named in 1.12.*

2. **For a research manuscript prepared for publication but not yet published** (if already published, please skip to Section 3):

2.1. **Title of the manuscript:** *Engaging cancer patients on their attitudes towards microbiome engineering technologies*

2.2. **Has the manuscript been uploaded to a preprint server (e.g., medRxiv)?** Yes, BioRxiv, 26th November 2024

2.3. **Link or DOI:** https://doi.org/10.1101/2024.11.25.625255

2.4. **Where is the work intended to be published?**

2.5. **Authors:** Kimberley A. Owen, Jack W. Rutter, Claire Holland, HB Trung Le, Philip Shapira, Clare Lewis, James M. Kinross, Chris P. Barnes

2.6. **Stage of publication:** Writing

3. **For multi-authored work, please provide a statement of contribution:**

KAO and JR carried out the work and wrote the manuscript. CPB helped write the manuscript. CH, CL, and PS helped with the qualitative thematic analysis. HBTL and JMK assisted with survey distribution. All authors approved the manuscript.

4. **In which chapter(s) of your thesis can this material be found?**

Chapter 6 - Engaging cancer patients on their attitudes towards microbiome engineering technologies

e-Signatures

e-Signatures confirming that the information above is accurate (this form should be co-signed by the supervisor/senior author unless this is not appropriate, e.g., if the paper was a single-author work.)

Candidate: _____

Date: _____

Supervisor/Senior Author (if applicable): _____

Date: _____

Acknowledgements

Firstly thank you to me, myself and I. For without me there would be no work at all.

Next, thank you to my supervisor, Prof Chris Barnes, for his support, guidance and patience throughout the BioDesign programme. Thank you for taking a chance on me, the one who breaks computers by looking at them and for keeping things entertaining with your consistent sarcasm over the past four years. Thank you to my second supervisor, James Kinross, for your enthusiasm and encouragement during my work. Thank you for the opportunity to observe surgery it was a privilege to be there. Thank you to Dr. Alex Fedorec and Dr. Ke Yan Wen for taking the time to teach and train me during the lockdown years. Thank you to Jack Rutter for all coding and modelling assistance, you are a computer angel. Thank you to Linda for being the one who gets all of my nonsensical lab questions and the one who handles all the lab fires!!! Thank you for keeping the lab going.

Thank you to the Barnes Girls (now just Barnes & Fedorec students): Alice, Qing, Chania, Kathleen, Casey, and Louie. For the company, the laughs and cries and most importantly the food. Thank you to everyone who has been in the Barnes group throughout the PhD, even during my break, your patience and kindness was much needed and appreciated.

I couldn't have done this without friends and family who helped me move flats and gave me lifts to train stations. Thank you mum and dad for your continued support even though you have no idea what I do, it means a lot. Thank you to Michael and Hayley for believing I could do this and Hayley for reading the work. Thank you Daisy (James) for being chef, chauffeur, and cleaner during the writing

phase, I am grateful for all you did so I could complete my degree. Thank you for being there during my break when I wasn't able to.

Thank you to the friends who took on way more than they needed to. To Alex and Charley, your help and friendship was so needed and you guys are the best technical theatre support anyone could ever need. To Bethan for being the best moaning post, ultimate academic advisor and friend. Thank you to Maha, Will and Danilo for giving me a space to help make a difference and believing I could do it. To friends from the CDT and the retreats we shared together, Cathal, Mallica, Danny, Eloise and Daniella thank you for being great cohort buddies.

To the UCL Stage Crew society and Chris Hoyle at the Bloomsbury theatre. I didn't get to take part in as many productions as I wanted but those that I did were amazing. Thank you for creating a society that's a safe and fun space for all students. To Harriet and Carmela thank you for everything. You were rocks that kept me afloat and I am forever grateful for your kindness and body guard services.

Finally, thank you to Jane Austen, and the BBC for being there at every exam season, at times when I am at my most stressed you have carried me through. To Taylor Swift for the best and first concert of my life, and for being the soundtrack to my writing. A cheers to Chad you really got me through this. A thank you to the ETC London office for adopting me, providing the best machine hot chocolates and chats while working. Lastly, a huge thank you to my little cartoon bacteria for assisting me in communicating my research both at conferences and competitions. You were amazing and so cute.

Contents

List of Figures

List of Tables

List of Abbreviations

AHL – acyl homoserine lactone

CRISPR – Clustered Regularly Interspaced Short Palindromic Repeats

cvaC – gene for microcin V

cvi – gene for immunity against microcin V

GFP – green flourescent protein

IPTG – Isopropyl ß-D-1-thiogalactopyranoside

K/O – knockout

OD – optical density measurement

qPCR – quantitative Polymerase Chain Reaction

RRI – Responsible Research and Innovation

SPoCK – Stabilised Population by Community Killing

Chapter 1

Introduction

‘I wish, as well as everybody else, to be perfectly happy; but, like everybody else, it must be in my own way.’

— Jane Austen, Sense & Sensibility

Contents

1.1 Synthetic biology

Synthetic biology is an interdisciplinary field that applies 'engineering tools and principles to design and engineer novel biologically-based parts, devices, and systems that do not exist in the natural world' [2]. At its base level synthetic biology has the potential to engineer new abilities by redesigning organisms for useful purposes [3]. The field leverages advanced tools such as DNA synthesis, genome editing, and computational biology to enable the reprogramming of life [4, 5]. Synthetic biology takes principles from engineering such as the design, build, test, learn cycle and uses them to systemise the field, improving efficacy and generalisability [6]. The impact of synthetic biology has the potential to provide solutions to some of the most pressing global challenges, such as climate change, food security, and human health [7].

The expertise that synthetic biology can contribute to research is already being realised. Microbes are being engineered for bioremediation, from *Escherichia coli* (*E. coli*) biosensors that can detect mercury and secrete mercury-absorbing proteins [8] to *E. coli* that can express catabolic enzymes for the degradation of oil spills [9]. By harnessing the metabolic capacities of these organisms, synthetic biology offers a more efficient and sustainable alternative to conventional oil clean up methods [10]. In fact, these technologies are nearing public use, for example, bacterial biosensors are being integrated with smartphones to detect unsafe levels of arsenic [11].

Synthetic biology has applications in biotechnology, where it is being used to create synthetic pathways for biofuel production. The gene editing tool, CRISPR, has been used to engineer a consortia of *Clostridium sp.* to convert the renewable feedstock lignocellulose into butanol, a much desired solvent [12]. This helps advancements towards reducing the dependence on fossil fuels, which aligns with global efforts to tackle climate change.

In the field of agriculture, synthetic biology is revolutionising crop production. For example, the microbial based fertiliser by Pivotbio, where a soil bacterium, *Klebisella variicola*, was engineered to constantly fix nitrogen. The *Klebsiella* nat-

urally live on the root of the desired crops, fixing nitrogen, therefore the nitrogen is not washed away by rain nor is it decomposed to nitrogen oxide (greenhouse gas) [13]. Other areas have worked to genetically engineer the crop itself; such as rapeseed, which was engineered to increase its yield whilst reducing its requirement for water [14]. Looking at healthier foods, there are works addressing reducing the fatty acid content of soya beans [15]. Innovations like these can improve food security and contribute to more sustainable agricultural practices.

Beyond agriculture and biotechnology, synthetic biology has a place in tackling human health and disease with the potential to develop engineered probiotics. The potential of synthetic biology to improve human health ranges from yeast that were engineered to express the anti-malarial compound, artemisinin [16], to human T-cells that were reprogrammed to express chimeric antigens that enable the immune system to target cancer cells [17]. It could be argued that the greatest contribution to global health, from synthetic biology, was the mRNA vaccine development used in the Covid-19 pandemic. A fully synthetic SARS-CoV-2 S gene was cloned onto a plasmid vector, and this was used as the template for the *in vitro* synthesis of the vaccine [18]. Further adaptations meant the protein was stabilised in the pre-fusion state [19, 18]. More importantly, for this work, synthetic biology is reshaping our understanding and manipulation of the human microbiome. Engineered bacteria that can sense disease states and then deliver tissue-specific therapeutics are already in development [20], alongside engineered phages for the treatment of bacterial infections and plant based vaccines producing virus-like particles to tackle human diseases [21]. Ultimately, these approaches will help minimise reliance on traditional untargeted therapies and help address challenges such as antibiotic resistance.

Synthetic biology holds transformative potential across diverse sectors, from environmental conservation and agriculture to human health. By enabling the design and engineering of biological systems, it offers innovative solutions to challenges that have long seemed insurmountable. As the field progresses, a balanced approach that integrates scientific innovation with responsible governance will be

crucial to ensure that synthetic biology achieves its potential while minimising risks to biodiversity, human health, and society.

1.2 Microbiome engineering and engineered live bacterial therapeutics

The microbiome is the collective genomes of all the microorganisms and the microbiota is classed as all the microorganisms inhabiting a particular environment [22, 23]. The human microbiota is a complex ecosystem implicated in numerous diseases, including neurological disorders [24, 25], inflammatory conditions like ulcerative colitis [26], and cancers [27]. This has driven the development of microbiome engineering techniques, including probiotics, faecal microbiota transplants (FMTs), and dietary modifications [28].

The microbiome has become a target of recent therapies, as its impacts on multiple health and disease states become apparent [29]. Current methods of targeting the microbiome involve using non-engineered probiotic strains that naturally exist [30]. There are examples of microbiome engineering with engineered bacteria, which include manipulating metabolites. For example an *E. coli* Nissle (*E. coli* with a high safety profile) was modified to degrade phenylalanine in the genetic disease phenylketonuria (PKU) [31]. Moreover, engineered bacterial therapies that can selectively eliminate specific microbes hold greater promise in treating conditions where one well known species is contributing to poor health outcomes.

Several microorganisms are known to play causative or antagonistic roles in human disease. For instance, *Enterococcus faecalis* (*E. faecalis*), a gut commensal [32], is implicated in urinary tract infections [33] and disrupts colonic tissue healing [34]. Additionally, *Clostridioides difficile* (*C. difficile*) is responsible for life-threatening diarrhoea, with high rates of recurrent infection despite existing antibiotic treatments [35] and infections caused by *Vibrio cholerae* lead to cholera, characterised by severe fluid loss that can prove fatal within hours [36, 37]. Similarly, *Fusobacterium nucleatum* (*F. nucleatum*), an oral and mucosal commensal, is

an oncogenic microorganism linked to colorectal cancer [38].

In Europe, colorectal cancer is one of the most commonly diagnosed cancers [39]. Therefore, therapies targeting specific microbes, such as *F. nucleatum* and *B. fragilis* in colorectal cancer, could transform outcomes by mitigating microbial contributions to immunosuppression and inflammation in the tumour microenvironment [40]. These onco-pathogens pose a real challenge with global prevalence of *F. nucleatum* and *B. fragilis* in colorectal cancer patients at 39.8% and 42.4% respectively [41]. *F. nucleatum* is a prognostic marker for poor outcomes in colorectal cancer [42]. It is believed it achieves this through multiple routes, including, modulating immune responses [43], disrupting epithelial tight junctions [44], increasing inflammation and oxidative stress [45], and facilitating chemo-resistance [46]. In the case of *B. fragilis* both enterotoxigenic and non-enterotoxigenic strains are linked to colorectal cancer [47]. Whilst the enterotoxigenic strains produce the toxin, fragilysin, the non-enterotoxigenic strains can damage epithelial barriers, inducing inflammation [48]. Current cancer treatments, including surgery, chemotherapy, and radiation [49], fail to address these microbial contributions, underscoring the need for targeted therapies.

Beyond transient probiotics, microbiome engineering has the potential to enable long-term manipulation of microbial communities for improved health but we need to understand these communities to attempt engineering them. In the human gut, microbial diversity correlates with health [50, 51], whereas its loss is linked to critical illnesses [52]. Conversely, the vaginal microbiome thrives with lower diversity, with increases often associated with diseased states [53]. Current microbiome engineering strategies include modulatory, additive, and subtractive approaches [54, 55]. Modulatory therapies involve non-living agents like prebiotics, while additive therapies introduce natural or engineered microbes. Subtractive therapies, such as bacteriophages or bacteriocins, selectively remove specific microbes. These approaches, however, must account for microbial competition and environmental pressures, which influence community dynamics.

Engineered Live Biotherapeutic Products (eLBPs) are genetically engineered

microorganisms designed for therapeutic or diagnostic purposes and could tackle the issues raised regarding, microbial competition and community dynamics. The eLBPs stand out as a promising innovation. By genetically modifying microorganisms, eLBPs enable precise therapeutic functions, offering advantages over traditional probiotics or synbiotics, such as enhanced control through genetic elements and reduced risks from native microbiota. Further, they provide precise control through genetic elements such as inducible promoters and defined strain chassis, minimising risks associated with native microbiota [56, 28]. Examples include an *E. coli* Nissle engineered to improve cancer therapy in mice. This was achieved by improving the mechanism of delivery of the engineered bacteria, coating them in a capsular polysaccharide that reduces bacterial immunogenicity and improves the therapeutic efficacy and safety [57]. Whilst, this example focused on delivery other examples focus on delivering the treatments, such as the *Lactococcus lactis* that was modified to produce interleukin-10 (IL-10) for colitis treatment. In mouse models this eLBP resulted in a 50% reduction in the disease and the local delivery of IL-10 reduced the therapeutic dose required, in addition to preventing colitis onset in IL-$10^{-/-}$ mice which normally spontaneously develop colitis [58]. However, despite the potential of eLPBPs, challenges remain, including risks of mutation, limited engineering tools for species beyond *E. coli* and *Lactobacillus*, and a lack of efficacy in human trials [59, 60].

Increasing numbers of eLBPs are entering clinical trials for cancer, metabolic diseases, and other conditions. For cancer, engineered strains like *Listeria monocytogenes* (ADXS11-001) target HPV-associated cancers [61], while *Salmonella*-based VXM01 [62] and *E. coli* Nissle 1917-based SYNB1891 [63] show promise in solid tumors and glioblastoma. For metabolic diseases, candidates like SYNB1618 [64] and SYNB1934 [65] degrade phenylalanine to mitigate phenylketonuria, while SYNB8802 [66] and NOV-001 [67] address enteric hyperoxaluria. However, many eLBPs have faced challenges in translation from preclinical studies to human efficacy, highlighting the need for advanced models, scalable manufacturing, and public acceptance.

The transformative potential of eLBPs lies in their ability to address unmet medical needs through precise microbial manipulation. By overcoming challenges in biocontainment, efficacy, and societal acceptance, eLBPs could redefine therapeutic approaches across diverse diseases. However, most work on eLBPs remain in pre-clincial phases of research [20]. Continued research, clinical trials, and regulatory progress will be pivotal in unlocking the full potential of microbiome engineering.

1.3 Bacteriocins

Bacteriocins are ribosomally synthesised antimicrobial peptides [68], produced and secreted by Gram-positive bacteria, Gram-negative bacteria, and archaea [69]. In Gram-negative bacteria, the two main classes of bacteriocins are microcins and colicins, both of which have a narrower spectrum of antimicrobial activity compared to those produced by Gram-positive bacteria [70]. Colicins are large, thermolabile peptides that can be further categorised into Group A and Group B based on their mode of import, which exploits nutrient uptake pathways in sensitive cells [71, 72]. Group A colicins utilise the Tol protein system, whereas Group B colicins enter via the Ton system [73]. In contrast, microcins are small, thermostable peptides that can be classified based on whether they are chromosome- or plasmid-encoded [70]. They are further divided into Class I and Class II microcins [74]: Class I microcins are low-molecular-weight peptides that undergo post-translational modifications, while Class II microcins have a larger molecular weight and are subdivided into Subclasses IIa, IIb, IIc, and IId [73] (Figure 1.1.

Class I bacteriocins are small peptides (<5 kDa) that contain unusual post-translational modifications, such as lanthionine, which forms covalent bonds resulting in internal ring structures. The most well-known example of a Class I bacteriocin is nisin A [75]. Nisin A is approved for use in the food industry by both the U.S. Food and Drug Administration (FDA) and the European Food Safety Authority (EFSA) and has recently demonstrated the ability to survive the harsh conditions of the gastrointestinal tract, facilitating microbiome engineering to restore a health-like state [76].

In contrast, Class II bacteriocins are larger (<10 kDa), unmodified, thermostable, cationic, hydrophobic peptides that lack lanthionine. They are subdivided into four groups: Class IIa (pediocin-like bacteriocins), Class IIb (two-peptide unmodified bacteriocins), Class IIc (circular bacteriocins), and Class IId (non-pediocin-like linear bacteriocins) [77]. Class IIa bacteriocins consist of a single peptide and exert bactericidal activity by disrupting membrane potential and increasing membrane permeability [78]. Class IId bacteriocins are linear peptides

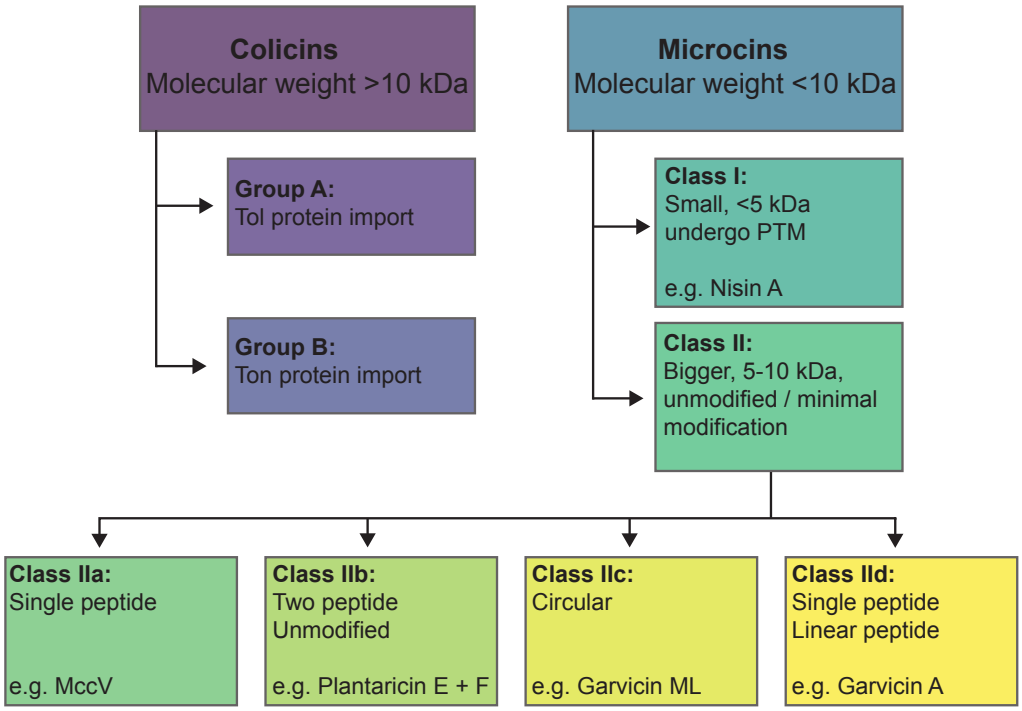

Figure 1.1: Bacteriocin classification
This flow chart highlights the current bacteriocin classification system. Some examples of the different Class II microcins are given.

that do not fit into the other three categories [79].

An example of a Class IIa microcin is Microcin V (MccV), produced by *E. coli*. Like most bacteriocins MccV is encoded within a gene cluster comprising four essential genes: an activity gene (encoding MccV), an immunity gene (encoding a protective peptide for the producer), and two genes that integrate into the ATP-binding Cassette (ABC) transporter system, facilitating MccV secretion [68, 80]. MccV is imported into sensitive cells via the CirA outer-membrane receptor and its uptake is TonB-dependent [68, 81]. The CirA, TonB, ExbB, and SdaC genes are essential for MccV-mediated killing [82]. MccV is naturally expressed under iron-depleted conditions [82, 83] and exerts its antimicrobial effect through membrane pore formation [84].

The greatest advantage of bacteriocins lies in their potential as antibiotic alternatives, as they employ different mechanisms to inhibit bacterial growth, preventing the creation of unoccupied niches that opportunistic pathogens could exploit [85].

Bacteriocins can selectively target and eliminate specific pathogens without harming commensal bacteria, preserving indigenous human microbiomes [86]. Unlike toxin-antitoxin systems, bacteriocin-based microbial control does not require engineering every cell in a population, only a single producer is needed [87].

Currently, the only known library of bacteriocin genes is the PARAGEN 1.0 collection, operated by Syngulon [88]. This collection comprises both chemically synthesised and *in vivo* produced bacteriocins, containing all the genetic elements necessary for *in vitro* cell-free synthesis of bacteriocins [1]. For this work it is important that the bacteriocins selected can be incorporated into plasmids for *in vivo* production by the eLBTs. Therefore, to build these plasmids the Modular Cloning (MoClo) [89] system was used. This is a digestion and ligation DNA assembly method, using standardised parts with pre-defined overhangs that allow for efficient plasmid assembly and easy interchangeability of parts, facilitating precise and adaptable engineering of the bacteriocins into genetic circuits [90].

1.4 Microbial population control

There are several methods for controlling microbial populations, including quorum sensing, metabolic flux regulation, and spatial segregation [91]. The primary motivation for microbial population control is to improve the yields of desired products in bio-manufacturing [92].

Quorum sensing has been successfully employed to enhance product yield, such as in the production of the flavonoid naringenin, where overall yield was increased by 60% [93]. Another example coupled quorum sensing with cell lysis, allowing *E. coli* to produce the enzyme required for isopropanol synthesis in a receiver strain [94]. In contrast, metabolic flux regulation does not rely on quorum sensing but instead depends on one strain utilising the metabolite output of another. This approach has been demonstrated in pathway-independent genetic control modules, which rebalance metabolic networks to favor glycolytic flux entering engineered pathways, thereby improving yields of myo-inositol, a key component for mammalian cell function [95], and glucaric acid, which has applications in disease treatment [96, 97]. The increased yields achieved through synthetic microbial communities enhance economic feasibility and provide a more sustainable alternative to conventional production methods [98].

Spatial segregation eliminates the need for engineering mutualism within microbial communities by physically separating strains to stabilise populations despite differences in growth rates [99]. This approach has been used to enhance production of complex metabolites, such as in a hydrogel-based co-culture where engineered *E. coli* produced L-dopa, which was subsequently converted by engineered *Saccharomyces cerevisiae* into betaxanthins, an antioxidant with applications in the food industry [100]. More broadly, efforts to control microbial populations aim to better understand microbial community dynamics, enabling their replication for practical applications. One example involves a synthetic predator-prey system, where the prey deactivates antibiotics targeting the predator while the predator produces a bacteriocin against the prey. The stability of this system was further altered by introducing an invader strain capable of killing both predator and prey [101].

Other systems looking into controlling microbial populations for the purpose of ensuring engineered microbes maintain their plasmids, have looked into Plasmid Segregational Killing (PSK) systems. The Barnes group developed the following systems with plasmid stabilising capabilites: axe/txe (toxin-antitoxin) system and the bacteriocin Microcin V (MccV) system [102]. These systems work by the plasmid containing both a toxin and an antitoxin, therefore after plasmid segregation, any cells that lose the plasmid no longer have the immunity to the toxin and are therefore killed. This prevents bacterial cells who lose the plasmid from outcompeting plasmid-containing cells and maintains control over the engineered bacterial cell population.

Beyond industrial applications, microbial population control has significant potential in therapeutic development, particularly in microbiome engineering for diseases with known microbial causative agents. eLBPs are gaining traction, as demonstrated by an engineered *Lactobacillus lactis* strain that successfully delivered human interleukin-10 (IL-10) to the gut in a Phase I clinical trial [103]. However, the *L. lactis* strain was cleared from the body within two days of treatment termination, highlighting a major challenge: engineered bacterial therapeutics struggle to persist in their target environments due to competition with native microbes. A self-regulating microbial system capable of controlling its population and interacting with surrounding microbes could overcome this limitation, offering a more effective and long-lasting therapeutic strategy. Microbiome engineering also presents an alternative treatment for diseases like colon cancer or recurrent *C. difficile* infection (CDI). However, transitory colonisation of probiotics reduces their efficacy, as their benefits cease once they are no longer administered [104, 105]. Even well characterised microbes cannot overcome transitory colonisation and the effects observed in mouse models of live bacterial therapeutics are rarely translated in human subjects [106]. For example, well-characterised microbes, such as *E. coli* Nissle, face limitations, with colonisation in mouse models ranging from 14 to 32 days depending on conditions [107, 108]. Furthermore, human colonisation is influenced by person-specific, strain-specific, and region-specific competition pressures

[109]. To address these challenges, the Barnes group developed the SPoCK 1 system, a combination additive/subtractive microbiome therapy designed to overcome the limitations of transitory colonisation and enhance therapeutic efficacy [87].

The SPoCK 1 system utilises bacteriocins to establish a dynamic win-lose cycle that enables niche creation within a microbial community [87]. Initially, the SPoCK 1 population decreases due to competitive exclusion, leading to lower levels of quorum sensing molecules in the environment (Figure 1.2). This reduction in quorum sensing molecules removes the inhibition of MccV production, allowing MccV to kill competing bacteria. Since SPoCK 1 carries an immunity protein (Cvi), it remains unaffected by MccV's activity and gains a competitive advantage. As the SPoCK 1 population grows, quorum sensing molecules accumulate, repressing MccV production and removing the SPoCK 1 competitive edge. The competitor strain population then recovers, and the cycle repeats again. In this way the SPoCK 1 system is able to maintain its population through niche creation while controlling the microbial populations around it. However, the model that predicted the SPoCK 1 system produced multiple versions with some estimated to be more robust[87]. This is important if the SPoCK system is to withstand changing environmental pressures, such as those in the human gastrointestinal tract.

Unlike current probiotics, which are transient due to gastrointestinal hurdles and competition from established microbial niches [110], a persistent live biotherapeutic could remain in the host for the duration of treatment, reducing the need for repeated dosing (a system such as the SPoCK 1 system). This is particularly relevant given that patient adherence to long-term medications is approximately 25% [111], and even multi-dose vaccine regimens, requiring only two to three doses, can have suboptimal uptake, as low as 25% to 35% in certain age groups [112]. Developing an engineered live biotherapeutic capable of sustained colonisation would address these challenges, offering a more reliable and effective treatment option.

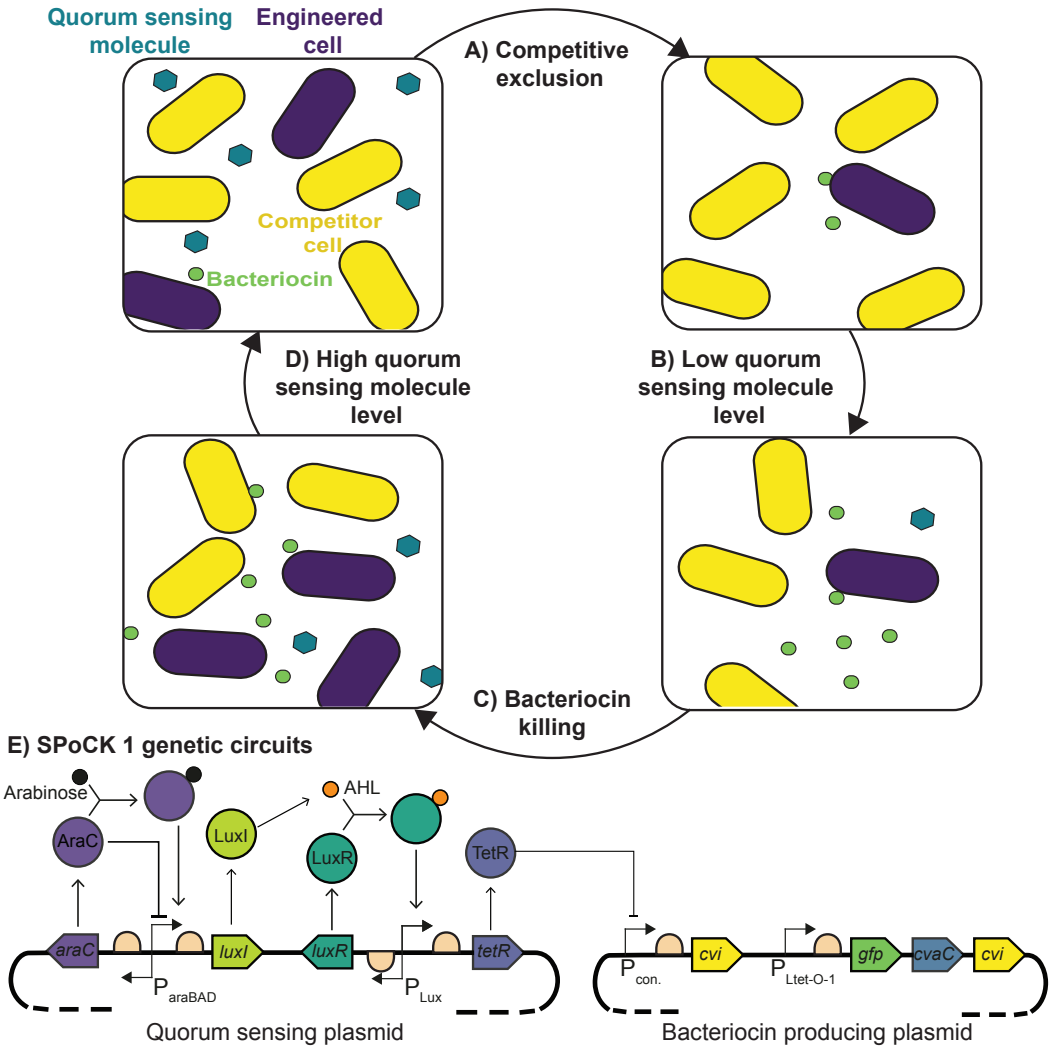

Figure 1.2: SPoCK 1 niche creation system

A) The engineered SPoCK 1 cell enters a new environment and is out competed. B) There are no quorum sensing molecules to repress bacteriocin production. SPoCK 1 produces bacteriocin. C) The bacteriocin kills the competitor strains, SPoCK 1 is protected by immunity. D) The levels of quorum sensing molecule produced by SPoCK 1 have increased and now repress bacteriocin production. SPoCK 1 loses its competitive advantage and is out competed once more. The cycle then begins again. E) The genetic circuits of the two plasmids used in the SPoCK 1 system in SBOL format. This figure is adapted from Fedorec et al, 2021 [87].

1.5 Biocontainment and kill switches

Biocontainment refers to preventing engineered bacteria from colonising undesired areas of the human body or escaping from defined geographical locations [113]. One approach for achieving this is to use non-commensal organisms as engineered strains. However, this strategy necessitates regular administration of the treatment, as non-commensal strains are typically outcompeted, a phenomenon observed with currently available probiotics [114]. Alternatively, commensal strains can be engineered to address this limitation. For example, one study engineered a commensal *Enterococcus faecalis* (*E. faecalis*) strain with a pPD1 defective conjugation plasmid expressing a bacteriocin. These engineered *E. faecalis* strains successfully outcompeted native *E. faecalis* strains and engineered *E. faecalis* lacking the pPD1 plasmid. In mouse models, the engineered strains effectively removed vancomycin-resistant *E. faecalis* from the intestine [86]. Using a microbe that naturally occupies the target niche avoids issues related to bacterial competition and minimises disruption to other microbial communities [86].

Kill switches are another key mechanism for biocontainment, enabling controlled shutdown of engineered bacteria [115]. Current kill switch designs encompass a variety of strategies. Metabolic auxotrophs, such as those used in the IL-10 *L. lactis* treatment, rely on external supplementation for survival [103]. Other examples include the 'Deadman' kill switch, which produces toxins to kill the host cell in the absence of a survival signal, with a fail-safe activated by IPTG addition [116], and the 'Passcode' Kill Switch, which requires complex inputs for cell survival [116]. Another example of a kill switch is where toxin production is triggered in response to low pH, this switch is enhanced with a counter mechanism that activates only after detecting low pH twice, increasing its robustness [117]. Auxotrophy based kill switches, including those employing non-canonical amino acids for survival, have gained popularity. By coupling essential enzymatic functions to non-canonical amino acids, engineered strains are unable to survive without them. However, this approach requires extensive genome editing, making it less practical for large-scale production [118]

Lysis circuits have been widely applied across various fields, including bacterial population management, kill switches for engineered strains, and delivery platforms. For example, a programmed lysis circuit (PLS) combines the PelB secretion peptide with (Figure 1.3) the cytotoxic protein colicin M (ColM) [119] (Figure 1.3A). This system employs a protease-trigger mechanism to regulate ColM degradation via TEVp, preventing premature entry into the periplasmic space. A protease-based regulatory switch with action and repression arms ensures delayed lysis, optimising the timing for product release. The PLS system has enabled metabolic division of labor (DOL), facilitating cell lysis after fermentation to release intracellular products such as poly(lactate-co-3-hydroxybutyrate) (PLH), which can then be used by other strains for production [119].

Another example is the synchronised lysis circuit (SLC), designed to regulate bacterial populations and enable drug delivery [120]. This system uses coupled positive and negative feedback loops to achieve oscillatory dynamics (Figure 1.3B). The quorum-sensing molecule AHL acts as a trigger, activating lysis once a threshold concentration is reached. Engineered in *Salmonella Typhimurium* (SL1344), this circuit was coupled with the anti-tumour toxin hemolysin E, demonstrating efficacy against HeLa cervical cancer cells in microfluidic models. When tested in colorectal tumours in mice, pulsatile bacterial population dynamics facilitated targeted therapeutic release without preloading drugs or requiring secretion machinery [120]. Further development included coupling the SLC with a nanobody antagonist of CD47, which is overexpressed in many cancers. In lymphoma mouse models, this system led to tumour shrinkage and regression after a single injection by maintaining a controlled bacterial population at the tumour site [121].

The SLC was also adapted into *S. Typhimurium* and *E .coli* to create 'ortholysis' circuits, which maintain stable co-cultures of metabolically competitive strains in microfluidic devices. This approach eliminated the need for external inputs to trigger lysis, offering potential beyond drug delivery by maintaining population equilibrium [122]. In another application, lysis circuits were used to transfer DNA from *E. coli* to *Bacillus subtillus*, a preferred host for synthetic biology. This in-

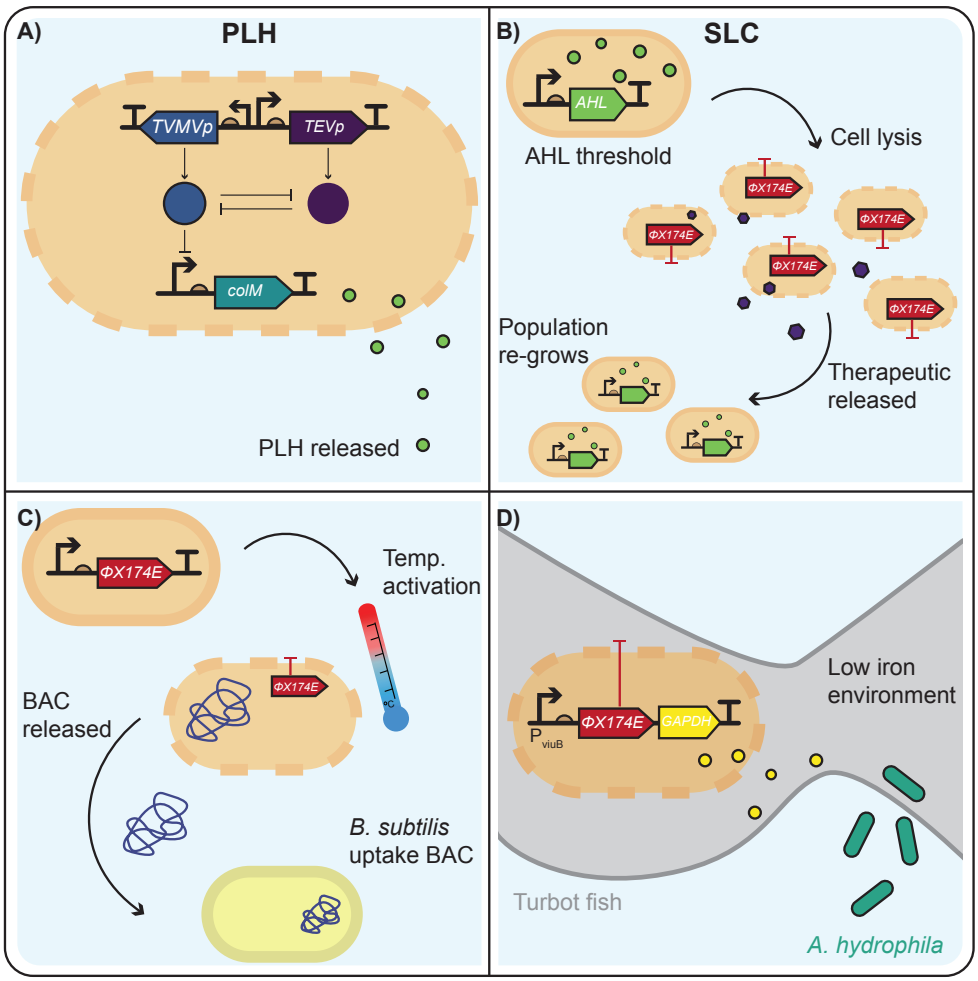

Figure 1.3: Current lysis circuits found in literature

A) The programmed lysis circuit (PLS). The PLS system uses the cytotoxic protein ColM to lyse open host cells. A protease trigger mechanism acts as the timer for the cell lysis, coupled with a protease based regulatory switch that ensures delayed lysis. B) The synchronised lysis circuit (SLC) uses the quorum-sensing molecule, AHL, as a trigger for cell lysis. The coupled positive and negative feedback loops create the oscillatory dynamics. C) The DNA transfer lysis system, uses cell lysis of *E. coli* to transfer a bacterial artificial chromosome (BAC) into the preferred host for protein expression, *B. subtilis*. D) Lysis systems have been used as vaccine delivery vehicles. Tested in turbot fish the system activates lysis in iron-depleted environments, releasing the vectored vaccine containing the *A. hydrophila* GAPDH protein, protective against infection by *A. hydrophila*.

volved utilising the ϕX174E lysis toxin to transfer a bacterial artificial chromosome (BAC) DNA (Figure 1.3C) and plasmid DNA, bridging the gap between tools assembled in *E. coli* and their use in *B. subtilis* [123].

Lysis circuits have also been harnessed for tumor-targeted therapy. One group engineered a probiotic *E. coli* Nissle (EcN) system to produce and release nanobodies, such as immune checkpoint inhibitors targeting PD-L1 and CTLA-4, at tumour sites. Controlled by the p_{Lux} promoter, the lysis circuit limited the engineered strain to the tumour site and enabled sustained therapeutic delivery in lymphoma and colorectal cancer models [124]. Another example involved an iron-regulated promoter (p_{viuB}) controlling the ϕX174E lysis gene in *E.coli* BL21(DE3). This system induced lysis in low-iron environments and was used to develop a vectored vaccine targeting *Aeromonas hydrophila* (*A. hydrophila*) (Figure 1.3D). Testing in turbot fish, an important food source [125], demonstrated its effectiveness in preventing infection and mortality [126].

Additionally, a *Salmonella* mRNA interferase regulation vector (SIRV) system was designed to induce self-lysis and release foreign antigens, activating the cGAS-STING immune pathway. To build this system required three chromosomal mutations in *Salmonella* and a plasmid carrying the desired antigen genes. To induce lysis this system utilised MazF, an mRNA interferase that regulates membrane damage, to trigger lysis and antigen release, showing promising results in mice and human cell lines for immune activation [127].

These examples highlight the versatility of engineered lysis circuits in applications ranging from drug delivery and pathogen control to tumour treatment and immune modulation. Despite these advances, there are no lysis circuits currently designed to deliver bacteriocins as cargo or target human oncogenic pathogens at tumour micro-environments. Using lysis circuits for bacteriocin delivery eliminates the need for specific export machinery tailored to each bacteriocin, offering a flexible and efficient solution. Thus, this study aimed to construct a simple inducible lysis circuit that can be easily adapted to deliver various bacteriocin cargos to therapeutically relevant sites.

1.6 Thesis objectives

In the interest of designing an engineered Live Bacterial Therapeutic (eLBT) with the potential to remain *in vivo* and target selected oncogenic bacteria, this work first looked at upgrading a previous system of microbial population control [87]. This was followed by a screening of bacteriocins to target the onco-pathogens, before combining the bacteriocin expression and bacteriocin delivery mechanisms. Lastly, public attitudes towards microbiome engineering and engineered live bacterial therapeutics were assessed.

Aim: To construct an engineered live bacterial therapeutic, designed to selectively kill oncogenic pathogens within colorectal cancer.

1. **Objective 1**: Design and construct the microbial population control system to deliver bacteriocins targeted to onco-pathogens. This will be achieved through modification of the microbial population control system, SPoCK.

2. **Objective 2**: Identify bacteriocins that can specifically target the onco-pathogens in colorectal cancer. This will be achieved through access to the PARAGEN bacteriocin library in collaboration with the industry partner, Syngulon.

3. **Objective 3**: Develop a kill switch bio-containment system to successfully deliver and destroy the engineered live bacteria. This will be achieved through combining bacteriocin expression and lysis in the MoClo format.

4. **Objective 4**: Assess and identify the public's attitudes towards engineered live bacterial therapeutics, to ensure acceptance of any such developed technologies in cancer treatment. This will be achieved through a public engagement survey.

Chapter 2

Methods

‘Beware; for I am fearless, and therefore powerful.’

— Mary Shelley, Frankenstein

Contents

2.1 Bacterial strains & plasmids

2.1.1 Bacterial strains

Table 2.1: Table of bacterial strains used in this work.

Chapter Ref.	Bacterial Strains	Characteristics
	SPoCK Strains	
	Escherichia coli	
3, 5	NEB DH5α	NEB chemically competent strain
3, 5	BW25113	Wild Type (Keio parent strain, LacZ K/O)
3	JW3910	Methionine auxotroph
5	BL21 (DE3)	T7 Expression Strain, deficient in proteases Lon and OmpT and resistant to phage T1 (fhuA2)
3, 5	JW2142	Keio collection CirA K/O (ΔcirA782::kan)
3	DH5α::PreCeKo	SPoCK Version 1.1 plasmid
3	JW_6343_01	SPoCK Version 1 system
3	JW_pMPES-AF01	SPoCK Version 1 plasmid
3	DH5α::pMPES_KAO01	SPoCK Version 2 plasmid
3	JW_6343_KAO01	SPoCK Version 2 system

Chapter Ref.	Bacterial Strains	Characteristics
3	JW2142::CeKo-ExpA	SPoCK Version 2.1 plasmid
3	JW2_6343_CeKoExpA	SPoCK Version 2.1 system
3	JW3_6343_CeKoExpA	SPoCK Version 2.1 system
3	BW2_6343_CeKoExpA	SPoCK Version 2.1 system
3	JW2142::pKAO02	SPoCK Version 3 plasmid
3	JW2142::pKAO02, pKAO052	SPoCK Version 3 system
3	JW_471	JW3910 with a streptomycin resistance plasmid
3	JW_637	JW3910 with a gentamicin resistance plasmid
	Bacteriocin Screens	
4	*Fusobacterium nucleatum subsp. nucleatum Knorr*	ATCC 25586
4	*Lactococcus lactis subsp. lactis*	IL1403
4	*Bacteroides fragilis*	ATCC 25185
4	*Enterococcus faecalis*	DSM 25700
4	*Enterococcus faecium*	NCTC 12202

Chapter Ref.	Bacterial Strains	Characteristics
	Lysis systems	
5	B21_IPTG	IPTG inducible circuit, in BL21(DE3), with the pAF06 plasmid
5	Lysara	Arabinose inducible lysis circuit, in BW25113, with the Lysara plasmid
5	Lysara:A53	Arabinose inducible lysis circuit and the pUC57-T7-AureocinA53 plasmid in BL21(DE3)
5	Lysara:BactA	Arabinose inducible lysis circuit and the pUC57-T7-BactofencinA plasmid in BL21(DE3)
5	Lysara:mccV	Arabinose inducible lysis circuit and the p15a_MccV plasmid in DH5 α.

2.1.2 Bacterial plasmids

Table 2.2: Table of bacterial strains used in this work.

Chapter Ref.	Bacterial Plasmids	Characteristics
	SPoCK Plasmids	
3	p63_AF043	Quorum sensing plasmid , used in SPoCK 1, 1.1, 2, 2.1
3	pMPES:AF01	SPoCK Version 1 plasmid
3	pre-CeKo	SpoCK Version 1.1 plasmid, Version 1 + SsrA tag
3	pMPES:KAO01	SPoCK Version 2 plasmid
3	CeKo1-ExpA	SPoCK Version 2.1 strain,*cvi*+SsrA
3	pKAO02	SPoCK Version 3 plasmid
3	pKAO052	Quorum sensing plasmid forSPoCK 3 system
3	pLac101-amp-CirA	plasmid containing the cirA receptor
3	pSEVA471	Streptomycin resistance
3	pSEVA637	Gentimicin resistance
	Lysara Plasmids	
5	pBADmTagBFB2	P_{araBAD} promoter PCR amplified from this plasmid
5	pAF06	IPTG inducible lysis circuit

Chapter Ref.	Bacterial Plasmids	Characteristics
5	Lysara_KAO07	Lysara arabinose inducible lysis circuit with kanamycin resistance
5	Lysara_ampicillin	Lysara arabinose inducible lysis circuit with ampicillin resistance
5	pUC57-T7-AureocinA53	IPTG inducible Bactofencin A expression plasmid, with kanmycin resistance
5	pUC57-T7-BactofencinA	IPTG inducible Bactofencin A expression plasmid, with kanmycin resistance
5	pUC57-T7-garML-S32-Npu	IPTG inducible Bactofencin A expression plasmid, with kanmycin resistance
5	A53_TU_EF	Aureocin A53 expression plasmid made with MoClo [128]
5	A53_noscars_TU_EF2	Aureocin A53 expression plasmid made with MoClo, without the scar sites between DNA parts[128]
5	garML_Npu_TU_EF	GarvicinML expression plasmid made with MoClo [128]
5	mccVCvi_TU_EF	Microcin V and immunity expression plasmid made with MoClo [128]
5	p15a_MccV	Microcin V and immunity with GFP expression plasmid

2.1.3 Bacterial culture

The strains were grown in their respective mediums with relevant antibiotics were required at the following working conditions in table2.3. *F. nucleatum* and *B. fragilis* were cultured in anearobic conditions, CO_2, H_2, N_2. *L. lactis*, *E. coli E. faecalis* and *E. faecium* were cultured in aerobic conditions, in 5% CO_2. All strains were cultured at 37°C, except *L. lactis* which was cultured at 30°C . Bacteria were kept in glycerol stocks and maintained at -70°C.

Table 2.3: Table of antibiotics and their working concentrations used in this work.

Antibiotic	**Working Concentration (μg/ml)**
Ampicillin	100
Chloramphenicol	25
Gentamicin	20
Kanamycin	50
Streptomycin	50

Table 2.4: Media used for Bacterial Growth

Bacterial Species	Media Name	Ingredients
Fusobacterium nucleatum & *Bacteroides fragilis*	BACTEC	BD BACTEC M Lytic Anaerobic medium
	Fastidious Anaerobic Broth (FAB)	Peptone 15.0 g/L, Yeast extract 10.0 g/L, Sodium thioglycollate 0.5 g/L,Sodium chloride 2.5 g/L, L-cysteine HCI 0.5 g/L, Resazurin 0.001 g/L, Sodium bicarbonate0.4 g/L, Haemin 0.005 g/L, Vitamin K 0.0005 g/L (EO labs)
	Brucella Blood Agar (BRU) & Supplemented broth	Anaerobesystems Pancreatic Digest of Casein 10.00g, Soy Peptone 3.00g, Meat Peptone 10.00g, Dextrose 1.00g, Yeast Extract 2.00g, Sodium Chloride 5.00g, Sodium Bisulfite 0.10g, L-Tryptophan 0.20g, Calcium Lactate 0.50g, Sodium Acetate 0.50g, Ascorbic Acid 0.10g, Hemin (0.1% solution) 5.00 mL, Vitamin K1 (1.0% solution) 1.00 mL, L-Cystine 0.40g, Sodium Hydroxide (4.0% solution) 4.00 mL, Agar 15.00g, Sheep Blood 45.50 mL, DI Water 1.00 L
Lactococcus lactis	GM17	GM17 broth (Sigma), Agar (Sigma), 0.5% glucose

Bacterial Species	Media Name	Ingredients
Escherichia coli	LB	200 mL diH2O, 4g LB Broth (Sigma), 3g Agar (Sigma)[1]
	M9	0.4% glycerol, 0.2% casamino, 0.4mg/ml thiamine, 0.002M/ 2mM MgSO4, 0.0001M / 0.1mM CaCl2, 1 X M9 salts acids

[1] Where making liquid broth, the ingredients are the same without the agar.

2.2 Plasmid creation

2.2.1 Polymerase Chain Reaction (PCR)

For the polymerase chain reactions (PCR) to construct the plasmids in this work the Q5 High-Fidelity DNA Polymerase system (M0491S, NEB)[129] was used. The PCR were performed in 25 μL volumes containing 1 μL of template DNA, 1×Q5 Reaction Buffer with 2 mM MgCl2, 200 μM dNTP mix, 1×Q5 High GC Enhancer, 0.5 μM forward or reverse primer, 0.02 U/μL Q5 High-Fidelity DNA polymerase, nuclease free water makes the reaction mix up to 25 μL. Thermocycling conditions included an initial denaturation at 98 °C for 30 seconds, denaturation at 98 °C for 10 s, annealing at required temperature (°C) for 30 s and extension at 72 °C for required length of time (varied for different PCR products), all three steps were repeated for a total of 30 cycles followed by a final 2 minute extension (not-tailored) at 72 °C. The reaction was ended by cooling at 10 °C to reduce condensation in the tubes.

2.2.2 Modular Cloning (MoClo)

Below is the list of MoClo parts used for plasmid construction in this work, alongside the plasmids they were used to construct. The reaction settings for the MoClo reaction are in table 2.6.

Table 2.5: Table of MoClo parts used to construct the plasmids

Plasmid	Part	Name	Notes
IPTG inducible plasmid	Vector	DVK_AE	(Kanamycin) Level 1 Vector backbone
	Promoter	p_{T7} (p18m)	Controls transcription of T7 RNA polymerase, induced by IPTG
	Ribosome Binding Site (RBS)	B0033m_BC	RBS was chosen

Plasmid	Part	Name	Notes
	Coding sequence (CDS)	ϕX174E	(ϕX174E) gene for phage lysis protein
	Terminator	L3S2P21	Modified L3S2P21 Terminator synthetic Voigt Terminator (T18m from CIDAR Ext.)
Lysara, arabinose inducible plasmid	Vector	DVK_AE or DVA_AE	Kanamycin and Ampicillin Level 1 Vector backbone
	Promoter	p_{araBAD}	Layer control araC regulatory gene in the opposite direction
	Ribosome Binding Site (RBS)	BCD8_BC	RBS library was used: B0032m_BC, B0033m_BC, B0034m_BC, BCD12_BC, BCD2_BC, BCD8_BC
	Coding sequence (CDS)	ϕX174E	(ϕX174E) gene for phage lysis protein
	Terminator	L3S2P21	Modified L3S2P21 Terminator synthetic Voigt Terminator (T18m from CIDAR Ext.)
A53_TU_EF	Vector	DVK_AE	Kanamycin Level 1 Vector backbone
	Promoter	J23106	Middle strength Anderson promoter
	Ribosome Binding Site (RBS)	BCD12_BC	
	Coding sequence (CDS)	*aucA*	Coding gene for aureocin A53 bacteriocin

Plasmid	Part	Name	Notes
	Terminator	B0015	MoClo part terminator
garML_Npu_TU_EF	Vector	DVK_AE	Kanamycin Level 1 Vector backbone
	Promoter	J23106	Middle strength Anderson promoter
	Ribosome Binding Site (RBS)	BCD12_BC	
	Coding sequence (CDS)	*Npu*	NpuIc, garvicin ML and NpuIn
	Terminator	B0015	MoClo part terminator
MccV_TU_EF	Vector	DVK_AE	Kanamycin Level 1 Vector backbone
	Promoter	J23106	Middle strength Anderson promoter
	Ribosome Binding Site (RBS)	BCD12_BC	
	Coding sequence (CDS)	CvaC and MccV	MccV and Cvi
	Terminator	B0015	MoClo part terminator
Another plasmid	Vector	DVK_AE	(Kanamycin) Level 2 Vector backbone
Another plasmid	Promoter	PlacUV5 (p19m)	Alternative promoter for inducible expression

2.2.3 SPoCK 2

Cultures of *E. coli* (MG1655) containing the SPoCK 1 plasmid (pMPES_AF01) in LB media, with relevant antibiotics, were grown overnight for 16 hours. The plasmid pMPES_AF01 (14920 bp) was mini-prepped following manufacturer's instructions (Monarch, NEB). PCR was used to amplify two sections of the plasmid, pMPES_AF01, primers with 20 bp pairs of homology between the two fragments are displayed in table _ (pMPES_001_F, and pMPES_003_F, italics are the overhangs). All PCR primers are listed in table (A.1). Dpn1 restriction digest (NEB) was used to remove any methylated DNA still present from the two PCR amplicons. Hi-Fi DNA assembly (NEB) was used to assemble the two amplicons resulting in the SPoCK2 plasmid, pMPES_KAO01. Plasmid pMPES_KAO01 was transformed into *E. coli* NEB 5-alpha via heat shock. Plasmids were checked for correct size by colony PCR and correct sequence by Sanger sequencing.

2.2.4 SPoCK 1.1

SPoCK 1.1 was constructed via PCR to amplify the mini-prepped plasmid pMPES_AF01, creating a vector (primers p.cvi.gBlock.F, cvi_qPCR7_R). PCR clean-up (NEB) and Dpn1 restriction digest (NEB) was used to remove any methylated DNA still present from the PCR amplicons. Hi-Fi DNA assembly (NEB) was used to assemble this vector and the g-block (IDT), cvi_SsrA_M2_gBlOCK.2 resulting in the SPoCK 1.1 plasmid, pre-CeKo. Plasmid pre-Ceko was transformed into *E. coli* NEB 5-alpha via heat shock. Plasmids were checked for correct size by colony PCR and correct sequence by Sanger sequencing.

2.2.5 SPoCK 2.1

Degradation tags were added to the immunity gene *cvi* to increase the degradation of the immunity protein Cvi (B.1). SPoCK 2.1 was constructed via PCR to amplify the mini-prepped plasmid pMPES_AF01, creating 2 halves with overhangs (primers, pMPES_001_F, cvi_qPCR7_R, pMPES_004_R, p.cvi.gBlock.F) compatible with the g-block (IDT), cvi_SsrA_M2_gBlOCK.2: TCTCTGCATTAATGTCTGCAATAT

GTTACTTTGTTGGTGATAATTATTATTCAATATCCGATAAGATAAAAAG
GAGATCATATGAGAACTCTGACTCTAAAAGGCCTGCAGCAAACGACGA
AAACTACGCTGCGAGCGTGTGAAGGTCCATGGTACGTACCCATAGATA
GGCGCCGTTATCGACTGGGCCTCATGGGCCTTCCGCTCACTGTAGATTA
atTAAACTGAAGCTTTCCACCATAATGCCAGCTACATATCCTGGTATTTT
TTTCCGATTATCTATAACTTGACGTGCAACGGAAATTTGCCGTTTAGCC
ACTTTACCGCTATTACCATGGCTACAATCAATCGTCCGAAAGTCACCA
GCctcctccccctgccgtcatccgtgcatcagatatgcactgagtatg (2.2.5). PCR clean-up (NEB) and Dpn1 restriction digest (NEB) was used to remove any methylated DNA still present from the PCR amplicon. Hi-Fi DNA assembly (NEB) was used to assemble the three parts. Resulting in the SPoCK 2.1 plasmid, CeKo-ExpA. Plasmid Ceko-ExpA was transformed into *E. coli* JW2142 via electroporation. Plasmids were checked for correct size by colony PCR and correct sequence by Sanger sequencing.

To create the RepA and MazE versions of SPoCK 2.1 the same primers as above were used to amplify the two halves of the plasmid, pMPES_AF01, two g-blocks with degradation tags RepA, MazE attached to *cvi* were ordered B.1. They were assembled as above and checked via colony PCR and sanger sequencing.

2.2.6 SPoCK 3

SPoCK 3 was constructed by creating two new plasmids. The first plasmid, pKAO02 was constructed by removing the inducible immunity gene *cvi* via PCR from the pMPES_KAO01 plasmid with the following primers, SPock2.2_1F, SPock2.2_1R, SPock2.2_2_F, SPock2.2_2R. A gel extraction kit (NEB) was used to isolate the expected PCR amplicon based on size followed by a Dpn1 restriction digest (NEB) to remove any methylated DNA still present from the two PCR amplicons. Plasmid pKAO02 was transformed into *E. coli* JW2142 via electroporation.

The second plasmid was attempted to be constructed by PCR to 1) amplify the required vector from the miniprepped plasmid p63_AF043 and 2) amplify the gene insert, CirA from the pLac101-amp-CirA plasmid. The aim was to have created a quorum sensing plasmid capable of producing the CirA receptor in response to

arabinose, pKAO052. The plasmid pKAO052 was transformed into *E. coli* JW2142 via electroporation. However, this was plasmid was not able to be built.

Plasmids were checked for correct size by colony PCR and correct sequence by Sanger sequencing.

2.2.7 p15a_MccV

In order to create a lysis system that can release a bacteriocin a MccV plasmid with no export machinery was created. The p15a_mccV plasmid was created via PCR to amplify the mini-prepped plasmid pMPES_AF01, creating a vector (primers in table:A.1). PCR clean-up (NEB) and Dpn1 restriction digest (NEB) was used to remove any methylated DNA still present from the PCR amplicons. Hi-Fi DNA assembly (NEB) was used to assemble this plasmid. The plasmid, p15a_mccV was transformed into *E. coli* JW2142 and JW3910 via electroporation. Plasmids were checked for correct size by colony PCR and correct sequence by Sanger sequencing.

2.2.8 MoClo plasmids

All plasmids that were constructed with MoClo parts are listed in the following table:2.5. In the MoClo reactions all parts were adjusted to 20 fmol/μL with the total reaction mix, 10 μL (table 2.6). The IPTG inducible lysis circuit was constructed using MoClo parts available in the kit [128], it was first transformed into NEB DH5α, then transformed into BL21(DE3) the T7 expression strain. The arabinose inducible lysis circuit, Lysara was constructed using MoClo [128], and finally transformed into *E. coli* BW25113. The level 0 promoter part, p_{araBAD} was amplified via PCR from the pBADmTagBFB2 plasmid, to include the *araC* gene, for tighter promoter control. See table 2.5 for level 1 transcriptional unit parts, including the options in the ribosome binding sequence library (RBS).

For the garvicinML bacteriocin expressing MoClo plasmid, the coding sequence part was obtained as G-block part GGTCTCAAATGatgattaaaattgcgaccc gcaaatatctgggcaaacagaacgtgtatgatattggcgtggaacgctatcataactttgcgctgaaaaacggctttatt gcgagcaactcaggagcttttactgcagctgggggaattatggcactcattaaaaaatatgctcaaaagaaattatgga aacagcttattgctgcattagtcgcgactggaatggctgcaggtgtagcaaaaactattgttaatgccgttagtgctggt

atggatattgccactgctttatcattgttctgcctgagctatgataccgaaattctgaccgtggaatatggcattctgccga
ttggcaaaattgtggaaaaacgcattgaatgcaccgtgtatagcgtggataacaacggcaacatttatacccagccgg
tggcgcagtggcatgatcgcggcgaacaggaagtgtttgaatattgcctggaagatggctgcctgattcgcgcgacc
aaagatcataaatttatgaccgtggatggccagatgatgccgattgatgaaatttttgaacgcgaactggatctgatgcg
cgtggataacctgccgaactag. The other parts are from the standard or extension MoClo kits.

Table 2.6: Table of reagents required for the MoClo reaction with the protocol used on the Thermocycler (Bio-Rad).

MoClo Reaction
DNA Part 20 fmol/ μL
T4 Ligase buffer (Promega)
T4 Ligase HC (Promega – 20U)
BsaI HF v2 OR 1 μL BbsI-HF
H_2O
Extended MoClo Program
25 cycles of:
37°C for 1min30s
16°C for 3 min.
Followed by:
50°C for 5 min
80°C for 10 min
12°C extended hold

2.2.9 Heat shock

For the plasmids that were transformed into NEB DH5-α (NEB) cells, they were transformed via heat shock.The following protocol was used, 2 μL of plasmid were used for 50 μL cells. Cells were placed on ice for 30 minutes, heat shock for 30 seconds at 42°C, cells immediately put on ice for 5 minutes. 950 μL SOC or LB media was added to a final volume of 1 mL as recovery media. Cells were incubated at 37°C for 1 hour. Cells were mixed by inversion and plated in several dilutions onto pre-warmed plates containing required antibiotics. Plates were incubated overnight at 37°C. For the moclo parts, blue/white screening assissted in colony selection. Followed by colony PCR that confirmed the size of the plasmids, successful plasmids were sent for sanger sequencing.

2.2.10 Electroporation

Plasmids that needed to be put into different strains or were unable to be transformed via heat shock were electroporated. For the full SPoCK systems there was a dual-transformation of the bacteriocin expressing and the quorum sensing plasmids.

Electrocompotent cells were made on the day following a protocol described by Datsenko & Wanner [130, 131]. 50 μL of cells were mixed with 1 μL of each plasmid (total plasmid DNA in mix was 2 μL). The plasmids were transformed into specified strains via electroporation into 1 mL cuvettes (MicroPulser, Bio-Rad). Recovery was 1 hour at 37°C in a shaking incubator in 1 mL warm SOC media (no antibiotics). Any other transformations using electroporation for this work were carried out the same way.

2.2.11 Colony PCR

For the polymerase chain reactions (PCR) to check the transformed colonies in this work the OneTaq QuickLoad system (M0486, NEB)[132] was used. The PCR were performed in 10 μL volumes containing 1 colony or 1 μLl of template DNA (positive controls), 1X OneTaq Quick-Load 2X Master Mix with Standard Buffer containing; 20 mM Tris-HCl, 1X Tartrazine, 25 units/ml OneTaq® DNA Polymerase,

22 mM KCl, 22 mM NH4Cl, 1.8 mM MgCl2, 5% Glycerol, 0.06% IGEPAL® CA-630, 0.05% Tween® 20, 0.2 mM dNTPs, 1X Xylene Cyanol, 0.2 μM forward or reverse primer, nuclease free water makes the reaction mix up to 10 μL. Thermocycling conditions included an initial denaturation at 94 °C for 10 minutes, denaturation at 94 °C for 30 seconds, annealing at required temperature (°C) for 30 seconds and extension at 68 °C for required length of time (1 minute per kb), all three steps were repeated for a total of 25 cycles followed by a final 5 min extension (not-tailored) at 68 °C. The reaction was ended by cooling at 10 °C to reduce condensation in the tubes.

2.2.12 Agarose gel

Where required a 0.8% or 1% agarose gel (Sigma), depending on the expected product size, was run with the PCR products. The Q5 High-Fidelity DNA Polymerase products required 1X Gel Loading Dye Purple (NEB). For the OneTaq QuickLoad 2X Master mix with Standard Buffer products no additional loading dye was required. Made with 1X TAE buffer (tris acetate EDTA, Severn Biotech Ltd.), Gelgreen nucleic acid stain (10,000X in DMSO, Biotium). The gel was run at 70 V for 45 minutes. For smaller fragments in this work a 1% agarose gel was used for the larger fragments 0.8% agarose gel was used.

2.2.13 Plasmid homology

To explore the genomic relationships between a plasmid and a reference genome, we developed a computational pipeline that integrates sequence alignment using BLAST and circular visualization through pyCirclize. The plasmid and genome sequences, provided as FASTA files, were processed to extract nucleotide sequences and determine their respective lengths. A BLAST database of the genome was constructed using the makeblastdb function from the BLAST+ suite, enabling efficient querying of the genome. The plasmid sequence was aligned to the genome using blastn, with alignment results exported in tabular format for subsequent analysis. The output was parsed into a structured DataFrame containing key alignment de-

tails, including start and end positions, percentage identity, and alignment lengths.

A circular visualisation of the alignments was generated using pyCirclize. The genome and plasmid were represented as circular sectors, with the plasmid scaled to enhance visual clarity. Genomic positions were annotated with axis ticks and labeled in megabases (Mb). Alignment links were plotted between the sectors to represent regions of homology identified by BLAST, connecting the corresponding loci on the plasmid and genome. The circular plot was exported as a PDF for visualization, and the processed alignment data were saved as a CSV file for further analysis. This approach provides a clear graphical representation of plasmid-genome relationships, facilitating the identification of homologous regions and their potential biological significance.

2.3 Killing Assays

2.3.1 SPoCK 2: lawn killing validation assays

Grew overnight cultures of a MccV sensitive strain (JW_471), a positive control (JW_pMPES-AF01) that only contains the SPoCK 1 plasmid, and the SPoCK2 strain (JW_6343_KAO01) all grown in relevant antibiotics in LB media. The streptomycin MccV sensitive strain (JW_471) was selected because we cannot be sure there are no SPoCK cells in the supernatant added to the bacterial lawn. To ensure that SPoCK cells could not grow we add streptomycin to the lawn media, which SPoCK does not have antibiotic resistance for, preventing any cells left in the supernatant from growing.

Overnight cultures were diluted 1:40 and left to grow for 4h, after which the cultures were centrifuged (1 minute at 13,000 rpm) and the supernatant removed, not disturbing the pellet of cells. The supernatant was put into clean 1.5 mL microcentrifuge tubes. To create the lawn, a water bath was set to 50°C. 1% and 0.5% LB agar (Sigma) were microwaved (until molten) and then placed in the water bath to cool to 50°C for 1 hour. The plate was made in two layers each 20 mL, the bottom layer contained 1.5% LB agar with streptomycin (1:1000). This was

then poured into a Onewell plate (Greiner bio-one) and allowed to dry. The top layer was made with 0.5% LB agar, with streptomycin (1:1000) and sensitive strain (JW_471, 1:100) added before being poured. Adding the bacteria to the media ensures a smooth lawn of bacterial growth. A mould for wells (made with PCR tubes fixed to a plastic frame) was placed onto the poured media and removed after the plate had dried. The respective supernatant was pipetted into the designated wells. Supernatant from SPoCK 2 were added to the wells with each volume in duplicate starting with 1 μL and ending with 15 μl of supernatant added. The controls were in singlets with 8 μL, 10 μL, 15 μL of supernatant added. The plate was left at 37°C overnight (18 hours) and imaged (iBright1500, Invitrogen by Thermo Fisher Scientific) the following morning.

2.3.2 SPoCK 2.1: lawn killing validation assays

Grew overnight cultures of MccV sensitive strains, JW3910, BW25113 along with the MccV insensitive strain, JW2142 and strains containing the SPoCK 2.1 system, JW2_6343_CeKoExpA, JW3_6343_CeKoExpA, BW2_6343_CeKoExpA in LB media with relevant antibiotics and 0.2% glucose to dampen the pLux promoter controlling TetR. The overnight cultures were diluted 1:100 and left to grow for 4h, after which the cultures were centrifuged for 10 minutes at 4.4. rpm. The bacterial cells were resuspended in phosphate buffer (oxoid) and adjusted to OD600nm 0.1. The plate was made with one layer containing 1.5% LB agar, 0.2% glucose and MccV sensitive strains JW3910, BW25113, and insensitive strains, JW2142 (1:100) respectively. The lawn was allowed to dry before 1 μL drops of the MccV-producing strains were pipetted onto the lawn. The plate was left at 37°C overnight (18 hours) and imaged (iBright1500, Invitrogen by Thermo Fisher Scientific) the following morning.

2.3.3 SPoCK 3: lawn killing validation assays

Grew transformant colonies, of JW2142::pKAO02 (bacteriocin producing plasmid only) in LB media with chloramphenicol for 4h. The plate was made from two

layers. The bottom layer was 20 mL 1.5% LB agar, the top layer was 0.5% LB agar, with MccV-sensitive strain, BW2113 (1:10) grown overnight. The lawn was allowed to dry before 2 μL drops of the 10 transformant colonies and BW25113 negative controls were pipetted onto the lawn. The plate was left at 37°C overnight (18 hours) and imaged (Iphone 6) the following morning.

2.3.4 AHL lawn killing validation assays: SPoCK 2.1

Grew overnight cultures of MccV sensitive strains, JW3910, BW25113 along with the MccV insensitive strain, JW2142 and strains containing the SPoCK 2.1 system, JW2_6343_CeKoExpA, JW3_6343_CeKoExpA, BW2_6343_CeKoExpA split into AHL and no-AHL groups. All strains were grown in LB media with relevant antibiotics and 0.2% glucose to dampen the pLux promoter controlling TetR and 10 μM AHL for the AHL groups. The overnight cultures were diluted 1:100 and left to grow for 4h, after which the cultures were centrifuged for 10 minutes at 4.4. rpm. The bacterial cells were resuspended in phosphate buffer (oxoid) and adjusted to OD_{600nm} 0.1. The plates were made with one layer containing 1.5% LB agar, 0.2% glucose, 10 μM AHL and MccV sensitive strains JW3910, BW25113, and insensitive strains, JW2142 (1:100) respectively. Control plates with no AHL were made the same as above minus AHL. The lawn was allowed to dry before 1 μL drops of the MccV- producing strains were pipetted onto the lawn. The plate was left at 37°C overnight (18 hours) and imaged (iBright1500, Invitrogen by Thermo Fisher Scientific) the following morning.

2.3.5 Pair colony drop assays

Grew overnight cultures of a sensitive strain (JW_471), a positive control (JW_pMPES-AF01) that only contains SPoCK 1 plasmid, and the SPoCK 2 strain (JW_6343_KAO01) all grown in relevant antibiotics in LB media. Overnight cultures were diluted 1:1000 and pipette into a 96-well plate (greiner bio-one) with relevant antibiotics. The iDot (Dispendix) was used to dispense the required volumes of the AHL inducer into the appropriate wells and the plate was sealed with

a Breathe-Easy membrane (Sigma-Aldrich). The plate was placed in a plate reader (Tecan Spark) and grown for 6h at 37°C with continuous double orbital shaking (2mm, 150 rpm). Measurements of absorbance (600 nm and 700 nm) were taken to check the cultures growth was normal. To prepare the plate for overnight incubation, a water bath was set to 50°C and 1% LB agar (Sigma) were microwaved (until molten) and then placed in the water bath to cool to 50°C for 1 hour. Once cooled to 50°C a serial dilution of 1% LB agar and AHL was set up, matching the AHL concentrations dispensed by the iDot. The LB agar and AHL mixes were pipetted into separate wells of a 6-well plate (ThermoScientific, Denmark) using a stripette. After the 6 hour incubation, 1 μL drops of each culture were pipetted onto the LB agar wells with the colony pairs pipetted next to each other but not touching. Plates were left to dry before being put in the incubator at 37°C overnight.

2.3.6 Pizza colony counting assay

The whole bacterial cell contents from one well per condition from a 96 microtitre plate (greiner bio-one) were diluted by serial dilution up to $10^{-}7$. Dilutions were thoroughly mixed by vortex before use. 5 μL was pipetted from each condition and each dilution along a grid on a 1.5% LB agar plate supplemented with 0.2% glucose were required. The plate was left to dry before being put in the incubator at 37°C overnight. The following morning the colonies inside each drop were counted. The plots were made using RStudio.

2.3.7 Microscopy

MccV-sensitive (JW3910), and both SPoCK1 and SPoCK2 strains were grown overnight. Co-cultures were set up by diluting overnight cultures to the same starting OD600 0.1 and then mixing together the pairs being tested in equal volumes. Cultures were incubated at 37°C for 6h with shaking. At 6h the co-cultures were centrifuged and resuspended in phosphate buffer (oxoid) at 10x the original culture volume. The co-cultures were then stained with propidium iodide (LIVE/DEAD BacLight Bacterial Viability Kit, Thermo Scientific, Rockford, IL, United States).

Microscope slides were prepared by making 1.5% agarose gel pads. 500 μL of 1.5% agarose were pipetted onto glass slides (Academy) and a 20 x 20 mm coverslip (Academy) added. When dry the coverslip was removed and the agarose was cut into 4 x 4mm squares. 5 μL of each experimental condition were pipetted onto the agarose pads. A 1 minute wait to allow the bacteria to burrow before adding the glass coverslip back and sealing with acrylic clear nail polish (Cutex). Samples were taken directly to the microscope (Olympus Widefield 1X81) and imaged at 20x with differential interference contrast (DIC), and 100x with phase contrast. Images were taken in the following channels; red for propidium iodide stain (ex = 490nm, em = 635 nm) and green for GFP fluorescence (ex = 480 nm, em = 500nm). Images were captured with the micromanager software (opensource) and edited in Fiji. Brightness was adjusted for DIC and phase images. Fluorescence signals were adjusted with "Auto" function for brightness/contrast in the channels tool [133].

2.3.8 Live / Dead Screening

The live/dead cell assay was performed using the LIVE/DEAD BacLight Bacterial Viability kit (Thermo Scientific, USA). In brief, *E. faecalis* were inoculated from glycerol stocks and grown in BHI media for approximately 18 hours at 37°C with shaking. Cultures were then diluted 1:20 and left to grow to an OD_{700} of 0.4. Cells were then split into 1 ml aliquots for each condition. For the 'none', 'EntA' and 'EntB' treatment groups cultures were supplemented with either 0 or 4 μg/ml of the respective bacteriocin and incubated for a further hour. The ethanol treated 'negative' control group was created as per the manufacturers instructions. After the one hour incubation all cultures were centrifuged and washed twice with PBS (Lonza, Belgium). The washed cells were then resuspended in PBS at 10x the original culture volume. Diluted cultures were supplemented with the SYTO-9 and propidium iodide dyes at a final ratio of 2:1 up to a total concentration of 3 μl/ml. Microscope slide agarose pads were prepared by adding 500 μl of 1.5% agarose to clean slides, following the instructions given by Skinner *et al* (2013)[134]. Five μl of culture from the selected treatment group was added to each agarose pad. After one minute, the agarose pads were covered by clean cover slips and sealed

with clear acrylic polish. The prepared samples were then imaged at 40x magnification with an Olympus Widefield 1X81 microscope (Olympus, Japan). Images were taken in the following channels; brightfield, TRITC (red) for propidium iodide stain (ex = 535nm, em = 617nm) and FITC (green) for SYTO-9 stain (ex = 485nm, em = 498nm), with a 50 ms exposure time. Images were collected and saved with the opensource 'Micro-Manager' software in Fiji[133]. All image analysis was performed in Fiji software. Collected images were first split into individual channels and converted to 8-bit. The FITC and TRITC images were then manually thresholded to identify the stained areas in the red and green channels. The thresholded areas were then measured and the ratio of red:green stained areas used to estimate the percentage of dead cells in each treatment group. Statistical analysis between treatment groups was performed in R, using an unpaired t-test. A p-value of less than 0.05 was deemed to show a significant difference between treatment groups.

2.4 Induction Assays

2.4.1 SPoCK 2: plate reader induction assays

Overnight cultures of the relevant strains SPoCK 1 (JW_6343_01), SPoCK2 (JW_6343_KAO01) and a sensitive strain (JW3910) were grown in M9 media. The overnight cultures were diluted 1:1000 in fresh M9 media with relevant antibiotics and grown for 2h at 37°C, with shaking. Diluted the cultures to OD700 of 0.1 with fresh M9 media, containing relevant antibiotics. 120 μL of each bacterial culture were added to their respective wells of a 96 microtitre plate (greiner bio-one). 125 μL of M9 media were added to the rows and columns at the end to mitigate against the end row/column effect.

For the arabinose induction the same overnight cultures and conditions as above, except the sensitive strain was JW_637 (gentamicin resistance). Cultures were diluted, as above, to OD_{700nm} of 0.1. Bacterial cultures at OD_{700nm} of 0.1 were pipetted into the top row. Serial dilutions down the rows resulted in a 1000-fold dilution of the starting concentration of cells. Pipetted 125 μL of M9 media

into the rows, leaving the first-row empty. Pipetted 187.5 μL of cells in M9 media into the first row. Mixed well with pipetting then removed 62.5 μL of M9 media and cells and dispensed this into 125 μL M9 media in the next row in the series. Repeated the steps above until the last row where the 62.5 μL were discarded into the waste. The iDot was used to dispense arabinose and the plate was sealed with a Breathe-Easy membrane (Sigma-Aldrich). Plate reader settings and analysis of results were kept as outlined above.

2.4.2 SPoCK 2.1: plate reader induction assays

Overnight cultures of the relevant strains, SPoCK 2.1 system (JW2_6343_CeKoExpA, JW3_6343_CeKoExpA, BW2_6343_CeKoExpA), sensitive strains (JW3910, BW25113) and an insensitive strain (JW2142) were grown in LB media with 0.2% glucose and with/without 10 μM AHL. Diluted the cultures to OD700 of 0.1 with fresh LB media, containing relevant antibiotics and 0.2% glucose. 120 μL of each bacterial culture were added to their respective wells of a 96 microtitre plate (greiner bio-one). 125 μL of LB media were added to the rows and columns at the end to mitigate against the end row/column effect.

For all Plate reader experiments the iDot (Dispendix) was used to dispense the required volumes of the AHL inducer into the appropriate wells and the plates were sealed with a Breathe-Easy membrane (Sigma-Aldrich). The plates were placed in a plate reader (Tecan Spark) and grown for 24h at 37°C with continuous double orbital shaking (2mm, 150 rpm). Measurements of absorbance (600 nm and 700 nm) and fluorescence (GFP: ex = 485 nm, em = 530 nm, mCherry: ex = 575 nm, em = 620 nm) were taken every 20 minutes using Tecan Spark Control software. The results were processed using the FlopR package [135]. Calibrated GFP (green fluorescence) / OD measurements were converted into standard units of molecule of equivalent fluorescein (MEFL). Plots for MEFL against increasing inducer levels were made in Rstudio [136], using the ggplot2 [137] and dplyr packages [138]. Final figures were compiled in Adobe Illustrator (line colours and title positions).

2.4.3 Lysara: plate reader induction assays

For the initial screening of the transformants the white colonies were resuspended in 20 μL of LB and 1 μL of the Lysara colony suspension was pipetted into 124 μL LB in a 96 microtitre plate (greiner bio-one) in both 0.2% glucose and without glucose. The plate was placed into the plate reader (Tecan Spark), allowing the colonies to grow for 2h. At 2h the iDot (Dispendix) was used to dispense 10 mM arabinose into each well. Colonies that lysed and remained dead until the end of the experiment (24h) were stored as glycerol stocks for further characterisation.

For subsequent characterisation assays of the Lysara arabinose inducible lysis system; the selected colonies were allowed to grow for 2h before addition of arabinose, controls were uninduced *E.coli* NEB 5α with the Lysara circuit. Empty *E.coli* NEB 5α was used as the negative control. Characterisation was conducted in both M9 and LB media with 0.2% glucose, unless no glucose is stated.

The same experimental setup was used for the time induction characterisation of Lysara the only difference being the arabinose was added at multiple timepoints. For the characterisation of arabinose concentration the setup was the same except arabinose concentrations differed and the time added remained the same.

2.5 Quantitative PCR (qPCR)

2.5.1 qPCR for gene expression

Quantitative real-time PCR (qPCR) was performed as in Hernandez-Miranda paper 80 by Dr William Andrews at the central molecular laboratory in the Cell and Developmental Biology department, UCL. Total RNA was extracted from *E. coli* using the QIAGEN RNeasy Plus kit (USA). For the SPoCK 2 samples, cells that were harvested after 4 hour and 6 hour treatment with different concentrations of AHL. For the bacteriocin expression plasmids, engineered cells were grown for 4 hours, for the IPTG-incubile cells 0.5 mM IPTG was added after cells had reached OD_{600nm} 0.4-0.5, then cells were left for 2-3 hours before being harvested for RNA extraction. RNA was treated with DNaseI to remove any remaining trace amounts of DNA.

cDNA was generated with 25 ng of RNA using the QIAGEN Whole Transcriptome Amplification kit, as described in the manufacturer's protocol. Primers for qPCR are in table 3. The qPCR was performed using Sybr Green reagent (Merck) on a Bio-Rad CFX96 Real-Time PCR Detector System (Bio-Rad). PCR conditions were 94°C for 2 min, followed by 40 three-step cycles of 94°C, 15 s; 60°C, 30 s; 72°C, 30 s. *rrsA* was used for endogenous reference gene controls. Each primer set amplified a single PCR product of predicted size, as determined by melt-curve analysis, after PCR and had approximately equal amplification efficiency when validated using a serial dilution of representative cDNA. Each qPCR was performed in triplicate, and relative quantification was determined according to the ΔΔCt method [139, 140]. A Mann-Whitney test was selected for statistical analysis because the sample size was small, and the data non-parametric.

2.6 Bacteriocin: synthesis, expression & screening

2.6.1 Bacteriocin selection

The methods used to identify the bacteriocins that can effectively kill *F. nucleatum* and *B. fragilis*. No bacteriocin genes were identified in a search of the *F. nucleatum* ATCC 25886 genome. Therefore, the search for bacteriocin genes was expanded to the bacterial genomes of bacteria commonly isolated with *F. nucleatum*, this yielded approximately 700 suspected bacteriocin genes. A further search of a bacteiocin databse, BactiBase identified a further two possible bacteriocins, predicted to target *F. nucleatum* were identified, Subtilosin A and Subtilosin X both produced by *B. subtilis*. Subtilosin A/X are both circular anti-microbial peptides, following on from this discovery the circular peptides from Syngulons PARAGEN collection [1] were added to the bacteriocin screen.

2.6.2 Bacteriocin synthesis

The chemically synthesised bacteriocins were produced at Syngulon and form part of the PARGAEN 1.0 collection [1]. These chemically synthesised bacteriocins

were put into vectors with T7 promoters/terminators, the recombinant vector amplified in *E. coli* DH10B (Thermo Scientific™) to produce the template for cell-free protein synthesis using the PURExpress *in vitro* protein synthesis kit (NEB) [1]. The *in vivo* produced bacteriocins were produced in *E. coli*DH10B and then the supernatant filtered. Final concentration of these constructs was diluted to 1 ng/μl.

2.6.3 Bacteriocin expression

The IPTG-inducible bacteriocin expression plasmids, were grown in 10 mL LB cultures overnight. The cultures were then diluted to OD_{600nm} 0.1 in 500 mL LB. Culutres were then induced with 0.5 mM IPTG once they had reached OFD_{600nm} 0.4-0.5. The cultures were left for 2-3 hours then centrifuged at 8,000g for 15 minutes. The supernatant was discarded and the cells re-suspended in 20 mL sonication buffer , samples were then left in -80 , until further use.

2.6.4 Bacteriocin screening assays

Bacterial cultures of *F. nucleatum* were grown for 72 hours in liquid media (Columbia blood media). Cells were diluted 1/10 into TA7 agar, without antibiotics and poured into One well plates (Thermo Scientific™) or pre-made columbia blood agar. Plates were left to dry in the Biosafety Level 2 cabinet for 10 minutes. Once dry 2 μL of each bacteriocin to be tested were drop pipetted onto the lawn. Plates were left to dry and then placed into the anearobic chamber for culturing. For the controls, overnight cultures of *E. coli* and *L. lactis* were used. *E. coli* as the control for microcins and colicins, *L. lactis* as a control for the circular antimicrobial peptides. LB and MG17 agar one well plates were prepared. Then *E. coli* and *L. lactis* cells were diluted 1/20 into TA7 agar, this layer was poured on top of the LB and MG17 plates. Once dry 2 μL of each bacteriocin were drop pipetted onto the lawns. Plates were left to dry and then placed in anaerobic conditions for overnight culture at 37°C.

An alternative bacterial lawn method was tested. A 25 mL petri dish of Columbia blood agar/Brucella agar was prepared. *F. nucleatum* and *B. fragilis* 48

hour cultures were smeared on top of the dried agar using a sterile cotton bud. Bacteriocin drops were dispensed as above using a multichannel pipette. Plates were left to dry and then placed in anaerobic conditions for overnight culture at 37°C.

For follow up screening and further work *F. nucleatum* and *B. fragilis* were cultured as follows. Streaked from a glycerol stock on Fastidious anaerobic agar (FAA) plates for 48 hours with and without 5% horse blood. Cultures were re-streaked onto fresh plates for a further 24 hours. Bacteria were diluted to OD600 nm at 0.1 and re-suspended in 150 μL fastidious anaerobic broth (FAB) medium which was spread onto a fresh plate. Plates were left for 5 minutes with the lid on to dry, after which the bacterial suspension was re-spread and the plates left to dry with the lid off. Once the plates were dry a sterile glass tube was used to punch 50 μL wells into the prepared bacterial lawns. 50 μL of tested bacteriocins and controls were placed into these wells. Plates were placed into the anaerobic chamber without inversion for overnight culture at 37°C.

2.6.5 Bacteriocin screens: oCelloScope

Bacteria were cultured on agar plates in anaerobic conditions for 48 hours. The bacterial strains to be tested were adjusted to a McFarland standard of 1 at 625 nm. This equates to approximately 3 x 10^8 cells / mL. The cells were then diluted 1/10, 1/100/ and 1/1000. There were 4 different media conditions tested for each strain at each dilution. Either the bacteria were suspended in complete media (Brucella/BACTEC) or suspended in the McFarland standard. The bacteria suspended in the McFarland standard lack any media to grow so this had to be added. This created a diluted media condition for both of the media types: Brucella/BACTEC. In a biosafety level 2 cabinet the following were set up for each well in the multi-well plate (96 wells), with all bacterial suspensions in triplicate: 180 μL bacterial suspension at 1, 1/10, 1/00, 1/1000 in either McFarland/BACTEC/Brucella, 20 μL BACTEC/Brucella media, 60 μL liquid paraffin.

The oCelloScope (BioSense Solutions, Farum Denmark) is an automated brightfield optical microscope that uses measurements of pixels to calculate bacte-

rial growth. The oCelloScope was set to record every 30 minutes for 18 hours. The growth curves from the tested strains were analysed at the end of the experiment. For *B. fragilis* the 1/100 dilution produced optimal growth curve patterns while *F. nucleatum* grows slower, a 1/10 dilution or less would be better. This needs to be confirmed. The McFarland standard with added BACTEC media worked best regarding imaging and growth curves. The complete Brucella media was too dark.

The Segmentation and Extraction Surface Area (SESA) normalized algorithm was used to obtain instrument derived growth values. This algorithm is object based and identifies bacteria within a scan area based on contrast against the background, and then calculates total bacterial surface area. This algorithm is less susceptible to artefacts caused by media precipitation, as observed with our BACTEC media and a selection of bacteriocins. Bacteria were inoculated onto fresh Brucella agar plates from growing strains. They were grown in anaerobic conditions for 48 hours at 37°C. The bacterial strains to be tested were adjusted to a McFarland standard of 1 at 625 nm. This equates to approximately 3 x 10^8 cells / mL. The bacterial cells were then diluted 1/100. In a biosafety level 2 cabinet the following were set up for each well in the multiwell plate (96 wells) with all bacterial suspensions in triplicate: 160 μL 1/100 bacterial suspension of McFarland standard 1, 20 μL BACTEC, 20 μL bacteriocin (final concentration 100μg/mL), 60 μL liquid paraffin. The multiwell plate was then placed in the oCellScope for static growth at 37°C for 24 hours. The liquid paraffin ensuring anaerobic conditions at all times.

2.6.6 Bacteriocin screens: Tecan Spark

For the initial growth tests of the bacterial strains to be tested they were adjusted to a McFarland standard of 1 at 625 nm. This equates to approximately 3 x 10^8 cells / mL. The bacterial cells were then diluted 1/100 in PBS and BACTEC media. The following were set up per well in a multiwell plate: 124 μL 1/100 bacterial suspension of McFarland standard 1, 14 μL bacteriocin (final concentration 100μg/mL), 60 μL liquid paraffin. Where a qPCR plate cover was used there was no liquid

paraffin. For the subsequent growth experiments and then the bacteriocin screening on the 5 short listed bacteriocins (Figures 4.1 and 4.4), the strains were adjusted to OD 600nm at 0.1. The bacteriocins were added to the final concentrations either 100μg/mL or 200μg/mL for *B. fragilis* or *F. nucleatum* respectively. For the Aureocin A53 concentration curves serial dilutions to intermediate concentrations diluted in molecular biology grade water (Corning) were created so that the following final concentrations were in the wells 200 μg/mL, 100 μg/mL, 50 μg/mL, 25 μg/mL, 12.5 μg/mL, 6.25 μg/mL, 3.12 μg/mL, 1.56 μg/mL, 0.78 μg/mL, 0.39 μg/mL, 0.19 μg/mL.

The multiwell plate was placed in a plate reader (Tecan Spark) and grown for 24 hours at 37°C without continuous double orbital shaking for *F. nucleatum* experiments and with the continuous double orbital shaking (2mm, 150 rpm) for *B. fragilis*. Measurements of absorbance (600 nm and 700 nm) were taken every 20 minutes using Tecan Spark Control software. The results were processed using the FlopR package [135]. Plots for Optical Density (OD) against time were made in Rstudio [136], using the ggplot2 [137] and dplyr packages [138]. Where the standard error of the mean was calculated the following equation was used with the dplyr package:

$$SE = \sqrt{\frac{\sum(\text{OD.se})^2}{n}}$$

Final figures were compiled in Adobe Illustrator (line colours and title positions).

2.7 Protein purification

2.7.1 Sonication

The cells requiring isopropyl-β-D-thiogalactoside (IPTG) induction were cultured as 10 mL overnight , diluted into 500 mL adjusted to OD_{600nm} 0.1. Then at OD $_{600nm}$ 0.4-0.5 IPTG was added to a final concentration of 0.5 mM. For strains with constitutive bacteriocin expression they were grown overnight in 10 mL, then diluted into 500 mL adjusted to OD_{600nm} 0.1. All samples were collected when they had reached $\approx$ OD_{600nm} 1.0. The+ cells were pelleted by centrifugation at 8,000 g

for 15 min at 4°C. The cells were resuspended in 20 mL ice-cold 20 mM phosphate buffer, pH 6.0 with 1 M NaCl, and lysed by sonication (5 cycles of 30 s at 75% maximum intensity, with 30 s incubation in ice in between the cycles) in a 450 Digital Sonifier (Branson Ultrasonics, Connecticut, United States). The insoluble cell debris was pelleted by centrifugation at 8,000 g, for 15 min at 4°C. The sonicated samples were then stored at -20°C until further use.

2.7.2 Ammonium sulphate precipitation

E. coli cultures were pelleted by centrifugation at 3,400g for 10 minutes and supernatants poured into 1L flasks containing stir bars. Ammonium sulphate salt was then slowly added to each 200 mL sample to reach 70% saturation concentration at 4°C. Samples were mixed by rotation at 4°C overnight. The following day, proteins were pelleted by centrifugation at 11,000g at 44°C for 15 minutes. Supernatant was removed, and the pelleted precipitate was resuspended in 1 mL sterile deionised water and stored at -20°C.

Chapter 3

Engineering bacteriocin delivery systems

‘You must do the thing you think you cannot do.’

— Eleanor Roosevelt, 1960

Contents

3.1 Introduction

3.1.1 Bacterial competition

One of the main challenges facing an engineered Live Bacterial Therapeutic (eLBT) is competition from host microbes. Bacterial competition comes in both passive and active forms. In passive competition the goal is to self-serve and not actively harm competitors, a microbe uses up, or depletes, the supply of nutrients, indirectly harming the competitor. Whereas active competition, the goal of which is to eliminate a competitor, causes deliberate harm, for example through the production of a toxin [141, 142]. There are three ecologically stable long term outcomes of competition: (1) one of the microbes wins and the other loses, (2) a metabolic niche is created because the two strains use different resources, or (3) territorial niches are created where each of the microbes keep to their own space (possible on solid structures such as mucous membranes) [142]. These ecologically stable outcomes provide potential solutions that the eLBTs could utilise to overcome the challenge of bacterial competition inside a host environment. Metabolic niches have been explored with quorum sensing molecules manipulating the metabolism of bacterial populations in synthetic microbial communities, creating a metabolic niche [93, 97]. However, a metabolic niche is not always possible. An alternative system would utilise a dynamic win-lose cycle as a competition outcome ultimately allowing the stable colonisation of the host. This is the reasoning behind the Stabilised Population by Community Killing (SPoCK) niche creation system, which uses bacteriocins common in bacterial genomes [143] to control the population of competitors to make a space for itself through a win-lose cycle. Once established in its dynamic niche, the SPoCK system can promote a healthy microbiome state by correcting perturbations that result in disease [54].

3.1.2 SPoCK

Modelling from previous work suggested that in order to construct a more robust system to withstand environmental pressures, the new SPoCK system would require ‘self-killing’ capability [87]. To produce this upgraded SPoCK system, multiple

SPoCK systems were created (Figure 3.1) from the original SPoCK system, SPoCK 1 [87]. In SPoCK 1 *cvi* expression is constitutive, so SPoCK 1 is continually protected from MccV. Whereas, in SPoCK 2 *cvi* expression is under the control of the quorum sensing molecule. High concentration of the quorum sensing molecule in the SPoCK 2 system results in the inhibition of both the bacteriocin (MccV) and the immunity (Cvi). This leaves SPoCK 2 vulnerable to 'self-killing'. In the SPoCK 1.1 system a degradation tag has been added to the *cvi* under the repressible promoters control, however the system still contains constitutive immunity and is expected to behave as SPoCK 1. The SPoCK 2.1 system is an improvement on SPoCK 2, whereby the degradation tag has been added to the *cvi* under the repressible promoters control, with no constitutive immunity in this system the system is expected to show signs of 'self-killing' as the immunity should be removed in the presence of the quorum sensing molecule. The SPoCK 3 system is an alternative way of controlling 'immunity' to the bacteriocin. In this system all immunity was removed and the CirA receptor that MccV requires to bind to a susceptible cell, was placed under an inducible promoter, in the presence of the quorum sensing molecule the Cir receptor is produced and the cells are susceptible to MccV we should observe the 'self-killing'. The SPoCK systems are designed to regulate their own populations as well as those of competitors around them. SPoCK 2, SPoCK 2.1 and SPoCK 3 directly regulates themselves, through self-killing. All systems are regulated by competitive exclusion when MccV production is inhibited.

It is sometimes desirable to tune synthetic circuits beyond the stage of transcription. A popular method of altering the dynamics of translated proteins in a system is to modify them with a degradation tag. The most well studied, and arguably the most popular, is the small stable RNA A (SsrA) tag. In native systems the SsrA tag is an 11 residue sequence that is added by the transfer-messenger RNA (tmRNA), to the C-terminal of peptides that are trapped in stalled ribosomes during translation [144]. The SsrA tag signals these peptides for degradation by cytoplasmic proteases including ClpXP, ClpAP and Lon [145, 146] and requires the assistance of adapter proteins e.g. SspB [147].

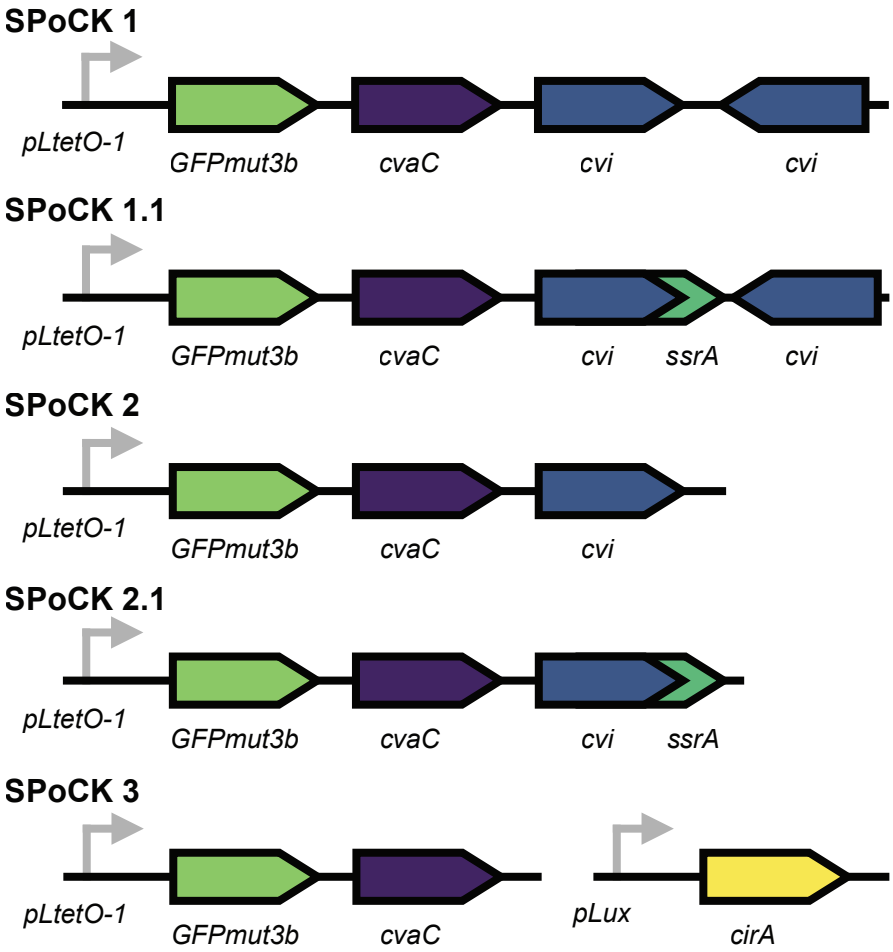

Figure 3.1: Genetic circuits in SBOL visual format of the SPoCK systems
Genetic circuits in the synthetic biology open langauge (SBOL) format of the SPoCK systems created in this work, except SPoCK 1 system which is from previous work by Alex Fedorec [87]. In SPoCK 1 and SPoCK 1.1 there is constitutive immunity, *cvi* expression, denoted by the reverse arrow. All other circuits are under controllable promoters. Acyl homoserine lactone (AHL), the quorum sensing molecule represses the promoter, p_{LtetO}. Whereas, the p_{Lux} promoter in the SPoCK 3 system is induced by the presence of AHL. In all SPoCK systems, the immunity is controlled by the Cvi protein, except SPoCK 3 where the immunity is controlled by the presence/absence of the MccV susceptible receptor, CirA, on the host cells surface.

There are multiple variants of the native SsrA tag (AANDENYALAA), with the C-terminal residues playing a role in the rate of degradation. The the Ala-Ala being the most important part to recruit ClpXP [148]. Altering the three C-terminal residues changes the rate of degradation, with fewer and further away alanine residues reducing the rate of degradation [149]. SsrA tag variants have been characterised in *E. coli* with tolerated, but not preferred residues such as Serine being incorporated alongside aspartic acid that reduces ClpXP and ClpAP degradation [150, 151].

The degradation dynamics of a variety of protein degradation tags have been studied using fluorescent reporter proteins as a marker of degradation efficiency [152, 151]. The purpose of utilising the protein degradation tags in this work, was to remove any lingering immunity protein from the engineered cell once its transcription had been switched off. This work attempted to use a weaker version (ASV) of the wild type SsrA tag (LAA), as well as the RepA and MazE protein degradation tags in an effort to control the degradation of the immunity protein, Cvi, in the SPoCK 2.1 system.

Ultimately the goal of the SPoCK system is to act as a delivery system for bacteriocins that target specific bacteria in the cancer microbiomes. This work is part of the umbrella of microbiome engineering. Theoretically, this chapter presents upgraded systems, SPoCK 2, SPoCK 2.1, SPoCK 3, with highly controlled colonisation and selective killing.

3.2 Results

3.2.1 The SPoCK 2 plasmid is successfully created and able to Kill MccV susceptible strains

The first step of the project was to create the plasmid that would be the bacteriocin producing plasmid of the SPoCK 2 system (app. C). To create this, the two regions from the SPoCK 1 plasmid were amplified via PCR (for primers see A.1) and then assembled by HiFi DNA assembly. The constitutive immunity gene (*cvi*) and dead space were removed to create a smaller SPoCK 2 plasmid 8,162 bp compared to the parent plasmid, SPoCK 1, 14,290 bp. Figure 3.2A, shows the sequencing alignments for the SPoCK 2 plasmid compared to the original SPoCK 1 plasmid. The junctions where the two amplified regions were assembled are correct for SPoCK2, indicated by the solid red arrows. The sequences showed a lack of alignment to the SPoCK1 plasmid which confirms that the constitutive immunity gene (*cvi*) and dead spaces were successfully removed.

The next step was to confirm that the SPoCK 2 plasmid was able to produce functional MccV, this was tested through lawn killing assays, SPoCK 2 supernatant was added to lawns of MccV sensitive strains. We expected to see zones of killing with the supernatant from SPoCK 1 (positive control) and SPoCK 2 (Figure 3.2B). We expected no zones of killing with the supernatant from *E. coli* strain JW3910 (negative control). From Figure 3.2B it is observed that there are zones of killing for both SPoCK 1 and SPoCK 2, and no zones for the negative control. A range of volumes of supernatant were tested, and we observed zones of killing from 7 μL for SPoCK 2. The zones of killing increase as the volume of supernatant from SPoCK 2 increases, until 13 μL. The zones of killing do not increase in size with increasing volume after this point. Although it appears there are zones of killing below 7 μL, these zones were not clear, and following the principles of determining a minimum inhibitory concentration (MIC) [153], only clear zones with no cloudiness to indicate bacterial growth were counted as zones of killing.

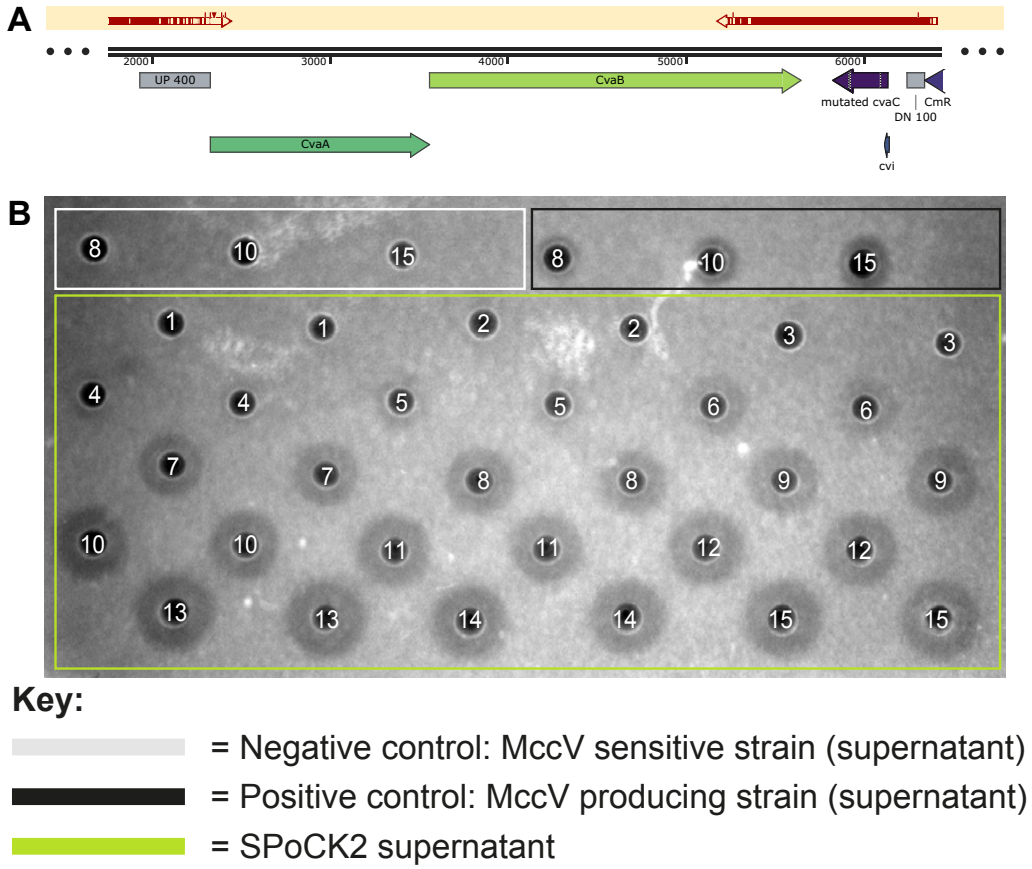

Figure 3.2: Successful creation of the SPoCK 2 plasmid that can kill MccV susceptible strains

A) Sanger sequencing alignments visualised on SnapGene. For the SPoCK 2 alignment the filled red arrows indicate bases that align. The two regions sent for sequencing were the 'junctions' created through joining the two sections. B) Image of the lawn killing assay. Lawn was made with a MccV sensitive strain JW3910 (*E. coli*). Supernatant from the incubation of JW3910 (MccV sensitive strain), SPoCK1 and SPoCK2 were pipetted into the wells. The plate was incubated overnight at 37°C and imaged the next morning. White bar is the supernatant from the sensitive strain added to the wells (negative control), the black bar is the supernatant from SPoCK1 added to the wells (positive control). The green bar is the supernatant from SPoCK2 added to the wells with each volume in duplicate. Numbers on wells are the volumes of supernatant pipetted into that well. Controls are one replicate.

3.2.2 Establishing the killing efficacy of SPoCK 2

To better understand the efficacy of SPoCK 2 killing of MccV sensitive cells, a modified version of the LIVE/DEAD staining assay was used. With this technique cells were only stained with propidium iodide (PI), only the dead cells in the cultures were stained red. SPoCK 2 contains the green fluorescent protein (GFP), therefore would appear green. Whereas the MccV sensitive strain, would appear grey/black as it has no intrinsic fluorescence and the SYTO-9 green dye was not used. In the SPoCK 2 dead control, yellow/orange is expected as the cultures would express GFP, green, and be stained in red (Figure 3.3A). Alive SPoCK 2 cells would appear green, as they would only express GFP and not take up PI (Figure 3.3B). This control confirms that SPoCK 2 can be successfully stained when dead. In the SPoCK 2 monoculture there were red cells present, these were expected to be orange/yellow as in the control (Figure 3.3A). As this was a monoculture all cells present must be SPoCK 2 therefore, it is believed that in the time gap from staining to imaging the GFP would have entered the supernatant, and therefore the GFP staining of the SPoCK 2 cells is less bright compared to the PI staining, hence the observed red rather than distinct orange of the dead control. In the co-cultures (Figure 3.3C) as expected there are green cells, SPoCK 2, and black cells (MccV sensitive strain). However, the red cells in this culture also express GFP, therefore they are dead SPoCK 2 cells and not dead MccV sensitive cells. It was hoped that this assay would shine some light on the efficacy of SPoCK 2 killing with MccV, however this has not been possible due to the lack of killing observed with the staining.

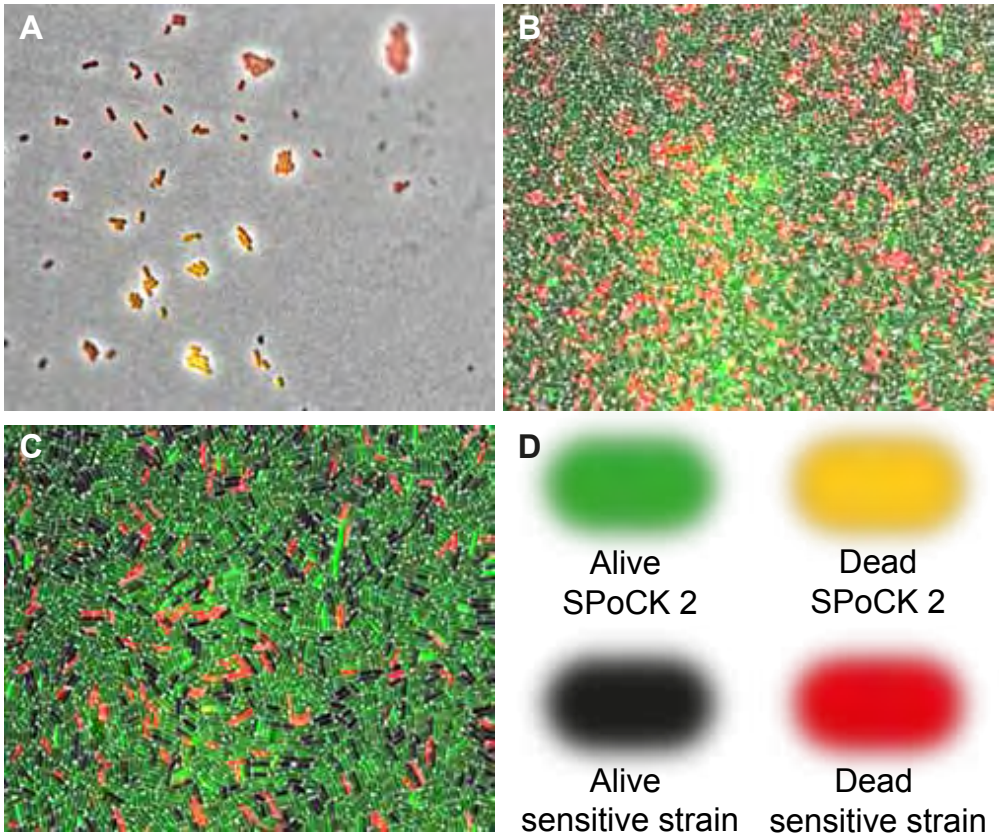

Figure 3.3: SPoCK 2 is successfully imaged, expressing GFP

A) SPoCK 2 dead control, incubated with 70% ethanol before staining. Cells appear orange/yellow because of the GFP expression (green) and the dead cell stain propidium iodide (red). B) SPoCK 2 monoculture, red cells are SPoCK 2. All cells are expressing GFP (green). C) SPoCK 2 co-cultured with the MccV sensitive strain. Black cells are the MccV sensitive strain not expressing GFP. Red cells are the dead SPoCK 2 cells as they also express GFP. D) Key denoting the fluorescent colours we expected to see from this assay for each cell population and cell status (dead or alive). Images are 100x composite images of cells, in phase contrast, green and red channels, taken on Olympus Widefield.

3.2.3 SPoCK 2 successfully responds to repressors

Moving on from determining the efficacy of SPoCK 2 killing, as we know it kills, the next step was to determine whether the SPoCK 2 system could successfully respond to the repressor, the quorum sensing molecule, Acyl homoserine lactone (AHL). In this circuit, the presence of AHL switches off production of *cvaC* (bacteriocin) and*cvi* (immunity). Shown in Figure 3.4A, AHL induces the production of the Tet repressor (TetR), which represses the pTet promoter. Using the reporter protein GFP for *cvaC* expression, the expected observation was a decrease in fluorescence of GFP, in both SPoCK systems as we increased the concentration of AHL. There was not expected to be any change in the control strains (lacking SPoCK system) (Figure 3.4B). The SPoCK systems behaved as expected, with an increasing AHL concentration there was a decrease in GFP fluorescence, as expected there was no change in the control strain. The SPoCK 2 strain behaved as was expected, with decreasing GFP expression in the presence of increasing AHL concentrations, confirming that the SPoCK 2 system responds to the repressor, AHL. The pattern observed for the SPoCK 2 strain was observed in the positive control, SPoCK 1. Repression of *cvaC* in SPoCK 1 has already been characterised and GFP expression confirmed a good marker for *cvaC* expression. This has not yet been done for SPoCK 2.

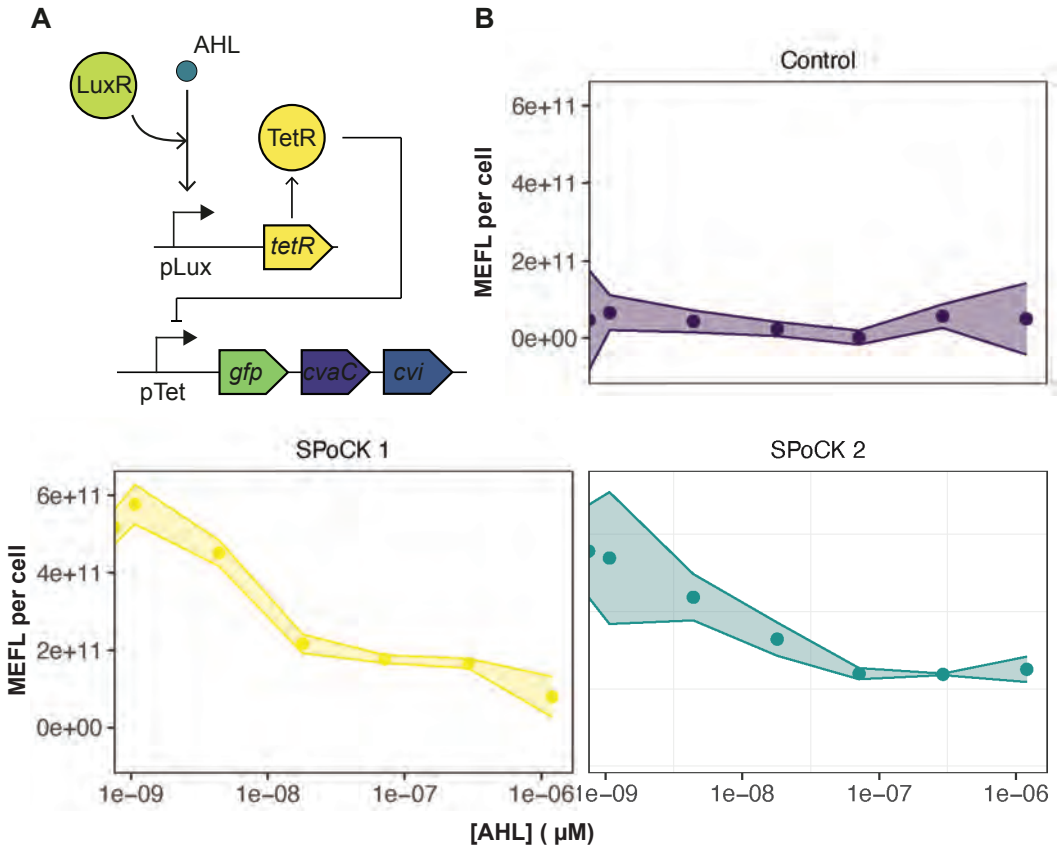

Figure 3.4: *cvaC* (bacteriocin) gene expression is inhibited in the presence of the repressor, AHL, in the SPoCK 2 system.

A) diagrammatic representation of the mechanism of AHL repression on bacteriocin (cvaC) and immunity (*cvi*) gene expression. In the presence of AHL, TetR is expressed. TetR represses the pTet promoter controlling*cvaC* and*cvi* expression. B) Graph shows the molecules of equivalent fluorescence (MEFL) with increasing AHL concentrations at steady state. GFP is a marker of bacteriocin production. The control strain (black), JW3910, contains no plasmids that can respond to AHL. SPoCK1 (blue) acts as a positive control, already confirmed that AHL inhibits*cvaC* expression. SPoCK2 is shown in green. AHL concentration increases left to right. The graph is a snapshot of one time point, approximately steady state (4 hours). The points are the median of triplicate data, and the shaded ribbons are the standard error of the median.

3.2.4 GFP is a good marker of MccV production in SPoCK 2

Whilst, in the SPoCK 1 system it is confirmed that GFP is a good marker for *cvaC* expression and ultimately MccV prodcution, this had not yet been tested in the SPoCK 2 system. Therefore, the next steps were to determine whether GFP was a reliable reporter for MccV production in the SPoCK 2 system. SPoCK 2 was cultured in AHL and the supernatant was pipetted onto a lawn of a MccV sensitive strain (Figure 3.5). In the presence of high AHL concentrations, no killing is expected on the MccV-sensitive lawn. Conversely, at low or absent AHL levels, zones of killing should appear on the MccV-sensitive lawn. Equally, no zone of killing is expected from the negative control, a MccV sensitive strain, whereas, zones of killing are expected for the MccV producing strain, SPoCK 1 the positive control (Figure 3.5). In the presence of no AHL (0 μM) zones of killing were observed (Figure 3.5), denoted by the dark ring around the well, as seen in for the positive control. In contrast, in the presence of higher AHL concentrations (10 μM) no zones of killing were observed. There was a clear AHL concentration dependent size of killing zone. As the AHL concentration increased, the size of the killing decreased. Overall, this AHL concentration dependent killing zone effect confirms the results presented previously (Figure 3.5B), that GFP is a good reporter for the expression and production of the MccV bacteriocin.

3.2.5 *cvi* is successfully repressed in SPoCK 2

Once it had been confirmed that the expression of the bacteriocin MccV was being properly repressed in the presence of AHL, the next step was to determine whether the production of immunity, Cvi, was also responding to AHL. A colony-drop assay (see Methods 2.3.5) was used to determine whether the SPoCK 2 cells were susceptible to MccV killing after AHL repression. If the production of imunity was being successfully repressed, the SPoCK 2 cells cultured in AHL would be susceptible to killing by MccV. It was expected that SPoCK 2 cells grown in high concentrations of AHL would be killed by the MccV producing strain next to them as their immunity would be switched off. Whereas, it was expected that the SPoCK 2 cells grown

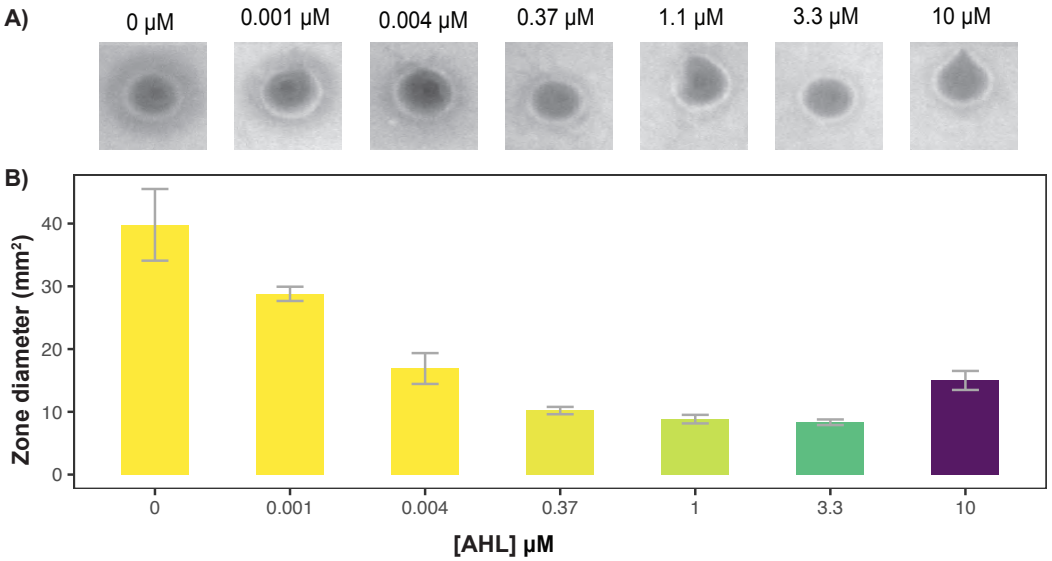

Figure 3.5: GFP is a good marker for MccV production
The strains were grown in different AHL concentrations, and the supernatant pipetted into the wells. A) The zones of killing observed when the SPoCK 2 strain was cultured in different AHL concentrations. B) The mean diameter (mm^2) of the zone of killing is represented by bars, the standard error of the mean is represented as error bars. Increasing AHL concentrations result in smaller or no zones of killing of the MccV sensitive strain. The AHL concentration increases from yellow, 0 μM, to purple, 10 μM (left to right).

in no AHL or low concentrations would not be killed as their immunity would still be produced. Additionally, it was expected that the two SPoCK 2 strains next to each other cultured in 10 μM AHL would display evidence of self killing. The controls worked as expected, with the MccV sensitive strain being killed by the MccV producing strain this is observed by a crescent shaped colony of MccV sensitive strain whereby the cells closest to the MccV producing colony had died (Figure 3.6). As this MccV sesitive strain contains no circuit to produce MccV, it does not respond to AHL, and this is observed in the middle panel (Figure 3.6). The third panel contains, SPoCK 2 and a MccV producing strain. There was no evidence of SPoCK 2 killing in the 10 μM AHL group. Furthermore, there was no evidence of SPoCK 2 'self-killing' in the presence of AHL. This suggests that the immunity is not being switched off as the circuit design intended.

In order to identify whether the immunity at the transcription level was being repressed in the SPoCK 2 system, quantitative PCR (qPCR) analysis was conducted.

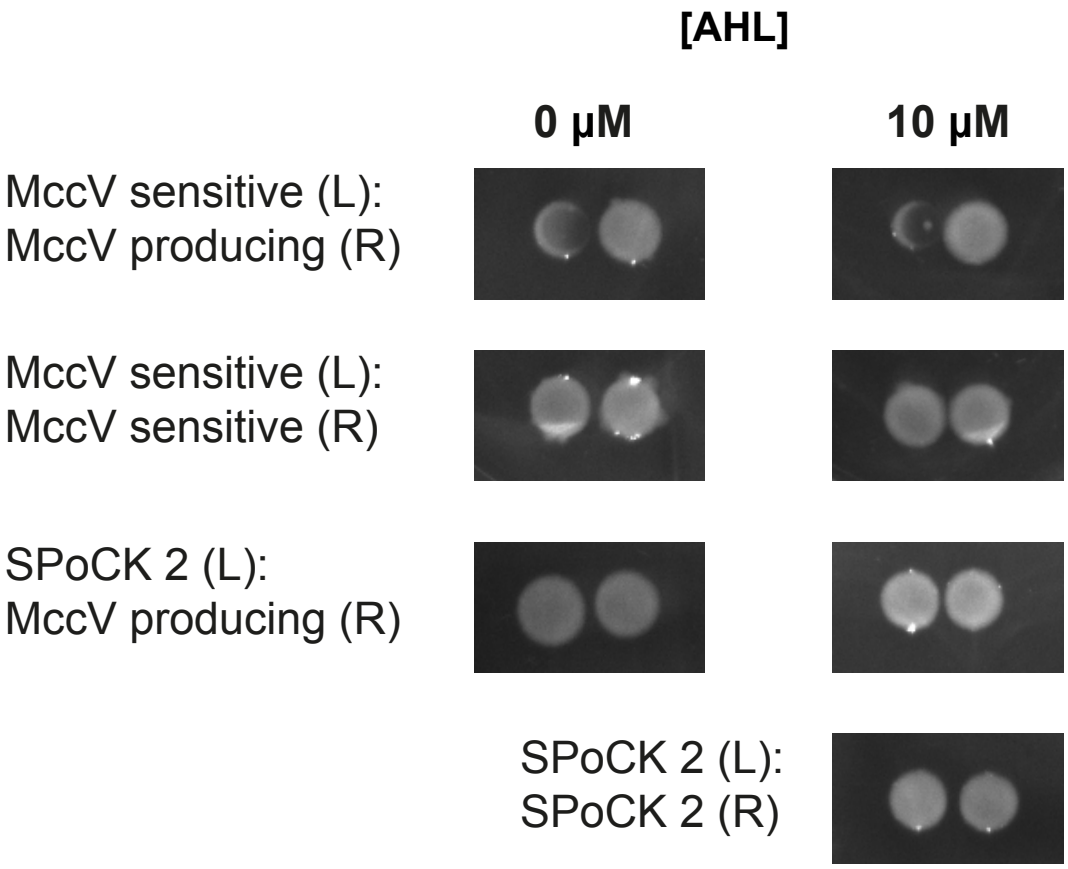

Figure 3.6: No evidence of *cvi* inhibition in the presence of AHL
Strains were grown in 10 μM AHL and 0μM AHL. Then 1 μL colonies were pipetted next to each other. The positive control (top panel) shows the MccV sensitive strain being killed by the MccV producing strain. Negative control is two colonies of the MccV sensitive strain next to each other (second panel). At 10 μM an additional control was added, two SPoCK2 colonies next to each other (bottom panel).

This is a direct measurement of gene expression and could identify whether the genetic circuit was responding to AHL. If SPoCK 2 was behaving as expected then, in the presence of AHL, there should be a reduction in in the expression of the *cvi* and*cvaC* genes for immunity and bacteriocin production respectively. A diagrammatic representation of what happens at the genetic level upon AHL addition is shown in Figure 3.7A. The fold changes represent the difference in gene expression when compared to the no AHL group. The fold changes for both *cvi* (yellow) and *cvaC* (blue) are negative for all concentrations of AHL, which meant in the presence of AHL there was reduced expression of both *cvi* and *cvaC* as expected (Figure 3.7B). There was not much difference observed in the fold changes for 0.01 μM and

0.3 μM AHL (Figure 3.7B) and this trend was the same for both *cvi* (yellow) and *cvaC* (blue). Whereas, for 10 μM AHL fold changes approximately 10x larger are observed when compared to the lower AHL concentrations. The bars represent the average fold changes, the dots represent the individual measurements. The reduction in gene expression between 0.01 μM and 10 μM, and 0.3 μM and 10 μM, are statistically significant. The p-values for concentrations compared to 10 μM for both *cvaC* and *cvi* were statistically significant, the p-value was 0.0011. Whereas, for 0.01 μM and 0.3 μM AHL for the *cvaC* gene, the p-value is p = 0.2424 and for the *cvi* gene, the p-value is p = 0.0898. These are not statistically significant. These results indicated that the SPoCK 2 circuit was successfully responding to the repressor AHL.

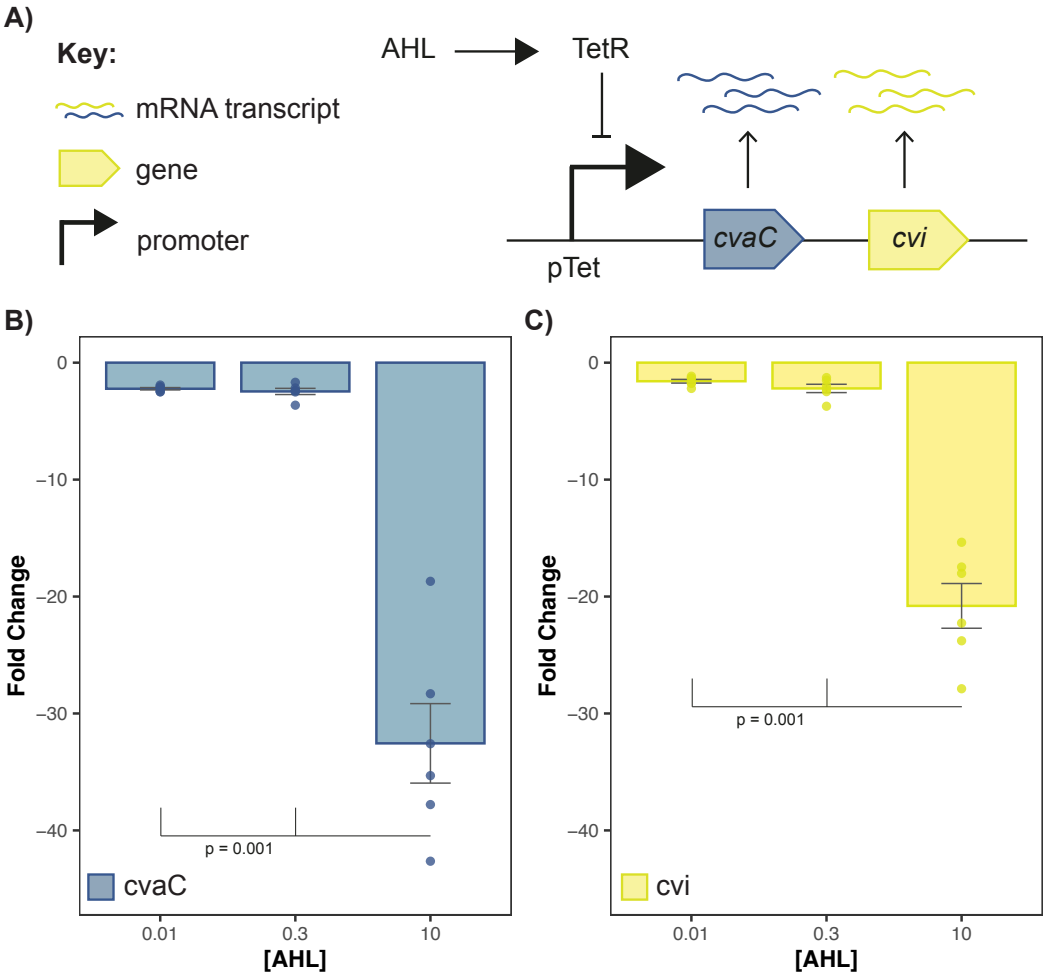

Figure 3.7: AHL represses the gene expression of*cvaC* (bacteriocin) and *cvi* (immunity)

A) Diagrammatic representation of the expected outcome of AHL repression on gene transcription. AHL induces production of TetR, TetR represses the pTet promoter repressing the expression of *cvaC* and *cvi*. B) The qPCR fold change data relative to the control group, 0 μM AHL, and then normalised to the housekeeping gene *rrsA* (16s rRNA). Average fold changes are shown by the bars, the individual measurements (sextuplicate) are shown by darker coloured dots. Fold changes shown are negative compared to the control. Data is shown for mRNA extracted after a 6 hour incubation with the relevant AHL concentration. The p-values are displayed on the graph with the relevant combinations, obtained from a Mann-Whitney test.

3.2.6 SPoCK 2 does not respond to an inducer

Once confirmed that the SPoCK 2 system responded to the repressor, AHL, confirmation was needed as to whether the SPoCK 2 system would respond to the inducer arabinose (Figure 3.8A). This was tested through plate reader bacterial culture experiments whereby arabinose was added to different starting cultures of SPoCK 2 cells. In this set up it is expected that both SPoCK 1 and the control strain (lacking any SPoCK system) would be unaffected by the addition of the arabinose because the control strain cannot respond and SPoCK 1 contains constitutive immunity. On the other hand the SPoCK 2 system, when induced with arabinose would cease production of the bacteriocin and immunity, having no constitutive immunity like SPoCK 1, the SPoCK 2 cells would start to die from residual MccV (Figure 3.8B). The decrease in optical density (OD) measurements for SPoCK 2 would have represented cell death and proved SPoCK 2 has 'self-killing' ability. This effect would have been observed first in the lower density starting cultures, and the highest arabinose concentrations, as there would be more arabinose per bacterial cell in the well. However, there were no growth differences observed between SPoCK 1, the negative control or SPoCK 2 (Figure 3.8C). It appeared as though SPoCK 2 was not responding to arabinose induction as it grew normally. Therefore, from these assays there was no evidence that the SPoCK 2 system was responding as it had been designed.

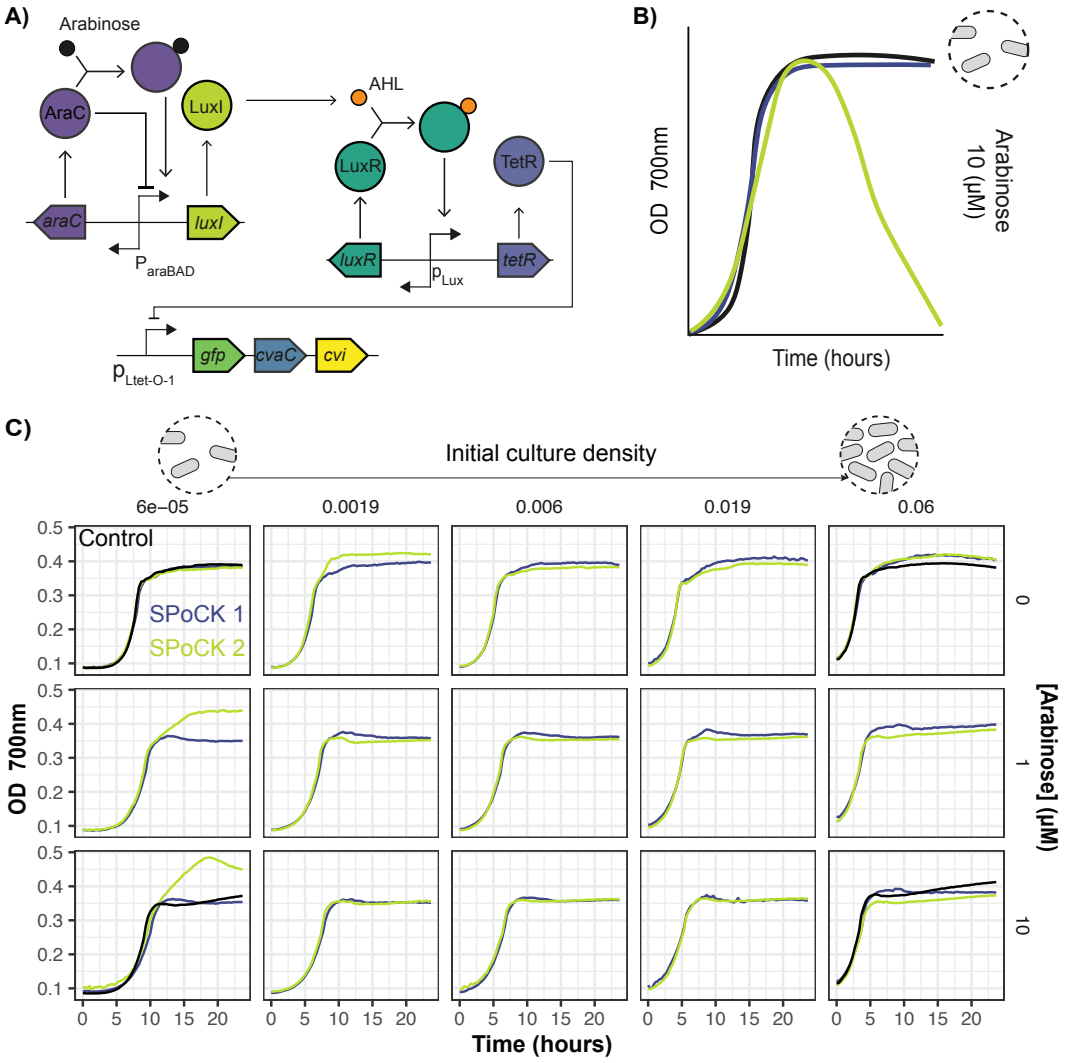

Figure 3.8: SPoCK 2 system does not respond to the inducer, arabinose

A) Diagrammatic representation of the SPoCK 2 system. Addition of arabinose would initiate production of AHL. AHL would switch off production of*cvaC* (bacteriocin) and*cvi* (immunity) gene expression via production of TetR. B) Diagram of the expected results. Expected to see a decline in growth of SPoCK 2 earliest in the highest arabinose concentration and lowest initial cell density. No growth effects on SPoCK 1 or the control. C) Arabinose has no effect on SPoCK 2. The initial cell culture densities, increase panels left to right. The rows show the different arabinose concentrations, with increasing arabinose concentration down the rows. Optical density as a measure of cell growth is on the Y axis, with time over a 24 hour period on the X axis. Key shown on diagram. The difference between the lowest and highest cell densities is 1000-fold.

3.2.7 Engineering immunity degradation

As the qPCR results confirmed that the SPoCK 2 system does respond to AHL induction by switching off the production of immunity, it was hypothesised that potentially the reason 'self-killing' was not observed was because the immunity protein itself was still present. In *E. coli* bulk proteins can have half lives as long as 70 hours, even proteins considered 'abnormal' have half lives of up to 1 hour [154, 155]. Therefore, it is not unreasonable to assume that a protein, such as Cvi, that offers immunity to a bacteriocin would have an extended half life. In order to obtain that 'self-killing' functionality that promises to create a more robust microbial population control system, the Cvi protein needs to be controlled at the protein level. The most efficient way to remove the Cvi protein faster was to add a protein degradation tag like the SsrA C-terminal tags that are a part of the hosts own protein degradation systems [149]. Currently, there are several mutants of the SsrA tag available each with different rates of protein degradation. To mitigate against selection pressures of the host cell to mutate, the weakest degradation tag was selected to try first. Additionally, to further reduce the risk of burden on cells, all circuits were transformed into a MccV non-susceptible cell, the CirA K/O strain (JW2142). The first step was to add the chosen degradation tag (SsrA mutant), to the *cvi* gene under the inducible promoters control. Through PCR two regions from the SPoCK 1 bacteriocin expression plasmid were amplified and together with a g-block (containing the SsrA tag) they were assembled into the SPoCK 2.1 plasmid (8221 bp) (Appendix C). Figure 3.9A shows the correct sequencing alignments for the junctions used to make this plasmid.

Further characterisation confirmed that the SPoCK 2.1 system, with both the bacteriocin producing plasmid and the quorum sensing plasmid, could still produce active MccV (Figure 3.9B). The SPoCK 2.1 system was transformed into three *E. coli* strains, two MccV-susceptible (JW3910, BW25113) and one MccV non-susceptible strain (JW2142). As expected, we see killing of the MccV-susceptible cells and no killing of the MccV non-susceptible cells. MccV with no bacterial cells was used as the positive control for MccV killing and the MccV susceptible lawn

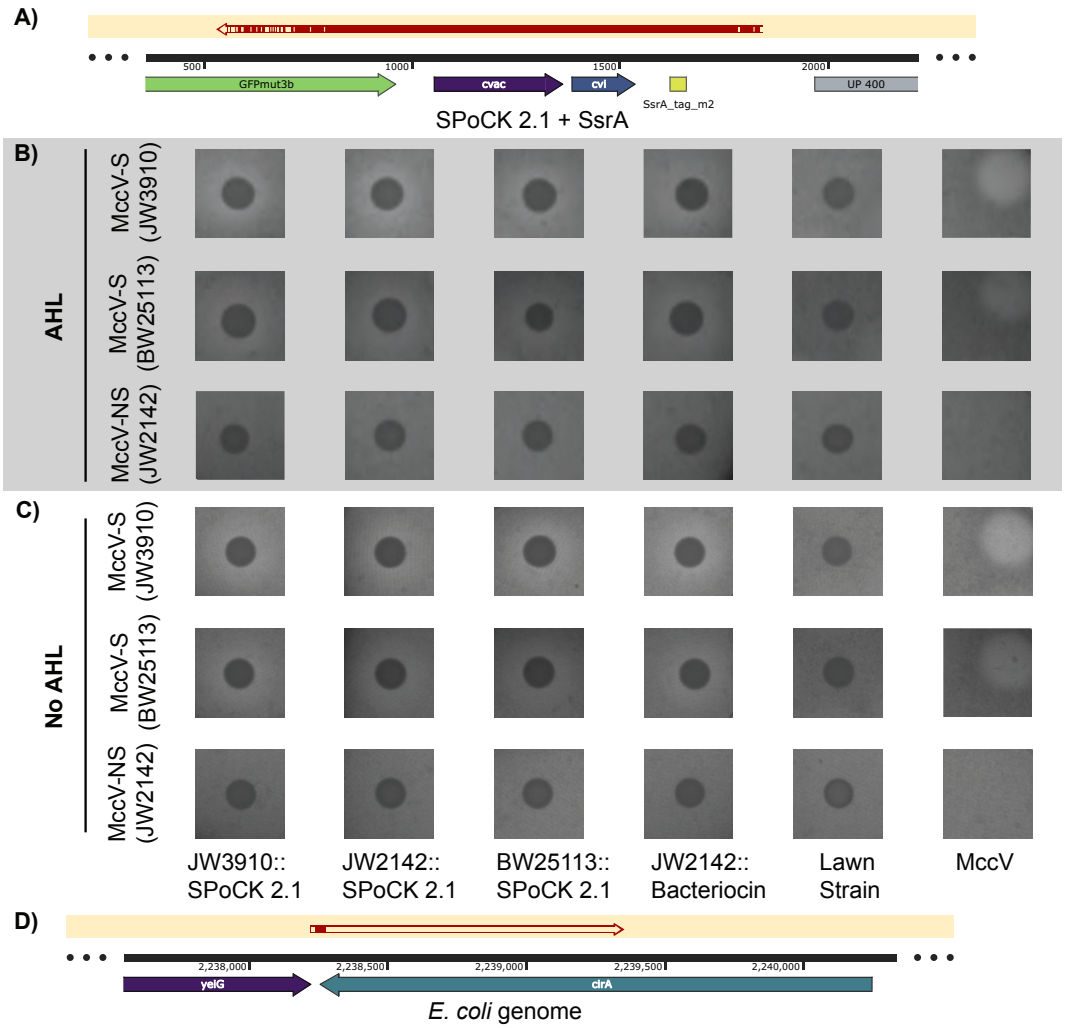

Figure 3.9: Construction of the SPoCK 2.1 system and successful killing
A) The SPoCK 2.1 plasmid map with the DNA alignment of the sanger sequencing results. The SsrA tag (yellow) is successfully incorporated into the plasmid. B) The lawns of MccV-susceptible (MccV-S) and MccV non-susceptible (MccV-NS) strains of *E. coli* in the presence of AHL. C) MccV-S and MccV-NS in the absence of AHL. D) alignment of the genome of SPoCK 2.1, can see that *cirA* has been removed. This means that SPoCK 2.1 is immune to killing, it is inside strain JW3910 (*E. coli*).

bacterial cells were used as a negative control of killing (Figure 3.9B).

The next steps were to check if the SPoCK 2.1 system was responsive to AHL, before investigating if this system became MccV-susceptible. To test this, bacterial lawns were constructed to observe the expected effects of the quorum sensing molecule, AHL, on the SPoCK 2.1 system. In this setup, if SPoCK 2.1 is responding to AHL there should be no zones of killing because the addition of AHL would have switched off the production of MccV. Thus rendering the SPoCK 2.1 system incapable of killing MccV-susceptible strains. However, the SPoCK 2.1 system displayed zones of killing in the presence of AHL (Figure 3.9B). This suggested that it was not responding to the repressor AHL. Further investigation revealed that the genomic copy of the CirA receptor, the receptor that MccV requires to enter susceptible cells and kill them, had mutated (Figure 3.9D). This meant that the SPoCK 2.1 system had become resistant to MccV and would never have been able to display the 'self-killing' functionality being sought after.

3.2.8 SPoCK 2.1 with degradation tags RepA, MazE was not built

The explanation that perhaps the SsrA tag was too powerful at degrading the Cvi protein, appeared plausible to explain the genomic mutation of the CirA receptor in order for the bacterial cells to escape MccV killing in the absence of an immunity protein upon AHL repression. As the weakest SsrA tag was attempted first and resulted in mutational escape, other potential protein degradation tags were investigated. Both the RepA and MazE tags are recorded as weaker than the wild type SsrA tag [151]. However, in this work it had proved impossible to assemble these constructs (Figure 3.10).

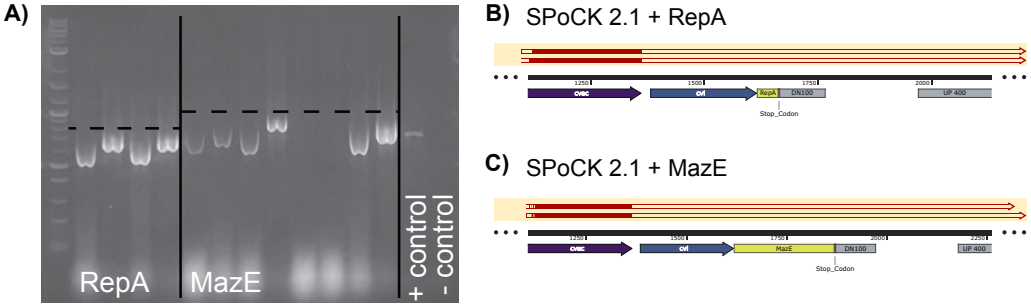

Figure 3.10: SPoCK 2.1 with RepA and MazE were unsuccessful
A) Colony PCR products for the SPoCK 2.1 systmem with both RepA (818 bp) and MazE (1022 bp) degradation tags added, expected product sizes are dashed lines. 0.8% agarose gel ran for 45 mins at 70V. Sanger sequencing alignments of the B) RepA and C) MazE constructs.

3.2.9 SPoCK 1.1

It proved challenging to construct some of the SPoCK plasmids, and through the process of creating the SPoCK 2.1 plasmid, the SPoCK 1.1 plasmid was made. This system still contains the constitutive immunity (Figure 3.1) but the inducible immunity, Cvi, now has an SsrA degradation tag. However, due to the presence of constitutive immunity, this system should behave exactly the same as the original SPoCK system. This plasmid was unable to be tested further due to the failed correct construction of the plasmid (Figure 3.11A). The region that contains the trans-

port machinery, CvA and CvaB [156], required for the secretion of MccV from the host cell is missing (Figure 3.11A). Alongside evidence that the SPoCK 1.1 plasmid was not functional because there were no zones of killing on a MccV susceptible lawn to suggest the presence of the bacteriocin MccV (Figure 3.11B).

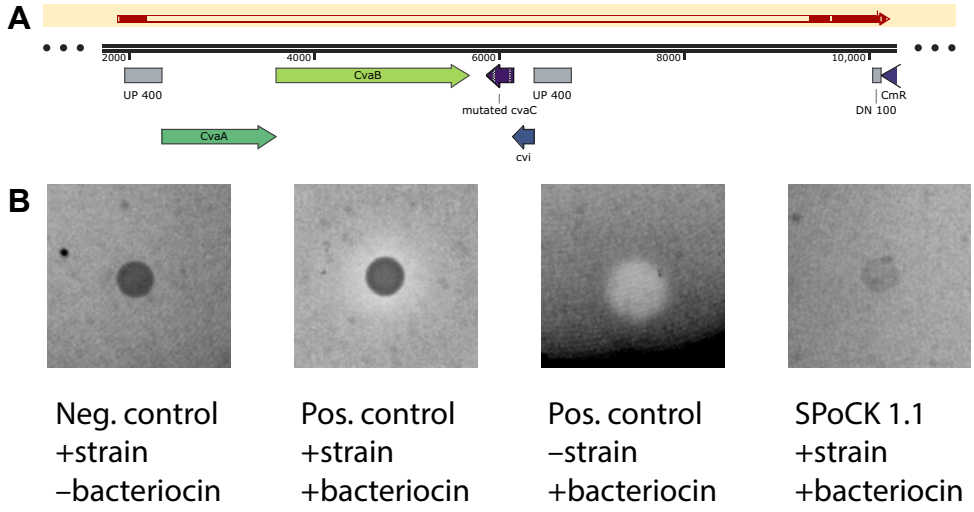

Figure 3.11: Construction of the SPoCK 1.1 bacteriocin killing plasmid
A) The sanger sequencing alignments confirm the unsuccessful construction of the SPoCK 1.1 plasmid. Missing sequences for export machinery required for the export of MccV. B) Lawns of MccV susceptible *E. coli*. The positive control strain was the SPoCK 1 system.

3.2.10 An alternative approach to modulate bacteriocin susceptibility

As it had became clear controlling the immunity of the SPoCK systems through the Cvi protein may be unattainable, an alternative method of controlling the immunity of the system was employed. Inspired by the genomic mutation of the CirA receptor in order for SPoCK 2.1 to escape MccV killing, the idea to capitalise on this feature of MccV having only one receptor to kill susceptible cells was formed. In this case rather than turning off immunity, the system would switch on susceptibility. The immunity gene was removed from the AHL repressed circuit, creating the SPoCK 3 bacteriocin producing plasmid (Figure 3.12A), and the *cirA* gene was added to the quorum sensing plasmid under the control of AHL, although this was not successfully built (Figure 3.12B). Together the two plasmids made the SPoCK 3 system. In the presence of AHL, the bacteriocin production would be switched off, and production of the CirA receptor would be switched on, leading to the host cell becoming susceptible to secreted MccV in the culture medium. The SPoCK 3 bacteriocin producing plasmid was successfully able to produce active MccV, killing MccV-susceptible cells in a bacterial lawn (Figure 3.12B). The quorum sensing plasmid containing *cirA* was not successfully built therefore, ultimately the SPoCK 3 system was unable to be built.

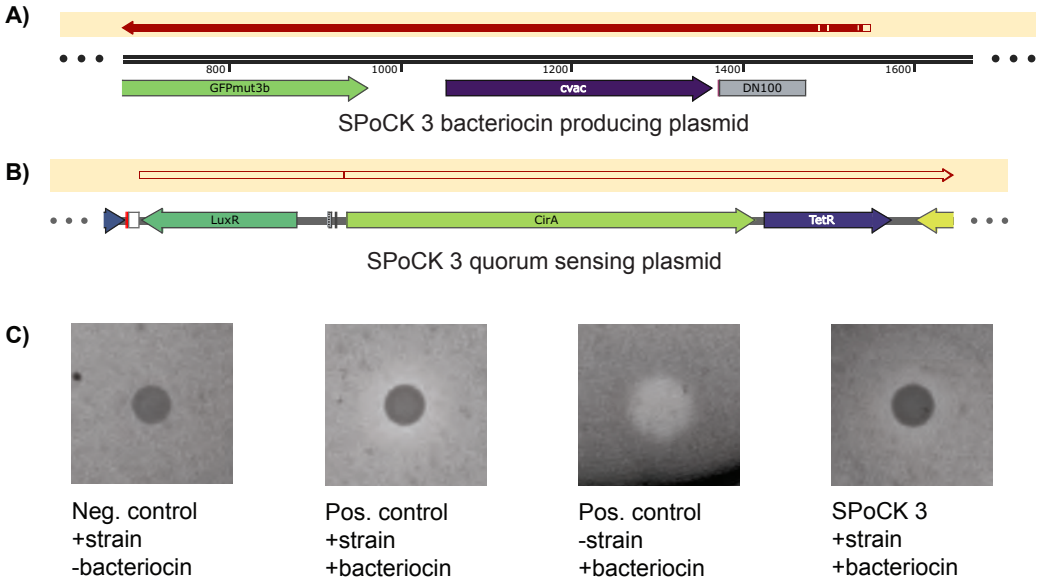

Figure 3.12: SPoCK 3 bacteriocin producing plasmid

A) The sanger sequencing alignments of the SPoCK 3 bacteriocin producing plasmid. This plasmid has all immunity removed and was transformed into the *E. coli* JW2142 K/O. B) The sanger sequencing alignments of the inserted *cirA* gene into the quorum sensing plasmid. There was no alignment. C) The bacterial lawn of *E. coli* BW25113, sensitive to MccV. The colonies are the negative control *E. coli* JW3910, the positive control SPoCK 1 and SPoCK 3 *E. coli* JW2142 containing the SPoCK 3 bacteriocin producing plasmid. The zones of inhibition, denote MccV activity. Image taken on IPhone 13, edited in Adobe Illustrator, converted to greyscale and colour balance set to 10% white.

3.3 Discussion

The SPoCK systems in this work are summarised in Table 3.1. The SPoCK 2 system was successfully constructed and shown to be repressed by AHL, as confirmed by qPCR analysis (Figure 3.7). This demonstrated effective transcriptional regulation of the *cvi* and *cvaC* genes, validating the foundational design of this SPoCK 2 system. Furthermore, efforts were made to address the hypothesised issue of prolonged Cvi protein activity due to its assumed long half-life. This included the SsrA degradation tag successfully incorporated into the Cvi protein, creating the newer SPoCK 2.1 system. However, while these advancements represented important steps in this work there were significant challenges that prevented the SPoCK 2 and then later, SPoCK 2.1 and SPoCK3 systems from functioning as intended.

Table 3.1: Comparison of the SPoCK systems in this work.

SPoCK System	Status	Details
SPoCK 1	Complete	Original system that was characterised [87]
SPoCK 1.1	Failed	Could not build the bacteriocin (MccV) producing plasmid
SPoCK 2	Built	There was no evidence of the desired self killing function
SPoCK 2.1	Built	The genomic copy of *cirA* was mutated rendering the cells immune to the desired self killing
SPoCK 3	Failed	Could not build the quorum sensing plasmid containing the CirA receptor, which was required for controlling the immunity within the system

One major issue was the lack of self-killing functionality in the SPoCK 2 system. Despite successful transcriptional repression of the *cvi* and *cvaC* genes, the Cvi protein's persistence within the cell appeared to continue conferring immunity to MccV, thus preventing the expected 'self-killing' response. In SPoCK 2.1, the addition of the SsrA degradation tag seemed to resolve this persistence issue, but it is believed that the tag potentially degraded the Cvi protein too effectively, even in the absence of AHL repression. This resulted in a loss of immunity, particularly evident in engineered cells with mutated genomic *cirA* gene or lacking functional

Table 3.2: Size comparison of degradation tags used compared to the original protein, Cvi.

Name	Amino Acid length	% of Cvi protein
Cvi	78	
RepA	15	19
MazE	83	106
SsrA	13	16.7

MccV altogether.

An additional complication arose from the small size of the Cvi protein (78 amino acids). Structural predictions by Alphafold suggest that the protein has 2 alpha helical domains that fold over to be in close proximity, as well as 2 transmembrane domains [157]. It is likely the addition of a degradation tag could interfere with any potential membrane integration and binding (Table 3.2). The addition of an 11-amino-acid SsrA degradation tag may have disrupted proper folding or membrane integration, rendering the protein non-functional. This structural interference likely explains why the system failed to retain immunity while simultaneously escaping through mutation. Attempts to incorporate alternative degradation tags, such as MazE and RepA, were unsuccessful due to failures during Gibson DNA assembly, as indicated by sequencing data (Figure 3.10). These issues underscore the technical challenges faced in constructing functional plasmid systems that involve bacteriocins and immunity that effect the host cell.

The limitations of the live/dead assay further complicated the evaluation of system functionality. The inability to use the SYTO-9 dye (green) otherwise it would be impossible to differentiate the cell populations apart due to the presence of GFP (green) in the SPoCK 2 system, could have altered how the assay functioned as SYTO-9 and PI are optimised together. Equally perhaps 6 hours was not enough time for the MccV sensitive strains to be incubated with the SPoCK 2 strains. Up until this point all killing assays had been on solid media, potentially the way MccV targets cells would differ in liquid media. Next steps to observe killing by the SPoCK strains in liquid co-cultures could include flow cytometry time lapse studies to try and capture the point at which MccV begins to kill sensitive strains as

it was likely missed with the microscopy conducted here as a single time point. Extending the incubation times or adapting to the experiment to flow cytometry might improve the reliability of these experiments.

This work contributes to the further development of microbial control systems, building on the design and creation of the original SPoCK 1 system [87]. The challenges encountered in this study are not unique, as designing systems capable of 'self-killing' in a living host is widely recognised as difficult. Currently, achieving effective 'self-killing' functionality appears to require multiple layers of regulation to prevent mutational escape, ensuring that the only escape mechanism for the engineered strain is cell death [119, 120, 122]. Most systems employing 'self-killing' functionality use it as a form of biocontainment rather than as a core component of their purpose. Such systems often rely on complex regulatory mechanisms, including genomic deletions of SOS response genes, multi-input circuits, and modified CRISPR-Cas9 systems [158]. Systems more similar to SPoCK, such as toxin-antitoxin systems [159], rely on a single regulatory layer where daughter cells lacking the plasmid are killed by toxins secreted by the population, while those retaining the plasmid survive [102]. However, the purpose of such systems is typically to prevent plasmid loss, whereas the goal of SPoCK is to robustly regulate its own population. The upgraded SPoCK systems were kept under antibiotic pressures, so their ability to conduct plasmid segregational killing has not been characterised in this work and is something that would need to be assessed if SPoCK were to be used an eLBP.

Future work should focus on improving the assembly and incorporation of alternative degradation tags, such as exploring variants of the SsrA tag with reduced degradation activity [152]. Investigating the structural effects of degradation tags on the Cvi protein through *in vitro* folding studies or computational modelling will provide valuable insights into the observed loss of function. Additionally, optimising experimental approaches to evaluate system functionality, such as using flow cytometry with alternative dyes, may offer more reliable and informative assessments. Finally, further exploration of the dynamics between induction, repression,

and degradation within the system is necessary to refine the balance between immunity and self-killing.

Chapter 4

Screening bacteriocins targeting the cancer microbiome

‘None of us want to be in calm waters all our lives.’

— Jane Austen, Persuasion

Contents

4.1 Introduction

4.1.1 Onocogenic pathogens

The gut microbiome, composed of bacteria, fungi, viruses, and phages, contains more microbes than human cells and is often referred to as a 'hidden metabolic organ' [160, 161]. It plays a crucial role in maintaining health and combating pathogenic infections by influencing neural, endocrine, humoral, immunological, and metabolic pathways [162]. However, dysbiosis of the microbiome has been implicated in various human diseases, including type II diabetes and inflammatory bowel disease [163]. Unsurprisingly, members of the gut microbiome have also been associated with human cancers, particularly colorectal cancer [164].

Several microbes have been identified as significant contributors to the progression and prognosis of colorectal cancer. This work focuses on two key oncogenic pathogens: *Fusobacterium nucleatum* (*F. nucleatum*), a known oral pathogen [38], and *Bacteroides fragilis* (*B. fragilis*). Both are markers of poor prognosis in colorectal cancer [165].

These oncogenic pathogens possess several mechanisms that enable them to promote colorectal cancer. Evidence suggests that *F. nucleatum* can be intracellular [166], although whether this occurs during early or late carcinogenesis remains unclear. This intracellular nature is believed to contribute to genome instability and mutation, as *F. nucleatum* has been linked to increased microsatellite instability (short DNA repeat variations commonly observed in colorectal cancer). [167, 168]. Additionally, *F. nucleatum* disrupts epithelial tight junctions [44] , promoting epithelial-mesenchymal transition (EMT), a key step in cancer metastasis.

Furthermore, *F. nucleatum* has been linked to increased production of pro-inflammatory cytokines [169] and microRNA-21, both of which promote cancer cell growth and invasion [170]. *F. nucleatum* also secretes vesicles that induce pro-inflammatory pathways and oxidative stress, leading to intestinal epithelial cell death [45]. Additionally, it produces formate, a metabolite associated with chemoresistance in lung cancer patients [46]. Formate production by *F. nucleatum* is also linked to increased glutamine dependence in highly metastatic cancers

and the initiation of a cancer stem cell-like state, which promotes tumour growth, resistance to treatment, and tumour initiation [171].

The enterotoxigenic *B. fragilis* (EBf) is known for producing fragilysin, a toxin that forms biofilms [42], facilitating the growth of other pathogens. However, even non-enterotoxigenic strains of *B. fragilis* are associated with poor health outcomes. These strains damage epithelial tight junctions, promoting EMT in cancer cells [47]. Additionally, *B. fragilis* induces inflammatory intestinal responses in inflammatory bowel diseases, which are precursors to colorectal cancer [48]. Recent studies have directly linked *B. fragilis* to colorectal cancer [172] and identified its role in inflammatory bowel diseases [42]. No significant differences in clinical outcomes have been observed between enterotoxigenic and non-enterotoxigenic *B. fragilis* strains [173]; therefore, it can be assumed that antimicrobial agents against a non-enterotoxigenic strain of *B. fragilis* will serve as a model for both the enterotoxigenic and non-enterotoxigenic strains. As a result, the non-enterotoxigenic *B. fragilis* will be used in this work.

The interaction between gut bacteria and chemotherapy agents, where gut bacteria interfere with chemotherapy has been well-documented [174]. Notably, *F. nucleatum* has been implicated in promoting chemotherapy resistance [175, 176]. Several gut bacteria can metabolise chemotherapy agents into inactive forms, such as the conversion of gemcitabine into its inactive state, leading to chemotherapeutic resistance. In a colon cancer mouse model, antibiotic treatment eliminated this resistance [177]. Similar findings were observed in humans, except the effect of adding antibiotics was dependent on the chemotherapeutic agent, where antibiotics enhanced the efficacy of oxaliplatin but not irinotecan [178]. Pretreatment with antibiotics targeting anaerobic bacteria improved disease-free survival by 25.5% in some studies [179]. However, concurrent use of antibiotics during chemotherapy has been linked to reduced 3-year disease-free survival rates, suggesting that gut dysbiosis during treatment may increase the risk of cancer recurrence [180].

Based on the promising results from the aforementioned antibiotic trials, it is hypothesised in this work that removing *F. nucleatum* from the colorectal tumour

micro-environment could re-sensitise patients to chemotherapy and improve clinical outcomes. However, despite advances in understanding the role of bacteria in the tumour micro-environment, there is still no method to selectively eliminate onco-pathogens. While antibiotics have demonstrated efficacy in improving patient outcomes, alternative, targeted strategies are needed to selectively remove onco-pathogens like *F. nucleatum* and *B. fragilis* from the tumour micro-environment.

4.2 Results

4.2.1 Optimising the growth of *F. nucleatum* & *B. fragilis*

Both *F. nucleatum* and *B. fragilis* are obligate anaerobes, their growth in the laboratory requires strict anaerobic conditions. The initial challenge was finding ways to culture these anaerobic bacteria inside a plate reader so that optical density (OD) measurements that correspond to bacterial growth could be obtained. This was important to measure any killing of screened bacteriocins in subsequent liquid culture experiments. Two approaches to creating anaerobic conditions were tested; 1) sealing the individual wells of bacterial cell culture with a layer of liquid paraffin oil, 2) sealing the whole plate with a transparent qPCR plate cover (Figure 4.1). In the case of *F. nucleatum* smoother growth curves were obtained when the cultures were grown with a qPCR plate seal (Figure 4.1A). However, noisier growth curves were observed for *B. fragilis* with the qPCR plate cover compared to the paraffin oil seal (Figure 4.1B) and faster growth was observed with the qPCR plate seal in *B. fragilis*. Due to the logistical difficulties with applying liquid paraffin over applying a qPCR plate cover, using a qPCR plate cover to maintain anaerobic conditions for plate reader measurements was adopted for all future experiments.

During these initial growth experiments it was noted that *F. nucleatum* was forming aggregates. *F. nucleatum* is known to often form aggregates and has high auto co-aggregation compared to other species [181]. During these experiments the co-aggregates formed by *F. nucleatum* could be seen by eye, which explained the noisy readings taken with the plate reader. The co-aggregation in *F. nucleatum* utilises the membrane adhesion protein, RadD. There are reports that this can be blocked by lysine, which uses RadD as a receptor, thereby blocking co-aggregation of *F. nucleatum* [182]. Lysine along with arginine [183] was added to the FAB media to see if it helped reduce the co-aggregation of *F. nucleatum*, as well as adding a minimally defined medium as there were reports rich mediums (i.e. FAB) promote aggregation (Figure 4.1C). No differences in growth curves were observed when these amino acids were added to the medium, both isolated and as a pair. This is likely because they are targeting pathways that *F. nucleatum* uses to co-aggregate

with other species, promoting biofilm formation, not targeting the pathways responsible for self-aggregation. No growth of *F. nucleatum* was observed when cultured in minimally defined medium, EZ rich. Despite *F. nucleatum* being considered an obligate anaerobe, it appears that it can be aerotolerant [184]. It is possible that conditions inside the cover of the qPCR plate were not strictly anaerobic and this lead to self-aggregation and biofilm formation in *F. nucleatum*. However, it should be noted that *B. fragilis* is considered an anaerobic indicator strain and this grew without issue under this experimental setup. Regardless, to improve the anaerobic conditions subsequent experiments used autoclavable tape to seal the edges of the qPCR plate cover, this has reduced the impact of aggregation but not removed the effect entirely.

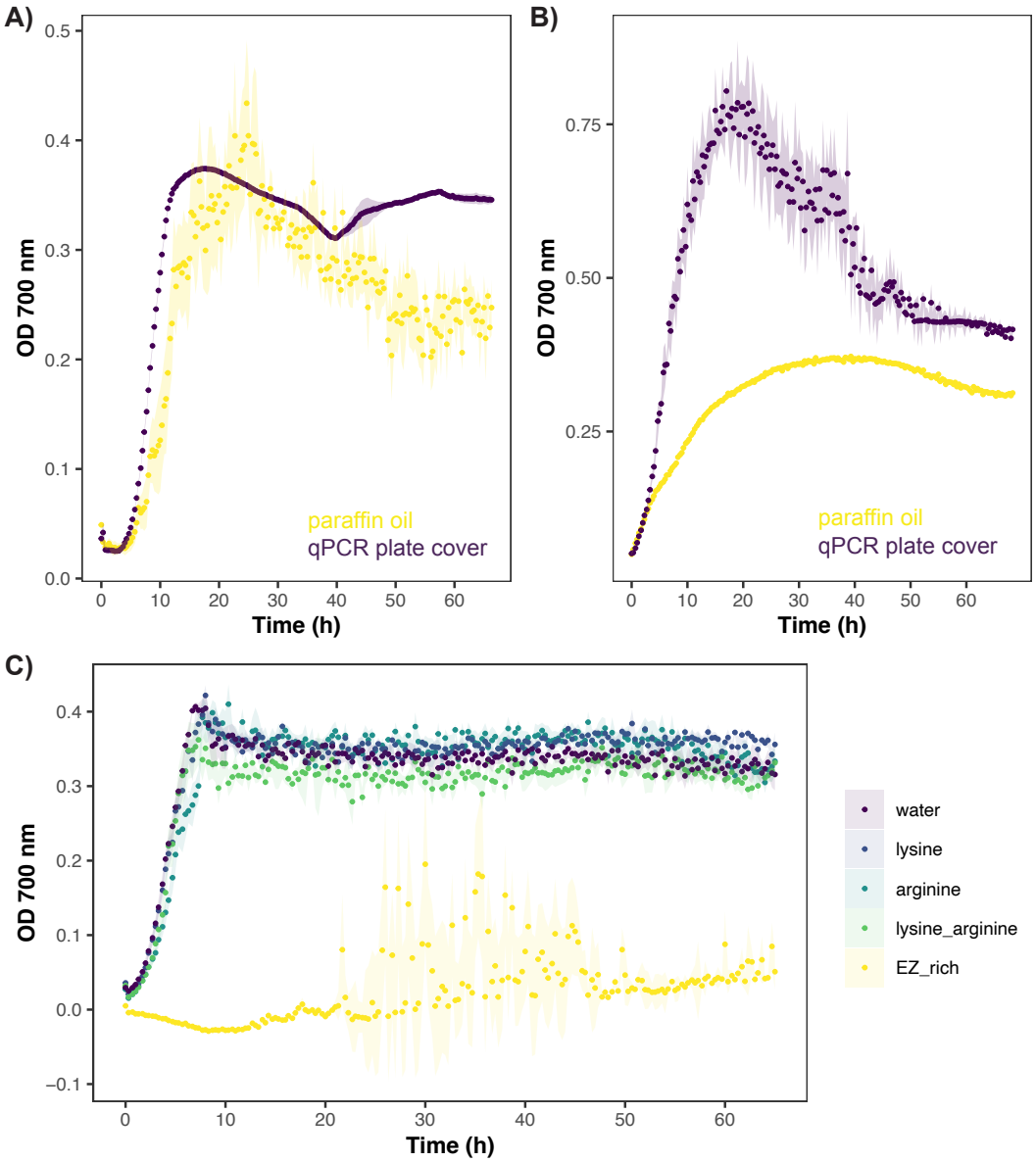

Figure 4.1: Successfully cultivating obligate anaerobes for bacteriocin screening
A) *F. nucleatum* growth with paraffin oil and a qPCR plate cover to create anaerobic conditions. B) *B. fragilis* growth with paraffin oil and qPCR plate cover to create anaerobic conditions. Both of these are in the plate reader. C) the growth of *F. nucleatum* with different supplements added. This was to try and reduce the auto-aggregation of *F. nucleatum* during the experiments. Shaded areas are the standard error of the median and the solid lines are the median of triplicate data points.

4.2.2 Bacteriocins successfully kill *F. nucleatum* & *B. fragilis* in solid media

Currently, there are few identified bacteriocins capable of effectively targeting *F. nucleatum*. A literature search returns limited options and bacteriocin databases such as Bactibase [185] suggest only one possibility: subtilosin. As a result, the initial step in identifying suitable bacteriocins involved screening a wide range of bacteriocins. These synthetic bacteriocins were sourced from the PARAGEN collection [1] provided by our industrial partner, Syngulon. The bacteriocins that formed the initial screen are presented in Table 4.1.

Several bacteriocins successfully killed *F. nucleatum*, as evidenced by the 'halos' or zones of killing (Figure 4.2) observed when the bacteriocins were applied to *F. nucleatum* and *B. fragilis* lawns. Among these, Aureocin A53 (class IId) displayed high efficacy, effectively killing both *F. nucleatum* and *B. fragilis* (Figure 4.2A).

Another promising bacteriocin, Garvicin ML [186], was provided by Dr. Borerro as supernatant collected from its native producer, *Lactococcus garvieae*. The supernatant was tested on blood plates (growth medium agar supplemented with blood) without a bacterial lawn (Figure 4.2C, top panel). While the unpurified supernatant showed no signs of red blood cell lysis, fractions subjected to purification steps displayed evidence of lysis. Specifically, the SF+ fraction, obtained after ammonium sulphate precipitation followed by a cationic exchange column, showed a zone of red blood cell lysis. This was further confirmed by the presence of erythrocyte ghosts. When red blood cells lyse they leave behind the empty protein scaffold of the cell appearing ghost-like on a microscope [187] (Figure 4.2C, bottom panel). Subsequent purification steps, including hydrophobic exchange chromatography, also exhibited red blood cell lysis in fractions such as OE (hydrophobic exchange column eluate) and OF+ (flowthrough from the hydrophobic interaction column). These results suggest that the red blood cell lysis observed on blood lawns is likely due to the presence of ammonium sulphate in the purified Garvicin ML fractions, rather than the bacteriocin itself.

Table 4.1: Table of the bacteriocins screened against the onco-pathogens, *F. nucleatum* and *B. fragilis*. The bacteriocins come from the PARAGEN collection [1]. CSP - chemically synthesised peptides and *in vivo* - peptides produced *in vivo*.

Bacteriocins Tested	**Produced by**	**Synthesised**
Acidocin LF221B	*Lactobacillus gasseri LF221*	CSP
Aureocin A53	*Staphylococcus aureus*	CSP
Bacteriocin L-1077	*Ligilactobacillus salivarius L-1077 (NRRL B-50053)*	CSP
Bactofencin A	*Ligilactobacillus salivarius*	CSP
Blpk	*Streptococcus salivarius*	CSP
Cerein 7B	*Bacillus cereus*	CSP
Ent1071A + B	*Enterococcus faecalis BFE 1071*	CSP
Ent50-52	*Enterococcus faecium (NRRL B-30746)*	CSP
Enterocin 7A	*Enterococcus faecium*	CSP
Enterocin 7B	*Enterococcus faecium*	CSP
Enterocin E760	*Entercococcus spp.*	CSP
Epidermicin Ni01	*Staphylococcus epidermidis 224*	CSP
Garvicin KS-A + B +C	*Lactococcus garvieae KS1546*	CSP
Garvicin ML	*Lactococcus garvieae DCC43*	*in vivo*
Lacticin FA - FX	*Lactobacillus johnsonii VPI 11088*	CSP
Lacticin Q	*Lactococcus lactis*	CSP
Lacticin Z	*Lactococcus lactis QU 14*	CSP
Lacticin Zβ*	modified by Syngulon	CSP
Lactococcin B	*Lactococcus lactis*	CSP
Lactococcin Gα + Gβ	*Lactococcus lactis*	CSP
Lactococcin Qα + Qβ	*Lactococcus lactis QU 4,*	CSP
Plantaricin E + F	*Lactobacillus plantarum*	CSP
Plantaricin NC8α + β	*Lactobacillus plantarum*	CSP
Plantaricin Sα + β	*Lactobacillus plantarum LPCO10*	CSP
sAbp118 α (Salivericin Pα)	*Lactobacillus salivarius*	CSP
sCerein X_A	*Bacillus cereus*	CSP
sEntL50A	*Pedicoccus pentosaceus*	CSP
sEntL50B	*Enterococcus faecium*	CSP
SlvV	*Streptococcus salivarius*	CSP
SlvV*	modified by Syngulon	CSP
SlvW	*Streptococcus salivarius*	CSP
SlvY	*Streptococcus salivarius*	CSP
SlvZ	*Streptococcus salivarius*	CSP

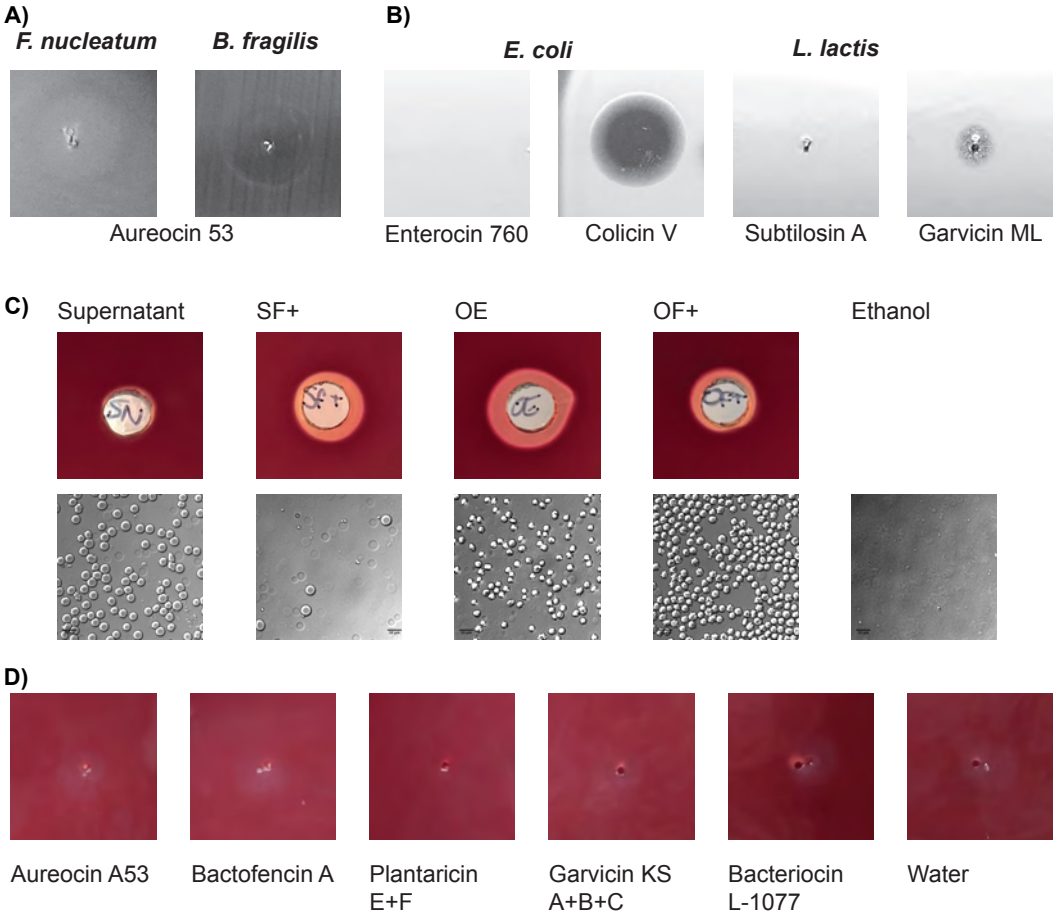

Figure 4.2: Bacteriocins successfully kill *F. nucleatum* and *B. fragilis* in solid media A) Some examples of a Bacteriocin that successfully killed *F. nucleatum* and *B. fragilis*. The shaded circles are the 'halos' which signify the killing zones. B) The controls of the presence and absence of killing zones, they show killing and no killing on sensitive strains. C) The top panel shows the discolouration on the horse blood plates with the addition of Garvicin ML supernatant and subsequent protein purified fractions. There are no bacterial lawns on these plates. The bottom panel shows the microscope images of the same fractions incubated with the same horse blood. The last image is lysed red blood cells with 70% ethanol, here you can see the 'erythrocyte ghosts'. These are red blood cells that have been lysed and all of their cellular contents have leaked out [187]. The microscope images were taken at 40X on olympus Widefield, scale bars are 10 μm. D) FAA plate + 5% horse blood with synthetic bacteriocins applied. There is no sign of lysed blood cells from the addition of the synthetic bacteriocins to the blood plates. The bacteriocins came from the PARAGEN collection [1]. Except the Garvicin ML fractions that were gifted by Dr. Juan Borrero del Pino.

It is important that the bacteriocins used do not harm human cells if they are to be used for therapeutic applications. Therefore, to confirm that other bacteriocins

do not cause red blood cell lysis, they were tested on 5% horse blood plates without bacterial lawns (Figure 4.2D). No zones of red blood cell lysis were observed, confirming that the synthetic bacteriocins do not harm red blood cells. This finding is promising, as any bacteriocins selected for therapeutic applications must not damage human cells. The absence of red blood cell lysis provides preliminary evidence that these bacteriocins are unlikely to harm human cells, supporting their potential suitability for therapeutic use.

4.2.3 Pixel based methods to determine bacterial cell growth are insufficient when testing proteinaceous antimicrobial compounds against *B. fragilis* and *F. nucleatum*

After the initial testing of the bacteriocins in solid media, the next step involved testing the killing of these bacteriocins in liquid media. A routine method, at Cliniques universitaires Saint-Luc (UCLouvain), for testing a panel of antibiotics against patient bacterial strains involves the use of the oCelloScope^{TM} [188]. The oCellScope^{TM} is an automated brightfield optical microscope that uses measurements of pixels to calculate bacterial growth. The SESA algorithm identifies all objects in a scan and then calculates the total surface area covered by the objects [188]. The bacteriocins that were screened in the solid media stage were taken forward to be screened in liquid media, BACTEC, by the oCellScope^{TM}.

From the initial screen, the effect of killing with one bacteriocin was particularly prominent, the class IIc circular bacteriocin, Garvicin ML. The killing effect of Garvicin ML was more pronounced against *B. fragilis*. Figure 4.3A shows *B. fragilis* growing in the absence of bacteriocin Garvicin ML (green) and then with the addition of the bacteriocin Garvicin ML (purple). Initially in the presence of the bacteriocin, *B. fragilis* grows until approximately 5 hours, where we observe a decrease in SESA measurements that correlate to cell death. Based on the images taken by the oCelloScope^{TM} we can conclude that the action of Garvicin ML led to cell lysis of *B. fragilis*. The image, taken at 24 hours, reveals a lack of bacterial cells in the media (Figure 4.3), which suggests cell death caused by cell lysis

induced by the bacteriocin Garvicin ML. From these experiments, no other bacteriocins appeared to have an effect on the growth of *B. fragilis*.

We were unable to obtain a clear growth curve for the growth of *F. nucleatum* as a control because it did not grow; therefore, we were unable to elucidate any effective bacteriocins against *F. nucleatum* using the technique of recording cell growth and death with the oCelloscope^{TM}.

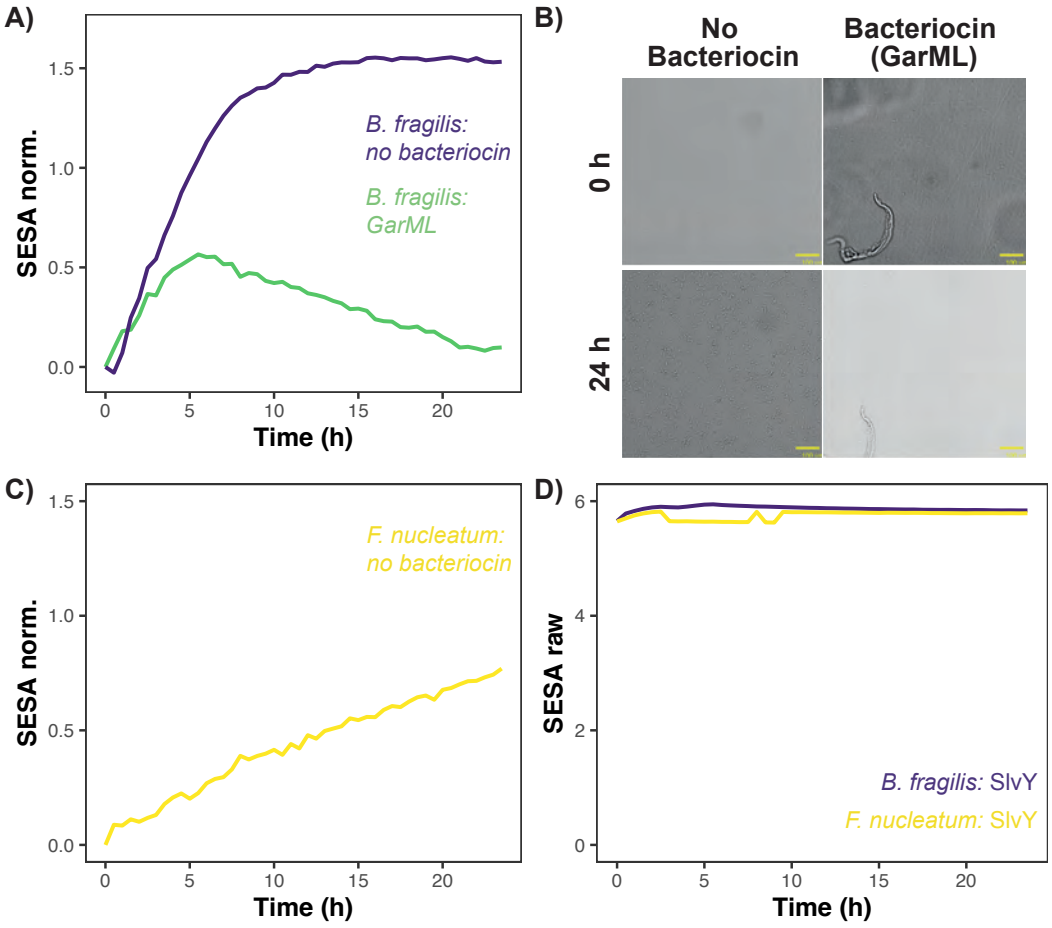

Figure 4.3: Bacteriocin Garvicin ML successfully kills *B. fragilis*
A) SESA normalised growth data for *B. fragilis* with (green) and without (purple) the bacteriocin Garvicin ML added. B) The images taken by the oCelloScope^{TM} at 0 hours and 24 hours. There are no bacteria in the images at 24 hours of *B. fragilis* incubation with the bacteriocin, Garvicin ML. C) SESA normalised growth of *F. nucleatum*. This is not a normal growth curve for *F. nucleatum*. D) SESA raw values plotted to show the impact on the measurements by the bacteriocins that precipitated in the medium. This plot uses the example of bacteriocin SLvY that visibly precipitated when added to the medium. BACTEC^{TM} media is used in all cases.

Multiple issues arose from measuring bacterial cell death with bacteriocins using the oCelloscope™. Either there was no change in the growth curves of *B. fragilis* with bacteriocins added or the bacteriocins precipitated in the medium, for example SlvY (Figure 4.3D). The raw SESA measurements are plotted for SlvY, for both strains, to highlight the extent to which the precipitation of bacteriocin in the growth medium interfered with the oCelloScope™ measurements. This precipitation made it impossible to record the bacterial growth curves with this technique. Therefore, the results of testing the bacteriocins against *F. nucleatum* and *B. fragilis* in liquid culture using the oCelloScope™ remain inconclusive. Alternative methods of measuring bacterial cell death with bacteriocins were explored.

4.2.4 *F. nucleatum* and *B. fragilis* are successfully killed by bacteriocins in liquid media

Due to inconclusive results from the liquid media screen using the oCelloScope™ technique, an alternative method was employed. It was hypothesised that measuring optical density, while less precise than pixel-based measurements, would provide more reliable results. This is because the less precise measurements mean that the precipitation of bacteriocins in the medium would have less impact on optical density measurements compared to the pixel-based techniques. As a result, all subsequent bacteriocin measurements in liquid culture were performed using a plate reader (Tecan Spark) (see Methods 2.6.6).

Five promising candidates from the PARAGEN collection identified in the initial solid and liquid screens were selected for further testing (Table 4.2). These bacteriocins were chosen based on their diverse classes, modes of action, structures, reduced propensity to precipitate in liquid media, and practical availability for this study. The results of bacteriocin Garvicin ML effectively killing *B. fragilis* were unable to be repeated. The supernatant containing Garvicin ML was active against the indicator strain, *L. lactis* (Figure 4.2B), but no killing was observed on either test strain. The discolouration observed on the blood agar plates was attributed to the presence of ammonium sulphate, which was used during the protein purification

process (Figure 4.2C) to concentrate the Garvicin ML bacteriocin from the supernatant of its producer, *Lactococcus garvieae* DCC43. The inclusion of Garvicin ML, a class IIc circular bacteriocin, was intended to complete the investigation of all four subclasses of class II bacteriocins.

Table 4.2: Table of bacteriocins selected for this work, and some of their properties

Bacteriocin	Class	Mode of Action	Amino acids	Notes	References
Aureocin A53	IId	membrane permeabilisation	51	single peptide	[189, 190]
Bactofencin A	IId	membrane disruption through electrostatic interaction	22	positively charged	[191]
Bacteriocin L-1077	IIa	membrane disruption	37	sensitive to proteolytic enzymes	[192]
Garvicin KS A+B+C	IId	inhibitory growth effect	32–34	three peptides	[193, 194]
Plantaricin E+F	IIb	targets membrane receptor CorC	33–34	narrow spectrum two peptides	[195]

The selected bacteriocins were tested on both solid and liquid media, with bacterial growth measured using optical density readings on a plate reader (Figure 4.4). Panels A and B illustrate the bacteriocins' effectiveness in killing *B. fragilis* and *F. nucleatum*, respectively. In the solid media screens, clear zones of killing were observed for Aureocin A53, Garvicin KS A+B+C, and Plantaricin E+F. However, in liquid culture, Aureocin A53 showed effective killing comparable to antibiotics (positive controls), while the killing effect of the others was less pronounced. When compared to the water growth controls in liquid culture, Bactofencin A and Garvicin KS A+B+C negatively affected the growth of both strains, though not as significantly as the antibiotics or Aureocin A53.

The discolouration of blood agar when Aureocin A53 was applied to the lawns

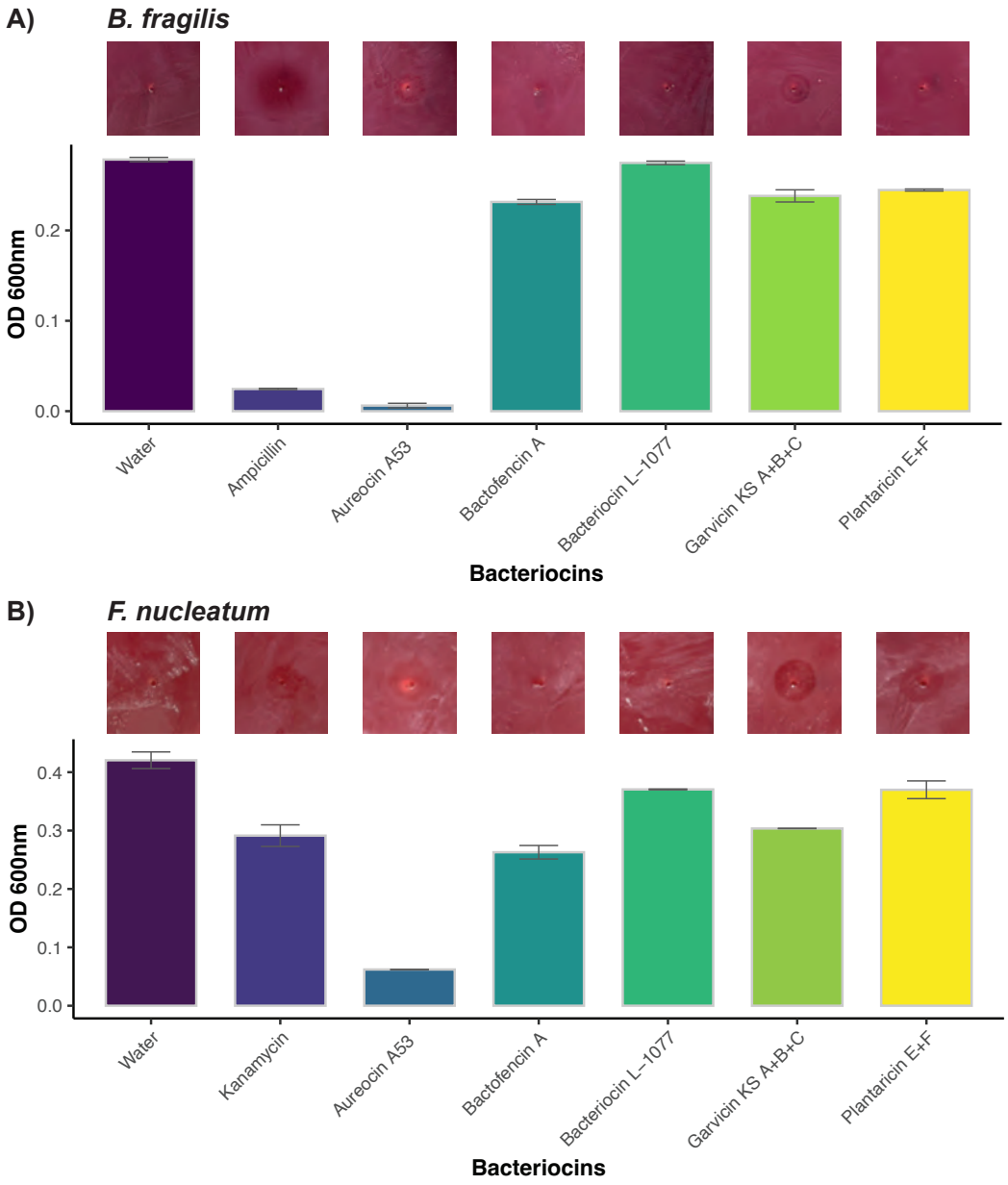

Figure 4.4: Aureocin A53 is the most potent bacteriocin against the onco-pathogens *B. fragilis* and *F. nucleatum*

A) Solid culture of FAA + 5% horse blood with a lawn of *B. fragilis*. The liquid culture is FAB medium with the bacteriocin added to a final concentration of 100 μg/mL B) Solid culture of FAA + 5% horse blood with a lawn of *F. nucleatum*. The liquid culture is FAB medium with the bacteriocin added to a final concentration of 200 μg/mL. The optical density measurements are taken at 20 hours. The solid media experiments are captured after overnight growth ($\approx$ 16 hours). The bars are the mean of duplicate experiments and the error bars are the standard error of the mean.

was not due to the bacteriocin lysing red blood cells, as in the case of the Garvicin ML fractions (Figure 4.2C), but rather the contents of the lysed *F. nucleatum* and *B. fragilis* cells (Figure 4.4A, B). This was confirmed by adding the synthetic bacteriocins to a blood plate without a bacterial lawn, where no discolouration of the red blood cells was observed (Figure 4.2D). Whereas, when testing the supernatant and purified aliquots of Garvicin ML bacteriocin, there was discolouration of the blood on the blood agar plates. This was the result of the ammonium sulphate, used in the protein purification process, lysing the red blood cells (Figure 4.2C). This can be seen by the formation of erythrocyte ghosts upon addition of the purified fractions. These are not seen with the supernatant alone (before any protein purification).

4.2.5 *B. fragilis* is more sensitive to killing by Aureocin A53 than *F. nucleatum*

To further quantify the potency of the bacteriocin Aureocin A53, a concentration curve was constructed. As indicated by previous screening experiments (Figure 4.4), a concentration of 100 μg/mL was sufficient to kill *B. fragilis*, while 200 μg/mL was required to kill *F. nucleatum*. The indicator strain *Bacteroides subtilis* (*B. subtilis*) for Aureocin A53 killing was added to the concentration curve, as a control for Aureocin A53 sensitivity.

From the concentration curve (Figure 4.5), it is clear that the indicator strain is more sensitive to Aureocin A53 than the two onco-pathogens (*F. nucleatum* and *B. fragilis*). The indicator strain, *B. subtilis*, was killed at 6.25 μg/mL. Among the two onco-pathogens, *B. fragilis* is more susceptible being killed at 50 μg/mL. Whereas, *F. nucleatum*is only killed at 200 μg/mL.

This difference in sensitivity may be explained by the gram status of the three bacteria. *B. subtilis* is a gram-positive bacterium, while both onco-pathogens are gram-negative. Since gram-positive bacteria have one cell wall layer, they are generally more susceptible to membrane-permeabilising bacteriocins like Aureocin A53. Furthermore, *B. subtilis* and the natural producer of Aureocin A53 (*Staphylococcus aureus*), are natural competitors [196], which could explain the heightened sensitiv-

ity of *B. subtilis* to the bacteriocin. Nonetheless, both *B. fragilis* and *F. nucleatum* are sensitive to Aureocin A53 at concentrations comparable to typical laboratory working concentrations of antibiotics.

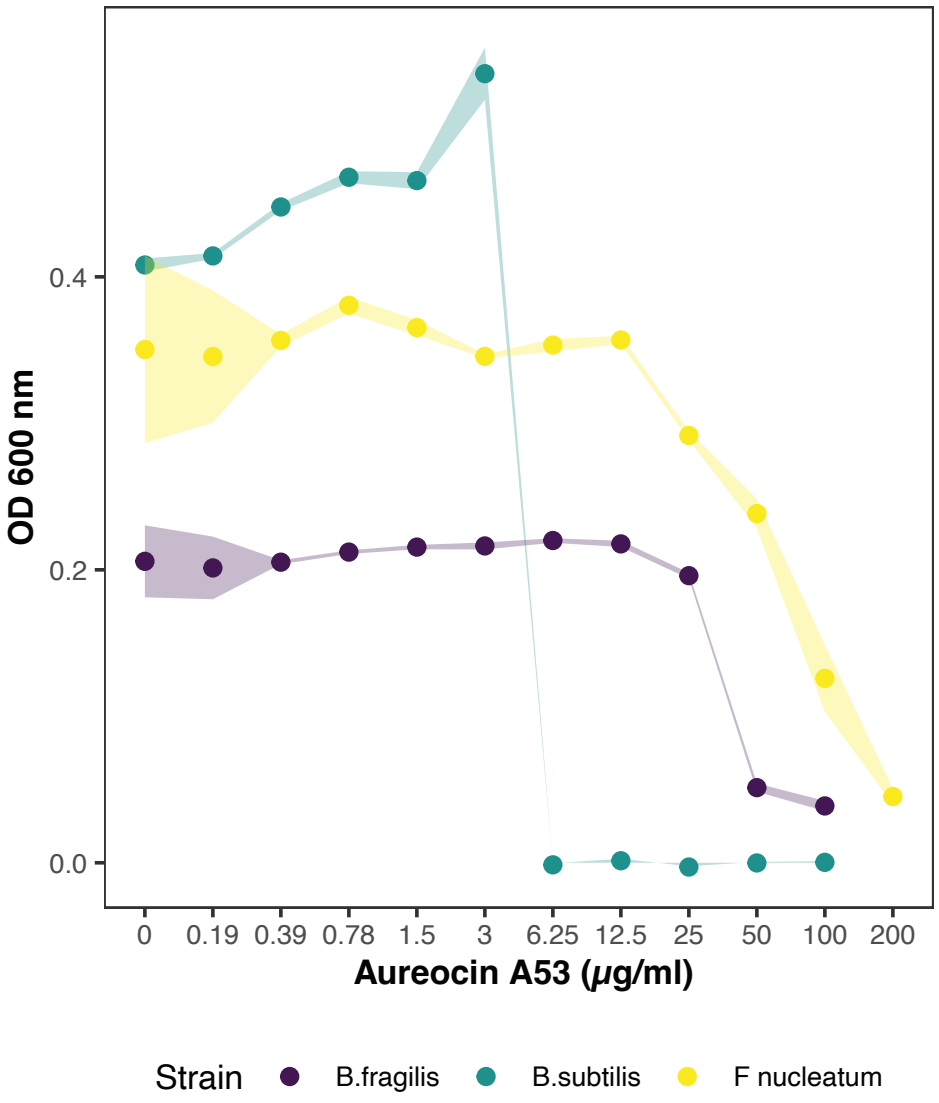

Figure 4.5: *B. fragilis* is more sensitive to killing by Aureocin A53 than *F. nucleatum*
The Aureocin A53 concentration curve reveals the susceptibility of *B .subtilis*, *F. nucleatum*, and *B. fragilis* to chemically synthesised Aureocin A53. The most sensitive to Aureocin a53 was the indicator strain, *B .subtilis*, followed by *B. fragilis* and *F. nucleatum*. The concentration curve was constructed on a log scale, starting with 200 µg/mL for *F. nucleatum* and 100 µg/mL for *B. fragilis* and *B .subtilis*.

4.3 Discussion

In this chapter, I investigated the ability of the panel of bacteriocins, from the PARAGEN collection, to kill the oncogenic strains *F. nucleatum* and *B. fragilis*. This involved optimising their growth and developing methods for bacteriocin screening in liquid culture, alongside testing the bacteriocins themselves. From this panel Aureocin A53 and Bactofencin A showed particular promise at effectively targetting the oncogenic strains.

The successful cultivation of the obligate anaerobes *F. nucleatum* and *B. fragilis* under laboratory conditions suitable for high-throughput screening of bacteriocins was achieved. To maintain anaerobic conditions, a qPCR plate seal secured with autoclave tape was used, providing a practical and effective method for obtaining optical density measurements. Despite challenges associated with the self-aggregation and biofilm formation of *F. nucleatum*, both strains were successfully cultivated, and their growth curves were measured. Notably, *B. fragilis* exhibited a faster growth rate, doubling every 2.1 hours, than *F. nucleatum* which had a doubling time of 3.8 hours. These results are comparable to the literature that cites *B. fragilis* having a doubling time of 1 hour [197] and *F. nucleatum* a doubling time of 3.5 hours [198]. The slight difference in the growth rate of *B. fragilis* measured here could be explained by the conditions not being completely anaerobic within the plate, this observation is supported by the auto-aggregation of *F.nucleatum* also thought to be due to the presence of some oxygen. The difference in growth rates between the two onco-pathogenic strains is important, because the bacteriocins were added at the same time for both strains and this may influence how the bacteriocins interact with the strains. It is important to consider the growth rates of bacterial strains as this effects efficacy, for example antimicrobial agents are most effective during the exponential growth phase [199].

Screening of bacteriocins from the PARAGEN collection identified several candidates capable of killing *F. nucleatum* and *B. fragilis*. Aureocin A53 and Bactofencin A demonstrated bactericidal effects on solid media, with distinct zones of killing observed on *F. nucleatum* and *B. fragilis* lawns. Among these, Aure-

ocin A53 showed the highest efficacy in liquid culture, with bactericidal activity comparable to antibiotics. However, technical challenges arose during liquid media assays using the oCelloScope^{TM}, as precipitation of certain bacteriocins, such as SlvY, interfered with the accuracy of growth curve measurements. This prompted a transition to optical density measurements using a plate reader, which provided more reliable results and enabled the identification of bacteriocins effective in both solid and liquid culture.

A concentration curve for Aureocin A53 was subsequently generated, providing insight into the sensitivity of the pathogens to this bacteriocin. However, due to a limited supply of chemically synthesised Aureocin A53, this experiment could only be conducted as a single replicate. Subsequent lawn assays corroborated the observed trend that *B. fragilis* is more sensitive to Aureocin A53 than *F. nucleatum*. Furthermore, discolouration observed in blood agar assays, initially suspected to indicate haemolytic activity, was found to result from bacterial cell lysis rather than direct erythrocyte damage. The exception was the purified fractions of Garvicin ML, where the ammonium sulphate used during purification caused erythrocyte lysis (Figure 4.2C, D). Importantly, other tested bacteriocins, including Aureocin A53, did not cause red blood cell lysis, a crucial consideration for therapeutic applications.

The two bacteriocins demonstrating the greatest killing efficacy in liquid culture were Bactofencin A and Aureocin A53, with Aureocin A53 being a single peptide requiring no post-translational modifications and Bactofencin A remaining active without disulfide bond formation. These were identified as promising candidates for incorporation into the lysis delivery system, Lysara, constructed using the Moclo platform [128]. While Aureocin A53 displayed stronger activity against the indicator strain *B. subtilis* compared to the onco-pathogens *F. nucleatum* and *B. fragilis*, its efficacy was consistent with previous studies. For example, concentrations of 128 μM (770 μg/mL) and 16 μM (96 μg/mL) of Aureocin A53 were required to kill *Staphylococcus aureus* and *Enterococcus faecium*, respectively [190], with one study reporting a MIC of 0.29 μg/mL for *E. feacium* [200]. In this

work, 200 μg/mL was required to kill *F. nucleatum*, and 50 μg/mL was sufficient for *B. fragilis*. These values were calculated in liquid culture, whereas previously reported concentrations were determined using solid media.

This study demonstrated that Aureocin A53 does not harm red blood cells, an important step in evaluating its therapeutic potential. This correlates with *in vivo* studies, in the *Galleria mellonella* (moth) model, that observed no harm caused by synthetically synthesised Aureocin A53 [201]. Although the screened bacteriocins effectively killed onco-pathogens, challenges were encountered during bacterial culture, such as *F. nucleatum* aggregation, and with bacteriocin precipitation in media, which occasionally rendered oCelloScope^{TM} results unreadable.

It is worth noting that *F. nucleatum* DNA is found at higher levels in the early stages of colorectal cancer [202]. This raises the question of whether bacteriocin-based systems should be administered early in colorectal cancer development. Furthermore, bacteriocins could potentially be repurposed for vaccine-like technologies. For example, a vaccine targeting *F. nucleatum*, such as one utilising recombinant Fn-AhpC protein, has been shown to reduce *F. nucleatum* levels in mouse colorectal cancer models and induce strong humoral immunity (antibody production by B cells) [203].

Future work not covered in this study includes screening the selected bacteriocins against commensal strains to confirm specificity. Potential commensal strains to investigate include members of the human gut: *Prevotella copri*, *Bacteroides vulgatus*, *Bacteroides ovatus*, and *Akkermansia muciniphila* [204, 205]. Whilst it is possible to achieve strain specificity with bacteriocins, as demonstrated with strains of *Clostridium difficile* [206], due to the pore-forming mechanism of action by Aureocin A53, it is unlikely to exhibit high specificity, as such modes of action are generally broad-spectrum. Thus far it has been recorded that Aureocin A53 displays activity against a wide range of bacteria, including *Staphylococcus simulans* [200], *STaphylococcus aureus*, *Staphylococcus epidermidis*, *Streptococcus sp.*, *Enterococcus faecalis*, *Micrococcus luteus* [207], *Listeria innocua* (food pathogens) and *Listeria monocytogenes* [208]. Additionally, there has been some evidence that

Auroecin A53 displays a slight toxic effect against murine monocytic-macrophages [209] however, this has not yet been observed in humans, and in this work there was no evidence of Aureocin A53 being cytotoxic to equine red blood cells. Nevertheless, high specificity may not be essential. Bacteriocins have modes of action distinct from those of antibiotics [85] and, even if Aureocin A53 is not highly specific, its specificity may still be sufficient to serve as an alternative to antibiotics in the current context of antibiotic resistance.

Chapter 5

Delivery of bacteriocins through engineered lysis

'Nothing is impossible, the word itself says 'I'm possible'!'

— Audrey Hepburn, 1929 - 1993

Contents

5.1 Introduction

5.1.1 Payload bacteriocins: Aureocin A53 & Bactofencin A

The bacteriocins Aureocin A53 and Bactofencin A displayed antimicrobial activity against both onco-pathogens being tested in this work. Their unique structural properties, no signal peptide, and lack of post-translational modifications (PTM) make them perfect candidates to be incorporated into a lysis delivery system. The circular bacteriocin Garvicin ML, whilst unable to display killing against the onco-pathogens, was included as a control of successful bacteriocin killing.

Aureocin A53 is a 6,012.5 Da, cationic, and tryptophan-rich antimicrobial peptide composed of 51 amino acid residues [189, 207]. It is produced by *Staphylococcus aureus* (*S. aureus*) and encoded by the *aucA* gene on the pRJ9 plasmid [210]. The pRJ9 plasmid also encodes genes for ABC transporters, which confer immunity by actively pumping Aureocin A53 out of the bacterial cell, preventing self-destruction [211]. Unusually, for a bacteriocin, Aureocin A53 lacks a typical leader sequence or signal peptide [189]. This feature, along with the absence of biosynthetic enzymes near the structural gene, suggests that no PTM are required for its antimicrobial activity, making it an ideal candidate for screening against oncogenic pathogens in this work [189].

Aureocin A53 exhibits potent antimicrobial activity which is formally measured by the minimum inhibitory concentration (MIC). The MIC is defined as the lowest concentration of an antibacterial agent that prevents visible growth of the strain [153]. Aureocin A53 has shown potent activity against gram-positive bacteria such as *Enterococcus faecium*, with an MIC of 0.29 μg/mL [200]. This is comparable to MICs of antibiotics reported in clinical isolates of *F. nucleatum* with values ranging from 0.25 μg/mL to 1 μg/mL for penicillin to chloramphenicol respectively [212]. It should be noted these values are from solid agar results not liquid culture experiments. Its bactericidal action involves rapid membrane permeabilisation, leading to the efflux of essential cellular components, dissipation of membrane potential, and the cessation of macromolecular synthesis [200]. This ultimately results in cell lysis and death.

The unique structural features and stability of Aureocin A53 enhance its potential for a wide range of applications, including food preservation and as an alternative to traditional antibiotics. Its stability under various environmental conditions further supports its suitability for these applications, as it can maintain its activity in a variety of settings [208].

In addition to Aureocin A53, Bactofencin A is a novel cationic bacteriocin that is produced by *Lactobacillus salivarius* DPC6502 (a strain isolated from the porcine intestine) [213]. This 22 amino-acid peptide contains an intramolecular disulphide bond between cysteine residues at positions 7 and 22, which stabilises the peptide and forms a large C-terminal loop [214, 191]. Bactofencin A exhibits potent antimicrobial activity against several clinically relevant pathogens, including *S. aureus* and *Listeria monocytogenes* [215]. Its mechanism of action involves interaction with the bacterial cell membrane, leading to cell death. The bacteriocin's effectiveness is closely linked to its primary structure, including the N-terminal charge and the formation of the disulfide bond [215].

Unlike many other bacteriocins, Bactofencin A's immunity is conferred by a teichoic acid D-alanyltransferase (dltB) [216] homolog located downstream of its structural gene [213]. The dltB gene is involved in the d-alanylation of teichoic acids in the cell wall, a modification that reduces the net negative charge of the bacterial surface, thereby decreasing susceptibility to cationic antimicrobial peptides. Heterologous expression of this gene in susceptible strains confers specific immunity to Bactofencin A, distinguishing it from other bacteriocins that rely on dedicated immunity proteins [213].

Given its potent antimicrobial properties and unique immunity mechanism, Bactofencin A holds great promise for therapeutic applications targeting antibiotic-resistant bacteria. Its ability to effectively target pathogens such as *S. aureus* and *L. monocytogenes* underscores its potential in clinical settings, particularly in the context of combating emerging antibiotic resistance [215].

Although initially promising (Figure 4.3), the bacteriocin Garvicin ML later proved unable to kill the onco-pathogens being investigated in this work. It is in-

cluded here on a bacteriocin expressing plasmid, as part of the collaboration with the industry partner Syngulon, as a positive control for plasmid expression of bacteriocin killing. It is unique in its expression as it circularises via split inteins, which are proteins that can self excise leaving exposed overhangs [217]. The wild type Garvicin ML is produced by *Lactococcus garvieae* DCC43 [218]. Circular bacteriocins such as Garivicin ML are gaining interest as therapeutics due to their stable nature [219].

5.1.2 Modelling bacteriocin expression & secretion

Modelling bacterial growth curves is a fundamental approach in microbiology to understand how bacterial populations grow over time under given environmental conditions. One of the most widely used models for bacterial growth is the logistic growth model, which accounts for both the initial exponential increase in cell numbers and the eventual plateau as resources become limited [220].

The logistic growth model improves upon simple exponential models by incorporating a carrying capacity (K): the maximum population size that the environment can sustain. This model provides a more realistic depiction of bacterial growth, especially in closed systems such as batch cultures, where nutrient limitations and environmental changes influence population dynamics [221].

Understanding bacterial growth dynamics is essential for various applications, including antibiotic development, industrial fermentation, and synthetic biology, where precise control over microbial populations is required [222]. For this work bacteriocin release via secretion and lysis was modelled in order to help guide and explain observations of the wet lab work.

5.1.3 Bacteriocin expression platforms

Bacteriocin expression has gained increased attention in recent years, particularly in the context of food applications [1]. One promising approach involves inserting naturally occurring plasmids into Generally Recognised As Safe (GRAS) strains, which can be used in food production. This method leverages native biosynthetic

genes to express bacteriocins in a food-safe environment, offering a potential pathway for the application of these antimicrobial peptides in food safety and preservation [223].

To enhance bacteriocin expression, various strategies have been explored. One approach involves modifying the leader peptide to increase expression levels, potentially improving the yield and activity of the bacteriocin [224]. In addition, the construction of modular synthetic circuits has been proposed to express a range of bacteriocins with diverse leader peptides, allowing for more versatile and tunable production systems [90].

Furthermore, yeast have been explored as alternative hosts for bacteriocin expression. This eukaryotic system offers advantages, including the ability to perform post-translational modifications that are not always achievable in prokaryotic systems, potentially enhancing the bioactivity and stability of the expressed bacteriocins [225].

In parallel, another team has successfully engineered *Escherchia coli* Nissle (EcN) to express the bacteriocins Actifencin and Bacteroidetocin A; targeting the following microbes *Bacteroides* and *Lactobacillus*. This provides further evidence for the feasibility of using engineered probiotics as a platform for bacteriocin production. However, their *in vivo* work (mice) could not recapitulate the inhibitory patterns they observed *in vitro* and *ex vivo* [226].

This chapter presents the development of a bacteriocin expression platform in an engineered strain, designed to use lysis as a mechanism for delivering active bacteriocins to target onco-pathogens within the tumour micro-environment. Where previous attempts have focused on secreting the bacteriocins [90], this attempt focuses on lysis as a simpler solution for versatile bacteriocin delivery. Lysing open engineered host cells has the added benefit of reinducing immune responses [227], a desirable effect in the context of a tumour. The platform constructed here integrates the arabinose inducible lysis circuit, Lysara, with the bacteriocins identified in previous chapters, Aureocin A53 and Bactofencin A.

5.2 Results

5.2.1 Challenges in IPTG induced cell lysis

An Isopropyl β-D-thiogalactopyranoside (IPTG) inducible lysis circuit was initially selected as the circuit design (Figure 5.1). IPTG was selected because it is a structural analogue of allolactose (the natural inducer of the lactose operon) [228]. Beneficially, its concentration remains constant during experiments because it is not metabolised by bacterial cells [228]. When present, IPTG binds to the lac repressor resulting in the lac repressor removing its repression of the P_{lacUV5} promoter. Therefore, transcription of the chromosomal T7 RNA polymerase can begin. The T7 RNA polymerase is then able to bind to and activate T7 promoters [229]. The IPTG-inducible circuit was constructed using the MoClo [128] standard parts.

A total of 24 transformants were tested for their response to IPTG induced cell lysis in a plate reader assay Figure (5.1). The transformants were grown for 2 hours before the addition of IPTG (100 μM). Of these 24 transformants, 12 initially showed signs of responding to IPTG induction but quickly developed resistance and became unresponsive within 1–2 hours. The remaining 12 transformants exhibited no response to IPTG-induced cell lysis at any point. Notably, none of the transformants were completely killed by the induction process.

This system utilised bacteriophage T7 RNA polymerase, which is encoded on the chromosome and specifically recognises the T7 promoter. This polymerase is capable of transcribing approximately eight times faster than *E. coli* RNA polymerase and its expression is controlled by the P_{lacUV5} promoter [230]. P_{lacUV5}, a strong variant of the wild-type P_{lac} promoter, is inducible by IPTG and does not rely on intracellular cyclic AMP levels or the CRP (cyclic AMP receptor protein). This was the promoter used in this initial circuit design. However, P_{lacUV5} is known to exhibit greater leakiness compared to the wild-type Lac operon, resulting in low levels of T7 expression and protein production even in non-induced cells [230]. This leaky expression is thought to drive mutations in the expressed gene, contributing to the observed resistance of the screened transformants.

This system was unsuitable for proteins with high toxicity or significant growth

burdens [230]; such as the lysis protein, ϕX174E encoded by the MoClo kit, used in this circuit. This suggests that the resistance observed among the transformants may be linked to its incompatibility with toxic genes such as the ϕX174E gene used to create this lysis system.

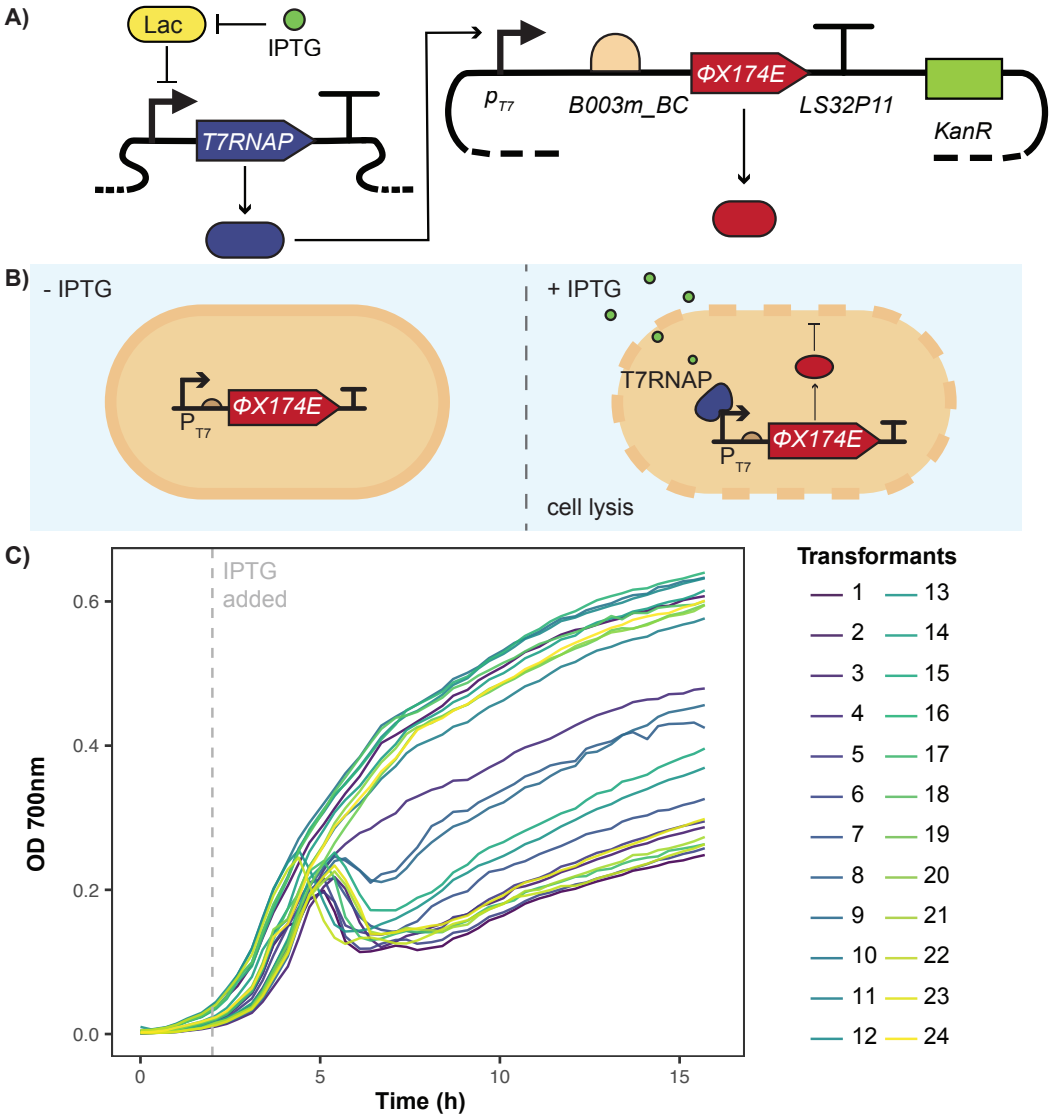

Figure 5.1: IPTG inducible lysis circuit partially responds to IPTG induction
A) The genetic constructs built and involved in this system, in the synthetic biology open language format (SBOL). B) Diagrammatic representation of the IPTG inducible circuit. In the absence of IPTG there is no T7 RNA polymerase (T7RNAP) to activate the T7 promoter. When IPTG is added the T7RNAP can bind the T7 promoter inducing transcription of the lysis gene, ϕX174E. C) Twenty four transformants containing the IPTG inducible lysis circuit (colours) were induced with IPTG at 2 hours (grey dashed line). OD_{700nm} measurements were taken over 16 hours. Data is one replicate, each well = one transformant.

5.2.2 Construction of the arabinose-inducible Lysis circuit: Lysara

Following the unsuccessful performance of the IPTG-inducible lysis circuit, an arabinose-inducible lysis circuit, termed Lysara, was developed to address the challenges of resistance and leaky expression. The P_{araBAD} promoter is induced by the addition of arabinose (Figure 5.2A), this promoter has very low background expression levels and can be further dampened by the addition of glucose, through catabolite repression. Glucose reduces cAMP which dampens the P_{araBAD} promoter [231] and reduces leakiness of the promoter when it is meant to be in the OFF state.

Lysara operates by being in the OFF state in the absence of arabinose, where the protein AraC represses the promoter P_{araBAD}. Upon the addition of arabinose, AraC undergoes a conformational change and releases its repression of P_{araBAD}. This leads to the expression of the lysis toxin (ϕX174E), which works by lysing the host cell via the inhibition of peptidogylcan synthesis of gram-negative cell walls, causing pore formation in the outer membrane [232] (Figure 5.2A). A screening of 24 transformants, containing the Lysara circuit, was conducted with arabinose (10 mM) introduced at the 2 hour time point (Figure 5.2B). Colonies that successfully lysed in response to arabinose induction were selected for further characterisation (Figure 5.3).

During further characterisation, a negative control strain was added, a host without the Lysara plasmid. The negative control did not respond to arabinose and grew without any signs of burden, as expected (Figure 5.3B). This confirmed that the addition of 10mM arabinose produced no toxic effects to the bacterial cells and that the cells would not lyse without the Lysara circuit present. This is not true for colony 5 (Figure 5.3D), which showed abnormal growth curves in the absence of arabinose suggesting burden on the cells. This was evidenced by colony 5 only reaching an Optical Density (OD) measurement of OD_{700} 0.3 compared to the control strain (Figure 5.3B), which achieved 0.58. In the presence of arabinose, colony 5 was observed to develop resistance and regrow. All 3 replicates of colony 5 followed this pattern. Other than colony 5, all other colonies grew comparable to the

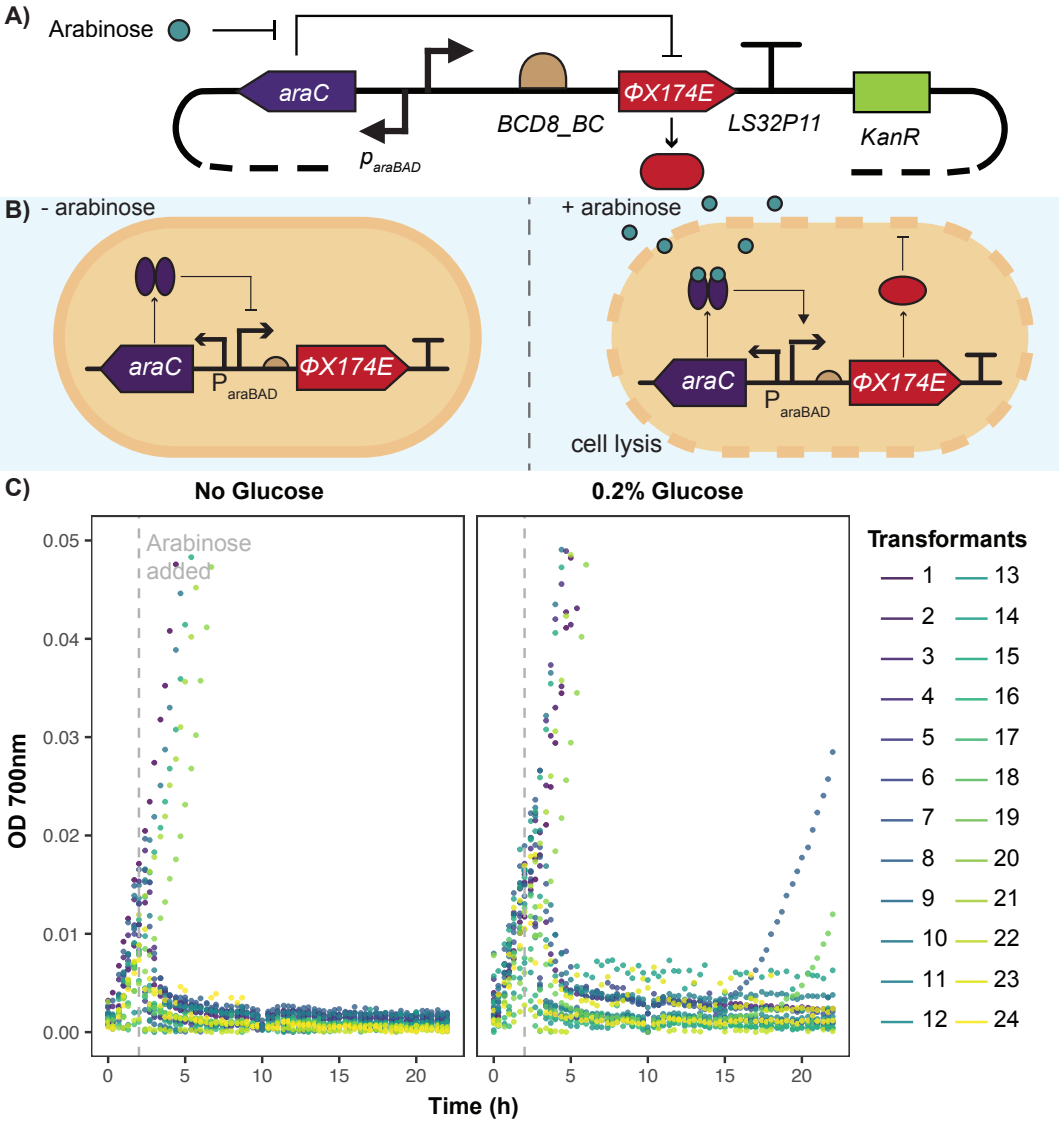

Figure 5.2: Lysara colonies successfully respond to arabinose and lyse host cells
A) The genetic constructs built to make this system, in the synthetic biology open language format (SBOL). B) Diagrammatic representation of the Lysara, arabinose inducible lysis circuit. In the absence of arabinose, AraC prevents RNA polymerase binding and transcription. Upon the addition of arabinose, AraC undergoes conformational change allowing RNA polymerase to access the P_{araBAD} promoter, inducing transcription. C) The Lysara arabinose inducible transformant colonies were resuspended in LB medium and placed into wells in the plate reader to grow, each colour is an individual colony with and without glucose. Arabinose (10μM) was added at 2 hours (dotted grey line). The transformant colonies were measured for 24 hours to observe any resistance.

negative control in the absence of arabinose.

For colony 11, the strain grew comparably to the negative control (Figure 5.3E). Upon addition of arabinose, despite all replicates lysing, by the end of the experiment all replicates had developed resistance and were beginning to regrow. Regarding colony 18 (Figure 5.3F), only one of the replicates developed resistance by the end of the experiment and this is thought to be due to spontaneous mutations that remove the burden of the lysis circuit, Lysara, on the host cell. There was a small growth burden observed in the engineered host cells as the colonies reached OD_{700} 0.45 rather than OD_{700} of 0.58 of the negative control strain (non-engineered). This defect is to be expected as the lysis circuit would place burden on the engineered cells [233].

Among the screened transformants taken forward to this stage, colony 3 was the only one that demonstrated consistent lysis without developing resistance (Figure 5.3C). Colony 3 was subsequently used in all downstream experiments. Overall, the Lysara system effectively demonstrates lysis behaviour upon arabinose induction.

To confirm that the glucose added to the media was not interfering with the lysis circuit, colony 3 was tested in conditions with and without both glucose (0.2%) and arabinose (Figure 5.4). In the conditions with glucose and no arabinose, colony 3 grows better than without glucose, reaching an OD_{700} of 0.6 (better growth than the control strain) (Figure 5.3B). This was expected because the bacteria can use glucose as a carbon food source. However, in the absence of glucose and no arabinose, colony 3 displayed abnormal growth curves, this was expected because without the glucose to dampen the P_{araBAD} promoter, the circuit would be leaky and therefore express the lysis toxin, ϕX174E and lyse itself. From the growth curve it can be observed that this curve flattens, presumably because the colony had mutated to escape the killing burden.

In the presence of glucose and arabinose (Figure 5.4), colony 3 initially grew better than without glucose (turquoise line) and responde to arabinose induction at 2 hours, observed by a sharp decrease in OD_{700} measurements. This was maintained

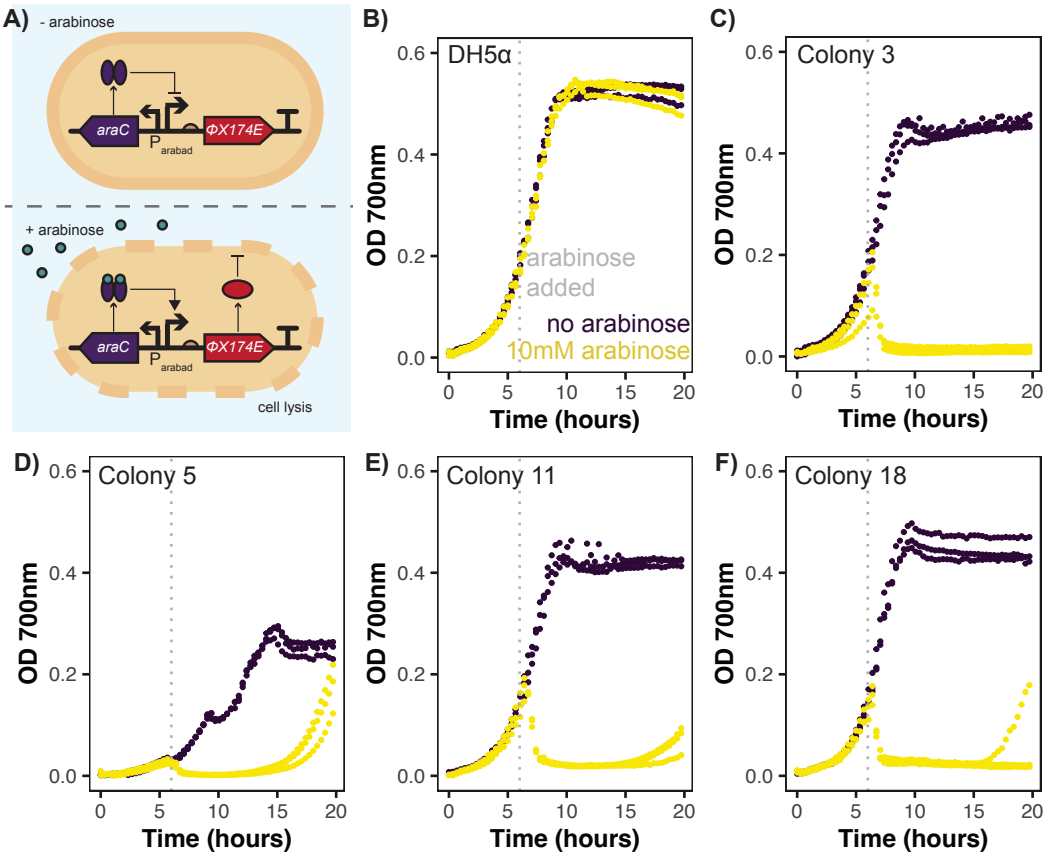

Figure 5.3: Successful construction of the arabinose-inducible lysis circuit, Lysara
A) Diagrammatic representation of the Lysara system with and without the induction of arabinose. In the absence of arabinose the AraC regulatory protein binds to sites (O and I1) upstream of the P_{araBAD} promoter which blocks transcription. Upon the addition of arabinose, the AraC complex now binds to sites I1 and I2, transcription can now begin from the P_{araBAD} promoter. B) NEB DH5α, empty strain control, does not contain the lysis circuit, Lysara. C) Colony 3 , this colony was taken forward for all other experiments. D - F) Colonies, 5, 11, and 18 respectively that were screened at this stage. Arabinose (10 mM) was added to all colonies B-F, at 6 hours (grey dashed line). Dots plotted are the 3 triplicate values from one experiment.

until 15 hours where a change in OD_{700} was observed, indicating regrowth of the cells. However, colony 3 does not fully recover its growth, unlike the arabinose induced 'no glucose' (purple line) group, which reached almost the same OD_{700} as the control. Colony 3 in these conditions, arabinose induced and no glucose, developed resistance faster and recovered its growth, unlike the arabinose induced glucose group.

Therefore, the overall effect of glucose in the media provided an additional carbon source for the cultures and effectively dampened the P_{araBAD} promoter activity, reducing the leaky expression of ϕX174E and reducing the resistance observed. The colony 3 cultures, grown in glucose-supplemented media, exhibited improved lysis responses and delayed resistance compared to those grown without glucose, where unresponsive cells resumed growth.

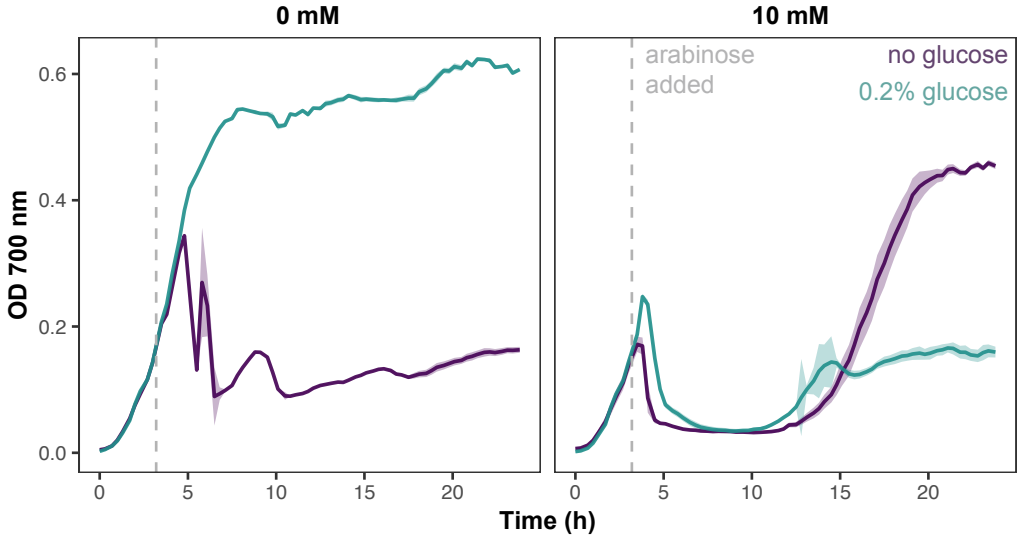

Figure 5.4: Glucose successfully dampens the leakiness of the Lysara circuit Lysara induced with arabinose (10 mM) in the presence and absence of glucose in LB medium. Increased cyclic AMP (cAMP) binding to the cAMP activator protein (CAP) can also stimulate AraC binding to I1 and I2, initiating transcription. However, the addition of glucose to the media decreases cAMP, which reduces binding to CAP, reducing AraC activation and ultimately represses the P_{araBAD} promoter [234]. The lines represent the median value of triplicate data from a single experiment. The ribbons represent the standard error of the median. The dashed line at 2 hours marks the addition of the inducer, arabinose (10 mM).

5.2.3 Lysara: characterising arabinose concentration and time of induction

The Lysara system was evaluated in both M9 minimal media and LB rich media, both supplemented with 0.2% glucose. As expected the strain grew better in LB rich media, compared to the minimal media, M9 because there are less energy sources in the M9 minimal media. The growth curves of Lysara in different arabinose concentrations and with arabinose added at different time points were characterised using optical density measurements as a measure of bacterial growth (Figure 5.5). Figure 5.5A and 5.5C display the growth under varying concentrations of an inducer (0, 2, 4, and 10 mM) added at 2 hours. Figure 5.5B and 5.5D represent growth curves for cultures with the inducer, arabinose (10 mM), added at different time intervals (0, 2, 4, 6, and 7 hours).

In LB media, lysis was observed only at the highest arabinose concentration (10 mM) (Figure 5.5A), whereas, in M9 media, concentrations as low as 4 mM successfully induced lysis (Figure 5.5C). This is thought to be due to the number of bacterial cells present in the cultures at the point of arabinose induction. The more bacterial cells present, the more arabinose is required to induce each bacterial cell. Similarly, since bacterial cells can use arabinose as a carbon source, it is possible that at lower arabinose concentrations but higher cell densities, the lysis circuit fails to activate. This could occur because the bacteria first metabolize the available arabinose before it can induce the circuit, as *E. coli* possesses ABC transporters for arabinose uptake [235]..

Regarding the multiple time points, arabinose at 10 mM was added to both LB (Figure 5.5B) and M9 (Figure 5.5D) over 2, 4, 6, and 7 hours. Lysara cultured in LB media responded to arabinose induction at all times tested (Figure 5.5B). However, resistance developed when arabinose was added at 2, 4 and 6 hours. The experiment had to stop at 24 hours so it is not possible to determine whether resistance would have developed from the cultures induced at 7 hours. By 24 hours there was no bacterial re-growth observed. When the cultures are induced later on, for example at 6 hours compared to 2 hours, resistance develops faster. For 2 hour induction,

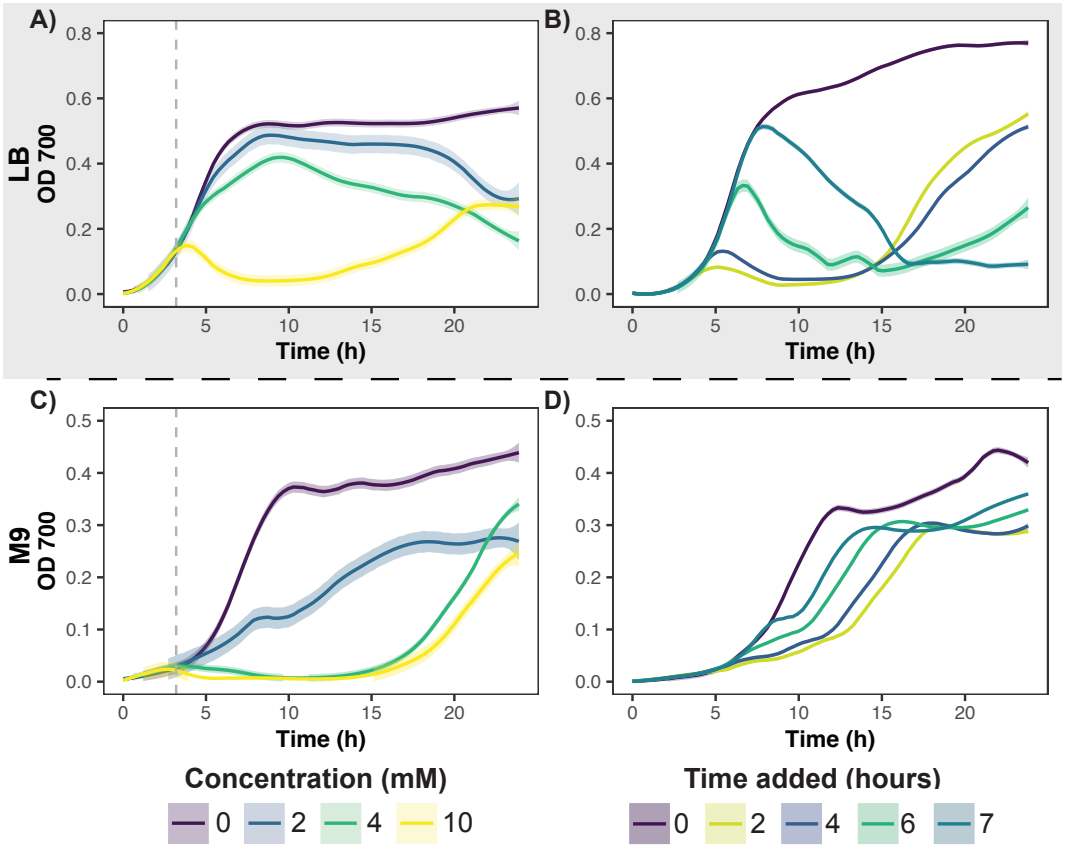

Figure 5.5: Lysara circuit successfully lyses in a range of arabinose concentrations and multiple time points

Panels show the bacterial growth measured by optical density (OD_{700nm}) over time. Panel A) and C) display the growth under varying concentrations of the inducer arabinose (0, 2, 4 and 10 mM) added at 2 hours. For panels A) and C), the lines represent the smoothed average median OD values over time, for each concentration, from triplicate data, while the shaded regions indicate the standard error of the average median. The dashed vertical line at 2 hours is when the 10 mM arabinose was added. Panel B) and D) display the growth curves for the bacterial cultures with the inducer, arabinose (10mM) added at different time intervals (0, 2, 4, 6, and 7 hours). The Lysara circuit is tested in LB medium in panels A) and B) and in M9 medium in panels C) and D). All media contained 0.2% glucose. For panels B) and D), the lines represent the median values and the shaded regions the standard error (SE) of the median from triplicate data from one experiment.

resistance can be seen by the emerging growth curve at 13 hours, compared to 17 hours for the 6 hour induction. Resistance observed from earlier arabinose inductions appears greater (steeper growth curve) in the 24 hour cycle of the experiment.

For M9 media (Figure 5.5D) the cultures appeared to not grow well and, whilst there can be observed a shift in time taken for the cultures to grow, none of the cultures appear to respond to arabinose and lyse. At a 2 hour induction, there is the most obvious effect on the cultures growth being delayed. When arabinose was added at 7 hours, the cultures entered the exponential phase at 6 hours, the same as the control (no arabinose added). In contrast, without arabinose addition, the culture appeared to enter the exponential phase at 13 hours. For 7 hours, it is clear there is a brief plateau in the cultures growth before it develops resistance. Potentially this suggests that as the circuit is growing in minimal M9 media, the cultures are using the arabinose as a carbon source before it can efficiently activate the lysis circuit. Although, as the growth is delayed, this does suggest some cells are responding to the circuit. However, as these die the resistant cells then take over.

Overall, higher arabinose concentrations elicited faster Lysara responses but also accelerated resistance development. Despite some variation, likely due to random mutations, the Lysara system consistently responded to arabinose across experiments.

5.2.4 Lysara: characterising host cell death and arabinose re-induction

Once it had been confirmed that Lysara responds to the inducer arabinose, the next steps were to determine whether the circuit could completely lyse bacterial populations and, if not, whether it could withstand repeated induction at varying arabinose concentrations.

Induction, at arabinose concentrations ranging from 0 mM to 10 mM, was assessed in LB media Figure 5.6. No arabinose or re-induction was used as a control of bacterial growth without arabinose induction and lysis (Figure 5.6A). When 2 mM arabinose (Figure 5.6B) was added at 2 hours and 4 hours, no effect on bacterial

growth was observed. The growth curves for 2 mM in the first induction were the same as the control growth curves (Figure 5.6A). However, re-induction at 26 hours shifted the growth curve, resulting in a delay of approximately two hours compared to cultures induced at 4 and 28 hours, which displayed no anomalies in growth.

At 4 mM arabinose (Figure 5.6C), a slight decrease in optical density (OD) was noted in cultures induced at 2 hours, but there was no evidence of lysis when arabinose was added at 4 hours. Upon re-induction at 26 hours, the 2-hour culture exhibited a temporary plateau in growth before recovery. A similar plateau was observed in the 4-hour group re-induced at 28 hours.

At 6 mM arabinose (Figure 5.6D), bacterial lysis was evident in cultures induced at 2 hours, as indicated by a decrease in OD. However, these cultures recovered after approximately 12 hours. Re-induction at 26 hours resulted in no response to arabinose, and the culture reached a higher OD (0.6) than the no-arabinose control (OD 0.5), suggesting a potential loss-of-function mutation leading to a reduced plasmid burden. In contrast, the 4-hour group exhibited a growth plateau upon induction, without recovery within the first 24 hours. Upon re-induction at 28 hours, the 4-hour group initially responded with a decrease in OD but became resistant, resuming exponential growth by 38 hours.

At 8 mM arabinose (Figure 5.6E), both the 2-hour and 4-hour inductions caused reductions in bacterial growth. The 2-hour group exhibited a steep decline in OD but became resistant after 12 hours, re-entering exponential growth. Re-induction of the 2-hour group at 26 hours produced no response to arabinose, and the culture again achieved a higher OD than the control. For the 4-hour group, induction caused a steady decline in OD, and re-induction resulted in delayed re-growth, with no observed recovery until approximately 35 hours.

At the maximum concentration of 10 mM arabinose (Figure 5.6F), both the 2-hour and 4-hour groups initially displayed sharp decreases in OD, indicating cell lysis. The 2-hour group recovered growth within 12 hours, showing resistance to re-induction at 26 hours and achieving a higher OD than the control. The 4-hour group exhibited a steady decrease in OD during the initial induction and minimal

growth until 33 hours (during the re-induction), at which point exponential growth resumed.

The data suggest that the lysis circuit does not respond to arabinose during re-induction, likely due to mutations conferring resistance to the circuit. The mutations may involve the Lysara plasmid itself, direct mutations of the lysis gene ϕX174E or an *E. coli* host gene SlyD, which is required for lysis induced by ϕX174E (lysis gene E) [236]. SlyD, a member of the FK506-binding protein (FKBP) family, has been implicated in lysis resistance due to recessive mutations. These mutations include deletions in the slyD locus, which contains three open reading frames. Such deletions prevent the lysis gene from inducing cell death and have been previously associated with the inability of ϕX174E to successfully lyse the host cell [237].

To assess the efficacy of the lysis circuit in eliminating all bacterial cells, colony counts were conducted 24 hours after arabinose induction (Figure 5.6G). Arabinose was added at two time points: 2 hours and 4 hours. The colony counts for both conditions demonstrated a reduction in viable cells at arabinose concentrations of 4 mM and 10 mM compared to controls without arabinose. However, these counts were conducted as single replicates, limiting the reliability of the findings. The data suggest that the lysis circuit does not completely eliminate all cells, as indicated by the presence of viable colonies after induction. Colony counts were performed using a 5 μL "pizza spotting" plating method (2.3.6) [238].

In conclusion, while the plate reader data confirm a reduction in optical density following arabinose induction, the colony counts reveal that the lysis circuit does not achieve complete eradication of the bacterial population. This is further confirmed by the re-growth of cultures during the re-induction stage. The variability in bacterial death and regrowth observed in these re-induction experiments could potentially be explained by mutations in the slyD gene within the genomic DNA of the Lysara *E.coli* strain. Further investigation is necessary to confirm this hypothesis i.e. sequence the resistant strains to identify mutations in the plasmid or the slyD gene.

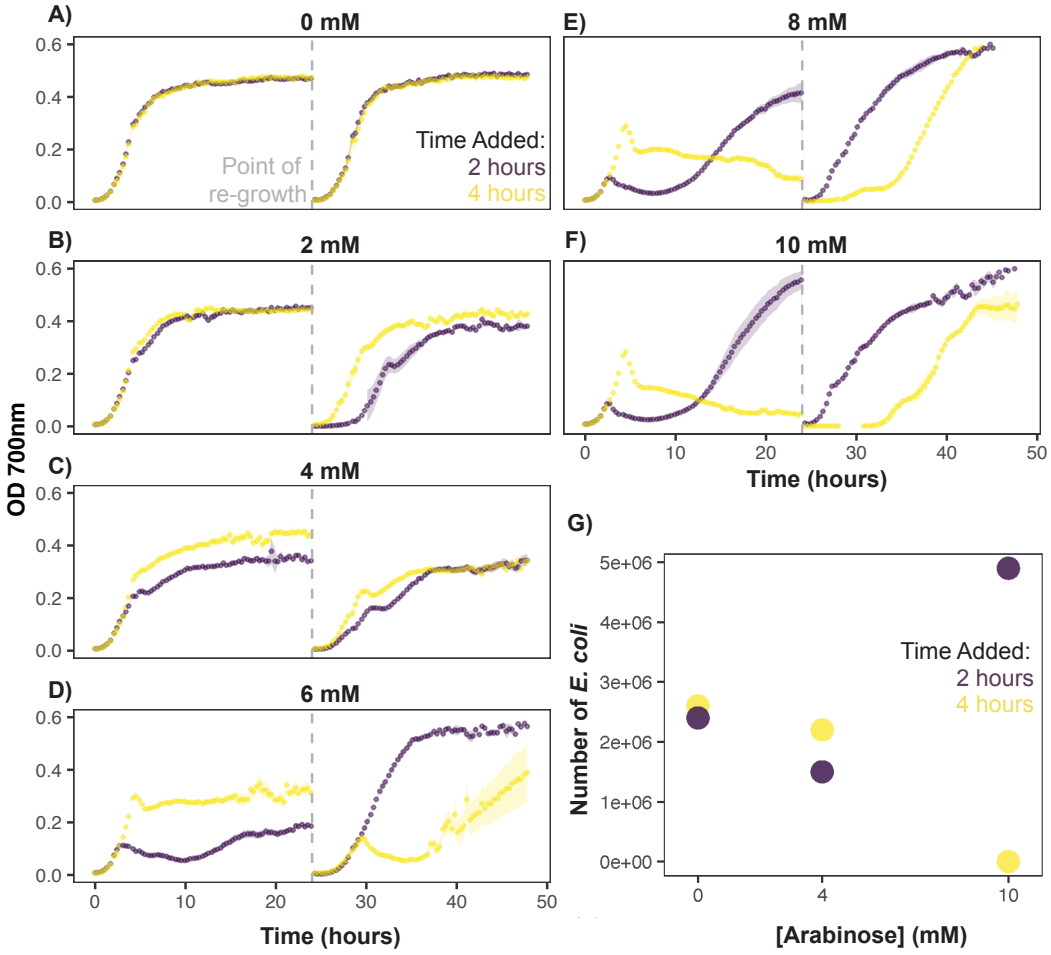

Figure 5.6: Lysara does not respond to re-induction with arabinose

A - F) The Lysara system was induced with arabinose at 2 and 4 hours and incubated for 24 hours (LB medium). The cultures were then diluted into fresh LB medium and re-induced with arabinose at 2 or 4 hours (corresponding to the induction time they previously had). The points are the median values, and the shaded regions are the standard error of the median for triplicate data from one experiment. The panels A - F) are different arabinose concentrations added at 2 and 4 hours. A) control panel no arabinose is added, B) 2 mM, C) 4 mM, D) 6 mM, E) 8 mM, and F) 10 mM. G) These are the colony counts for 0, 4, and 10 mM arabinose after the end of the first experiment at 24 hours. There are less viable *E. coli* cells after the addition of 4 and 10 mM arabinose compared to no arabinose, apart from the 2 hour induction point at 10 mM which appears to be an outlier. The colony count data is one replicate.

5.2.5 Lysara: characterising functional protein expression

The next steps aimed to determine whether a functional protein could be obtained from the supernatant of lysed host cells using the Lysara arabinose-inducible lysis circuit. Lysara cultures were grown in a plate reader and induced with 10 mM arabinose at 4, 6, and 8 hours. These time points were selected based on prior experiments confirming that the circuit lyses effectively at 4 hours, allowing sufficient time for the host cells to express the green fluorescent protein (GFP) [239], used as a marker for protein expression and activity.

In this experiment, GFP was placed under the control of a constitutive promoter (Figure 5.7A). As the host cells grew, GFP accumulated in the cytoplasm. Upon arabinose induction, host cell lysis occurred, releasing GFP into the media. GFP in the supernatant was then measured to confirm the system's ability to express a functional protein and export it into the media through the Lysara system.

Measurements from the different induction time points (Figure 5.7B) demonstrated that GFP could be detected in the supernatant of lysed cultures. Statistical analysis revealed significant differences in GFP levels between uninduced controls and induced cultures at 4 and 6 hours of arabinose induction. However, at 8 hours, no significant difference in GFP levels was observed between the induced and uninduced cultures. This result aligns with expectations, as the Lysara system becomes less responsive to arabinose at higher optical densities, which were reached by 8 hours of growth. The greatest difference in GFP levels between induced and uninduced cultures was observed at the 4-hour induction time point.

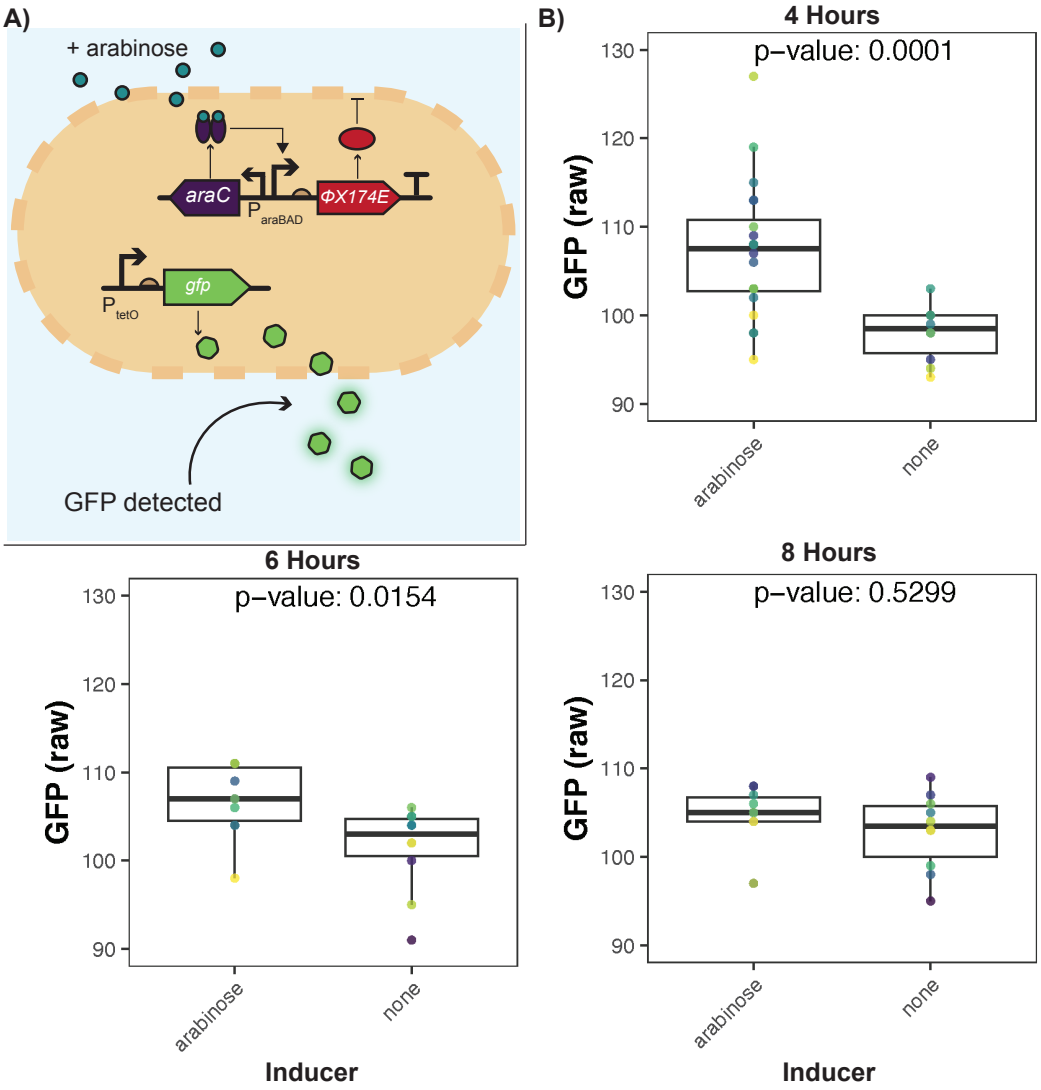

Figure 5.7: Lysara system successfully kills host cells and produces functional GFP protein

A) diagrammatic representation of the dual transformed host, containing both the Lysara circuit and a circuit that expresses green fluorescent protein (GFP) with the bacteriocin, MccV. The GFP circuit is constitutive, constantly producing GFP. GFP is not secreted out of the host cell. When the Lysara circuit is activated by the addition of the inducer, arabinose, the host cell is lysed and the GFP enters the medium. This GFP in the supernatant can be measured with a plate reader. B) the GFP raw values when arabinose is added at 4 hours, 6 hours, and 8 hours. The individual points (different colours) are different wells. The p-values are from the T-test and are displayed on their corresponding panel. The greatest difference in GFP values between induced and un-induced is observed at 4 hours.

5.2.6 Lysara: modelling the lysis circuit

To complement the characterisation experiments, a model of the Lysara system coupled with bacteriocin expression was constructed. The objective of this model was to investigate the relationship between bacterial growth, bacteriocin production, and the timing of arabinose induction. Additionally, the model allowed comparisons between bacteriocin production in secretion-based systems, such as the PACMAN system [90] (secretion is shown in Figure 5.9A), and the Lysara lysis-based system. Alongside comparing the dynamics of secretion of bacteriocins vs lysis of bacteriocins. The secretion system was first modelled at varying growth rates to establish a baseline growth rate for simulating the lysis circuit. Modelling this system provides a valuable framework for predicting responses before experimental testing, offering a preliminary set of parameters for optimal induction timing.

There were models made for two different production systems:

1. Secretion system - equivalent to strains based on PACMAN [90] and SPoCK [102]. The model could be improved by adding a term for secretion rate that models bacteriocins moving from a ‘produced’ to ‘secreted’ state.

2. Lysis system - based on the arabinose-inducible Lysara plasmid.

All simulations were run in Python 3.9.7 with Spyder v5.1.5, using a MacBook Pro (2020, intel core i5, 16GB RAM). The following Table (5.1) lists all of the assumptions made in these models:

Table 5.1: The assumptions made for both models and then assumptions made that are specific to each model

Both Models	**Secretion Model**	**Lysis Model**
All strains follow logistic growth. This ignores any effects that the Lysara plasmid has on the growth dynamics of the host strain.	Any bacteriocin molecules produced are secreted immediately. Therefore, the number of bacteriocin molecules produced in the model is equivalent to molecules secreted. In practice, molecules are likely secreted at a slower rate.	The p_{araBAD} promoter has no leakage. Therefore, no cells are lysed before arabinose is added, and the presence of the lysis plasmid does not affect strain growth.
There is a limit on the internal concentration of bacteriocin molecules that is feasible. This stops bacteriocin production when a threshold has been reached.		Bacteriocin production stops at the point lysis is induced. This likely leads to a slight underestimation of the total bacteriocin molecules released, as not all cells are lysed instantaneously after the addition of the inducer.

Models	Secretion	Lysis
Bacteriocin degradation is negligible. No degradation terms for intracellular or secreted bacteriocins are included in either model.		Lysed cells release 100% of the bacteriocins they have produced. In reality, it is possible that some bacteriocins are not released during lysis.

For the secretion model, bacterial growth was simulated as given in equation (5.1):

$$\frac{dy}{dt} = y\_s(t) \cdot \mu_{Ec} \cdot \frac{1 - y\_s(t)}{A} \tag{5.1}$$

Where y_s(t) is the optical density at each timepoint in the secretion model, μEc is the bacterial growth rate and A is the maximum carrying capacity. Bacteriocin molecules were then produced at a constant rate, as given in equation (5.2):

$$m_b(t) = m_b(t-1) + (y(t) \cdot k_p) \tag{5.2}$$

Where m_b is the total number of bacteriocin molecules produced at each timepoint and k_p is the rate of bacteriocin production. For the lysis system, the logistic growth in equation (5.1) was modified to include a lysis term resulting in equation (5.3):

$$\frac{dy}{dt} = y\_l(t) \cdot \mu_{Ec} \cdot \frac{1 - y\_l(t)}{A} - (y\_l(t) \cdot k_l) \tag{5.3}$$

Where k_l is the rate of cell lysis and is adjusted such that $k_l = 0$ before the addition of the arabinose inducer. Bacteriocin production up to the point of induction was modelled using equation (5.2). The number of bacteriocin molecules released after lysis-induction was simulated by multiplying the number of bacteriocin molecules produced at the point of induction by the fraction of lysed cells, as given in equation

(5.4):

$$m_r(t) = m_b(t_i) \cdot c_l(t)/c_t \tag{5.4}$$

Where $m_r(t)$ is the number of released bacteriocin molecules, $m_b(t_i)$ is the number of intracellular bacteriocin molecules at the time of induction, $c_l(t)$ is the number of lysed cells at time t and c_t is the total number of cells.

The differential equations for the lysis model are shown below. Growth is modelled through a logistic growth equation

$$\frac{dy\_l}{dt} = r \cdot y\_l \cdot \left(1 - \frac{y\_l}{K}\right),$$

where y_l is the optical density (bacterial population size) in the lysis population, r is the growth growth rate and K is the carrying capacity. The induction of lysis is modelled through an inducer-lysis model

$$\frac{dy\_l}{dt} = r \cdot y\_l \cdot \left(1 - \frac{y\_l}{K}\right) - \text{lysis\_factor} \cdot y\_l,$$

where lysis_factor = lytic_rateif $t \geq$ induction_time, otherwise lysis_factor = 0

All parameter estimates are given in Table 5.2 below. For rates of production and lysis the values used were rough estimates from Bionumbers [240]. The values for growth rates, starting OD and carrying capacity were chosen to match the growth curves observed with the PACMAN [90] bacteriocin expression strains.

Table 5.2: Parameter descriptions and values

Parameter	Description	Units	Value
μ_{Ec}	Growth rate of *E. coli*	min^{-1}	0.005 - 0.025
$y(0)$	Starting optical density	OD	0.05
A	Maximum carrying capacity	OD	0.6
k_p	Rate of bacteriocin production	$\text{mols} \cdot \text{min}^{-1}$	-
k_l	Rate of cell lysis	$\text{OD} \cdot \text{min}^{-1}$	-

Validating the production of functional bacteriocins in wet-lab experiments has proven challenging. This model serves as a guide to pinpoint the optimal arabi-

nose induction time, aiming to maximise the concentration of bacteriocin produced within host cells.

The timing of lysis circuit induction is critical. Figure 5.9 presents simulations of three different arabinose induction times: 2 hours (Figure 5.9A), 8 hours (Figure 5.9B), and 16 hours (Figure 5.9C). Early induction (Figure 5.9A) does not allow sufficient bacterial growth. The simulations show that longer growth periods for engineered host cells result in increased bacteriocin production, with cells reaching their maximum intracellular bacteriocin levels by approximately 14 hours (Figure 5.9D).

The simulations suggest that secretion systems yield a higher overall bacteriocin concentration (Figure 5.8). Assuming complete secretion of bacteriocins, the secretion system achieves extracellular levels of approximately $\approx 1.6 \times 10^{13}$ molecules (Figure 5.8, Figure 5.10), with optimal production observed around 8 hours (Figure 5.8B). In contrast, the lysis system reaches extracellular bacteriocin levels of approximately $\approx 0.55 \times 10^{13}$ molecules at 8 hours (Figure 5.9B), which is about 3-fold less than the secretion system at the same time, and $\approx 1.0 \times 10^{13}$ molecules at 16 hours of arabinose induction (Figure 5.9C). From these simulations it is clear that the lysis system will produce less bacteriocin than the secretion system (Figure 5.10) this is important when conducting wet lab experiments, as it may be harder to identify active bacteriocin from the lysis systems.

As anticipated, increasing the growth rate of the host strain correlates with higher bacteriocin concentrations. In these models no fitness burden was assumed for the lysis plasmids, in practice this may not be the case. This may further affect the amount of bacteriocin released. This highlights the importance of considering strain fitness when optimising antimicrobial activity.

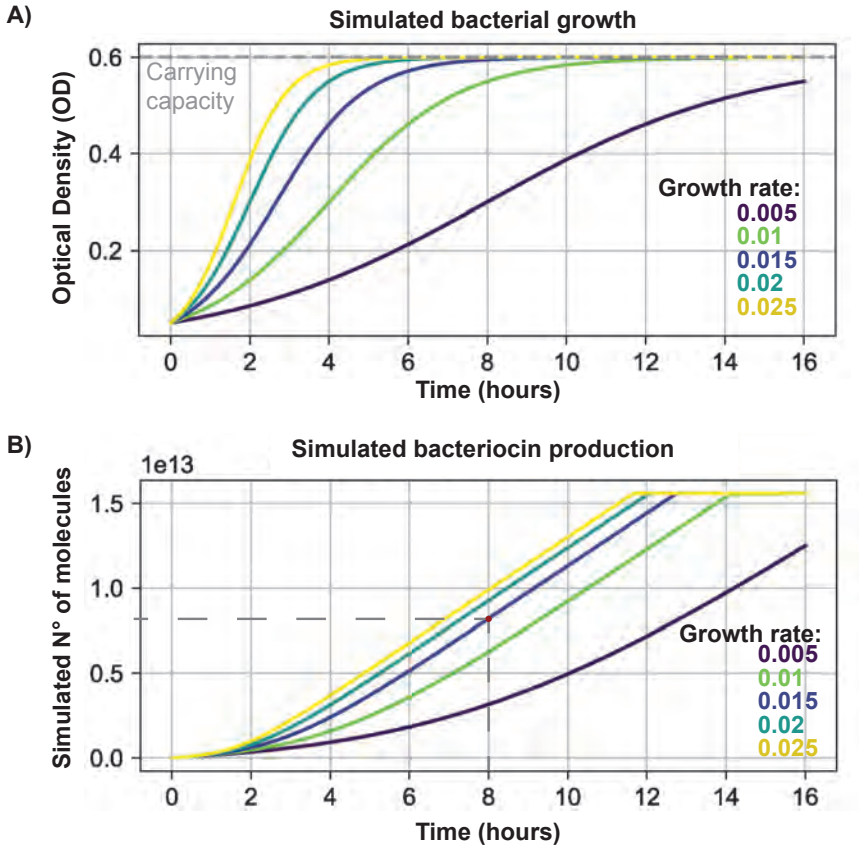

Figure 5.8: Model of the amount of bacteriocin released by secretion

A) Simulated bacterial growth rates. Different bacterial growth rates were tested to observe the effect on the bacteriocin production. B) The simulated bacteriocin production that corresponds to the relevant growth rate is displayed. The faster the growth rate the faster the maximum amount of bacteriocin was produced. However, the time taken to reach the maximum growth rate between 0.025, 0.02, and 0.015 is quite small. There is a bigger effect on bacteriocion production observed with the slowest growth rates 0.0 and the biggest effect observed on bacterial growth and bacteriocin production with the slowest growth rate 0.005. The grey dotted line intercepts the 8 hour induction point of the same growth rate as the simulated lysis circuit shown in Figure 5.9.

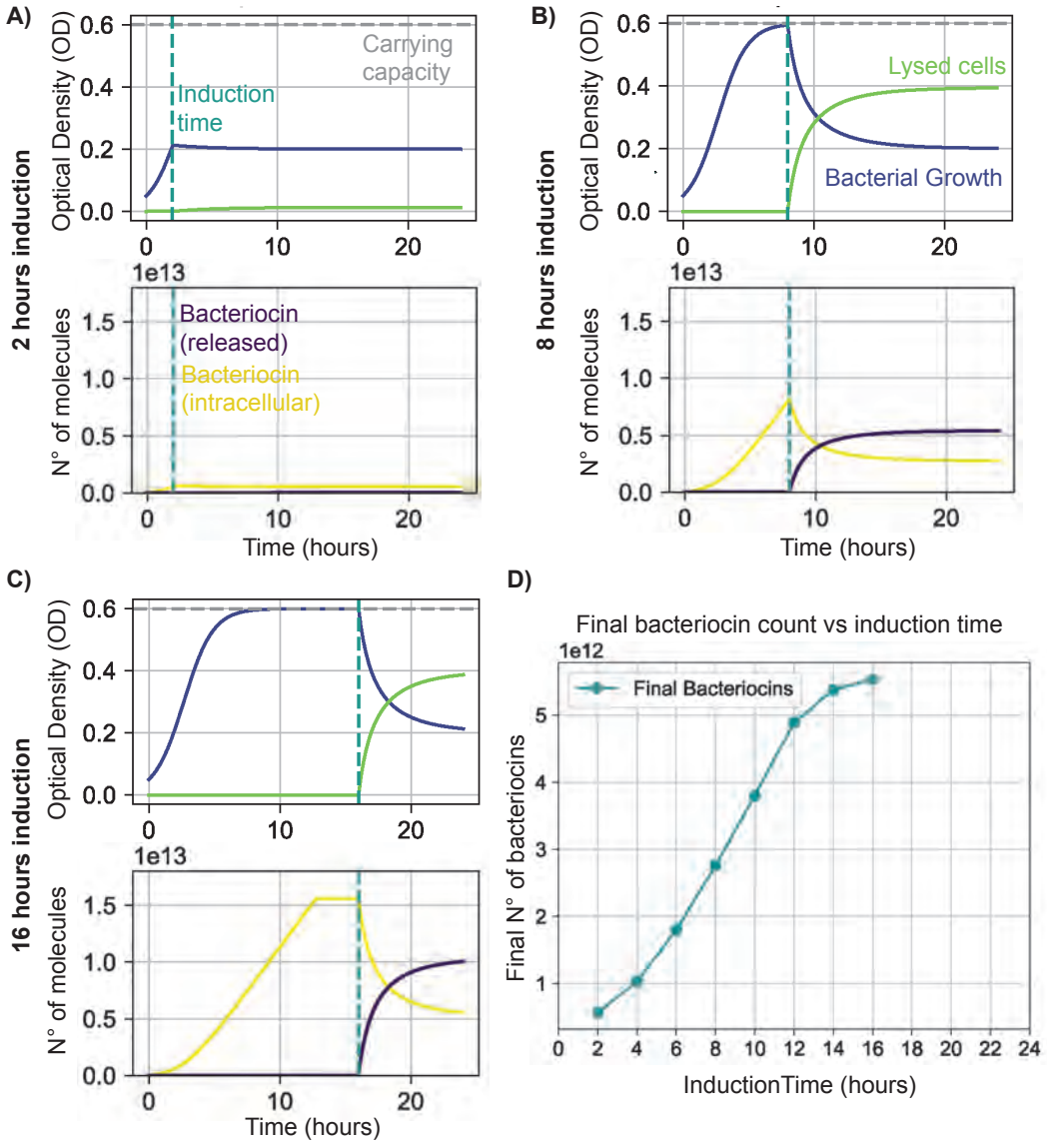

Figure 5.9: Model of the amount of bacteriocin released by lysis

The top panels show the bacterial cell growth over time and the proportion of live cells to lysed cells. The growth rate (dark blue) and the bacteriocin produced (lime green). A) Arabinose induction at 2 hours induction, B) 8 hours induction, and C) 16 hours induction. The bottom panels show the amount of bacteriocin that is intracellular (yellow) and extracellular (purple). The grey dashed line is the carrying capacity of the cell. Arabinose induction is the turquoise dashed line. D) the final count of the bacteriocin produced at each simulated arabinose induction time point.

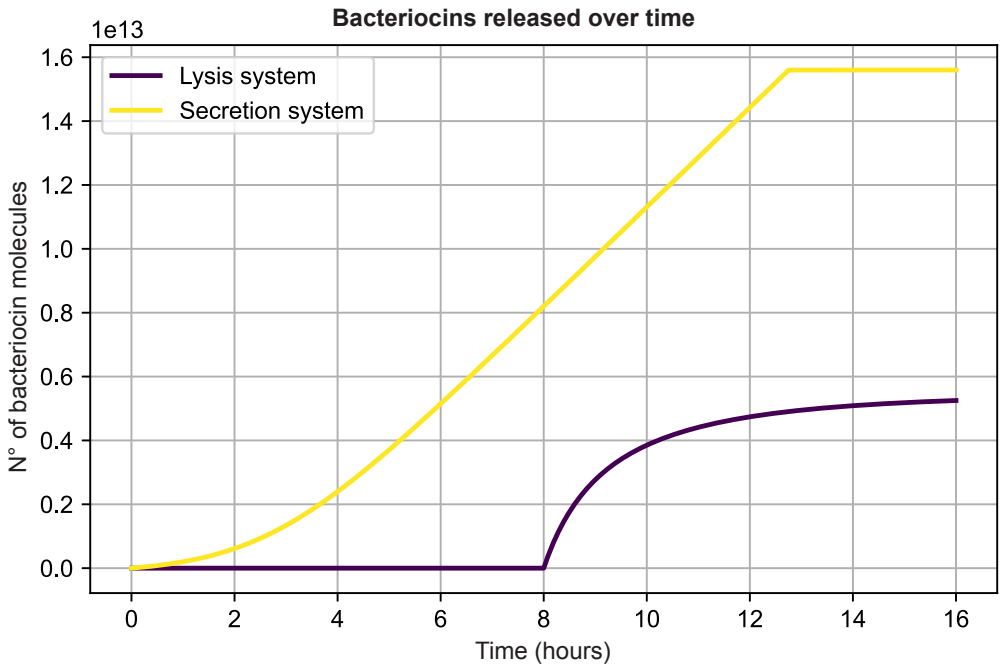

Figure 5.10: Model of the amount of bacteriocin released by the secretion system versus the lysis system

Bacteriocin release by the secretion system (yellow) and the lysis system (purple) over time. The secretion system continuously releases bacteriocin and the lysis system only releases upon induction. The growth rate is set to 0.015 for both systems and lysis induction is set to 8 hours.

5.2.7 Growth analysis of bacteriocin-producing plasmids

Following the characterisation of the Lysara lysis circuit, the next steps involved the construction and testing of bacteriocin-producing plasmids. The bacteriocins Aureocin A53, Bactofencin A, and Garvicin ML were initially expressed from pUC57 plasmids, under the control of a T7 system, and induced by IPTG. Furthermore, Aureocin A53 (A53:moclo and A53ns:moclo) and Garvicin ML (garML:moclo) were successfully integrated into the MoClo modular cloning system, while attempts to clone Bactofencin A into the MoClo system were unsuccessful.

Given the modelling predictions of the Lysara circuit, it was hypothesised that the fitness of engineered strains would impact their growth rates, and thus bacteriocin production. To investigate this, the growth of engineered strains was compared to non-engineered host strains, cultured under bacteriocin-expressing conditions. Growth was monitored over 16 hours through optical density (OD_{700nm}) measurements (Figure 5.11A,B,C).

The engineered strains were divided into two categories: those with constitutive bacteriocin expression and those with inducible expression. The exception was the strain producing MccV, which expressed the bacteriocin constitutively but was not constructed using the MoClo system. Some engineered strains exhibited growth rates comparable to their host controls. For example, the strain containing the MccV MoClo plasmid (mccV:moclo) showed no growth defect relative to its host, JW2142 (Figure 5.11B). In contrast, strains engineered to express Aureocin A53, Bactofencin A, and Garvicin ML displayed reduced growth compared to their host controls.

In *E. coli* NEBExpress, the non-engineered host entered exponential phase at approximately 1.5 hours, reaching a final OD_{700nm} of ≈ 0.6. Similarly, the strain containing the MccV MoClo plasmid exhibited comparable growth. However, the strain carrying the Aureocin A53 MoClo plasmid (A53:moclo) showed delayed exponential phase entry at ≈ 4 hours and reached a lower final $OD_{700nm}$of ≈ 0.5. The strain producing Garvicin ML demonstrated even slower growth, entering exponential phase at ≈ 5 hours and achieving a final OD_{700nm} of ≈ 0.45. To address potential

issues caused by the MoClo system's scar sites, short DNA sequences between genetic elements, a scarless Aureocin A53 plasmid (A53ns:moclo) was constructed. This strain appeared to grow better than the control (Figure 5.11A). However, visible cell debris in the wells interfered with OD_{700nm} readings, a feature confirmed by observing the overnight cultures of this strain, where clustered cell debris was clearly visible in the medium.

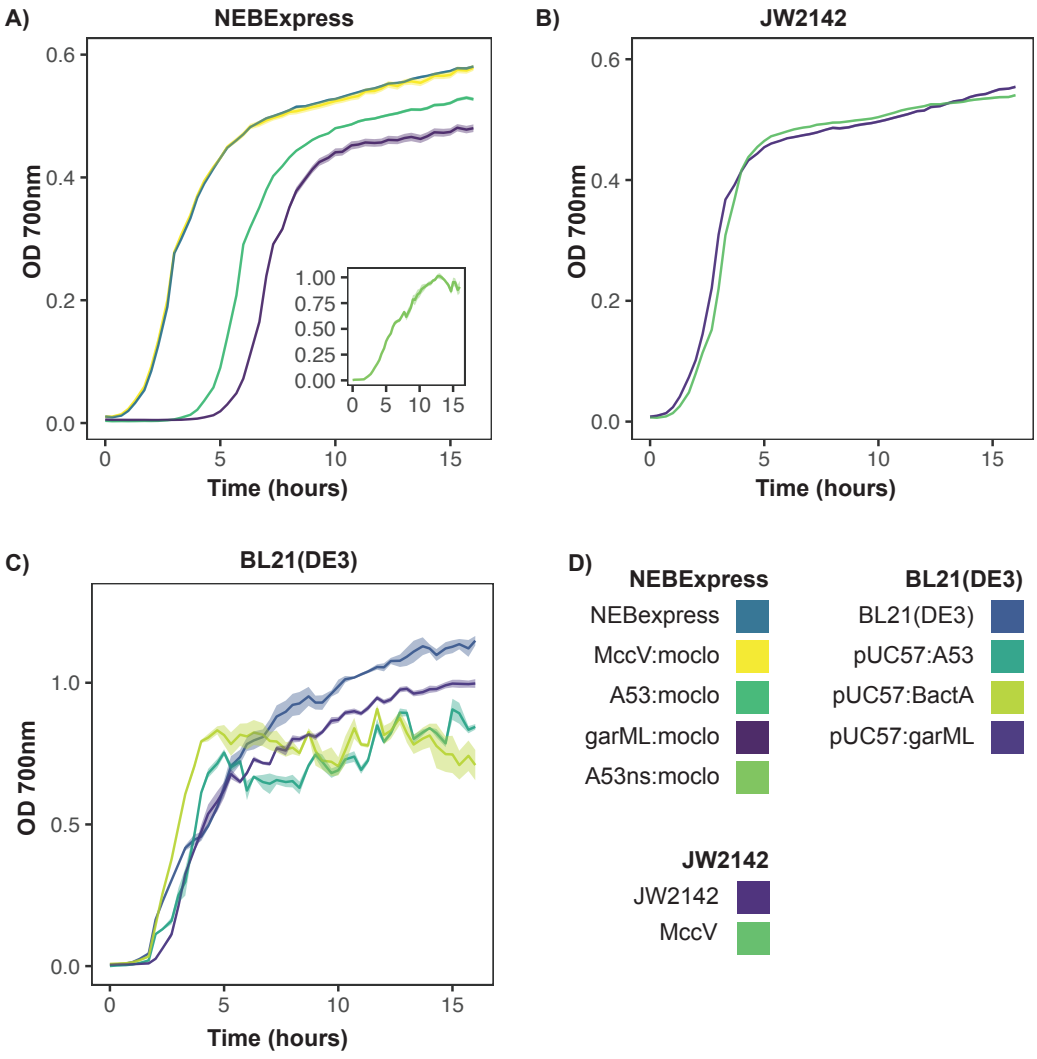

Figure 5.11: Engineered strains have a growth burden compared to controls Engineered strains were characterised in a growth fitness test compared to the non-engineered host controls. All host strains are *E. coli*. A) Strains that were built in NEBExpress. The host control shown here is NEBExpress (dark blue line). Insert: NEBExpress engineered host containing the A53ns:moclo plasmid. B) Strains that were built in the host control, JW2142 (purple line). C) Strains that were built in the host control, BL21(DE3) (blue line). Measurements are OD_{700nm}, the lines are the median of triplicate data, and ribbons are the standard error of the median.

In *E. coli* BL21(DE3), growth of the inducible bacteriocin-producing strains followed a different pattern. All strains, including the host, entered exponential phase at ≈ 2 hours (Figure 5.11C). However, the engineered strains failed to reach the same final OD_{700nm} as the host (final OD_{700nm}) ≈ 1.2). The strain containing pUC57:garML reached ≈ 0.9, while pUC57:A53 and pUC57:BactA reached ≈ 0.75 and ≈ 0.6, respectively. Additionally, the OD_{700nm} readings for these strains were noisy due to the presence of cell debris, likely resulting from cell lysis observed during the experiment.

Overall, while the MccV-producing strain showed no fitness defect either in its MoClo format or the non-MoClo format, strains expressing Aureocin A53, Bactofencin A, and Garvicin ML exhibited reduced growth rates compared to their hosts. The scarless A53ns:moclo plasmid showed promising results but suffered from artifacts caused by cell debris. In *E. coli* BL21(DE3), inducible strains demonstrated consistent exponential phase entry but failed to reach the same final growth levels as the non-engineered host. This gives some insight into the fitness cost of producing different bacteriocins in different hosts and with different expression platforms. It highlights that potentially it may not be possible to find one expression approach for all bacteriocins.

5.2.8 Successful mRNA expression of constructed bacteriocin expressing plasmids

The next critical step after sequencing the constructed plasmids was to determine whether the circuits were functioning as intended. Quantitative PCR (qPCR) was chosen as the optimal method to confirm successful transcription from the constructed plasmids.

The qPCR results confirmed that both the reduced plasmid (derived from the pMPES AF01 plasmid [87], containing MccV and Cvi) and the MoClo plasmid (also containing MccV and Cvi) successfully expressed mRNA (Figure 5.12) at levels comparable to the positive control plasmid, SPoCK1 (pMPES AF01) [87]. For MccV expression, SPoCK1 and MccV(moClo) both displayed fold changes of

4.2, while the reduced plasmid MccV had a fold change of 2.8. For Cvi expression, SPoCK1 and MccV(moClo) reached fold changes of approximately 4.3, while the reduced plasmid had a fold change of 2.8. These results demonstrate that transcription from both the MoClo and reduced plasmids is robust and comparable to established systems.

Despite these transcriptional results, post-transcriptional and post-translational challenges appeared to impact bacteriocin activity. While SPoCK1 exhibited killing activity, no killing of sensitive strains was observed with either the reduced plasmid or the MoClo plasmid.

The lack of observed bacteriocin activity is likely due to differences in release mechanisms. Unlike SPoCK1, which secretes MccV, the reduced and MoClo plasmids rely on lysis mediated by the Lysara system. This lysis-based release bypasses essential post-translational modifications, such as the formation of disulfide bonds, which are critical for bacteriocin functionality. Disulfide bonds typically form in the periplasm [241], and their absence renders the bacteriocin inactive. To address this issue, it is proposed that disulfide bond-forming agents, such as glutathione (GSH) [242], be added during arabinose-induced lysis to facilitate proper folding and restore bacteriocin activity.

In the case of Aureocin A53, the pUC57-A53 plasmid exhibited higher mRNA expression (fold change of 3.5) when compared to the MoClo plasmid expressing A53, which showed a fold change of 1.8.

A reverse trend was observed for Garvicin ML expression. The MoClo plasmid expressing Garvicin ML (GarML(moClo)) showed a higher fold change (5.2) compared to the pUC57-GarML plasmid (4.2). However, despite high mRNA levels, no killing activity was detected for GarML(moClo).

The qPCR results underscore several challenges affecting bacteriocin production and activity, particularly those related to post-translational modifications and plasmid design. Addressing these issues will be essential to improve the reliability and efficacy of the system.

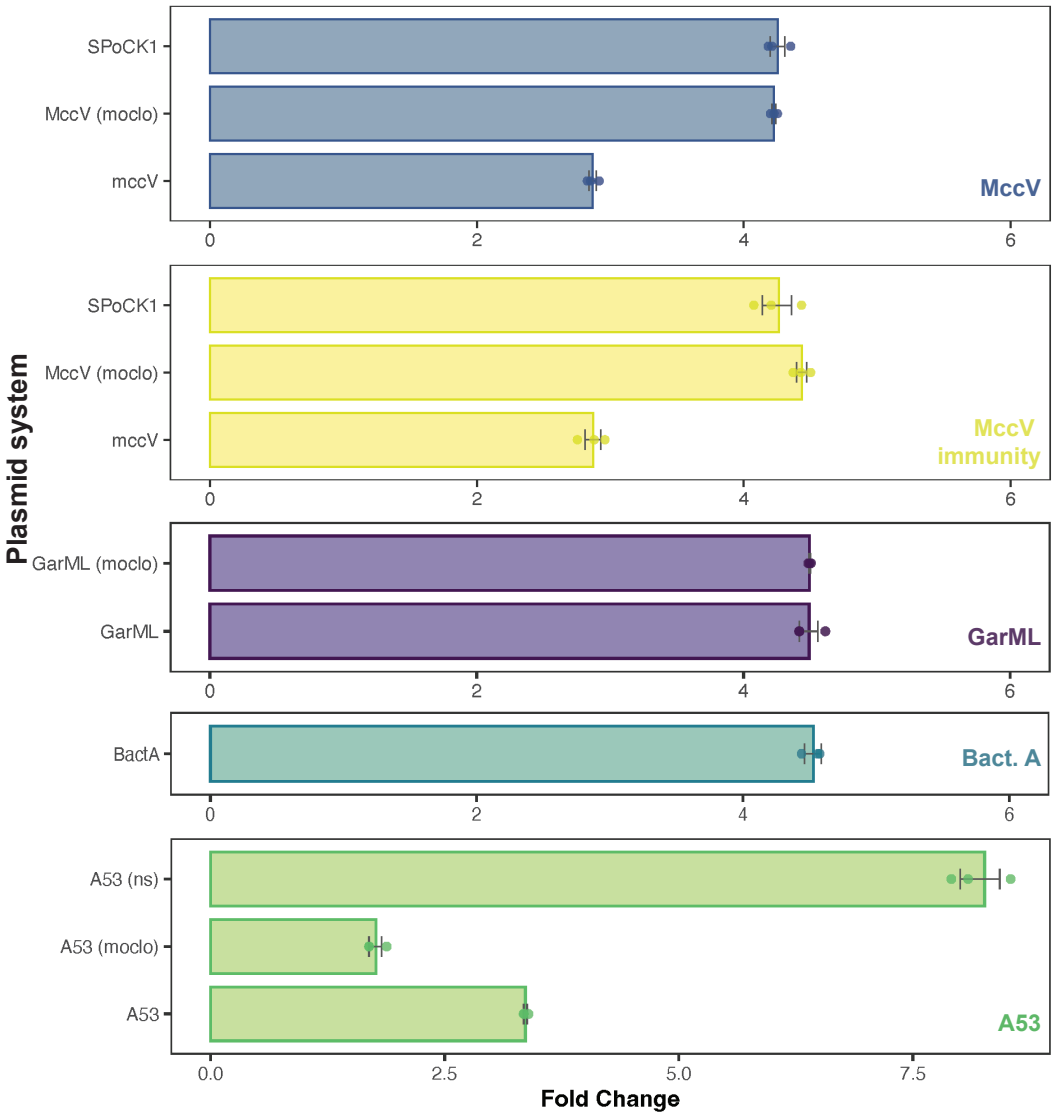

Figure 5.12: Engineered strains are successfully producing mRNA of selected bacteriocins

Fold changes for mRNA expression of bacteriocins tested. Fold changes are relative to the negative controls and adjusted to the house keeping gene *rrsA*. The bars are the mean fold change, the error bars are the standard error of the mean. There are a minimum of 3 replicates for each condition.

5.2.9 Homology match between the MoClo plasmids and the *E. coli* chromosome

To identify other potential issues that could be responsible for the lack of observed killing in the bacteriocin expressing plasmids, the next step was to complete homology mapping. This revealed sequence similarities in the terminator of the Aureocin A53 plasmid construct (A53:moclo) (Figure 5.13). The terminator, B0015, had multiple regions of homology with the *E. coli* genome, which could lead to unintended recombination or interference. To address this, the terminator was replaced with non-homologous sequences such as LS32PI1. It was hypothesised that this would fix issues with protein expression through blocking of any unintended recombination.

Another potential factor interfering with the formation of functional proteins could be the scar sites present in the MoClo plasmids. To address this, a scar-free Aureocin A53 plasmid (a53ns:moclo) was constructed. However, when this plasmid, which lacked scar sites and contained the non-homologous terminator LS32PI1, was sequenced, it revealed a 954 bp insertion. A BLAST search on NCBI identified this insertion as an IS4-like element, specifically the ISVsa5 family transposase, which had integrated between the kanamycin resistance gene and the origin of replication. These are mobile genetic elements capable of excising and inserting themselves without requiring DNA homology [243].

5.2.10 Lysara & bacteriocin expression successfully kill a sensitive strain

To test the functionality of the Lysara circuit in conjunction with bacteriocin production, a dual transformation approach was employed. Cells were transformed with the pUC57-Aureocin A53 and pUC57-Bactofencin A plasmids along with the Lysara lysis circuit. Cultures were initially induced with IPTG to activate bacteriocin expression from the pUC57 plasmids. After three hours, sufficient time for bacteriocin protein synthesis [239], arabinose (10 mM) was added to induce the Lysara lysis circuit. The cultures were incubated for an additional two hours

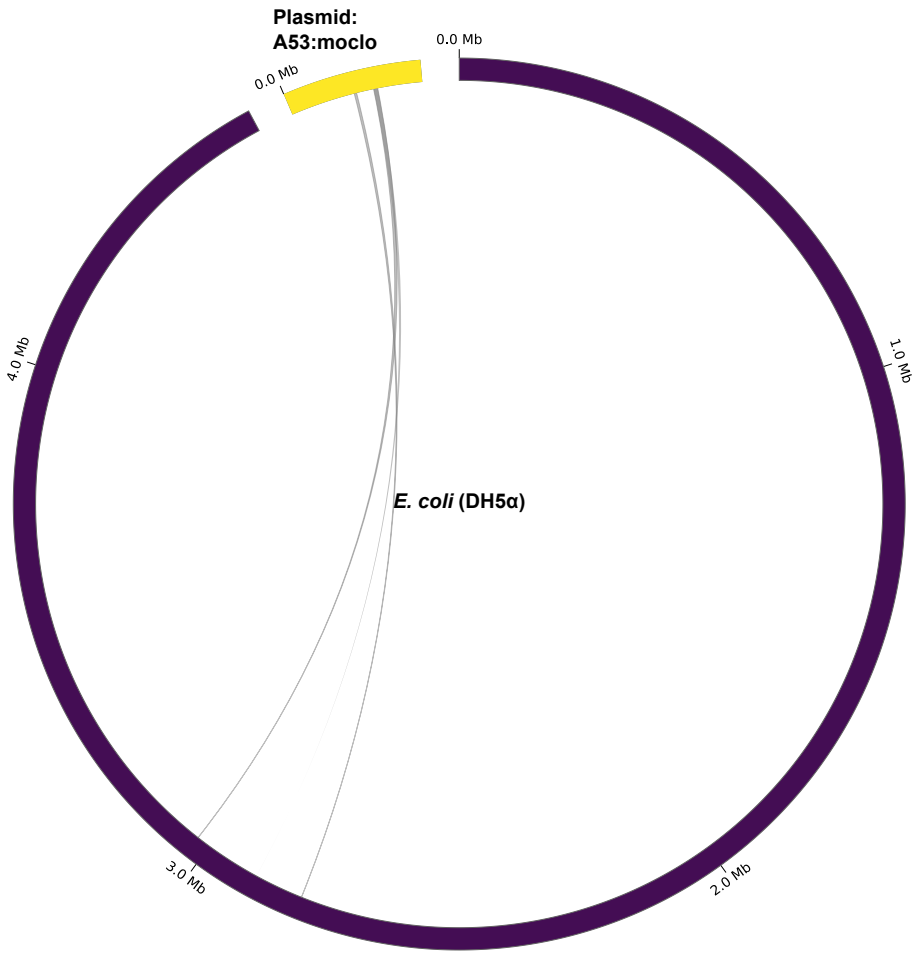

Figure 5.13: Regions of homology between the terminator in the designed moclo circuits and the host *E. coli strains*

The genome map (purple circle) shows regions of homology between the terminators being used in the moclo circuits and the initial host *E. coli* DH5α strain. This is the strain that is designed to be highly competent so is the strain used to build the MoClo constructs.

to allow complete cell lysis before proceeding with centrifugation and ammonium sulphate precipitation to isolate the bacteriocins.

The extracted bacteriocin containing supernatant was applied to a lawn of *B. subtilis* and zones of killing were assessed. Observations revealed distinct zones of inhibition (Figure 5.14B), with Aureocin A53 producing a significantly larger zone of killing compared to Bactofencin A. Quantitative measurements of the zones (Figure 5.14A) further supported these observations: the control (cells containing

only the Lysara lysis circuit) produced a killing zone of 35 mm², which likely represents non-specific effects from lysed cell contents. In contrast, Bactofencin A generated a zone of 93 mm², while Aureocin A53 demonstrated a substantially larger zone of 140 mm².

The other engineered constructs were tested in isolation, without the lysara circuit (Figure 5.14C, D). These engineered systems constitutively produce bacteriocins. They were cultured for 4 hours and then prepared for sonication to mechanically lyse open the cells. However, there was no evidence of any active bacteriocins in the collected supernatant, as there were no zones of killing present on the tested lawns. The A53 producing MoClo strains were tested against the indicator strain *B. subtilis* 168 and the MccV producing MoClo strain was tested against the indicator strain *E. coli* BW25113. These strains were not taken forward from this point as there was no sign they were producing functional bacteriocins.

Overall, while some engineered strains did not demonstrate killing of indicator strains, these results confirm that the Lysara lysis circuit successfully facilitates the release of functional bacteriocins capable of effectively targeting sensitive strains. Unlike naturally occurring systems [70], or previously engineered bacteriocin expression platforms [90], this approach does not rely on secretion tags or specialised export mechanisms. Instead, the lysis system effectively releases multiple bacteriocins while enforcing biocontainment by lysing the host cell during bacteriocin delivery.

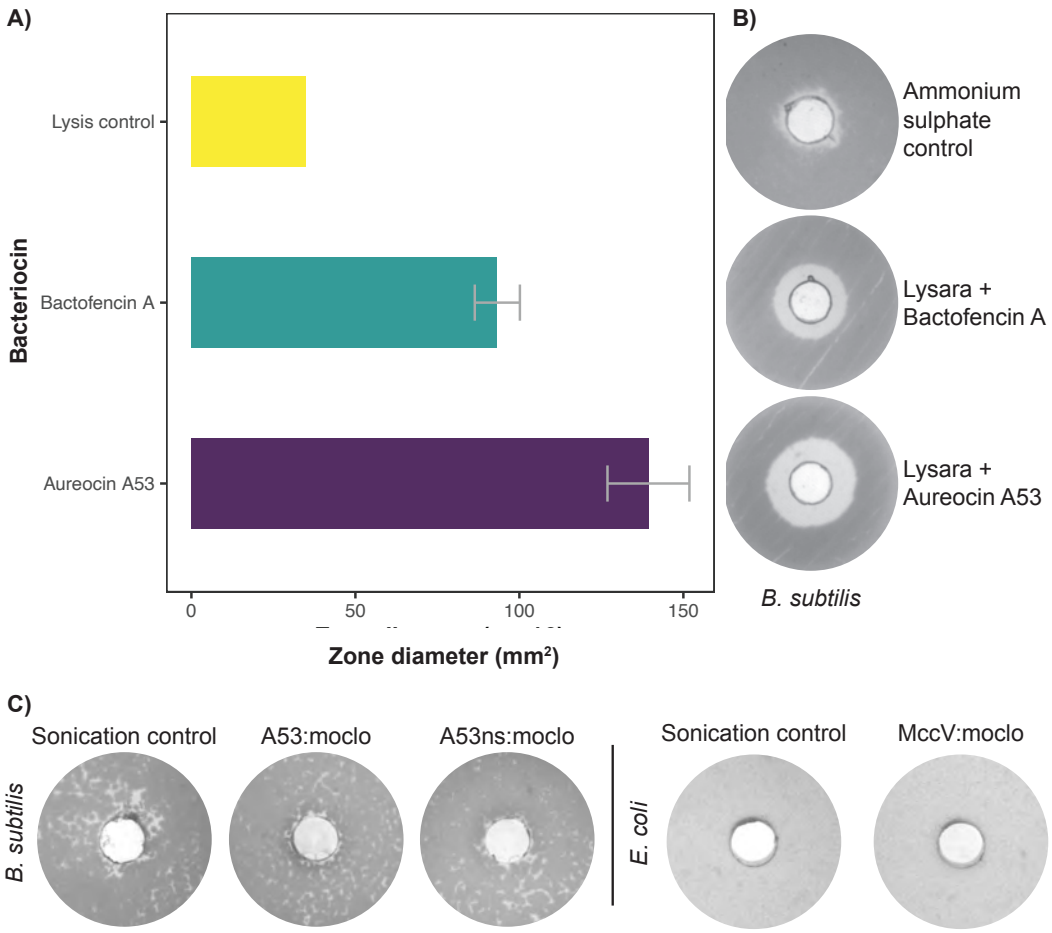

Figure 5.14: Lysara & bacteriocin dual expression successfully kill *B. subtilis*
A) the mean area of the zone of killing on the sensitive strain. The grey error bars are the standard error of the mean. For the Lysara:Aureocin A53 there are three replicates, for the Lysara:Bactofencin A, there are two duplicates, and for the control there is no mean or standard error as only one replicate is plotted. Panel B) the corresponding images of the zones of killing on a *B. subtilis* lawn (sensitive indicator strain) for each condition; Lysara:Aureocin A53, Lysara:Bactofencin A, and the control, Lysara circuit only. Panels A) and B) are from the ammonium sulphate precipitation of the dual plasmid systems, other than the lysis control which is Lysara only (single plasmid). Panel C) the engineered strains tested on sensitive lawn of *B. subtilis*. Panel D) the engineered strains tested on sensitive lawn of *E. coli*. For C) and D) these are the bacteriocin-producing plasmids, the cells were mechanically lysed via sonication.

5.3 Discussion

The work in this chapter represents a step forward in the development of engineered lysis systems and bacteriocin-producing plasmids. It demonstrates both the successes and challenges associated with advancing modular synthetic biology tools. The Lysara circuit, combined with bacteriocin-expressing plasmids, enabled the effective release of functional antimicrobial peptides, as evidenced by the clear zones of killing observed (Figure 5.14B). Notably, the Lysara:Aureocin A53 system displayed robust activity against indicator strains, validating its potential for targeted bacteriocin delivery. While less potent than Aureocin A53, Bactofencin A also demonstrated clear activity against indicator strains when delivered via the Lysara system. The differences in bacteriocin efficacy may be attributed to inherent potency or release efficiency through the Lysara system, both of which warrant further investigation.

Key achievements include the successful integration of the arabinose inducible Lysara circuit with bacteriocin production (Figure 5.14), the utility of GFP as a proof-of-concept reporter for protein release (Figure 5.7B), and the identification of critical dependencies on induction timing and arabinose concentration (Figure 5.5A-F). These findings underscore the importance of tightly regulated lysis systems in achieving precise control over bacterial population dynamics and protein release, crucial for future bio-therapeutic applications, such as engineered live biotherapeutics.

However, several challenges were encountered. Resistance development and variability in lysis efficiency across experimental conditions were notable hurdles. The use of arabinose as an inducer introduced regulatory complexity as it can serve as a carbon source for cells, leading to variable responses. This was further supported by the emergence of resistance (Figure 5.6), suggesting the Lysara system is susceptible to mutational escape. Sequencing of the transcriptional unit confirmed no mutations in the ϕX174E lysis gene E, implying that escape likely occurred in the slyD locus, a known mechanism for evasion of ϕX174E, induced lysis [237]. Whole-genome sequencing could confirm this hypothesis. Potential solutions in-

clude reducing selective pressure through weaker promoters or optimising the promoter system.

Initial exploration of an IPTG-inducible system was abandoned due to promoter leakiness and subsequent resistance in host strains (Figure 5.1). Arabinose was selected next as it has shown promise as a sweetener replacement in food and drink [244], making it safe for use in humans. It was further beneficial as the arabinose inducible system could be dampened with glucose (Figure 5.4), complications likely arose from arabinose utilisation as an energy source. A more suitable inducer for *in vivo* use, such as anhydrotetracycline (aTc), may address these issues. Recent work has demonstrated the utility of aTc-inducible circuits for therapeutic delivery, with complete repression in the absence of aTc and effective induction upon addition of the inducer, alongside methods to detoxify tetracyclines from samples [245].

Due to time and resource constraints, the number of bacteriocins tested was limited. Future work should expand the repertoire of bacteriocins, focusing on those with profiles similar to Aureocin A53 and Bactofencin A, which do not require post-translational modifications or secretion peptides. From the plasmids that did not work (Figure 5.14C, D), it became clear this was likely due to the lack of post-translational modifications e.g. disulphide bond formation that is required for folding and happens in the periplasm, a step that is skipped in the Lysara system. Optimising bacteriocin concentrations is also essential. For instance, concentration curves for Aureocin A53 indicated that oncopathogenic strains such as *F. nucleatum* and *B. fragilis* were less sensitive to Aureocin A53 compared to the gram-positive indicator strain *B. subtilis* (Figure 4.5). This was further corroborated by the zones of killing observed with the Lysara:Aureocin A53 system, which produced a 13.35 mm diameter zone of killing against the gram positive *B. subtilis* (Figure 5.14B). These findings align with previous work showing larger zones of killing (22–24 mm) against the gram positive *Listeria monocytogenes* in the dairy industry [208].

Despite the promising results, the reliance on cell lysis for bacteriocin release raises questions about scalability, consistency, and trade-offs between growth and

lysis. While some systems have achieved lysis with repeated re-induction capabilities such as the synchronised lysis circuit [120], this was not observed with Lysara and could be an area for future investigation. Additionally, co-culture experiments with susceptible strains may provide further insights, as lawn assays and concentration curves suggest higher bacteriocin efficacy in liquid media compared to solid media assays.

In wet-lab experiments, the lysis circuit has displayed inconsistent behaviour across replicates, with the circuit failing to respond when the inducer is added at later time points. This inconsistency is likely due to insufficient arabinose availability at higher optical densities, where arabinose may be metabolised as an energy source instead of inducing the circuit. This phenomenon is not currently captured in the lysis model but could be replicated by adjusting the lysis rate as a function of induction timing.

In summary, the Lysara system demonstrated strong potential, enabling arabinose-induced lysis, effective delivery of functional bacteriocins against indicator strains, and functioned well as a bio-containment mechanism. However, resistance development, variability in responses, and suboptimal bacteriocin concentrations need to be addressed. Future efforts should focus on identifying *in vivo* compatible inducers, optimising induction timing to improve bacteriocin yields, and expanding testing in co-culture systems to maximise the therapeutic potential of the Lysara:Aureocin A53 system.

Chapter 6

Engaging cancer patients on their attitudes towards microbiome engineering technologies

'Who's afraid of little old me? ... Well, you should be'

— Taylor Swift, The Tortured Poets Department

Contents

6.1 Introduction

Responsible research and innovation (RRI) is an integral part of scientific research. It has the ability to ensure the research being conducted is desired by relevant stakeholders and that it delivers on its promises, while minimising future negative outcomes. As stated by the Engineering and Physical Sciences Research Council (EPSRC), RRI accepts that scientific research can: raise questions and dilemmas, be ambiguous, and be unpredictable [246]. To address these points, stakeholders of the research need to be involved early in the experimental process. This aligns with the EPSRCs Anticipate, Reflect, Engage, Act (AREA) framework [247]; where, through stakeholder engagement, research can be modified and ultimately provide a greater benefit to the end users.

In the field of engineering biology, public acceptance has been identified as a general block to advancements in the field [248]. This stresses the need for public engagement early during research to identify and mitigate any concerns that may not have been envisioned by the primary researchers. This is in alignment with the EPSRC RRI initiative and recent studies by the European commission (EC), which encouraged consulting the public on research regarding genetic techniques [249]. Within this study we look at public perceptions of microbiome engineering, specifically for the design of new cancer therapeutics.

Microbiome engineering falls under the broad umbrella of genetic engineering, as it often involves the genetic modification of microbes [250]. Although not yet commonly available, many engineered microbes are undergoing human clinical trials [251]. Despite this promise, and the likely imminent approval of some of these products, there has been limited research exploring the public's attitudes towards these technologies.

In light of this current lack of knowledge, we can look towards previous works on genetically modified (GM) foods as a comparison of general public opinion of genetically engineered products. A sizeable portion of the general population will have come into contact with GM foods, so it is a useful starting point for exploring public attitudes towards genetic engineering as a whole. Public attitudes to-

wards GM foods are complex, with concerns ranging from unexpected long term health consequences to unintentional environment harm. People want to be aware of where and when genetic modifications are being used in the food chain, from genetically engineered animal feed given to livestock to genetically engineered substances present in the final edible product [252]. Furthermore, the public appear to have a greater awareness of the limitations of genetic modifications than they do for the benefits. In some cases, even when the benefits are known, their influence does not outweigh the negative perceptions [253].

Ultimately, GM foods differ from the proposed eLBT medicines both in composition and intended purpose. Although there is some research suggesting that the application of the GM product is less important than the type of gene manipulation involved [254], other research suggests that, within the EU, the way the GM product is applied greatly influence the acceptance of the technology [255]. In addition, it appears that the application of genetic modifications in the context of medicine meets with higher approval than other fields of genetic engineering, including GM foods [256, 257].

An early assessment of sustainability can be used to identify aspects of a research project that need addressing. The results, presented in a RADAR diagram created by the Manchester RRI team, were the first step in this project looking at the views of relevant stakeholders. The RADAR diagram provided numerical scores for project elements and was supported by an initial purposive sampling study.

In the case of engineered live biotherapeutics, the primary stakeholders will be cancer patients. To date, there have been many studies investigating public attitudes towards genetic engineering in foods but few exploring genetic engineering in the context of the microbiome and cancer treatment. The EC's stance on public engagement on genetic techniques coupled with the EPSRC AREA framework, and the current lack of evidence, led us to launch a survey to assess attitudes towards microbiome engineering as a general principle and, more specifically, for the creation of novel cancer therapeutics.

There was one overall aim of this work, to assess current attitudes to micro-

biome engineering in the context of cancer treatment. There were two hypotheses associated with this aim. It was hypothesised that: H1. Individuals that have been personally affected by cancer, are more open to new treatments (H1). H2. Individuals are more comfortable with items they perceive as "natural" over "engineered" bacteria (H2).

6.2 Results

6.2.1 Quantitative survey design

The survey was created using Opino software, with access provided by UCL. The survey questions were designed to ascertain current attitudes of the general public towards using engineered live bacteria in medicine, specifically as part of cancer treatments. The survey contained 21 questions, including the choice to consent, and encompassed quantitative and qualitative question types, from multiple choice tick box answers to open text answers, and questions requiring the participant to rank choices. The first section of the survey contains questions relating to current cancer treatments, the second section of the survey assesses participants prior knowledge on probiotics and microbiome engineering, the final section of the survey measures participants comfortability with different / new concepts for example, CAR-T cell therapies. All patients had to be over the age of 18 and informed consent was obtained from all respondents.

6.2.2 Survey distribution

The survey was promoted on the Cancer Research UK Patient Involvement webpage https://www.cancerresearchuk.org/get-involved/volunteer/patient-involvement/involvement-opportunities/survey-can-we-engineer-live-bacteria-to-treat-cancer). The survey was also advertised on email newsletters by the Patient Experience Research Centre https://www.imperial.ac.uk/patient-experience-research-centre/ and Independent Cancer Patients Voice Network http://www.independentcancerpatientsvoice.org.uk/. The survey was also shared and re-tweeted on X (formerly Twitter). The survey questions are available in the appendix (E).

Table 6.1: Definitions of key terms

Word	Definition
Bacteria	Bacteria are small organisms, or microscopic living things, that can be found in nearly all natural environments. They live on our skin and inside our bodies. Some bacteria may cause infection and disease. However, many other bacteria help us to digest our food, produce vitamins (such as B12 and K) and fight off other bacteria.
Probiotics	Probiotics are live microorganisms (such as bacteria) that are intended to have health benefits when consumed or applied to the body. They can be found in fermented foods, dietary supplements, and beauty products. Probiotics have so far shown some promise in the treatment of diarrhoea, bacterial vaginosis, and irritable bowel syndrome (IBS).
Microbiome Engineering	A microbiome is a community of microorganisms (bacteria, fungi, etc.) that live together within a specific environment, like the human gut. Microbiome engineering aims to modify these communities in a predictable way, for example, for the treatment of diseases within the body. There are currently many ongoing clinical trials for the treatment of disease with live microorganisms.
GMO	A genetically modified organism (GMO) is any organism which has had its genetic material, or DNA, modified in a laboratory. Genetically modified crops are routinely produced and consumed in the USA, though not yet in the UK and Europe. As microbiome engineering may involve the use of GMOs, the following questions will explore your opinions on the use of GMOs.

6.2.3 Data analysis

The survey Closed on 31st December 2022, 23:59. The collected data was downloaded using Opinio software as an csv file and quantitative data analysis performed in R (version: 4.1.2). Incomplete submissions and respondents with no personal connection to cancer (either first or second hand) were removed from further analysis.

For qualitative data, in the form of short text answers, thematic analysis was conducted [258]. This analysis was performed following the 5 steps of thematic analysis as detailed by Braun and Clarke 2006 [258]: 1, read the data and identify

codes, 2, code the data, 3, identify themes, 4, review the themes, 5, define and name the themes (6.2). An inductive coding approach was used as this is data led and we did not know what themes to expect (deductive coding) (6.2.

Theme	Definition
Trust	Explicit mentions of trusting health care professionals and their recommendations.
Social connection	Considering the impact of this technology on the self and on other people.
Optimism	Positive tone in responses towards microbiome engineering. There is excitement and hope towards these technologies.
Understanding	Participants express their lack of knowledge or desire for more information on a topic that is new to them.

Table 6.2: Themes and their definitions identified during the thematic analysis of the qualitative open text responses in the survey.

Statistical analyses was performed in R (version: 4.1.2). Firstly, the responses to each question were grouped into comfortable (mildly comfortable and very comfortable), uncomfortable (mildly uncomfortable and very uncomfortable) and unsure (do not know and neutral). A Fisher's Exact test was then performed on the grouped responses for each relevant question 6.2.11. All conditions tested were assessing against whether the respondent was comfortable with using eLBTs to treat cancer in future.

Data visualisation was performed in RStudio (version: 2022.07.2, [136]), using the ggplot2 package[137] and Adobe Illustrator (version: 28.5).

6.2.4 RADAR diagram

The following definitions (6.3) were used to construct the RADAR diagram in collaboration with the Manchester based RRI team as part of the early assessment of sustainability workshop hosted as part of the CDT in BioDesign Engineering [259].

Table 6.3: Definitions and descriptions of the terminology used in the early assessment of sustainability

Keyword	Description/Definition
feedstock	sources, availability, cost, geography, community, and environmental impacts
process	extraction/purification, cost, intellectual property, industrial disruption, and consumer responses
product/outcome	functionality, characteristics, cost, market competitiveness, geography, community, consumer response, environmental, and end-of-life implications
Traffic Light System	
Green	This project looks good for this aspect given current understanding.
Amber	There is not enough yet known to judge whether this project/target will deliver satisfactorily for this aspect.
Red	The current evidence suggests this project will face problems for this aspect.

6.2.5 Limitations of study

This study was designed as a preliminary exploration of public opinion towards microbiome enegineering technologies. The study did not collect any ethnicity, socio-economic or geographical data. Coupled with the limited number of responses to this survey, it is not possible to draw detailed conclusions of how different factors impact on a the publics willingness to accept these new technologies.

6.2.6 Literature search

Search terms “public attitude microbiome engineering” “public attitudes genetic engineering”, “public attitudes genetic engineering medicine” On Google Scholar and NCBI.

6.2.7 Study Design

The use of purposive sampling was to ensure the survey was fit for purpose and that the questions put to the public would answer the hypothesis we designed (Appendix E). There were 108 complete responses from the trial of purposive sampling. This was expected because the purposive sampling was primarily friends and family. The majority of respondents were 18 - 39 years old (Figure 6.1A) and were predominantly associated with cancer through a second hand relationship (Figure 6.1B). Surgery ranked as the most comfortable cancer treatment option available, closely followed by immunotherapy. Unsurprisingly, doctors were ranked as the most trustworthy source of information and the large pharmaceutical companies the least trustworthy. In these groups most people have heard of and understand the benefits of probiotics but were almost split 50:50 regarding awareness of the limitations. More than 70 respondents said they would/do take probiotics to supplement their diet and/or to treat a medical condition. Importantly, 75% of respondents said they approve of microbiome engineering technologies (Figure 6.1C). This dropped for approval of GMO foods to 54% (Figure 6.1C) which, as discussed previously, is expected as public acceptance of GMO is generally lower. Promisingly, using engineered human cells and natural bacterial cells to treat cancer was met with great

support, over 80% of respondents felt comfortable using either of these (Figure 6.1D). Only slightly less was observed for engineered bacterial cells, at 76% (Figure 6.1D). These initial purposive sampling results gave some insight into what would be expected of the formal public engagement survey. However, as mentioned, this sampling contained friends and family, university attendees, and healthcare professionals to a higher extent. This explains the overwhelmingly positive attitude towards microbiome engineering observed in these results. These results do not reflect the general public, by age, cancer relationship, or background. However, the purposive sampling ensured the functionality of the survey and enabled initial testing of the output. This lead to the successful launch of the survey onto publicly available platforms.

6.2.8 Demographics of survey respondents

The survey received a total of 102 full responses. Due to the small sample size, responses from participants that had no connection to cancer (5) were removed from further analysis. More than half of the remaining participants were over the age of 60 (59%). A quarter of participants were between 40 and 59 years old (24.4%), the remaining participants were between the ages of 18 and 39 years old (16.5%). A full breakdown is given in figure (6.2). This was a better spread of ages compared to the purposive sampling, but leaned more towards the older age bracket.

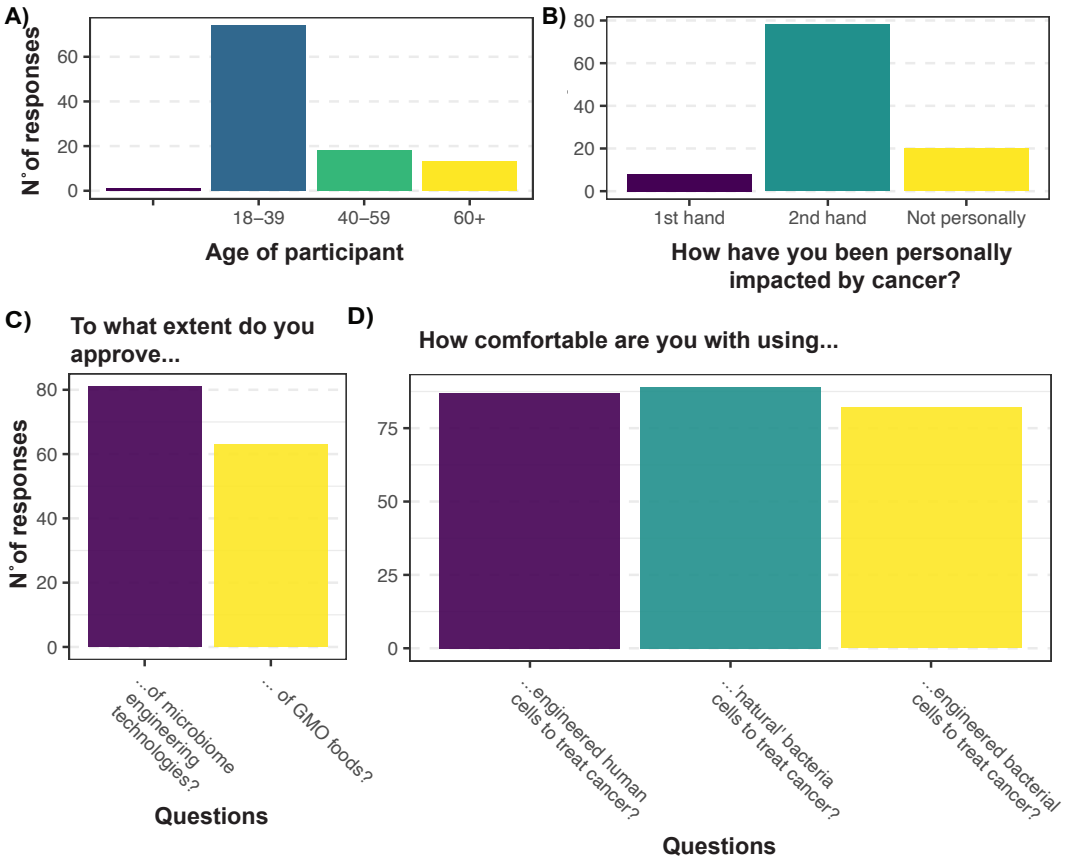

Figure 6.1: Initial results from the purposive sampling are not representative of the general population

A) Age distribution of the participants of the purposive sampling. B) The participants relationship to cancer, 1st hand being they have had cancer, 2nd hand being they know a close relation (friend or family) who has had cancer, or no personal connection. C) The number of participants who approve of microbiome engineering and GMO foods as a principle. Mildly approve and strongly approve were combined for this. D) The number of participants who are comfortable with using engineered human cells, natural bacteria or engineered bacteria. Mildly comfortable and very comfortable were combined.

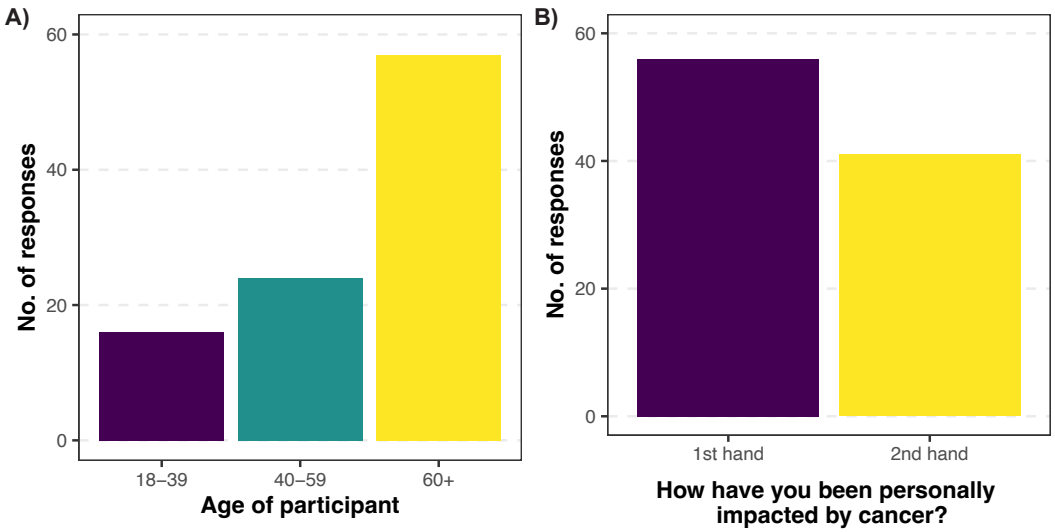

Figure 6.2: Demographic information collected from the survey
The demographics of the participants of the survey. A) The ages of the participants. B) The relationship to cancer for each participant. 'No connection to cancer' was removed as the sample was too small and would contaminate the rest of the results.

6.2.9 Prior knowledge of concepts

All participants were provided with definitions of the key concepts explored in the survey (these definitions are provided in the Supplementary Information) and then asked to state whether they had previously heard of the topics. The majority of respondents (95) had previously heard of probiotics. It is clear that probiotics are a well known concept; for example the term 'probiotic' is often associated with dairy foods. In addition, during the initial Covid-19 outbreak, market reports predicted an increase in interest of probiotics within the food industry as the public associated probiotics with increased immune health [260]. This was confirmed by a Chr. Hansen study, which highlighted the consumer view of probiotics and positive views on how live bacteria can benefit human health [261]. This was further reflected by the fact that 86 respondents indicated they were aware of the proposed benefits of probiotics, whereas only 41 were aware of the limitations. This may indicate that probiotics do not have the negative connotations that surround GM foods. A further 72 respondents reported they would be comfortable taking probiotics as part of their diet, but only 64 would be comfortable taking them to treat a medical condition (Figure 6.3). This conflicted with some of the open comments, which suggested greater comfortability with genetic engineering in the context of medicine. One respondent also highlighted a perception that the regulatory governance of medicine is more robust than that of food products:

> *"I am far more comfortable as I believe the regulatory rigour / approval / testing etc to be higher"* – 2nd hand experience of cancer (40-59 age group).

In contrast to the widespread knowledge of probiotics, only 49 respondents had previously heard of microbiome engineering- suggesting the term is not yet commonly known.

6.2.10 Attitudes towards current cancer therapies

Firstly, we set out to check which sources prospective patients would trust for advice on cancer treatment. Overall doctors and clinicians were ranked as the most

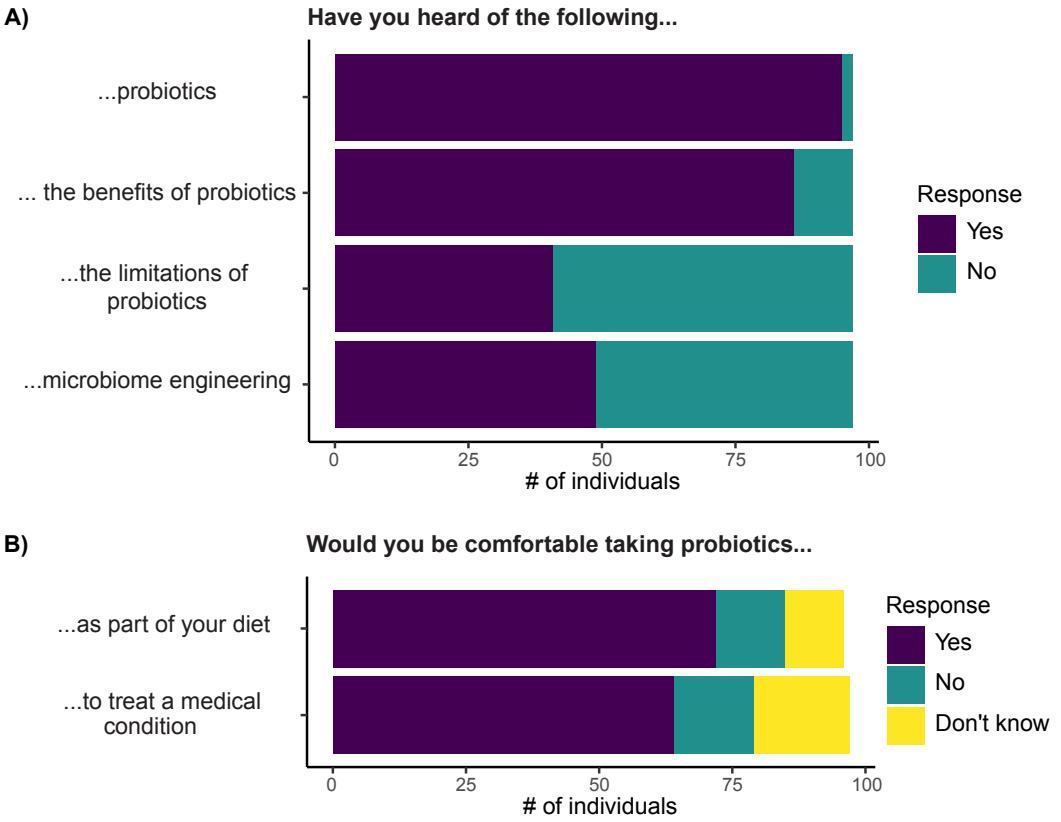

Figure 6.3: Comfortability of taking probiotics
A) Gauging the previous knowledge of the respondents regarding probiotics, their benefits and limitations, and microbiome engineering. B) Whether the respondents would be comfortable taking probiotics, either as part of their diet or to treat a medical condition.

trustworthy source (Figure 6.4A) this followed the same pattern of the purposive sampling results.

Pharmaceutical companies were ranked as the least trustworthy. This corroborates previous studies which investigated patient trust in healthcare professionals [262]. This is important as it highlights the sources of information patients trust and how future policy makers would be best positioned to deliver information on new therapeutics going forward. The theme of trust was prevalent in the open text answers, where the word was explicitly used 10 times. Many comments focused on trust in medical teams, with respondents indicating they are open to new treatments that are recommended by their clinicians:

"I'm intrigued and if my consultant recommended such treatment, I would

consent to it." – 1st hand experience of cancer (40-59 age group).

"I trust the doctors, surgeon and support team (nurses, dietitians etc) to make the choice that would aim to result in the best outcome for me." – 1st hand experience of cancer (40-59 age group)

"I'd be perfectly comfortable if clinician suggested the microbiome route." – 1st hand experience of cancer (60+ age group)

Next, we explored the cancer treatment options that respondents would be comfortable taking as part of their treatment plan. Of the treatment options provided, respondents were most comfortable with surgery, closely followed by immunotherapy (Figure 6.4B). This mirrors the previous purposive sampling results. Chemotherapy and radiation therapy were the most unpopular options. This is likely due to awareness surrounding the adverse side effects that are associated with these treatments. Although, it should be noted that over 70% of the respondents still indicated they would be comfortable with these treatments if available to them. Despite our hypothesis that live bacterial therapy would be a less popular treatment option (due to a lack of precedent for its use), a total of 77 respondents stated they would be comfortable with this treatment option. However, the issue of side effects comes up frequently in the open text comments (16 times). This links to a broader theme of social connection seen amongst the responses from participants. They are not only concerned about their own response to new therapies but also about how others may be affected, especially when potential side effects remain uncertain.

"If the microbiome can be modified in a predictable way that is beneficial to health I would be very comfortable with their use. However, most treatments have drawbacks or side effects. Without knowing what these might be I cannot be sure of whether I am comfortable with the technology." – 2nd hand experience of cancer (60+ age group).

"The knowledge of biology of microorganisms and the microbial engineering techniques need to improve in order to ensure that there are not side effects." – 2nd hand experience of cancer (18-39 age group).

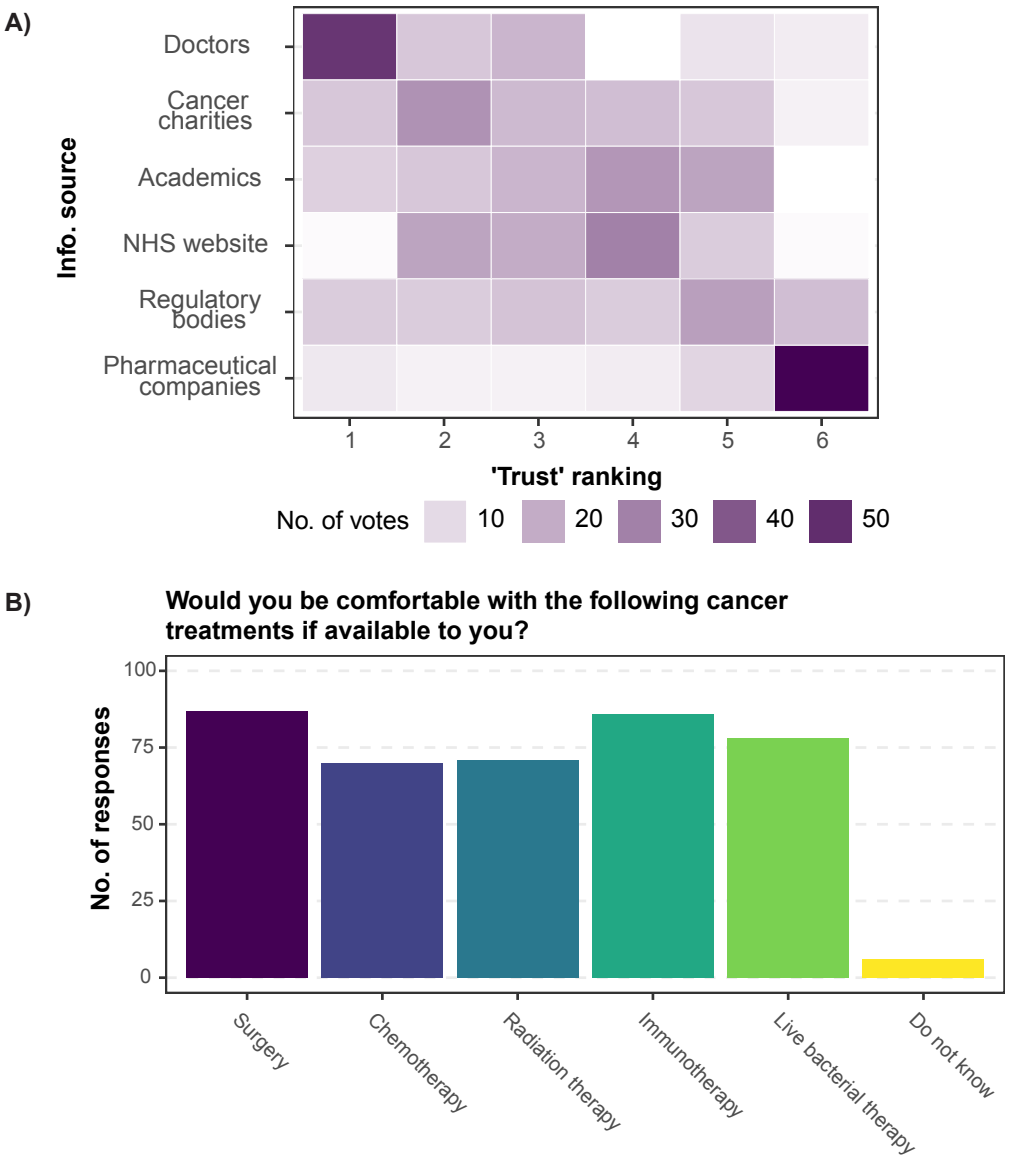

Figure 6.4: Participants trust clinicians

A) The trust square, ranked so that the information source rated the most trustworthy is at the top, and the least trustworthy is at the bottom. B) Participant responses on how comfortable they would be with cancer treatments, including live bacterial therapies.

"...would want certainty that this would not adversely impact anyone else eg future generations." - 1st hand experience of cancer (60+ age group).

6.2.11 Attitudes towards bacterial therapies

Following the positive overall attitude towards live bacterial therapies, we investigated whether these perceptions changed based on different situations. To this end, we asked participants to rank how comfortable they would be with using a number of different technologies (Figure 6.5). The majority of respondents stated they would be comfortable using microbiome engineering technologies in general. However, the majority of respondents stated they would be uncomfortable taking GM foods as part of their diet. This matches with previous responses and studies, highlighting the negative connotations associated with GM foods. The majority of participants stated they would be comfortable using engineered human cells to treat cancer (for example CAR-T therapy) and a similar response was seen towards using 'engineered' bacteria to treat cancer. An interesting comment from one participant highlighted how they had not perceived CAR-T cell therapy as a form of genetic engineering at all, potentially this led to them having less reservations regarding this kind of treatment over the proposed microbiome engineering techniques presented in the survey. This is perhaps a reminder that the terms used to describe these future treatments greatly impact whether or not they are positively perceived.

"Am very comfy with the concept of CAR-T, funnily enough have never thought of it as genetically modified cells" - 1st hand experience of cancer (40-59 age group)

Notably, more participants indicated they would be comfortable using 'natural' bacterial therapies than either engineering human cells or bacteria. This coincides with a previous work by the Nuffield Council on Bioethics which found some people do view natural medicines as safer, healthier, and more likely to do good than alternatives [263].

Participants who stated they were comfortable with the use of GM foods were found to be more likely to be comfortable with the use of engineered bacteria. There

was a positive correlation between those comfortable using engineered human cells and engineered bacteria. No significant correlation was found between age or relationship to cancer and comfort with using engineered bacteria (6.4). A full breakdown of the statistical analysis performed is given in the methods (6.2.3).

A united theme, among many of the free text answers, was the need for more information. The participants showed the desire to better understand this possible new treatment option. This theme of understanding, whereby participants expressed the desire to know more information regarding this treatment, or that they did not have the knowledge to assess this potential treatment for themselves, was prevalent across the age groups. There is a need from these participants to better understand what these treatments are and a need to correct misinformation. In some responses there was confusion between GM food and live engineered bacteria. This only serves to highlight how any new treatment needs to be accompanied by information campaigns, and that this is something patients want.

> *"It sounds promising, but i would want to know more about a treatment before accepting it."* - 1st hand experience of cancer (60+ age group)

> *"Agree with the theoretical principle but would need to have a lot more info before deciding to use it personally"* - 1st hand experience of cancer (40-59 age group)

The final identified theme centred on optimism towards these new therapies, with 22 comments connected to this theme. Many comments mentioned excitement and hope that these new therapies could bring about improvements in the current standard of cancer care.

> *"Microbiome engineering sounds very promising and far less invasive than some other treatments."* - 2nd hand experience of cancer (60+ age group)

> *"I think this would be a huge step forward. Being able to manipulate bacteria in a way which gets the body itself to fight the disease would be incredible."* - 2nd hand experience of cancer (40-59 age group)

"I'm a great believer in the human body's ability to use its own resources to counteract disease, and this is mobilising them with perhaps a little modification to do just that." - 1st hand experience of cancer (60+ age group)

"Modified bacteria have already shown they hold great potential." - 1st hand experience of cancer (60+ age group)

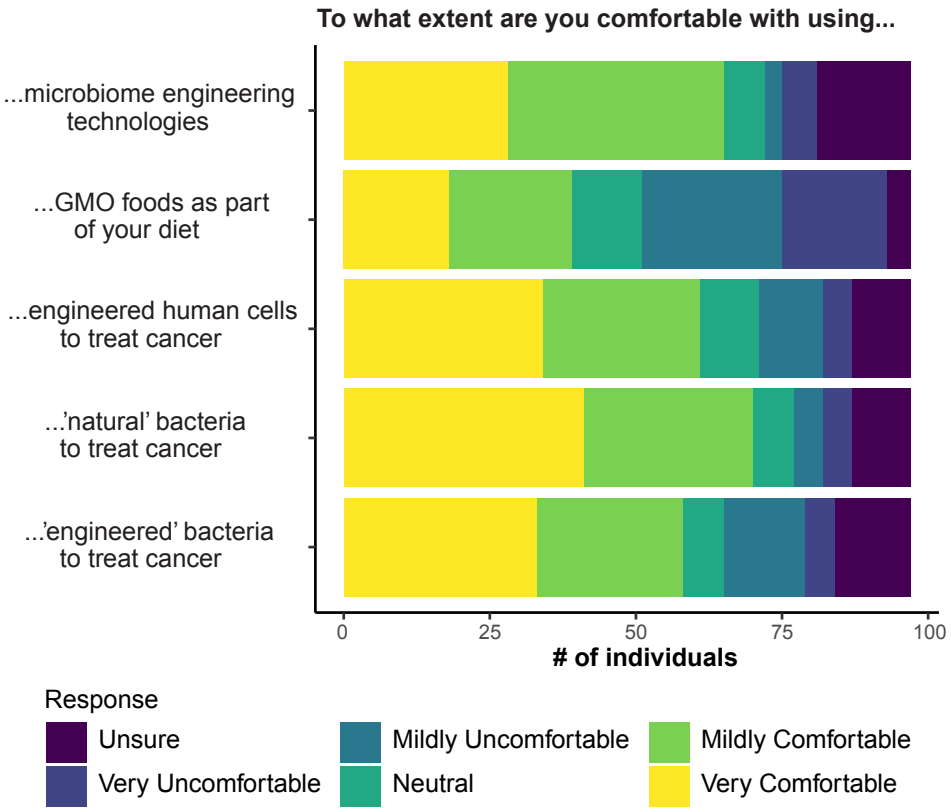

Figure 6.5: Comfortable with microbiome engineering and engineered live bacterial therapies

The participants responses to how comfortable they would be with using engineered cells (human or bacterial) in their diet or as part of a treatment plan. The response options are kept as they appear in the survey.

Table 6.4: Positive correlations exist between participants' opinions on GM foods or engineered human cells and whether they are comfortable with using engineered bacteria to treat cancer. No significant correlations exist between age or relationship to cancer and whether they are comfortable using engineered bacteria to treat cancer. The provided values are p-values from a two-sided T-test, with a p-value below 0.05 indicating statistical significance.

	Are you comfortable using engineered bacteria?		
	Number of participants (%)		
Characteristic	**Comfortable (n=58)**	**Uncomfortable (n=19)**	**p-value**
Age			0.4946
18 – 39	12 (%)	3 (%)	
40 – 59	15 (%)	5 (%)	
60+	31 (%)	11 (%)	
Fisher's Exact Test, Alt. hypothesis: 2 sided			
Relationship with cancer			1
First-hand relationship	33 (75%)	11 (25%)	
Second-hand relationship	25 (76%)	8 (24%)	
Fisher's Exact Test, Alt. hypothesis: 2 sided			
Comfortable with GMO			0.0039
Comfortable	30 (94%)	2 (6%)	
Neutral	2 (100%)	0 (0%)	
Uncomfortable	26 (60%)	17 (40%)	
Fisher's Exact Test, Alt. hypothesis: 2 sided			
Comfortable with engineered human cells			<0.0001
Comfortable	51 (93%)	3 (7%)	
Neutral	7 (78%)	2 (22%)	
Uncomfortable	0 (0%)	14 (100%)	
Fisher's Exact Test, Alt. hypothesis: 2 sided			

6.3 Discussion

Following the increase in clinical trials investigating the efficacy of using genetically modified bacteria to treat cancer, we wished to explore public attitudes towards these technologies. An initial purposive sampling study was conducted in order to ensure the suitability of the questions. Personal contacts such as friends and family completed this study. As expected from a sample such as this, most responses were positive. However, they did not reflect the attitudes of the general public, as the sample did not cover a range of ages and cancer relationships. The point of the purposive sample was to ensure the survey functioned and the output usable. In this regard, the purposive sample was successful and led to the launch of the main survey in the public domain.

It should be noted that the formal survey only received a total of 102 full responses and, due to this limited sample size, may not be representative of the wider public in general. However, the responses still provide a valuable insight into public perceptions surrounding these newly emerging technologies. The majority of participants in this study were comfortable with the concept of live bacterial therapies (both 'natural' and 'engineered') as cancer treatments, despite a lack of previous knowledge of these terms in some cases. In addition, positive correlations indicated that participants who are comfortable using GM foods or engineered human cells to treat cancer are also more comfortable using engineered bacterial therapies.

To further understand the attitudes of the participants towards microbiome engineering and engineered live bacterial therapies, we included open text questions. To identify the main themes of these responses and, therefore infer the attitudes of the participants, we conducted a thematic analysis. We were able to identify key themes that shaped the attitudes of the participants of this survey and support the results of the quantitative questions. For example, trust emerged as a main theme, with many respondents indicating they would be comfortable trusting their healthcare professionals if they recommended microbiome engineering technologies. However, it is important to note this survey likely introduced this bias by asking participants about trust in a previous question. However, it is an important

observation to help guide future avenues to enable successful implementation of new technologies in the future. Overall, these findings are promising for the future adoption of the many microbiome engineering technologies that are currently undergoing clinical trials.

Chapter 7

General conclusions

> ‘The hurried way is not the right way; you need time for everything - time to work, time to play, time to rest.”’
>
> — Hedy Lamarr, 1913-2000

It comes as no surprise that in 2010, the UK government identified synthetic biology as a disruptive technology of the future [264]. Given the transformative potential of this field across multiple sectors, and its existing global impact, synthetic biology is well-positioned to provide solutions to unresolved challenges in human health and disease. As demonstrated in this work, synthetic biology tools were employed to screen, build, and test constructs designed to selectively target pathogens, an objective that remains unattainable with currently available tools, namely antibiotics. This work successfully developed multiple bacteriocin delivery platforms; including the SPoCK 2 bacteriocin expression system and Lysara, the arabinose-inducible lysis system. Furthermore, bacteriocins capable of targeting the onco-pathogens *F. nucleatum* and *B. fragilis* were identified and, when combined with Lysara in a dual-plasmid system, demonstrated the ability to kill an indicator strain, *B. subtilis*. Additionally, a public engagement survey was initiated to assess cancer patients' attitudes toward microbiome engineering and engineered live biotherapeutics. Without public support, this work is of little value if it is not ultimately implemented.

Systems like SPoCK raise potential concerns, as their design (if built as predicted) would allow them to persist and control microbial populations for extended periods. Genetic engineering of microbes is already met with public apprehension [265], and such concerns could be amplified by systems with prolonged activity. To address this, the SPoCK system was coupled with Lysara, a lysis circuit functioning as a 'kill switch,' thereby integrating a biocontainment mechanism for controlled delivery. While SPoCK 2 successfully delivered the bacteriocin MccV and responded to exogenous AHL repressors, it failed to endogenously respond to AHL following arabinose induction. This was evident in the absence of 'self-killing', a key feature of the updated system. Although it remains unclear whether the SPoCK system was unresponsive to arabinose, it is likely that the complex dynamics of the bacteriocin-immunity protein interaction contributed to this failure. Efforts to address the stability of the immunity protein were ultimately unsuccessful. Despite this, the SPoCK 2 system was able to express and secrete MccV, effectively killing

sensitive cells and repressing bacteriocin and immunity gene transcription. However, its inability to undergo self-killing compromises its robustness, particularly in challenging environments such as the human gastrointestinal tract.

Initially designed as a biocontainment mechanism, the Lysara system showed considerable promise. Following the identification of bacteriocins targeting the onco-pathogens *F. nucleatum* and *B. fragilis*, it was hypothesised that Lysara could also function as a bacteriocin delivery system for peptides that do not require post-translational modifications. Aureocin A53 and Bactofencin A were identified as suitable candidates, as they are single-peptide bacteriocins that do not require disulphide bond formation. These bacteriocins demonstrated significant potential in liquid culture experiments, killing onco-pathogens at concentrations comparable to antibiotics [212]. Despite reports suggesting that Aureocin A53 may harm macrophages [209], this observation was based on murine macrophages, which are not always reliable models for human systems [266]. Importantly, this work confirmed that Aureocin A53 does not lyse red blood cells, though further studies using more clinically relevant models are required. Future work could involve organ-on-chip systems, allowing engineered live biotherapeutics to deliver bacteriocins directly to onco-pathogens in a physiologically relevant environment. Additionally, bacteriocins must be screened against a panel of commensal bacteria to assess specificity. However, selectively targeting onco-pathogens may prove challenging, necessitating alternative strategies such as vaccines to counteract onco-pathogen-induced effects, as has been explored for *F. nucleatum* [267].

Despite, positive results that Aureocin A53 does not harm in an *in vivo Galleria mellonella* model, the bacteriocin was also ineffective at killing the target pathogen *Enterococcus faecalis in vivo* [201]. This highlights how important it is to understand the protein dynamics of the bacteriocin and potentially that this work, which produced Aureocin A53 *in vivo* could see functionality of the bacteriocin itself when tested in *in vivo* models, compared to the synthesised bacteriocin which lack something to render them ineffective in and *in vivo* environment.

The Lysara system successfully responded to arabinose induction, lysing host

cells and delivering bacteriocins to sensitive cells, thereby demonstrating antimicrobial activity. However, the system exhibited resistance to re-induction and variability in response, which would be problematic in a therapeutic setting. Additionally, a trade-off was observed between bacteriocin production and the system's ability to respond to induction. Further investigation is needed to understand the mechanisms underlying resistance. If the resistance is not due to mutations in the lysis gene, identifying genomic loci responsible for host cell adaptation (potentially the SlyD locus, required for lysis by ϕX174E) will be essential. Modifying promoter strength to a weaker variant could mitigate resistance by reducing selection pressure on host cells. Growth curve analyses indicated that while the Lysara circuit itself did not impose a significant burden, the bacteriocin expression plasmids did, highlighting an important consideration for future system optimisation.

To enhance the therapeutic potential of Lysara, the inducer arabinose would need to be replaced. Arabinose can be exploited by pathogenic strains such as enterotoxigenic *E. coli*, which utilises it for virulence factor regulation [268]. While screening patients for pathogenic bacteria prior to treatment and localising biotherapeutics to tumour sites could reduce risks, these steps introduce additional complexity. Alternative inducers, such as IPTG, were initially explored but require further optimisation [269].

Regarding bacteriocin expression plasmids, some (such as the MccV plasmids) exhibited good growth but failed to demonstrate killing activity. MoClo-format Aureocin A53 and Bactofencin A plasmids exhibited poor growth and did not kill sensitive strains. Even when IPTG-inducible plasmids expressing these bacteriocins were combined with the Lysara circuit, killing was only observed in extremely sensitive indicator strains, not in onco-pathogens. This may be a concentration-dependent effect, as suggested by Aureocin A53 concentration curves. Additionally, it was assumed that chemically synthesised bacteriocins and *in vivo* expressed bacteriocins are functionally equivalent. Though this may not be the case, potentially explaining differences in killing efficacy. Furthermore, this work highlights the challenge of constructing a universal bacteriocin expression system. Evidence

suggests that not all bacteriocins can be expressed and secreted using a single system, a limitation observed in other studies [90].

If a single system cannot accommodate all bacteriocins and constructing multiple systems is impractical, alternative delivery strategies should be considered. Rather than lysing or secreting bacteriocins from the engineered host cell, targeted injection into bacterial cells could be explored [245]. This approach leverages the observation that certain bacteriocins are non-toxic externally but lethal when produced intracellularly. Another problem with eLBT is in how to deliver them to patients. One solution is to encapsulate the eLBT by engineering the bacterium's own encapsulation pathways [57]. However, this would require further modulation of the eLBT and would place increased burden on the strain. Another potential option could be to use existing osmotic pill samplers, which are 3D printed pills that respond to pH signals in the gastrointestinal tract, which are currently used to collect bacterial samples from different regions [270]. These could be instead adapted to deliver an eLBT to the desired location. Ideally, these functions would be combined so that the pill both collects microbiome samples and delivers the eLBT drug, allowing for monitoring of eLBT progress. eLBTs could also be paired with newer therapies such as monoclonal antibodies. Monoclonal antibodies are highly targeted and could help ensure the eLBTs reach the tumour site. Although pairing monoclonal antibodies with bacteria has been explored, those studies used un-engineered bacterial strains with known anti-tumour effects, rather than eLBTs [271]. There is merits in exploring this combination, as the targeted nature of monoclonal antibodies could reduce the engineering required for eLBTs to reach their target. This would lower the burden on the systems and could enable simpler designs in non pathogenic strains, which are currently favoured due to their ability to localise to tumour sites [272].

Regardless of the delivery strategy, public acceptance is crucial, not only for securing funding but also for ensuring the clinical adoption of these technologies. The public engagement survey conducted in this work yielded promising results. Participants expressed optimism about targeted therapies, particularly due to their potential

to minimise side effects compared to current treatments such as chemotherapy and radiotherapy. However, the survey lacked the statistical power to draw conclusions regarding correlations between participants' personal experiences with cancer and their attitudes toward microbiome engineering and engineered live biotherapeutics. Additionally, the sample was not representative of the general population. Nevertheless, this survey represents the first attempt to assess public attitudes toward these technologies in the context of cancer, and responses were generally positive. Notably, participants emphasized their trust in medical professionals. Moving forward, it will be critical to engage and educate healthcare providers early in the development process to ensure they are equipped to communicate these technologies to patients upon approval. Despite concerns regarding side effects and potential ecological succession, participants were receptive to innovative approaches to cancer treatment and were open to their clinical implementation.

This work highlights the complexity and challenges associated with engineering live bacterial therapeutics. The inconsistencies in bacteriocin expression plasmids, difficulties with plasmid constructs, and stability issues underscore the inherent challenges of working with living systems. However, the successes; development of the Lysara inducible lysis circuit, functional bacteriocin delivery, identification of bacteriocins targeting onco-pathogens, and positive public engagement responses, demonstrate the potential of synthetic biology to address real-world challenges, such as antibiotic resistance and targeted therapy development. Future work could refine these constructs into highly tunable systems or reconsider their design in light of bacteriocin expression limitations. Further investigation into bacteriocin expression and mode of action may be necessary to achieve the required specificity, potentially through the development of synthetic bacteriocins [273].

Appendix A

Primer table

‘The most effective way to do it, is to do it.’

— Amelia Earhart, 1897 - 1939

Table A.1: Table of all primers used in this work

Primer Name	Primers	Used in:	Product Size (bp)	Tm (C)	Gene Name	Type
Construction of SPoCK Systems						
pMPES_001_F [1]	agagttctttaatgatctccGAAGC ACACGGTCACACTG	SPoCK 2	3861	66		
pMPES_002_R[1]	ATTGATTGTAGCCATGG TAATAGC	SPoCK 2		62		
pMPES_003_F[1]	ttaccatggctacaatcaatCGTCC GAAAGT CACCAGC	SPoCK 2	4321	67		
pMPES_004_R[1]	GGAGATCATTAAAGAAC TCTGACTC	SPoCK 2		62		

[1]Primer3

Table A.1: Table of all primers used in this work

Primer Name	Primers	Used in:	Product Size (bp)	Tm (C)	Gene Name	Type
p.cvi.gBlock.F[1]	TCAGATATGCACTGAGTATGCCT	SPoCK 1.1, SPoCK 2.1	11606, 4276	58		
SPock2.2_1F [2]	taatactattgtcgaatttgctttcgaatttc	SPoCK 3		60		
SPock2.2_1R[2]	ccatggaccttggtatcttataaacaaacatcac	SPoCK 3	3326	57		
SPock2.2_2_F[2]	taagataccaaggtccatggtacgtacc	SPoCK 3	4227	63		
SPock2.2_2R[2]	caaattcgacaatagtattatttaatataagaaagaacagttattgg	SPoCK 3		59		
P.insCirA.F[2]	cagtggattatcgcttctagGGCCCcggcgaa	SPoCK 3	8129	70		

[2]NEBuilder

Table A.1: Table of all primers used in this work

Primer Name	Primers	Used in:	Product Size (bp)	Tm (C)	Gene Name	Type
P.insCirA.R[2]	attgttatccgctcacaattCattcgactat aacaaaccattttcttgcg	SPoCK 3		66		
P.CirA.F[2]	tggtttgttatagtcgaatGaattgtgagc ggataacaatttcacacag	SPoCK 3	2075	69		
P.CirA.R[2]	tccctagcttcgccgGGGCCctaga agcgataatccactgccataaagt	SPoCK 3		69		
P.PacI.cvaC.F [3]	CGCTGCTTAATTAACTGTG TGGATTGTCCAATAACTGT TC		2496 (S2) 6255 (S1)	59		

[3]The Lab

Table A.1: Table of all primers used in this work

Primer Name	Primers	Used in:	Product Size (bp)	Tm (C)	Gene Name	Type
ΔLacI_rev[3]	TCACTGCCCGCTTTCCAGTCG			64		
Construction of Lysara systems						
P.araC.A.F	ctagctgaagacatggagCAAACCCTATGCTACTCCGTCAAG	Lysara	1276	77		
P.araBAD.B.R2	cgtcgagaagacgtagtaATGGAGAAACAGTAGAGAGTTGCGA	Lysara		76		
CvaC23_F	cagggacgggGAAGCACACGGTCACACTG	p15a_mccV	3881	66.4		
CvaC23_R	cgcctgataaATTGATTGTAGCCATGGTAATAGC	p15a_mccV		62		

Table A.1: Table of all primers used in this work

Primer Name	Primers	Used in:	Product Size (bp)	Tm (C)	Gene Name	Type
Notransport23_F	tacaatcaatTTATCAGGC GATGGTTAATGCCC	p15a_mccV	6730	67		
Notransport23_R	cgtgtgcttcCCCGTCC CTGCCACTTCA	p15a_mccV		70		
Sanger Sequencing Primers						
pMPES_KAO01 _DN100_008_F [1]	ACGTACCCATAGATAGGCG C			58		
pMPES_KAO01 _CmR_005_R [1]	CAGGTTCATCATGCCGTCT			58		
MoClo Primers						

Table A.1: Table of all primers used in this work

Primer Name	Primers	Used in:	Product Size (bp)	Tm (C)	Gene Name	Type
VR	attaccgcctttgagtgagc	MoClo primers		65		depends on part
VF2	tgccacctgacgtctaagaa	MoClo primers		66		depends on part
qPCR Primers						
rrsA_qPCR1_F [4]	CTCTTGCCATCGGATGTGCCCA		105	59	*rrsA*	House Keeping
rrsa_qPCR1_R	CCAGTGTGGCTGGTCATCCTCTCA			58		
mccV_qPCR5_F [5]	GGCAATTTGTTGCAGGAGGA		116	59		
					cvaC	Bacterocin

[4](Peng, 2014; Zhou 2011)[274, 275]
[5]NCBI

Table A.1: Table of all primers used in this work

Primer Name	Primers	Used in:	Product Size (bp)	Tm (C)	Gene Name	Type
mccV_qPCR5_R[4]	CCCTAAACCGGATGGAGAC A					
mccV_qPCR6_F[4]	GTTGCAGGAGGAATTGGAG C		116	59		
mccV_qPCR6_R[4]	ATTGTTCCCCCTAAACCGG A					
cvi_qPCR7_F[4]	TGATTGTGTTTTTAGAGGA AAGGAC		70	58		
cvi_qPCR7_R[4]	TGCAGACATTAATGCAGAG AAGC			60	*cvi*	Immunity

Table A.1: Table of all primers used in this work

Primer Name	Primers	Used in:	Product Size (bp)	Tm (C)	Gene Name	Type
cvi_qPCR8_F[4]	AGAGGAAAGGACTTTTTAT CCATGC		77	59		
cvi_qPCR8_R[4]	TCACCAACAAAGTAACATA TTGCAG			58		

Appendix B

G-blocks

‘Don’t be intimidated by what you don’t know. That can be your greatest strength and ensure you do things differently from everyone else’

— Sara Blakely, 1971 - present

Table B.1: G-block sequences used in this work

G-block name	G-block sequence - 5' - 3'
cvi_SsrA_M2_gBLOCK2	TCTCTGCATTAATGTCTGCAATATGTTAC TTTGTTGGTGATAATTATTATTCAATATCC GATAAGATAAAAAGGAGATCATATGAGA ACTCTGACTCTAAAAGGCCTGCAGCAAAC GACGAAAACTACGCTGCGAGCGTGTGAA GGTCCATGGTACGTACCCATAGATAGGCG CCGTTATCGACTGGGCCTCATGGGCCTTC CGCTCACTGTAGATTAatTAAACTGAAGCT TTCCACCATAATGCCAGCTACATATCCTG GTATTTTTTTCCGATTATCTATAACTTGAC GTGCAACGGAAATTTGCCGTTTAGCCACT TTACCGCTATTACCATGGCTACAATCAAT CGTCCGAAAGTCACCAGCctcctccccccctgccgtc atccgtgcatcagatatgcactgagtatg

Continued on next page

Table B.1: G-block sequences used in this work (continued)

G-block name	G-block sequence - 5' - 3'
cvi_RepA_M_gBLOCK	TCTCTGCATTAATGTCTGCAATATGTTAC TTTGTTGGTGATAATTATTATTCAATATCC GATAAGATAAAAAGGAGATCATATGAGA ACTCTGACTCTAAAatgaatcaatcatttatctccgatat tctttacgcagacattgaaTGAAGGTCCATGGTACG TACCCATAGATAGGCGCCGTTATCGACTG GGCCTCATGGGCCTTCCGCTCACTGTAGA TTAatTAAACTGAAGCTTTCCACCATAATG CCAGCTACATATCCTGGTATTTTTTTCCGA TTATCTATAACTTGACGTGCAACGGAAAT TTGCCGTTTAGCCACTTTACCGCTATTACC ATGGCTACAATCAATCGTCCGAAAGTCAC CAGCctcctccccctgccgtcatccgtgcatcagatatgcactg agtatg

Continued on next page

Table B.1: G-block sequences used in this work (continued)

G-block name	G-block sequence - 5' - 3'
cvi_MazE_M_gBLOCK	TCTCTGCATTAATGTCTGCAATATGTTAC TTTGTTGGTGATAATTATTATTCAATATCC GATAAGATAAAAAGGAGATCATATGAGA ACTCTGACTCTAAAatgatccacagtagcgtaaagcgtt ggggaaattcaccggcggtgcggatcccggctacgttaatgcagg cgctcaatctgaatattgatgatgaagtgaagattgacctggtggatg gcaaattaattattgagccagtgcgtaaagagcccgtatttacgcttg ctgaactggtcaacgacatcacgccggaaaacctccacgagaatat cgactggggagagccgaaagataaggaagtctggtaaTGAAG GTCCATGGTACGTACCCATAGATAGGCGC CGTTATCGACTGGGCCTCATGGGCCTTCC GCTCACTGTAGATTAatTAAACTGAAGCTT TCCACCATAATGCCAGCTACATATCCTGG TATTTTTTTCCGATTATCTATAACTTGACG TGCAACGGAAATTTGCCGTTTAGCCACTT TACCGCTATTACCATGGCTACAATCAATC GTCCGAAAGTCACCAGCctcctccccctgccgtcat ccgtgcatcagatatgcactgagtatg

Continued on next page

Table B.1: G-block sequences used in this work (continued)

G-block name	G-block sequence - 5' - 3'
garmL_Npu_CD	GGTCTCAAATGatgattaaaattgcgacccgcaaatatctg ggcaaacagaacgtgtatgatattggcgtggaacgctatcataacttt gcgctgaaaaacggctttattgcgagcaactcaggagcttttactgc agctgggggaattatggcactcattaaaaaatatgctcaaaagaaatt atggaaacagcttattgctgcattagtcgcgactggaatggctgcag gtgtagcaaaaactattgttaatgccgttagtgctggtatggatattgc cactgctttatcattgttctgcctgagctatgataccgaaattctgaccg tggaatatggcattctgccgattggcaaaattgtggaaaaacgcattg aatgcaccgtgtatagcgtggataacaacggcaacatttatacccag ccggtggcgcagtggcatgatcgcggcgaacaggaagtgtttgaa tattgcctggaagatggctgcctgattcgcgcgaccaaagatcataa atttatgaccgtggatggccagatgatgccgattgatgaaatttttgaa cgcgaactggatctgatgcgcgtggataacctgccgaactag

Continued on next page

Table B.1: G-block sequences used in this work (continued)

G-block name	G-block sequence - 5' - 3'
mccVCvi_CD	TTAAGACGGGCGACAGATGACTAGTGGG
	TCTCAAATGATGAGAACTCTGACTCTAAA
	TGAATTAGATTCTGTTTCTGGTGGTGCTTC
	AGGGCGTGATATTGCGATGGCTATAGGA
	ACACTATCCGGGCAATTTGTTGCAGGAGG
	AATTGGAGCAGCTGCTGGGGGTGTGGCT
	GGAGGTGCAATATATGACTATGCATCCAC
	TCACAAACCTAATCCTGCAATGTCTCCAT
	CCGGTTTAGGGGGAACAATTAAGCAAAA
	ACCCGAAGGGATACCTTCAGAAGCATGG
	AACTATGCTGCGGGAAGATTGTGTAATTG
	GAGTCCAAATAATCTTAGTGATGTTTGTT
	TATAAGATACCAGGAGGAAACTGCTATG
	GATAGAAAAAGAACAAAATTAGAGTTGT
	TATTTGCATTTATAATAAATGCCACCGCA
	ATATATATTGCATTAGCTATATATGATTG
	TGTTTTTAGAGGAAAGGACTTTTTATCCA
	TGCATACATTTTGCTTCTCTGCATTAATGT
	CTGCAATATGTTACTTTGTTGGTGATAAT
	TATTATTCAATATCCGATAAGATAAAAAG
	GAGATCATATGAGAACTCTGACTCTAAAT
	GAAGGTAGAGACCTACTAGTAATCAGTTC
	TGGACCAGCGAGCTGTGCTGCGACTCGTG
	GCGTAATCATG

Appendix C

Plasmid maps

> ‘Think like a queen. A queen is not afraid to fail. Failure is another steppingstone to greatness.’
>
> — Oprah Winfrey, 1954 - present

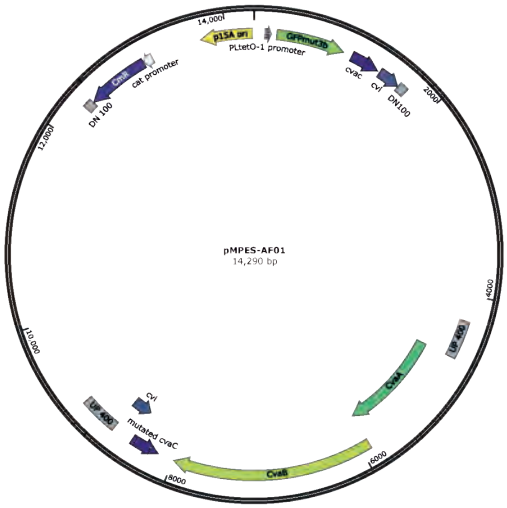

Appendix: SPoCK 1 bacteriocin producing plasmid

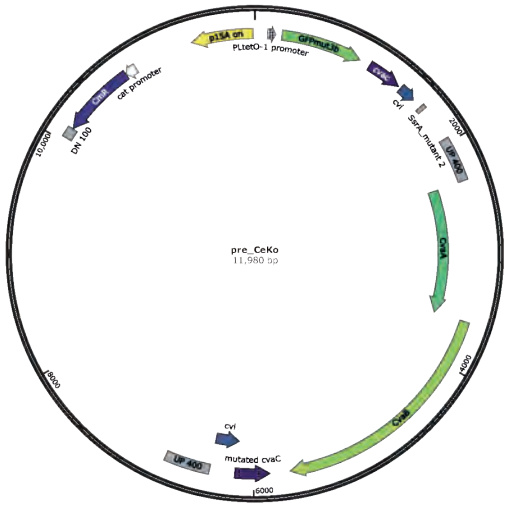

Appendix: SPoCK 1.1 bacteriocin producing plasmid

Created by SnapGene

Figure C.1: Plasmid maps
SPoCK 1 and SPoCK 1.1 bacteriocin producing plasmids.

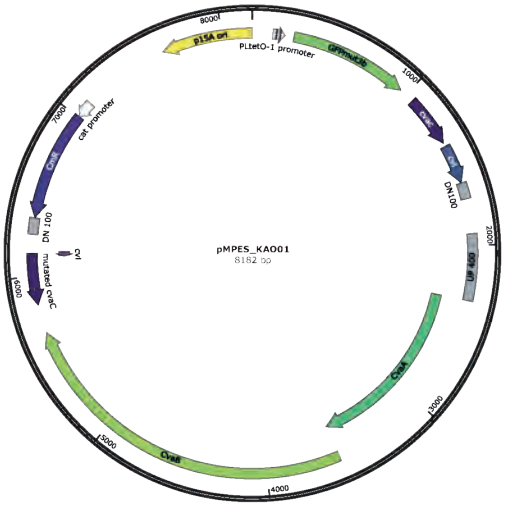

Appendix: SPoCK 2 bacteriocin producing plasmid

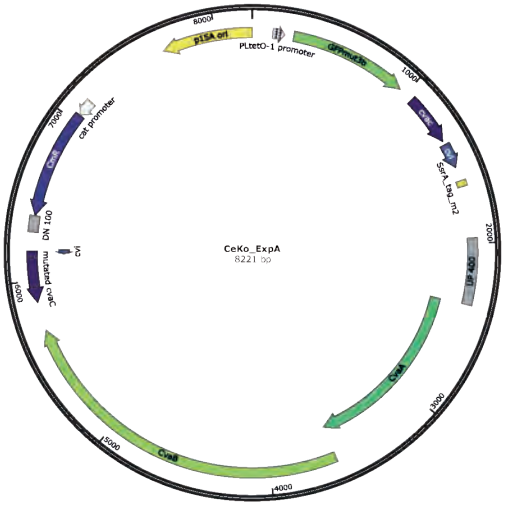

Appendix: SPoCK 2.1 bacteriocin producing plasmid

Created by SnapGene

Figure C.2: Plasmid maps
SPoCK 2 and SPoCK 2.1 bacteriocin producing plasmids.

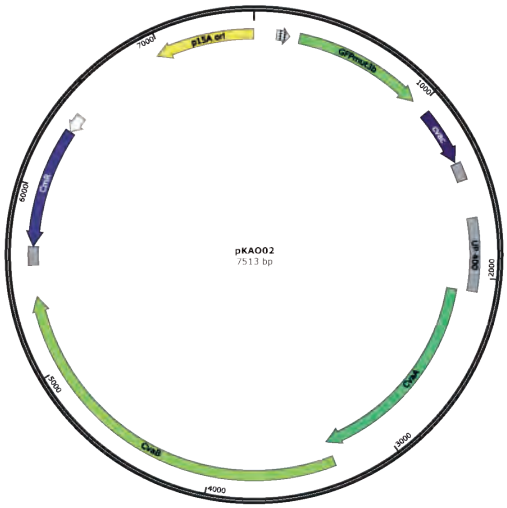

Appendix: SPoCK 3 bacteriocin producing plasmid

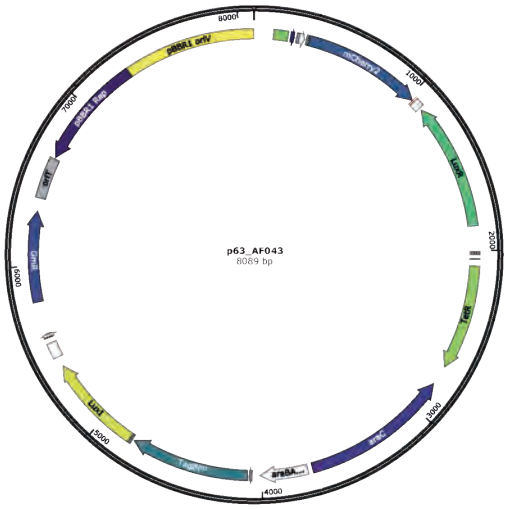

Appendix: SPoCK system quorum sensing plasmid

Created by SnapGene

Figure C.3: Plasmid maps
SPoCK 3 bacteriocin producing and SPoCK quorum sensing plasmids.

Appendix: SPoCK 3 quorum sensing plasmid

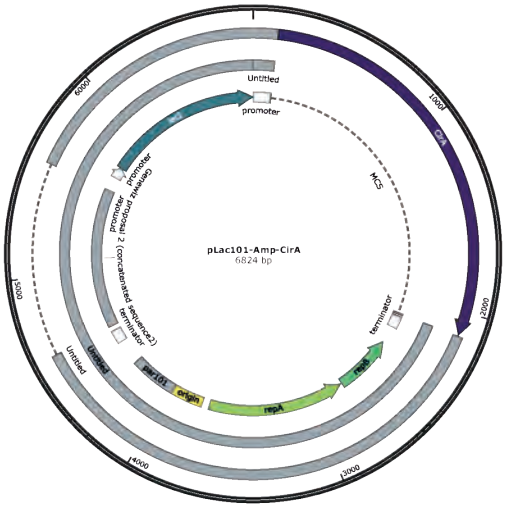

Appendix: *cirA* containing plasmid

Created by SnapGene

Figure C.4: Plasmid maps
SPoCK 3 quorum sensing and the *cirA* producing plasmids.

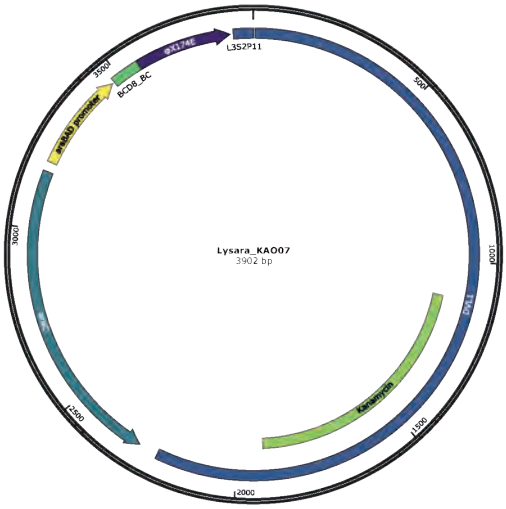

Appendix: Lysara, arabinose inducible lysis system plasmid

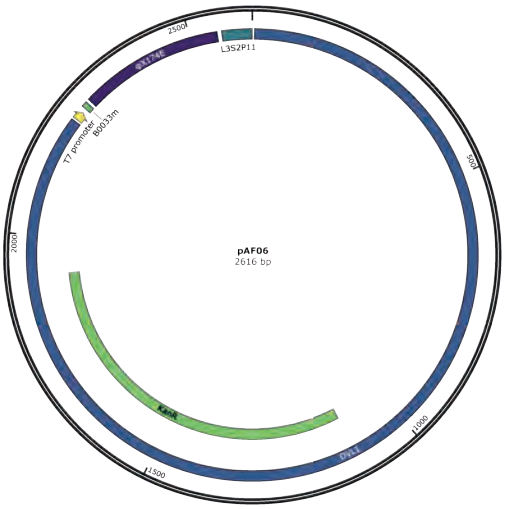

Appendix: IPTG Inducible plasmid

Created by SnapGene

Figure C.5: Plasmid maps
Lysara, the arabinose inducible, and the IPTG inducible lysis plasmids.

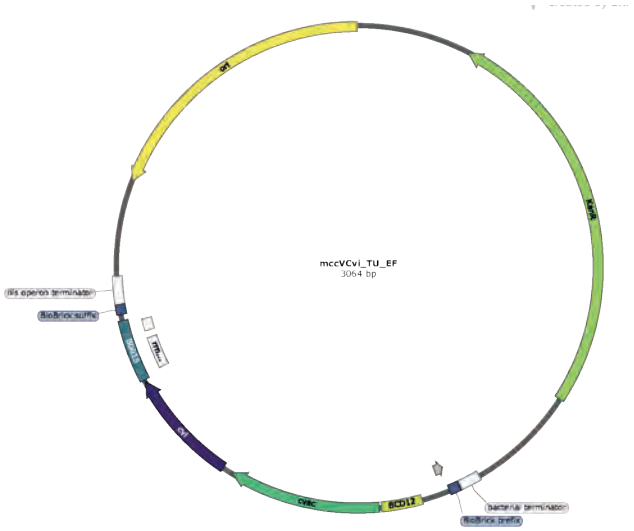

Appendix: MccV + Cvi as a moclo transcriptional unit

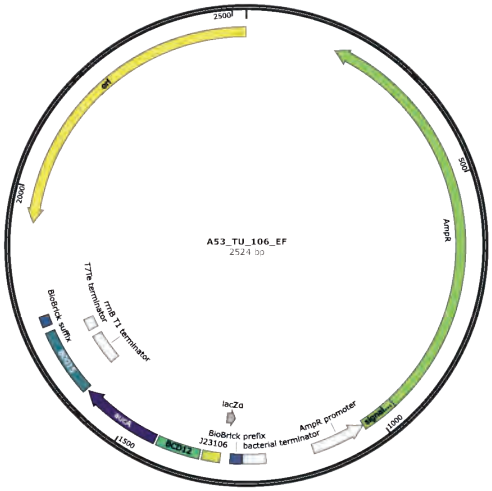

Appendix: A53 as a moclo transcriptional unit

Figure C.6: Plasmid maps
MccV + Cvi moclo plasmid and Aureocun A53 moclo plasmid.

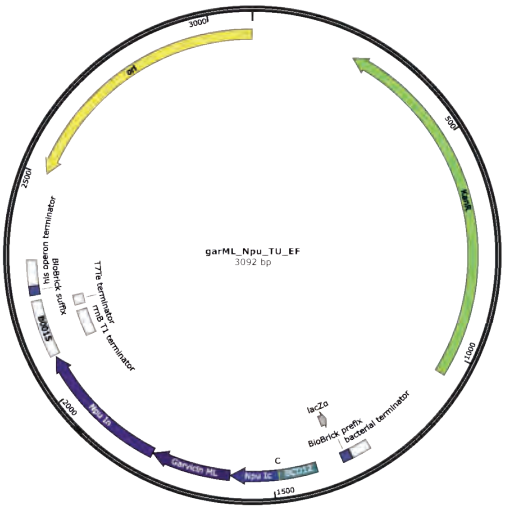

Appendix: GarML as a moclo transcriptional unit

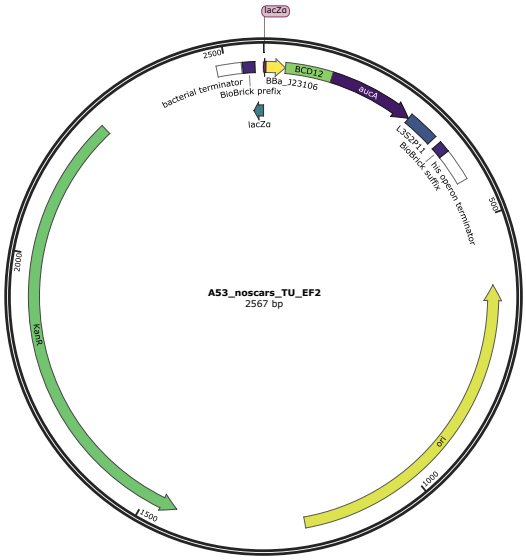

Appendix: A53 as a moclo transcriptional unit without the moclo scar sites

Created by SnapGene

Figure C.7: Plasmid maps

Garvicin ML moclo plasmid and Aureocin A53 without scar sites as a moclo plasmid.

Appendix D

SESA raw data

> ‘The way I see it, if you want the rainbow, you gotta put up with the rain.’
>
> — Dolly Parton, 2013

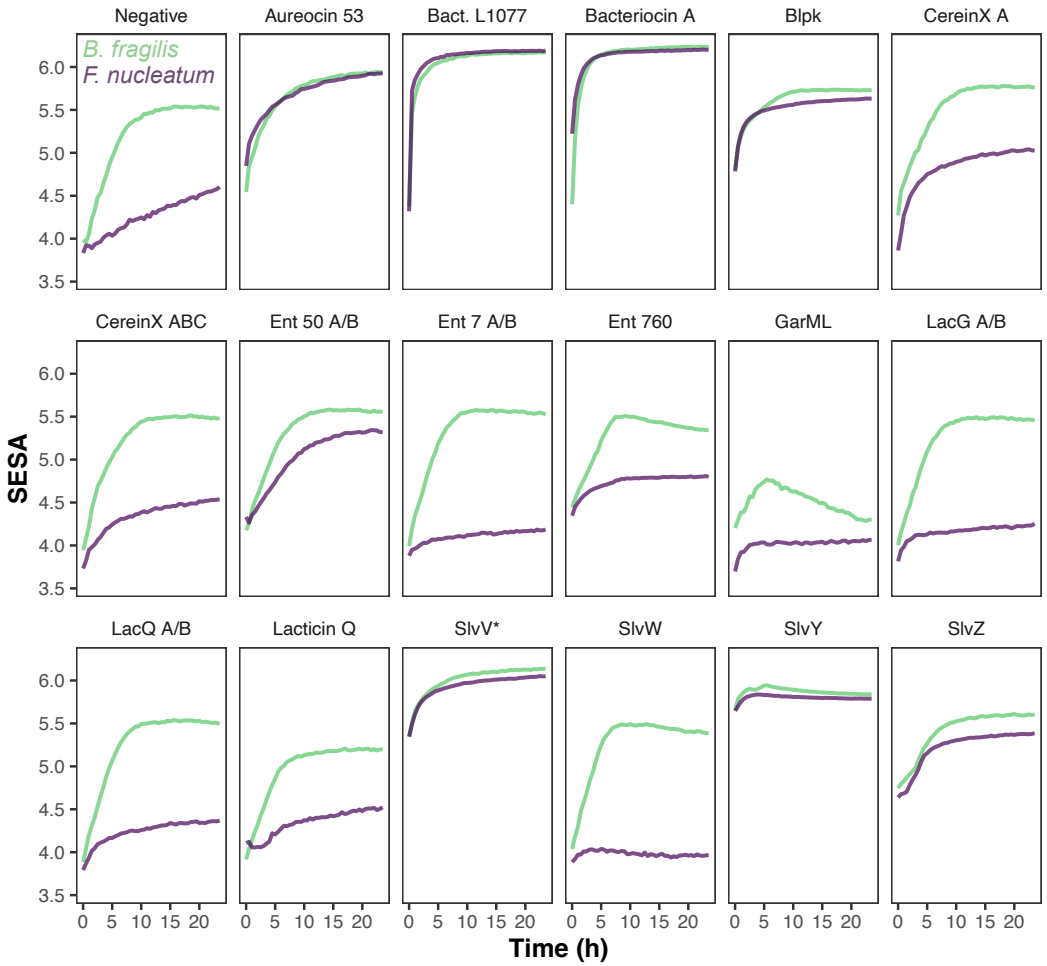

Figure D.1: The oCelloScope data, using the SESA values these are the raw numbers from the algorithm.

The negative plot contains the growth curves of *B. fragilis* and *F. nucleatum* with no bacteriocin present.

Appendix E

Survey questions

> ‘It took me quite a long time to develop a voice, and now that I have it, I am not going to be silent.’
>
> — Madeleine Albright, 2010

Section 1

Q1. Please select your age range from the groups below:

- A. 18-39
- B. 40-59
- C. 60+
- D. Prefer not to say

Q2. How have you personally been impacted by cancer?

- A. 1st hand (i.e., current patient/survivor of cancer)
- B. 2nd hand (i.e., first-degree relative of a patient who has been diagnosed with cancer)
- C. 3rd hand (i.e., friend/distant relative of a patient who has been diagnosed with cancer)
- D. Not personally impacted

Q3. Which of these potential cancer treatment options would you be comfortable taking if recommended (or have previously taken if applicable)?

- A. Surgery – removal of tumours through cutting them out of the body.
- B. Chemotherapy – use of drugs to kill cancer cells.
- C. Radiation – use of high-powered energy rays (such as X-rays) to kill cancer cells.
- D. Immunotherapy/Biological Therapy – use of the body's own immune system to fight cancer cells.
- E. Live bacterial therapy – use of live bacteria to target cancer inside the body.
- F. Do not know enough to answer.

Q4. Who would you trust to provide information on new cancer therapies and recommendations for promising treatments? Please rank these options from most trustworthy (1) to least trustworthy (6):

- A. Clinicians/doctors
- B. Regulatory bodies (e.g., Medicines & Healthcare products Regulatory Agency, European Medical Agency)
- C. Cancer charities
- D. NHS website and official resources (e.g., hospital flyers and brochures)
- E. Academic researchers
- F. Pharmaceutical/private research companies

Section 2

You will now be given a short description of the term 'Probiotics'. Please read the following statement carefully:

Probiotics are live microorganisms (such as bacteria) that are intended to have health benefits when consumed or applied to the body. They can be found in yogurt and other fermented foods, dietary supplements, and beauty products. Probiotics have so far shown some promise in the treatment of diarrhoea, bacterial vaginosis, and irritable bowel syndrome (IBS).

Q5. Please select the statement that best applies to you regarding probiotics:

- A. I had never heard of probiotics and I do not understand what they are.
- B. I had never heard of probiotics but I understand what they are now.
- C. I have heard about probiotics previously but do not understand what they are.
- D. I have heard about probiotics previously and I understand what they are.

Q6. Are you aware of the proposed benefits of probiotics?

- A. Yes
- B. No
- C. Do not know enough information to provide an opinion.

Q7. Are you aware of the limitations of probiotics?

- A. Yes
- B. No
- C. Do not know enough information to provide an opinion.

Q8. Would you/do you take probiotics to supplement your current diet? This includes regularly consuming items such as fermented foods or live yogurt.

- A. Yes
- B. No
- C. Do not know enough information to provide an opinion.

Q9. Would you/do you take probiotics to treat a disease/medical condition?

- A. Yes
- B. No
- C. Do not know enough information to provide an opinion.

Section 3

You will now be given a short description of the term 'microbiome engineering'. Please read the following statement carefully:

A microbiome is a community of micro-organisms (bacteria, fungi, etc.) that live together within a specific environment, like the human gut. Microbiome engineering aims to modify these communities in a predictable way, for example, for the treatment of diseases within the body.

Q10. Please select the statement that best applies to you regarding microbiome engineering:

- A. I had never heard of it and I do not understand what it is.
- B. I had never heard of it but I understand what it is now.
- C. I have heard about it previously but do not understand what it is.
- D. I have heard about it previously and I understand what it is.

Q11. Please rate to what extent you would approve/disapprove of microbiome engineering technologies:

- A. Strongly disapprove
- B. Mildly disapprove
- C. Neutral/no opinion
- D. Mildly approve
- E. Strongly approve
- F. Do not know enough to answer

Please explain your choice in a maximum of 100 words (this box can be left blank, please DO NOT include any information that could potentially identify you, i.e., name, exact age, where you live, health status, etc.):

[Open text box for responses]

Q12. If you disapprove of microbiome engineering, please highlight your major concerns and what, if anything, could be done to address them? (Please DO NOT include any information that could potentially identify you, i.e., name, exact age, where you live, health status, etc.):

[Open text box for responses]

You will now be given a short description of the term 'genetically modified organism'. Please read the following statement carefully:

A genetically modified organism (GMO) is any organism which has had its genetic material, or DNA, modified in a laboratory. As microbiome engineering

may involve the use of GMOs, the following questions will explore your opinions on the use of GMOs.

Q13. Please rate to what extent you approve/disapprove of consuming genetically modified foods (e.g., GM tomatoes) as part of your diet:

- A. Strongly disapprove
- B. Mildly disapprove
- C. Neutral/no opinion
- D. Mildly approve
- E. Strongly approve
- F. Do not know enough to answer

Q14. Please rate how comfortable you would be with using engineered (i.e., genetically modified) human cells as part of your cancer treatment plan (e.g., currently available CAR-T cell therapy):

- A. Very uncomfortable
- B. Mildly uncomfortable
- C. Neutral/no opinion
- D. Mildly comfortable
- E. Very comfortable
- F. Do not know enough to answer

Q15. In the future, how comfortable would you be with using natural live bacteria as part of your cancer treatment plan:

- A. Very uncomfortable
- B. Mildly uncomfortable

- C. Neutral/no opinion
- D. Mildly comfortable
- E. Very comfortable
- F. Do not know enough to answer

Q16. In the future, how comfortable would you be with using engineered (i.e., genetically modified) live bacteria as part of your cancer treatment plan:

- A. Very uncomfortable
- B. Mildly uncomfortable
- C. Neutral/no opinion
- D. Mildly comfortable
- E. Very comfortable
- F. Do not know enough to answer

Appendix F

Bacteria outreach

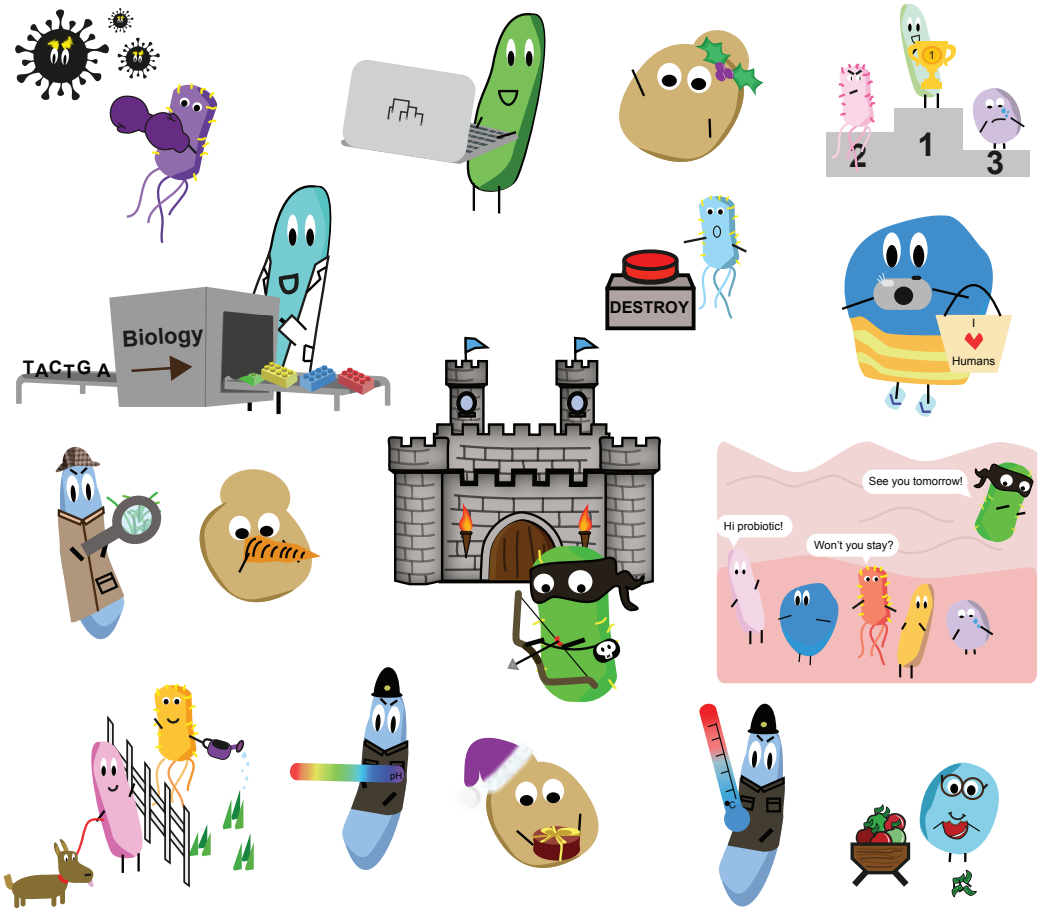

Figure F.1: Collection of the bacterial cartoons created during this PhD
Created using Adobe Illustrator, featuring festive yeast cells.

Bibliography

[1] Philippe Gabant and Juan Borrero. PARAGEN 1.0: A standardized synthetic gene library for fast cell-free bacteriocin synthesis. *Frontiers in Bioengineering and Biotechnology*, 7(SEP):213, 2019.

[2] Synthetic biology – EPSRC. https://www.ukri.org/what-we-do/browse-our-areas-of-investment-and-support/synthetic-biology/.

[3] NIH. Synthetic Biology. https://www.genome.gov/about-genomics/policy-issues/Synthetic-Biology.

[4] Genome-scale engineering for systems and synthetic biology | Molecular Systems Biology. https://www.embopress.org/doi/full/10.1038/msb.2012.66.

[5] D. Chandran, W. B. Copeland, S. C. Sleight, and H. M. Sauro. Mathematical modeling and synthetic biology. *Drug Discovery Today: Disease Models*, 5(4):299–309, December 2008.

[6] Benjamin Pouvreau, Thomas Vanhercke, and Surinder Singh. From plant metabolic engineering to plant synthetic biology: The evolution of the design/build/test/learn cycle. *Plant Science*, 273:3–12, August 2018.

[7] Secretariat of the Convention on Biological Diversity. CBD Technical Series No. 100 synthetic Biology. Technical Series 100, Secretariat of the Convention on Biological Diversity, April 2022.

[8] Pei Kun R. Tay, Peter Q. Nguyen, and Neel S. Joshi. A Synthetic Circuit for

Mercury Bioremediation Using Self-Assembling Functional Amyloids. *ACS Synthetic Biology*, 6(10):1841–1850, October 2017.

[9] Katherine E. French, Zhongrui Zhou, and Norman Terry. Horizontal 'gene drives' harness indigenous bacteria for bioremediation. *Scientific Reports*, 10(1):15091, September 2020.

[10] Bhairavi Doshi, Mika Sillanpää, and Simo Kalliola. A review of bio-based materials for oil spill treatment. *Water Research*, 135:262–277, May 2018.

[11] Xinyi Wan, Trevor Y. H. Ho, and Baojun Wang. Engineering Prokaryote Synthetic Biology Biosensors. In Gerald Thouand, editor, *Handbook of Cell Biosensors*, pages 1–37. Springer International Publishing, Cham, 2019.

[12] Zhiqiang Wen, Nigel P. Minton, Ying Zhang, Qi Li, Jinle Liu, Yu Jiang, and Sheng Yang. Enhanced solvent production by metabolic engineering of a twin-clostridial consortium. *Metabolic Engineering*, 39:38–48, January 2017.

[13] Karsten TEMME, Alvin TAMSIR, Sarah BLOCH, Rosemary CLARK, and Emily TUNG. Methods and compositions for improving plant traits, January 2017.

[14] Matija Stanic, Neil M.N. Hickerson, Rex Arunraj, and Marcus A. Samuel. Gene-editing of the strigolactone receptor BnD14 confers promising shoot architectural changes in Brassica napus (canola). *Plant Biotechnology Journal*, 19(4):639–641, 2021.

[15] Trans Fatty Acids and Coronary Heart Disease | New England Journal of Medicine. https://www.nejm.org/doi/full/10.1056/NEJM199906243402511.

[16] Stephanie H. Kung, Sean Lund, Abhishek Murarka, Derek McPhee, and Chris J. Paddon. Approaches and Recent Developments for the Commercial Production of Semi-synthetic Artemisinin. *Frontiers in Plant Science*, 9, January 2018.

[17] Paul F. Robbins, Richard A. Morgan, Steven A. Feldman, James C. Yang, Richard M. Sherry, Mark E. Dudley, John R. Wunderlich, Azam V. Nahvi, Lee J. Helman, Crystal L. Mackall, Udai S. Kammula, Marybeth S. Hughes, Nicholas P. Restifo, Mark Raffeld, Chyi-Chia Richard Lee, Catherine L. Levy, Yong F. Li, Mona El-Gamil, Susan L. Schwarz, Carolyn Laurencot, and Steven A. Rosenberg. Tumor Regression in Patients With Metastatic Synovial Cell Sarcoma and Melanoma Using Genetically Engineered Lymphocytes Reactive With NY-ESO-1. *Journal of Clinical Oncology*, 29(7):917–924, March 2011.

[18] Rino Rappuoli, Ennio De Gregorio, Giuseppe Del Giudice, Sanjay Phogat, Simone Pecetta, Mariagrazia Pizza, and Emmanuel Hanon. Vaccinology in the post-COVID-19 era. *Proceedings of the National Academy of Sciences*, 118(3):e2020368118, January 2021.

[19] Lisa A. Jackson, Evan J. Anderson, Nadine G. Rouphael, Paul C. Roberts, Mamodikoe Makhene, Rhea N. Coler, Michele P. McCullough, James D. Chappell, Mark R. Denison, Laura J. Stevens, Andrea J. Pruijssers, Adrian McDermott, Britta Flach, Nicole A. Doria-Rose, Kizzmekia S. Corbett, Kaitlyn M. Morabito, Sijy O'Dell, Stephen D. Schmidt, Phillip A. Swanson, Marcelino Padilla, John R. Mascola, Kathleen M. Neuzil, Hamilton Bennett, Wellington Sun, Etza Peters, Mat Makowski, Jim Albert, Kaitlyn Cross, Wendy Buchanan, Rhonda Pikaart-Tautges, Julie E. Ledgerwood, Barney S. Graham, and John H. Beigel. An mRNA Vaccine against SARS-CoV-2 — Preliminary Report. *New England Journal of Medicine*, 383(20):1920–1931, November 2020.

[20] Mark R. Charbonneau, Vincent M. Isabella, Ning Li, and Caroline B. Kurtz. Developing a new class of engineered live bacterial therapeutics to treat human diseases. *Nature Communications*, 11(1):1738, April 2020.

[21] Ina Balke and Andris Zeltins. Recent Advances in the Use of Plant Virus-Like Particles as Vaccines. *Viruses*, 12(3):270, February 2020.

[22] Gail A. M. Cresci and Kristin Izzo. Chapter 4 - Gut Microbiome. In Mandy L. Corrigan, Kristen Roberts, and Ezra Steiger, editors, *Adult Short Bowel Syndrome*, pages 45–54. Academic Press, January 2019.

[23] Gabriele Berg, Daria Rybakova, Doreen Fischer, Tomislav Cernava, Marie-Christine Champomier Vergès, Trevor Charles, Xiaoyulong Chen, Luca Cocolin, Kellye Eversole, Gema Herrero Corral, Maria Kazou, Linda Kinkel, Lene Lange, Nelson Lima, Alexander Loy, James A. Macklin, Emmanuelle Maguin, Tim Mauchline, Ryan McClure, Birgit Mitter, Matthew Ryan, Inga Sarand, Hauke Smidt, Bettina Schelkle, Hugo Roume, G. Seghal Kiran, Joseph Selvin, Rafael Soares Correa de Souza, Leo van Overbeek, Brajesh K. Singh, Michael Wagner, Aaron Walsh, Angela Sessitsch, and Michael Schloter. Microbiome definition re-visited: Old concepts and new challenges. *Microbiome*, 8(1):103, June 2020.

[24] Livia H. Morais, Henry L. Schreiber, and Sarkis K. Mazmanian. The gut microbiota–brain axis in behaviour and brain disorders. *Nature Reviews Microbiology*, 19(4):241–255, April 2021.

[25] Longsha Liu, Jun R. Huh, and Khalid Shah. Microbiota and the gut-brain-axis: Implications for new therapeutic design in the CNS. *eBioMedicine*, 77, March 2022.

[26] Roberta Caruso, Bernard C. Lo, and Gabriel Núñez. Host–microbiota interactions in inflammatory bowel disease. *Nature Reviews Immunology*, 20(7):411–426, July 2020.

[27] Beth A. Helmink, M. A. Wadud Khan, Amanda Hermann, Vancheswaran Gopalakrishnan, and Jennifer A. Wargo. The microbiome, cancer, and cancer therapy. *Nature Medicine*, 25(3):377–388, March 2019.

[28] Aoife M Brennan. Development of synthetic biotics as treatment for human diseases. *Synthetic Biology*, 7(1):ysac001, January 2022.

[29] Vincent B. Young. The role of the microbiome in human health and disease: An introduction for clinicians. *BMJ*, 356:j831, March 2017.

[30] Jee Loon Foo, Hua Ling, Yung Seng Lee, and Matthew Wook Chang. Microbiome engineering: Current applications and its future. *Biotechnology Journal*, 12(3):1600099, 2017.

[31] Marja K. Puurunen, Jerry Vockley, Shawn L. Searle, Stephanie J. Sacharow, John A. Phillips, William S. Denney, Benjamin D. Goodlett, David A. Wagner, Larry Blankstein, Mary J. Castillo, Mark R. Charbonneau, Vincent M. Isabella, Vasu V. Sethuraman, Richard J. Riese, Caroline B. Kurtz, and Aoife M. Brennan. Safety and pharmacodynamics of an engineered E. coli Nissle for the treatment of phenylketonuria: A first-in-human phase 1/2a study. *Nature Metabolism*, 3(8):1125–1132, July 2021.

[32] Katie L. Mason, Taylor A. Stepien, Jessamina E. Blum, Jonathan F. Holt, Normand H. Labbe, Jason S. Rush, Kenneth F. Raffa, and Jo Handelsman. From Commensal to Pathogen: Translocation of Enterococcus faecalis from the Midgut to the Hemocoel of Manduca sexta. *mBio*, 2(3):e00065–11, May 2011.

[33] Manshi Li, Fuhuo Yang, Yihan Lu, and Weifeng Huang. Identification of Enterococcus faecalis in a patient with urinary-tract infection based on metagenomic next-generation sequencing: A case report. *BMC Infectious Diseases*, 20(1):467, July 2020.

[34] Richard A. Jacobson, Kiedo Wienholts, Ashley J. Williamson, Sara Gaines, Sanjiv Hyoju, Harry van Goor, Alexander Zaborin, Benjamin D. Shogan, Olga Zaborina, and John C. Alverdy. Enterococcus faecalis exploits the human fibrinolytic system to drive excess collagenolysis: Implications in gut healing and identification of druggable targets. *American Journal of Physiology - Gastrointestinal and Liver Physiology*, 318(1):G1–G9, January 2020.

[35] Krishna Rao and Preeti N. Malani. Diagnosis and Treatment of Clostridioides

(Clostridium) difficile Infection in Adults in 2020. *JAMA*, 323(14):1403–1404, April 2020.

[36] Ana A. Weil, Rachel L. Becker, and Jason B. Harris. Vibrio cholerae at the Intersection of Immunity and the Microbiome. *mSphere*, 4(6):10.1128/msphere.00597–19, November 2019.

[37] Charurut Somboonwit, Lynette J Menezes, Douglas A Holt, John T Sinnott, and Paul Shapshak. Current views and challenges on clinical cholera. *Bioinformation*, 13(12):405–409, December 2017.

[38] Caitlin A. Brennan and Wendy S. Garrett. Fusobacterium nucleatum — symbiont, opportunist and oncobacterium. *Nature Reviews Microbiology 2018 17:3*, 17(3):156–166, December 2018.

[39] Lucía Cea Soriano, Montse Soriano-Gabarró, and Luis A. García Rodríguez. Trends in the contemporary incidence of colorectal cancer and patient characteristics in the United Kingdom: A population-based cohort study using The Health Improvement Network. *BMC Cancer*, 18:402, April 2018.

[40] Gregory D. Sepich-Poore, Laurence Zitvogel, Ravid Straussman, Jeff Hasty, Jennifer A. Wargo, and Rob Knight. The microbiome and human cancer. *Science (New York, N.Y.)*, 371(6536):eabc4552, March 2021.

[41] Fatemeh Sameni, Parisa Abedi Elkhichi, Ali Dadashi, Mohammad Sadeghi, Mehdi Goudarzi, Maedeh Pourali Eshkalak, and Masoud Dadashi. Global prevalence of Fusobacterium nucleatum and Bacteroides fragilis in patients with colorectal cancer: An overview of case reports/case series and meta-analysis of prevalence studies. *BMC Gastroenterology*, 25(1):71, February 2025.

[42] Yiwen Cheng, Zongxin Ling, and Lanjuan Li. The intestinal microbiota and colorectal cancer. *Frontiers in Immunology*, 11:3100, November 2020.

[43] Iradj Sobhani, Aurelien Amiot, Yann Le Baleur, Michael Levy, Marie-Luce Auriault, Jeanne Tran Van Nhieu, and Jean Charles Delchier. Microbial dysbiosis and colon carcinogenesis: Could colon cancer be considered a bacteria-related disease? *Therapeutic Advances in Gastroenterology*, 6(3):215–229, May 2013.

[44] Hua Liu, Xia Lu Hong, Tian Tian Sun, Xiao Wen Huang, Ji Lin Wang, and Hua Xiong. Fusobacterium nucleatum exacerbates colitis by damaging epithelial barriers and inducing aberrant inflammation. *Journal of Digestive Diseases*, 21(7):385–398, July 2020.

[45] Le Liu, Liping Liang, Chenghai Yang, Youlian Zhou, and Ye Chen. Extracellular vesicles of Fusobacterium nucleatum compromise intestinal barrier through targeting RIPK1-mediated cell death pathway. *Gut Microbes*, 13(1):1–20, 2021.

[46] Zhe Zhao, Kailun Fei, Hua Bai, Zhijie Wang, Jianchun Duan, and Jie Wang. Metagenome association study of the gut microbiome revealed biomarkers linked to chemotherapy outcomes in locally advanced and advanced lung cancer. *Thoracic Cancer*, 12(1):66–78, January 2021.

[47] Rachel V. Purcell, John Pearson, Alan Aitchison, Liane Dixon, Frank A. Frizelle, and Jacqueline I. Keenan. Colonization with enterotoxigenic Bacteroides fragilis is associated with early-stage colorectal neoplasia. *PLOS ONE*, 12(2):e0171602, February 2017.

[48] Heike E.F. Becker, Casper Jamin, Liene Bervoets, Annemarie Boleij, Pan Xu, Marie J. Pierik, Frank R.M. Stassen, Paul H.M. Savelkoul, John Penders, and Daisy M.A.E. Jonkers. Higher prevalence of bacteroides fragilis in crohn's disease exacerbations and strain-dependent increase of epithelial resistance. *Frontiers in Microbiology*, 12:1305, June 2021.

[49] Colon Cancer Treatment, by Stage | How to Treat Colon Can-

cer. https://www.cancer.org/cancer/types/colon-rectal-cancer/treating/by-stage-colon.html.

[50] María Eugenia Inda, Esther Broset, Timothy K. Lu, and Cesar de la Fuente-Nunez. Emerging frontiers in microbiome engineering. *Trends in Immunology*, 40(10):952–973, October 2019.

[51] Liam P. Shaw, Hassan Bassam, Chris P. Barnes, A. Sarah Walker, Nigel Klein, and Francois Balloux. Modelling microbiome recovery after antibiotics using a stability landscape framework. *The ISME Journal 2019 13:7*, 13(7):1845–1856, March 2019.

[52] Anuradha Ravi, Fenella D. Halstead, Amy Bamford, Anna Casey, Nicholas M. Thomson, Willem Van Schaik, Catherine Snelson, Robert Goulden, Ebenezer Foster-Nyarko, George M. Savva, Tony Whitehouse, Mark J. Pallen, and Beryl A. Oppenheim. Loss of microbial diversity and pathogen domination of the gut microbiota in critically ill patients. *Microbial Genomics*, 5(9):e000293, September 2019.

[53] Xiaodi Chen, Yune Lu, Tao Chen, and Rongguo Li. The female vaginal microbiome in health and bacterial vaginosis. *Frontiers in Cellular and Infection Microbiology*, 11:271, April 2021.

[54] Mark Mimee, Robert J. Citorik, and Timothy K. Lu. Microbiome therapeutics — Advances and challenges. *Advanced Drug Delivery Reviews*, 105:44–54, October 2016.

[55] Gautam Singhvi, Vishal Girdhar, Shalini Patil, Gaurav Gupta, Philip M. Hansbro, and Kamal Dua. Microbiome as therapeutics in vesicular delivery. *Biomedicine & Pharmacotherapy*, 104:738–741, August 2018.

[56] Andres Cubillos-Ruiz, Tingxi Guo, Anna Sokolovska, Paul F. Miller, James J. Collins, Timothy K. Lu, and Jose M. Lora. Engineering living therapeutics with synthetic biology. *Nature Reviews Drug Discovery*, 20(12):941–960, December 2021.

[57] Tetsuhiro Harimoto, Jaeseung Hahn, Yu-Yu Chen, Jongwon Im, Joanna Zhang, Nicholas Hou, Fangda Li, Courtney Coker, Kelsey Gray, Nicole Harr, Sreyan Chowdhury, Kelly Pu, Clare Nimura, Nicholas Arpaia, Kam W. Leong, and Tal Danino. A programmable encapsulation system improves delivery of therapeutic bacteria in mice. *Nature Biotechnology*, 40(8):1259–1269, August 2022.

[58] Lothar Steidler, Wolfgang Hans, Lieven Schotte, Sabine Neirynck, Florian Obermeier, Werner Falk, Walter Fiers, and Erik Remaut. Treatment of Murine Colitis by Lactococcus lactis Secreting Interleukin-10. *Science*, 289(5483):1352–1355, August 2000.

[59] Tanel Ozdemir, Alex J. H. Fedorec, Tal Danino, and Chris P. Barnes. Synthetic Biology and Engineered Live Biotherapeutics: Toward Increasing System Complexity. *Cell Systems*, 7(1):5–16, July 2018.

[60] Monica P. McNerney, Kailyn E. Doiron, Tai L. Ng, Timothy Z. Chang, and Pamela A. Silver. Theranostic cells: Emerging clinical applications of synthetic biology. *Nature Reviews Genetics*, 22(11):730–746, November 2021.

[61] John C. Flickinger, Ulrich Rodeck, and Adam E. Snook. Listeria monocytogenes as a Vector for Cancer Immunotherapy: Current Understanding and Progress. *Vaccines*, 6(3):48, September 2018.

[62] Wolfgang Wick, Antje Wick, Felix Sahm, Dennis Riehl, Andreas von Deimling, Martin Bendszus, Philipp Kickingereder, Philipp Beckhove, Friedrich Hubertus Schmitz-Winnenthal, Christine Jungk, Sébastien Wieckowski, Lilli Podola, Christel Herold-Mende, Andreas Unterberg, and Michael Platten. VXM01 phase I study in patients with progressive glioblastoma: Final results. *Journal of Clinical Oncology*, 36(15_suppl):2017–2017, May 2018.

[63] Daniel S. Leventhal, Anna Sokolovska, Ning Li, Christopher Plescia, Starsha A. Kolodziej, Carey W. Gallant, Rudy Christmas, Jian-Rong Gao,

Michael J. James, Andres Abin-Fuentes, Munira Momin, Christopher Bergeron, Adam Fisher, Paul F. Miller, Kip A. West, and Jose M. Lora. Immunotherapy with engineered bacteria by targeting the STING pathway for anti-tumor immunity. *Nature Communications*, 11(1):2739, June 2020.

[64] Marja K. Puurunen, Jerry Vockley, Shawn L. Searle, Stephanie J. Sacharow, John A. Phillips, William S. Denney, Benjamin D. Goodlett, David A. Wagner, Larry Blankstein, Mary J. Castillo, Mark R. Charbonneau, Vincent M. Isabella, Vasu V. Sethuraman, Richard J. Riese, Caroline B. Kurtz, and Aoife M. Brennan. Safety and pharmacodynamics of an engineered E. coli Nissle for the treatment of phenylketonuria: A first-in-human phase 1/2a study. *Nature Metabolism*, 3(8):1125–1132, August 2021.

[65] Kristin J. Adolfsen, Isolde Callihan, Catherine E. Monahan, Per Jr Greisen, James Spoonamore, Munira Momin, Lauren E. Fitch, Mary Joan Castillo, Lindong Weng, Lauren Renaud, Carl J. Weile, Jay H. Konieczka, Teodelinda Mirabella, Andres Abin-Fuentes, Adam G. Lawrence, and Vincent M. Isabella. Improvement of a synthetic live bacterial therapeutic for phenylketonuria with biosensor-enabled enzyme engineering. *Nature Communications*, 12(1):6215, October 2021.

[66] David Lubkowicz, Nicholas G Horvath, Michael J James, Pasquale Cantarella, Lauren Renaud, Christopher G Bergeron, Ron B Shmueli, Cami Anderson, Jian-Rong Gao, Caroline B Kurtz, Mylene Perreault, Mark R Charbonneau, Vincent M Isabella, and David L Hava. An engineered bacterial therapeutic lowers urinary oxalate in preclinical models and in silico simulations of enteric hyperoxaluria. *Molecular Systems Biology*, 18(3):e10539, March 2022.

[67] Caroline B. Kurtz, Yves A. Millet, Marja K. Puurunen, Mylène Perreault, Mark R. Charbonneau, Vincent M. Isabella, Jonathan W. Kotula, Eugene Antipov, Yossi Dagon, William S. Denney, David A. Wagner, Kip A. West, Andrew J. Degar, Aoife M. Brennan, and Paul F. Miller. An engineered E.

coli Nissle improves hyperammonemia and survival in mice and shows dose-dependent exposure in healthy humans. *Science Translational Medicine*, 11(475):eaau7975, January 2019.

[68] Fernando Baquero, Val F. Lanza, Maria Rosario Baquero, Rosa del Campo, and Daniel A. Bravo-Vázquez. Microcins in enterobacteriaceae: Peptide antimicrobials in the eco-active intestinal chemosphere. *Frontiers in Microbiology*, 10:2261, October 2019.

[69] Halil Ibrahim Kaya, Burcu Özel, and Ömer Şimşek. A natural way of food preservation: Bacteriocins and their applications. *Health and Safety Aspects of Food Processing Technologies*, pages 633–659, December 2019.

[70] Alexis Simons, Kamel Alhanout, and Raphaël E. Duval. Bacteriocins, antimicrobial peptides from bacterial origin: Overview of their biology and their impact against multidrug-resistant bacteria. *Microorganisms*, 8(5), May 2020.

[71] Iva Atanaskovic and Colin Kleanthous. Tools and approaches for dissecting protein bacteriocin import in gram-negative bacteria. *Frontiers in Microbiology*, 10(MAR):444199, March 2019.

[72] Eric Cascales, Susan K. Buchanan, Denis Duché, Colin Kleanthous, Roland Lloubès, Kathleen Postle, Margaret Riley, Stephen Slatin, and Danièle Cavard. Colicin biology. *Microbiology and Molecular Biology Reviews*, 71(1):158–229, March 2007.

[73] Shih Chun Yang, Chih Hung Lin, Calvin T. Sung, and Jia You Fang. Antibacterial activities of bacteriocins: Application in foods and pharmaceuticals. *Frontiers in Microbiology*, 5(MAY):241, 2014.

[74] Nicholas C. K. Heng and John R. Tagg. What's in a name? Class distinction for bacteriocins. *Nature Reviews Microbiology*, 4(2):160–160, February 2006.

[75] Rodney H. Perez, Takeshi Zendo, and Kenji Sonomoto. Novel bacteriocins from lactic acid bacteria (LAB): Various structures and applications. *Microbial Cell Factories*, 13(1):S3, August 2014.

[76] Catherine O'Reilly, Ghjuvan M. Grimaud, Mairéad Coakley, Paula M. O'Connor, Harsh Mathur, Veronica L. Peterson, Ciara M. O'Donovan, Peadar G. Lawlor, Paul D. Cotter, Catherine Stanton, Mary C. Rea, Colin Hill, and R. Paul Ross. Modulation of the gut microbiome with nisin. *Scientific Reports*, 13(1):7899, May 2023.

[77] Didem Deliorman Orhan. Chapter 18 - Bacteriocins Produced by Probiotic Microorganisms. In Dharumadurai Dhanasekaran and Alwarappan Sankaranarayanan, editors, *Advances in Probiotics*, pages 277–291. Academic Press, January 2021.

[78] Sa| Ennahar, Toshihiro Sashihara, Kenji Sonomoto, and Ayaaki Ishizaki. Class IIa bacteriocins: Biosynthesis, structure and activity. *FEMS Microbiology Reviews*, 24(1):85–106, January 2000.

[79] Ruilian Li, Jinsong Duan, Yicheng Zhou, and Jiawei Wang. Structural Basis of the Mechanisms of Action and Immunity of Lactococcin A, a Class IId Bacteriocin. *Applied and Environmental Microbiology*, 89(3):e00066–23, February 2023.

[80] María F. Azpiroz and Magela Laviña. Modular structure of microcin H47 and colicin V. *Antimicrobial Agents and Chemotherapy*, 51(7):2412–2419, July 2007.

[81] Justyna Mazurek-Popczyk, Justyna Pisarska, Ewa Bok, and Katarzyna Baldy-Chudzik. Antibacterial activity of bacteriocinogenic commensal escherichia coli against zoonotic strains resistant and sensitive to antibiotics. *Antibiotics 2020, Vol. 9, Page 411*, 9(7):411, July 2020.

[82] Heidi Chehade and Volkmar Braun. Iron-regulated synthesis and uptake of colicin V. *FEMS Microbiology Letters*, 52(3):177–181, August 1988.

[83] Virginia L Waterst and Jorge H Crosa. Colicin V virulence plasmids. *Microbiological Reviews*, 55(3):437–450, September 1991.

[84] Sylvie Rebuffat. Microcins. In A.J Kastin, editor, *Handbook of Biologically Active Peptides*, pages 129–137. Elsevier, 2013.

[85] Xing Jin, Weston Kightlinger, Yong Chan Kwon, and Seok Hoon Hong. Rapid production and characterization of antimicrobial colicins using Escherichia coli-based cell-free protein synthesis. *Synthetic Biology*, 3(1), January 2018.

[86] Sushma Kommineni, Daniel J. Bretl, Vy Lam, Rajrupa Chakraborty, Michael Hayward, Pippa Simpson, Yumei Cao, Pavlos Bousounis, Christopher J. Kristich, and Nita H. Salzman. Bacteriocin production augments niche competition by enterococci in the mammalian gastrointestinal tract. *Nature 2015 526:7575*, 526(7575):719–722, October 2015.

[87] Alex J.H. Fedorec, Behzad D. Karkaria, Michael Sulu, and Chris P. Barnes. Single strain control of microbial consortia. *Nature Communications 2021 12:1*, 12(1):1–12, March 2021.

[88] Startup in the labs. https://syngulon.com/startup-in-the-labs/, April 2018.

[89] Sonya V. Iverson, Traci L. Haddock, Jacob Beal, and Douglas M. Densmore. CIDAR MoClo: Improved MoClo Assembly Standard and New E. coli Part Library Enable Rapid Combinatorial Design for Synthetic and Traditional Biology. *ACS Synthetic Biology*, 5(1):99–103, January 2016.

[90] Jack W. Rutter, Linda Dekker, Chania Clare, Zoe F. Slendebroek, Kimberley A. Owen, Julie A. K. McDonald, Sean P. Nair, Alex J. H. Fedorec, and Chris P. Barnes. A bacteriocin expression platform for targeting pathogenic bacterial species. *Nature Communications*, 15(1):6332, July 2024.

[91] Katherine E. Duncker, Zachary A. Holmes, and Lingchong You. Engineered

microbial consortia: Strategies and applications. *Microbial Cell Factories*, 20(1):211, November 2021.

[92] Maziya Ibrahim, Lavanya Raajaraam, and Karthik Raman. Modelling microbial communities: Harnessing consortia for biotechnological applications. *Computational and Structural Biotechnology Journal*, 19:3892–3907, January 2021.

[93] Christina V. Dinh, Xingyu Chen, and Kristala L.J. Prather. Development of a quorum-sensing based circuit for control of coculture population composition in a naringenin production system. *ACS Synthetic Biology*, 9(3):590–597, March 2020.

[94] Hiroshi Honjo, Kenshiro Iwasaki, Yuki Soma, Keigo Tsuruno, Hiroyuki Hamada, and Taizo Hanai. Synthetic microbial consortium with specific roles designated by genetic circuits for cooperative chemical production. *Metabolic Engineering*, 55:268–275, September 2019.

[95] Dhani Raj Chhetri. Myo-Inositol and Its Derivatives: Their Emerging Role in the Treatment of Human Diseases. *Frontiers in Pharmacology*, 10, October 2019.

[96] Na Chen, Jingya Wang, Yunying Zhao, and Yu Deng. Metabolic engineering of Saccharomyces cerevisiae for efficient production of glucaric acid at high titer. *Microbial Cell Factories*, 17(1):67, May 2018.

[97] Apoorv Gupta, Irene M.Brockman Reizman, Christopher R. Reisch, and Kristala L.J. Prather. Dynamic regulation of metabolic flux in engineered bacteria using a pathway-independent quorum-sensing circuit. *Nature Biotechnology 2017 35:3*, 35(3):273–279, February 2017.

[98] Engineering microbial factories for synthesis of value-added products | Journal of Industrial Microbiology and Biotechnology | Oxford Academic. https://academic.oup.com/jimb/article/38/8/873/5994403.

[99] Hyun Jung Kim, James Q. Boedicker, Jang Wook Choi, and Rustem F. Ismagilov. Defined spatial structure stabilizes a synthetic multispecies bacterial community. *Proceedings of the National Academy of Sciences of the United States of America*, 105(47):18188–18193, November 2008.

[100] Trevor G. Johnston, Shuo-Fu Yuan, James M. Wagner, Xiunan Yi, Abhijit Saha, Patrick Smith, Alshakim Nelson, and Hal S. Alper. Compartmentalized microbes and co-cultures in hydrogels for on-demand bioproduction and preservation. *Nature Communications*, 11(1):563, February 2020.

[101] Feng Liu, Junwen Mao, Ting Lu, and Qiang Hua. Synthetic, Context-Dependent Microbial Consortium of Predator and Prey. *ACS synthetic biology*, 8(8):1713–1722, August 2019.

[102] Alex J.H. Fedorec, Tanel Ozdemir, Anjali Doshi, Yan Kay Ho, Luca Rosa, Jack Rutter, Oscar Velazquez, Vitor B. Pinheiro, Tal Danino, and Chris P. Barnes. Two new plasmid post-segregational killing mechanisms for the implementation of synthetic gene networks in escherichia coli. *iScience*, 14:323–334, April 2019.

[103] Henri Braat, Pieter Rottiers, Daniel W. Hommes, Nathalie Huyghebaert, Erik Remaut, Jean Paul Remon, Sander J.H. van Deventer, Sabine Neirynck, Maikel P. Peppelenbosch, and Lothar Steidler. A phase I trial with transgenic bacteria expressing interleukin-10 in crohn's disease. *Clinical Gastroenterology and Hepatology*, 4(6):754–759, June 2006.

[104] Chongxin Wang, Satoru Nagata, Takashi Asahara, Norikatsu Yuki, Kazunori Matsuda, Hirokazu Tsuji, Takuya Takahashi, Koji Nomoto, and Yuichiro Yamashiro. Intestinal microbiota profiles of healthy pre-school and school-age children and effects of probiotic supplementation. *Annals of nutrition & metabolism*, 67(4):257–266, November 2015.

[105] Violaine Rochet, Lionel Rigottier-Gois, Maléne Sutren, Marie-Noëlle Krementscki, Claude Andrieux, Jean-Pierre Furet, Patrick Tailliez, Florence

Levenez, Agnés Mogenet, Jean-Louis Bresson, Séverine Méance, Chantal Cayuela, Antony Leplingard, and Joël Dore. Effects of orally administered Lactobacillus casei DN-114 001 on the composition or activities of the dominant faecal microbiota in healthy humans. *British Journal of Nutrition*, 95(2):421–429, February 2006.

[106] Zhao Zhou, Xin Chen, Huakang Sheng, Xiaolin Shen, Xinxiao Sun, Yajun Yan, Jia Wang, and Qipeng Yuan. Engineering probiotics as living diagnostics and therapeutics for improving human health. *Microbial Cell Factories*, 19(1):1–12, March 2020.

[107] Michael Schultz, Sonja Watzl, Tobias A. Oelschlaeger, Heiko C. Rath, Claudia Göttl, Norbert Lehn, Jürgen Schölmerich, and Hans Jörg Linde. Green fluorescent protein for detection of the probiotic microorganism Escherichia coli strain Nissle 1917 (EcN) in vivo. *Journal of microbiological methods*, 61(3):389–398, 2005.

[108] Pichet Praveschotinunt, Anna M. Duraj-Thatte, Ilia Gelfat, Franziska Bahl, David B. Chou, and Neel S. Joshi. Engineered E. coli Nissle 1917 for the delivery of matrix-tethered therapeutic domains to the gut. *Nature Communications 2019 10:1*, 10(1):1–14, December 2019.

[109] Niv Zmora, Gili Zilberman-Schapira, Jotham Suez, Uria Mor, Mally Dori-Bachash, Stavros Bashiardes, Eran Kotler, Maya Zur, Dana Regev-Lehavi, Rotem Ben Zeev Brik, Sara Federici, Yotam Cohen, Raquel Linevsky, Daphna Rothschild, Andreas E. Moor, Shani Ben-Moshe, Alon Harmelin, Shalev Itzkovitz, Nitsan Maharshak, Oren Shibolet, Hagit Shapiro, Meirav Pevsner-Fischer, Itai Sharon, Zamir Halpern, Eran Segal, and Eran Elinav. Personalized gut mucosal colonization resistance to empiric probiotics is associated with unique host and microbiome features. *Cell*, 174(6):1388–1405.e21, September 2018.

[110] Shengyi Han, Yanmeng Lu, Jiaojiao Xie, Yiqiu Fei, Guiwen Zheng, Ziyuan

Wang, Jie Liu, Longxian Lv, Zongxin Ling, Björn Berglund, Mingfei Yao, and Lanjuan Li. Probiotic Gastrointestinal Transit and Colonization After Oral Administration: A Long Journey. *Frontiers in Cellular and Infection Microbiology*, 11:609722, March 2021.

[111] Jacqueline G Hugtenburg, Lonneke Timmers, Petra JM Elders, Marcia Vervloet, and Liset van Dijk. Definitions, variants, and causes of nonadherence with medication: A challenge for tailored interventions. *Patient preference and adherence*, 7:675–682, July 2013.

[112] Jennifer C. Nelson, Rachel C. L. Bittner, Lora Bounds, Shanshan Zhao, James Baggs, James G. Donahue, Simon J. Hambidge, Steven J. Jacobsen, Nicola P. Klein, Allison L. Naleway, Kenneth M. Zangwill, and Lisa A. Jackson. Compliance With Multiple-Dose Vaccine Schedules Among Older Children, Adolescents, and Adults: Results From a Vaccine Safety Datalink Study. *American Journal of Public Health*, 99(Suppl 2):S389–S397, October 2009.

[113] Leticia Torres, Antje KrügerKr, Eszter Csibra, Edoardo Gianni, and Vitor B Pinheiro. Synthetic biology approaches to biological containment: Pre-emptively tackling potential risks. *Essays in Biochemistry*, 60:393–410, 2016.

[114] Jan Claesen and Michael A. Fischbach. Synthetic microbes as drug delivery systems. *ACS Synthetic Biology*, 4(4):358–364, April 2015.

[115] Christopher M. Whitford, Saskia Dymek, Denise Kerkhoff, Camilla März, Olga Schmidt, Maximilian Edich, Julian Droste, Boas Pucker, Christian Rückert, and Jörn Kalinowski. Auxotrophy to Xeno-DNA: An exploration of combinatorial mechanisms for a high-fidelity biosafety system for synthetic biology applications. *Journal of Biological Engineering 2018 12:1*, 12(1):1–28, August 2018.

[116] Clement T.Y. Chan, Jeong Wook Lee, D. Ewen Cameron, Caleb J. Bashor,

and James J. Collins. 'Deadman' and 'Passcode' microbial kill switches for bacterial containment. *Nature Chemical Biology 2015 12:2*, 12(2):82–86, December 2015.

[117] Finn Stirling, Alexander Naydich, Juliet Bramante, Rachel Barocio, Michael Certo, Hannah Wellington, Elizabeth Redfield, Samuel O'Keefe, Sherry Gao, Adam Cusolito, Jeffrey Way, and Pamela Silver. Synthetic cassettes for pH-Mediated sensing, counting, and containment. *Cell Reports*, 30(9):3139–3148.e4, March 2020.

[118] Jeong Wook Lee, Clement T. Y. Chan, Shimyn Slomovic, and James J. Collins. Next-generation biocontainment systems for engineered organisms. *Nature Chemical Biology*, 14(6):530–537, June 2018.

[119] Wenwen Diao, Liang Guo, Qiang Ding, Cong Gao, Guipeng Hu, Xiulai Chen, Yang Li, Linpei Zhang, Wei Chen, Jian Chen, and Liming Liu. Reprogramming microbial populations using a programmed lysis system to improve chemical production. *Nature Communications*, 12(1):6886, November 2021.

[120] M. Omar Din, Tal Danino, Arthur Prindle, Matt Skalak, Jangir Selimkhanov, Kaitlin Allen, Ellixis Julio, Eta Atolia, Lev S. Tsimring, Sangeeta N. Bhatia, and Jeff Hasty. Synchronized cycles of bacterial lysis for in vivo delivery. *Nature*, 536(7614):81–85, August 2016.

[121] Sreyan Chowdhury, Samuel Castro, Courtney Coker, Taylor E. Hinchliffe, Nicholas Arpaia, and Tal Danino. Programmable bacteria induce durable tumor regression and systemic antitumor immunity | Nature Medicine. *Nature Medicine*, 25:1057–1063, 2019.

[122] Spencer R. Scott, M. Omar Din, Philip Bittihn, Liyang Xiong, Lev S. Tsimring, and Jeff Hasty. A stabilized microbial ecosystem of self-limiting bacteria using synthetic quorum-regulated lysis. *Nature Microbiology*, 2(8):1–9, June 2017.

[123] Mario Juhas and James W. Ajioka. T7 RNA polymerase-driven inducible cell lysis for DNA transfer from Escherichia coli to Bacillus subtilis. *Microbial Biotechnology*, 10(6):1797–1808, 2017.

[124] Candice R. Gurbatri, Ioana Lia, Rosa Vincent, Courtney Coker, Samuel Castro, Piper M. Treuting, Taylor E. Hinchliffe, Nicholas Arpaia, and Tal Danino. Engineered probiotics for local tumor delivery of checkpoint blockade nanobodies. *Science Translational Medicine*, 12(530):eaax0876, February 2020.

[125] Turbot | Our Complete Guide – The Fish Society. https://www.thefishsociety.co.uk/blogs/fishopedia/turbot.

[126] Lingyu Guan, Wei Mu, Jonathan Champeimont, Qiyao Wang, Haizhen Wu, Jingfan Xiao, Werner Lubitz, Yuanxing Zhang, and Qin Liu. Iron-Regulated Lysis of Recombinant Escherichia coli in Host Releases Protective Antigen and Confers Biological Containment. *Infection and Immunity*, 79(7):2608–2618, June 2011.

[127] Yu-an Li, Yanni Sun, Yuqin Zhang, Quan Li, Shifeng Wang, Roy Curtiss III, and Huoying Shi. A Bacterial mRNA-Lysis-Mediated Cargo Release Vaccine System for Regulated Cytosolic Surveillance and Optimized Antigen Delivery. *Advanced Science*, 10(33):2303568, 2023.

[128] Ernst Weber, Carola Engler, Ramona Gruetzner, Stefan Werner, and Sylvestre Marillonnet. A modular cloning system for standardized assembly of multigene constructs. *PloS one*, 6(2), 2011.

[129] NEB. Protocol for Q5® high-fidelity 2X master mix | NEB, 2023.

[130] Kirill A. Datsenko and Barry L. Wanner. One-step inactivation of chromosomal genes in Escherichia coli K-12 using PCR products. *Proceedings of the National Academy of Sciences of the United States of America*, 97(12):6640–6645, June 2000.

[131] J. Sambrook, E. R. Fritsch, and T. Maniatis. Molecular cloning: A laboratory manual (2nd ed. *Cold Spring Harbor Laboratory Press*, 1989.

[132] NEB. Protocol for OneTaq® quick-load 2X master mix with standard buffer (M0486) | NEB.

[133] Johannes Schindelin, Ignacio Arganda-Carreras, Erwin Frise, Verena Kaynig, Mark Longair, Tobias Pietzsch, Stephan Preibisch, Curtis Rueden, Stephan Saalfeld, Benjamin Schmid, Jean Yves Tinevez, Daniel James White, Volker Hartenstein, Kevin Eliceiri, Pavel Tomancak, and Albert Cardona. Fiji: An open-source platform for biological-image analysis. *Nature Methods 2012 9:7*, 9(7):676–682, June 2012.

[134] Samuel O. Skinner, Leonardo A. Sepúlveda, Heng Xu, and Ido Golding. Measuring mRNA copy number in individual Escherichia coli cells using single-molecule fluorescent in situ hybridization. *Nature Protocols*, 8(6):1100–1113, June 2013.

[135] Alex J.H. Fedorec, Clare M. Robinson, Ke Yan Wen, and Chris P. Barnes. FlopR: An open source software package for calibration and normalization of plate reader and flow cytometry data (ACS Synthetic Biology (2020) 9:9 (2258-2266) DOI: 10.1021/acssynbio.0c00296). *ACS Synthetic Biology*, 10(2):428, February 2021.

[136] R Core Team. R: The R project for statistical computing, 2022.

[137] H Wickham. Create elegant data visualisations using the grammar of graphics • ggplot2, 2022.

[138] Hadley Wickham, Mara Averick, Jennifer Bryan, Winston Chang, Lucy D', Agostino Mcgowan, Romain François, Garrett Grolemund, Alex Hayes, Lionel Henry, Jim Hester, Max Kuhn, Thomas Lin Pedersen, Evan Miller, Stephan Milton Bache, Kirill Müller, Jeroen Ooms, David Robinson, Dana Paige Seidel, Vitalie Spinu, Kohske Takahashi, Davis Vaughan, Claus

Wilke, Kara Woo, and Hiroaki Yutani. Welcome to the tidyverse. *Journal of Open Source Software*, 4(43):1686, November 2019.

[139] Kenneth J. Livak and Thomas D. Schmittgen. Analysis of relative gene expression data using real-time quantitative PCR and the 2-ΔΔCT method. *Methods (San Diego, Calif.)*, 25(4):402–408, December 2001.

[140] Clare Faux, Sonja Rakic, William Andrews, Yuchio Yanagawa, Kunihiko Obata, and John G. Parnavelas. Differential gene expression in migrating cortical interneurons during mouse forebrain development. *Journal of Comparative Neurology*, 518(8):1232–1248, April 2010.

[141] Melanie Ghoul and Sara Mitri. The ecology and evolution of microbial competition. *Trends in Microbiology*, 24(10):833–845, October 2016.

[142] Maria A. Bauer, Katharina Kainz, Didac Carmona-Gutierrez, and Frank Madeo. Microbial wars: Competition in ecological niches and within the microbiome. *Microbial Cell*, 5(5):215, May 2018.

[143] Diego Gonzalez and Despoina A.I. Mavridou. Making the best of aggression: The many dimensions of bacterial toxin regulation. *Trends in Microbiology*, 27(11):897–905, November 2019.

[144] A. Wali Karzai, Eric D. Roche, and Robert T. Sauer. The SsrA–SmpB system for protein tagging, directed degradation and ribosome rescue. *Nature Structural Biology 2000 7:6*, 7(6):449–455, June 2000.

[145] Soledad Moreno, Luis Felipe Muriel-Millán, Karen Rodríguez-Martínez, Cristian Ortíz-Vasco, Leidy Patricia Bedoya-PCrossed D Sign©rez, and Guadalupe Espín. The ribosome rescue pathways SsrA-SmpB, ArfA, and ArfB mediate tolerance to heat and antibiotic stresses in Azotobacter vinelandii. *FEMS Microbiology Letters*, 369(1):1–8, February 2022.

[146] Perumalraja Kirthika, Khristine Kaith Sison Lloren, Vijayakumar Jawalagatti, and John Hwa Lee. Structure, substrate specificity and role of lon pro-

tease in bacterial pathogenesis and survival. *International Journal of Molecular Sciences*, 24(4), February 2023.

[147] Christopher M. Farrell, Alan D. Grossman, and Robert T. Sauer. Cytoplasmic degradation of ssrA-tagged proteins. *Molecular Microbiology*, 57(6):1750–1761, September 2005.

[148] Xue Fei, Tristan A. Bell, Sarah R. Barkow, Tania A. Baker, and Robert T. Sauer. Structural basis of ClpXP recognition and unfolding of ssrA-tagged substrates. *eLife*, 9:1–39, October 2020.

[149] Julia M. Flynn, Igor Levchenko, Meredith Seidel, Sue H. Wickner, Robert T. Sauer, and Tania A. Baker. Overlapping recognition determinants within the ssrA degradation tag allow modulation of proteolysis. *Proceedings of the National Academy of Sciences*, 98(19):10584–10589, September 2001.

[150] Kathleen E. McGinness, Tania A. Baker, and Robert T. Sauer. Engineering controllable protein degradation. *Molecular Cell*, 22(5):701–707, June 2006.

[151] Nicholas C. Butzin and William H. Mather. Crosstalk between diverse synthetic protein degradation tags in escherichia coli. *ACS Synthetic Biology*, 7(1):54–62, January 2018.

[152] Sarah Guiziou, Vincent Sauveplane, Hung Ju Chang, Caroline Clerté, Nathalie Declerck, Matthieu Jules, and Jerome Bonnet. A part toolbox to tune genetic expression in Bacillus subtilis. *Nucleic Acids Research*, 44(15):7495–7508, September 2016.

[153] Beata Kowalska-Krochmal and Ruth Dudek-Wicher. The Minimum Inhibitory Concentration of Antibiotics: Methods, Interpretation, Clinical Relevance. *Pathogens*, 10(2):165, February 2021.

[154] Protein half-lives in E. coli - Bacteria Escherichia coli - BNID 109921. https://bionumbers.hms.harvard.edu/bionumber.aspx?s=n&v=2&id=109921.

[155] M. R. Maurizi. Proteases and protein degradation in Escherichia coli. *Experientia*, 48(2):178–201, February 1992.

[156] Sun-Young Kim, Jennifer K. Parker, Monica Gonzalez-Magaldi, Mady S. Telford, Daniel J. Leahy, and Bryan W. Davies. Export of Diverse and Bioactive Small Proteins through a Type I Secretion System. *Applied and Environmental Microbiology*, 89(5):e00335–23, April 2023.

[157] Uniprot. Cvi - colicin V immunity protein - escherichia coli | UniProtKB | UniProt.

[158] Austin G. Rottinghaus, Aura Ferreiro, Skye R. S. Fishbein, Gautam Dantas, and Tae Seok Moon. Genetically stable CRISPR-based kill switches for engineered microbes. *Nature Communications*, 13(1):672, February 2022.

[159] Nathan Fraikin and Laurence Van Melderen. Single-cell evidence for plasmid addiction mediated by toxin–antitoxin systems. *Nucleic Acids Research*, 52(4):1847–1859, February 2024.

[160] Kaijian Hou, Zhuo-Xun Wu, Xuan-Yu Chen, Jing-Quan Wang, Dongya Zhang, Chuanxing Xiao, Dan Zhu, Jagadish B. Koya, Liuya Wei, Jilin Li, and Zhe-Sheng Chen. Microbiota in health and diseases. *Signal Transduction and Targeted Therapy*, 7(1):1–28, April 2022.

[161] Andrew L. Goodman and Jeffrey I. Gordon. Our Unindicted Coconspirators: Human Metabolism from a Microbial Perspective. *Cell Metabolism*, 12(2):111–116, August 2010.

[162] Muhammad Afzaal, Farhan Saeed, Yasir Abbas Shah, Muzzamal Hussain, Roshina Rabail, Claudia Terezia Socol, Abdo Hassoun, Mirian Pateiro, José M. Lorenzo, Alexandru Vasile Rusu, and Rana Muhammad Aadil. Human gut microbiota in health and disease: Unveiling the relationship. *Frontiers in Microbiology*, 13, September 2022.

[163] Ohad Manor, Chengzhen L. Dai, Sergey A. Kornilov, Brett Smith, Nathan D. Price, Jennifer C. Lovejoy, Sean M. Gibbons, and Andrew T. Magis. Health and disease markers correlate with gut microbiome composition across thousands of people. *Nature Communications*, 11(1):5206, October 2020.

[164] Chi Chun Wong and Jun Yu. Gut microbiota in colorectal cancer development and therapy. *Nature Reviews Clinical Oncology*, 20(7):429–452, July 2023.

[165] Mara Roxana Rubinstein, Xiaowei Wang, Wendy Liu, Yujun Hao, Guifang Cai, and Yiping W. Han. Fusobacterium nucleatum promotes colorectal carcinogenesis by modulating E-cadherin/β-catenin signaling via its FadA adhesin. *Cell Host and Microbe*, 14(2):195–206, August 2013.

[166] Aleksandar D. Kostic, Dirk Gevers, Chandra Sekhar Pedamallu, Monia Michaud, Fujiko Duke, Ashlee M. Earl, Akinyemi I. Ojesina, Joonil Jung, Adam J. Bass, Josep Tabernero, José Baselga, Chen Liu, Ramesh A. Shivdasani, Shuji Ogino, Bruce W. Birren, Curtis Huttenhower, Wendy S. Garrett, and Matthew Meyerson. Genomic analysis identifies association of Fusobacterium with colorectal carcinoma. *Genome Research*, 22(2):292–298, January 2012.

[167] Tomomitsu Tahara, Eiichiro Yamamoto, Hiromu Suzuki, Reo Maruyama, Woonbok Chung, Judith Garriga, Jaroslav Jelinek, Hiro O. Yamano, Tamotsu Sugai, Byonggu An, Imad Shureiqi, Minoru Toyota, Yutaka Kondo, Marcos R.H. Estecio, and Jean Pierre J. Issa. Fusobacterium in colonic flora and molecular features of colorectal carcinoma. *Cancer research*, 74(5):1311, March 2014.

[168] Definition of microsatellite instability - NCI Dictionary of Cancer Terms - NCI. https://www.cancer.gov/publications/dictionaries/cancer-terms/def/microsatellite-instability, 02/02/2011 - 07:00.

[169] Chun-Hui Sun, Bin-Bin Li, Bo Wang, Jing Zhao, Xiao-Ying Zhang, Ting-Ting Li, Wen-Bing Li, Di Tang, Miao-Juan Qiu, Xin-Cheng Wang, Cheng-Ming Zhu, and Zhi-Rong Qian. The role of Fusobacterium nucleatum in colorectal cancer: From carcinogenesis to clinical management. *Chronic Diseases and Translational Medicine*, 5(3):178–187, September 2019.

[170] Yongzhi Yang, Wenhao Weng, Junjie Peng, Leiming Hong, Lei Yang, Yuji Toiyama, Renyuan Gao, Minfeng Liu, Mingming Yin, Cheng Pan, Hao Li, Bomin Guo, Qingchao Zhu, Qing Wei, Mary-Pat Moyer, Ping Wang, Sanjun Cai, Ajay Goel, Huanlong Qin, and Yanlei Ma. Fusobacterium nucleatum Increases Proliferation of Colorectal Cancer Cells and Tumor Development in Mice by Activating Toll-Like Receptor 4 Signaling to Nuclear Factor-κB, and Up-regulating Expression of MicroRNA-21. *Gastroenterology*, 152(4):851–866.e24, March 2017.

[171] Dominik Ternes, Mina Tsenkova, Vitaly Igorevich Pozdeev, Marianne Meyers, Eric Koncina, Sura Atatri, Martine Schmitz, Jessica Karta, Maryse Schmoetten, Almut Heinken, Fabien Rodriguez, Catherine Delbrouck, Anthoula Gaigneaux, Aurelien Ginolhac, Tam Thuy Dan Nguyen, Lea Grandmougin, Audrey Frachet-Bour, Camille Martin-Gallausiaux, Maria Pacheco, Lorie Neuberger-Castillo, Paulo Miranda, Nikolaus Zuegel, Jean Yves Ferrand, Manon Gantenbein, Thomas Sauter, Daniel Joseph Slade, Ines Thiele, Johannes Meiser, Serge Haan, Paul Wilmes, and Elisabeth Letellier. The gut microbial metabolite formate exacerbates colorectal cancer progression. *Nature Metabolism 2022 4:4*, 4(4):458–475, April 2022.

[172] Samin Zamani, Reza Taslimi, Akram Sarabi, Seyedesomaye Jasemi, Leonardo A. Sechi, and Mohammad Mehdi Feizabadi. Enterotoxigenic bacteroides fragilis: A possible etiological candidate for bacterially-induced colorectal precancerous and cancerous lesions. *Frontiers in Cellular and Infection Microbiology*, 9:449, January 2020.

[173] Yuriko Matsumiya, Mitsukuni Suenaga, Toshiaki Ishikawa, Marie Hanaoka,

Noriko Iwata, Taiki Masuda, Shinichi Yamauchi, Masanori Tokunaga, and Yusuke Kinugasa. Clinical significance of Bacteroides fragilis as potential prognostic factor in colorectal cancer patients. *Journal of Clinical Oncology*, 40(4_suppl):137–137, January 2022.

[174] Shiyu Li, Shuangli Zhu, and Jun Yu. The role of gut microbiota and metabolites in cancer chemotherapy. *Journal of Advanced Research*, 64:223–235, October 2024.

[175] Ta Chung Yu, Fangfang Guo, Yanan Yu, Tiantian Sun, Dan Ma, Jixuan Han, Yun Qian, Ilona Kryczek, Danfeng Sun, Nisha Nagarsheth, Yingxuan Chen, Haoyan Chen, Jie Hong, Weiping Zou, and Jing Yuan Fang. Fusobacterium nucleatum promotes chemoresistance to colorectal cancer by modulating autophagy. *Cell*, 170(3):548–563.e16, July 2017.

[176] Leila Dadgar-Zankbar, Zahra Elahi, Aref Shariati, Azad Khaledi, Shabnam Razavi, and Amin Khoshbayan. Exploring the role of Fusobacterium nucleatum in colorectal cancer: Implications for tumor proliferation and chemoresistance. *Cell Communication and Signaling*, 22(1):547, November 2024.

[177] Potential role of intratumor bacteria in mediating tumor resistance to the chemotherapeutic drug gemcitabine. https://www.science.org/doi/10.1126/science.aah5043.

[178] Hiroo Imai, Ken Saijo, Keigo Komine, Yuya Yoshida, Keiju Sasaki, Asako Suzuki, Kota Ouchi, Masahiro Takahashi, Shin Takahashi, Hidekazu Shirota, Masanobu Takahashi, and Chikashi Ishioka. Antibiotics Improve the Treatment Efficacy of Oxaliplatin-Based but Not Irinotecan-Based Therapy in Advanced Colorectal Cancer Patients. *Journal of Oncology*, 2020(1):1701326, 2020.

[179] Menglin Wang, Benoit Rousseau, Kunyu Qiu, Guannan Huang, Yu Zhang, Hang Su, Christine Le Bihan-Benjamin, Ines Khati, Oliver Artz, Michael B. Foote, Yung-Yi Cheng, Kuo-Hsiung Lee, Michael Z. Miao, Yue Sun,

Philippe-Jean Bousquet, Marc Hilmi, Elise Dumas, Anne-Sophie Hamy, Fabien Reyal, Lin Lin, Paul M. Armistead, Wantong Song, Ava Vargason, Janelle C. Arthur, Yun Liu, Jianfeng Guo, Xuefei Zhou, Juliane Nguyen, Yongqun He, Jenny P.-Y. Ting, Aaron C. Anselmo, and Leaf Huang. Killing tumor-associated bacteria with a liposomal antibiotic generates neoantigens that induce anti-tumor immune responses. *Nature Biotechnology*, 42(8):1263–1274, August 2024.

[180] Benoit Rousseau, Marc Hilmi, Ines Khati, Anthony Turpin, Antoine Andremont, Charles Burdet, Nathalie Grall, Joana Vidal, Philippe Jean Bousquet, and Christine Le Bihan. Impact of antibiotics (ATB) on the recurrence of resected colorectal cancer (CRC): Results of EVADER-1 a nation-wide pharmacoepidemiologic study. *Journal of Clinical Oncology*, 38(15_suppl):4106–4106, May 2020.

[181] Maribasappa Karched, Radhika G. Bhardwaj, and Sirkka E. Asikainen. Coaggregation and biofilm growth of Granulicatella spp. with Fusobacterium nucleatum and Aggregatibacter actinomycetemcomitans. *BMC Microbiology*, 15(1):114, May 2015.

[182] Chenggang Wu, Yi-Wei Chen, Matthew Scheible, Chungyu Chang, Manuel Wittchen, Ju Huck Lee, Truc T. Luong, Bethany L. Tiner, Andreas Tauch, Asis Das, and Hung Ton-That. Genetic and molecular determinants of polymicrobial interactions in Fusobacterium nucleatum. *Proceedings of the National Academy of Sciences*, 118(23):e2006482118, June 2021.

[183] Akito Sakanaka, Masae Kuboniwa, Shuichi Shimma, Samar A. Alghamdi, Shota Mayumi, Richard J. Lamont, Eiichiro Fukusaki, and Atsuo Amano. Fusobacterium nucleatum Metabolically Integrates Commensals and Pathogens in Oral Biofilms. *mSystems*, 7(4):e0017022, August 2022.

[184] Vania L. Silva, Claudio G. Diniz, Denise C. Cara, Simone G. Santos, Jacques R. Nicoli, Maria Auxiliadora R. Carvalho, and Luiz M. Farias.

Enhanced pathogenicity of *Fusobacterium nucleatum* adapted to oxidative stress. *Microbial Pathogenesis*, 39(4):131–138, October 2005.

[185] BACTIBASE. Bacteriocin: Subtilosin, 2023.

[186] Nuria Peña, Michael J. Bland, Ester Sevillano, Estefanía Muñoz-Atienza, Irene Lafuente, Mohamed El Bakkoury, Luis M. Cintas, Pablo E. Hernández, Philippe Gabant, and Juan Borrero. In vitro and in vivo production and split-intein mediated ligation (SIML) of circular bacteriocins. *Frontiers in Microbiology*, 13, November 2022.

[187] Sebastian Himbert, Richard J. Alsop, Markus Rose, Laura Hertz, Alexander Dhaliwal, Jose M. Moran-Mirabal, Chris P. Verschoor, Dawn M. E. Bowdish, Lars Kaestner, Christian Wagner, and Maikel C. Rheinstädter. The Molecular Structure of Human Red Blood Cell Membranes from Highly Oriented, Solid Supported Multi-Lamellar Membranes. *Scientific Reports*, 7(1):39661, January 2017.

[188] Chiara Canali, Erik Spillum, Martin Valvik, Niels Agersnap, and Tom Olesen. A digital time-lapse, bright field technology to drive faster, higher throughput label-free bioanalysis. www.biosensesolutions.dk, 2025.

[189] Daili Jacqueline Aguilar Netz, Regula Pohl, Annette G. Beck-Sickinger, Thorsten Selmer, Antonio J. Pierik, Maria do Carmo de Freire Bastos, and Hans-Georg Sahl. Biochemical Characterisation and Genetic Analysis of Aureocin A53, a New, Atypical Bacteriocin from *Staphylococcus aureus*. *Journal of Molecular Biology*, 319(3):745–756, June 2002.

[190] Jeella Z. Acedo, Marco J. van Belkum, Christopher T. Lohans, Kaitlyn M. Towle, Mark Miskolzie, and John C. Vederas. Nuclear Magnetic Resonance Solution Structures of Lacticin Q and Aureocin A53 Reveal a Structural Motif Conserved among Leaderless Bacteriocins with Broad-Spectrum Activity. *Biochemistry*, 55(4):733–742, February 2016.

[191] Paula M. O' Connor, Eileen F. O' Shea, Paul D. Cotter, Colin Hill, and R. Paul Ross. The potency of the broad spectrum bacteriocin, bactofencin A, against staphylococci is highly dependent on primary structure, N-terminal charge and disulphide formation. *Scientific Reports*, 8(1):11833, August 2018.

[192] Edward A. Svetoch, Boris V. Eruslanov, Vladimir P. Levchuk, Vladimir V. Perelygin, Evgeny V. Mitsevich, Irina P. Mitsevich, Juri Stepanshin, Ivan Dyatlov, Bruce S. Seal, and Norman J. Stern. Isolation of lactobacillus salivarius 1077 (NRRL B-50053) and characterization of its bacteriocin, including the antimicrobial activity spectrum. *Applied and Environmental Microbiology*, 77(8):2749, April 2011.

[193] Raj Kumar Thapa, Hanne Cecilie Winther-Larsen, Dzung B. Diep, and Hanne Hjorth Tønnesen. Preformulation studies on novel garvicin KS peptides for topical applications. *European Journal of Pharmaceutical Sciences*, 151:105333, August 2020.

[194] Saurabh Dubey, Dzung B. Diep, Øystein Evensen, and Hetron M. Munang'andu. Garvicin KS, a Broad-Spectrum Bacteriocin Protects Zebrafish Larvae against Lactococcus garvieae Infection. *International Journal of Molecular Sciences*, 23(5):2833, March 2022.

[195] Dustin D. Heeney, Vladimir Yarov-Yarovoy, and Maria L. Marco. Sensitivity to the two peptide bacteriocin plantaricin EF is dependent on CorC, a membrane-bound, magnesium/cobalt efflux protein. *MicrobiologyOpen*, 8(11), November 2019.

[196] David J. Gonzalez, Nina M. Haste, Andrew Hollands, Tinya C. Fleming, Matthew Hamby, Kit Pogliano, Victor Nizet, and Pieter C. Dorrestein. Microbial competition between Bacillus subtilis and Staphylococcus aureus monitored by imaging mass spectrometry. *Microbiology*, 157(Pt 9):2485–2492, September 2011.

[197] J C Frantz and R E McCallum. Growth yields and fermentation balance of Bacteroides fragilis cultured in glucose-enriched medium. *Journal of Bacteriology*, 137(3):1263–1270, March 1979.

[198] A. H. Rogers, P. S. Zilm, N. J. Gully, A. L. Pfennig, and P. D. Marsh. Aspects of the growth and metabolism of Fusobacterium nucleatum ATCC 10953 in continuous culture. *Oral Microbiology and Immunology*, 6(4):250–255, August 1991.

[199] R H Eng, F T Padberg, S M Smith, E N Tan, and C E Cherubin. Bactericidal effects of antibiotics on slowly growing and nongrowing bacteria. *Antimicrobial Agents and Chemotherapy*, 35(9):1824–1828, September 1991.

[200] Daili Jacqueline Aguilar Netz, Maria do Carmo de Freire Bastos, and Hans Georg Sahl. Mode of action of the antimicrobial peptide aureocin A53 from Staphylococcus aureus. *Applied and environmental microbiology*, 68(11):5274–5280, November 2002.

[201] Nele Hofkens, Zina Gestels, Saïd Abdellati, Philippe Gabant, Hector Rodriguez-Villalobos, Anandi Martin, Chris Kenyon, and Sheeba Santhini Manoharan-Basil. Protective effect of microbisporicin (NAI-107) against vancomycin resistant Enterococcus faecium infection in a Galleria mellonella model. *Scientific Reports*, 14(1):4786, February 2024.

[202] Jun Yu, Qiang Feng, Sunny Hei Wong, Dongya Zhang, Qiao yi Liang, Youwen Qin, Longqing Tang, Hui Zhao, Jan Stenvang, Yanli Li, Xiaokai Wang, Xiaoqiang Xu, Ning Chen, William Ka Kei Wu, Jumana Al-Aama, Hans Jørgen Nielsen, Pia Kiilerich, Benjamin Anderschou Holbech Jensen, Tung On Yau, Zhou Lan, Huijue Jia, Junhua Li, Liang Xiao, Thomas Yuen Tung Lam, Siew Chien Ng, Alfred Sze-Lok Cheng, Vincent Wai-Sun Wong, Francis Ka Leung Chan, Xun Xu, Huanming Yang, Lise Madsen, Christian Datz, Herbert Tilg, Jian Wang, Nils Brünner, Karsten Kristiansen, Manimozhiyan Arumugam, Joseph Jao-Yiu Sung, and Jun Wang. Metage-

nomic analysis of faecal microbiome as a tool towards targeted non-invasive biomarkers for colorectal cancer. *Gut*, 66(1):70–78, January 2017.

[203] Song-He Guo, Hai-Fang Wang, Zhi-Gang Nian, Yi-Dan Wang, Qiu-Yao Zeng, and Ge Zhang. Immunization with alkyl hydroperoxide reductase subunit C reduces Fusobacterium nucleatum load in the intestinal tract. *Scientific Reports*, 7:10566, September 2017.

[204] Ophelia S Venturelli, Alex C Carr, Garth Fisher, Ryan H Hsu, Rebecca Lau, Benjamin P Bowen, Susan Hromada, Trent Northen, and Adam P Arkin. Deciphering microbial interactions in synthetic human gut microbiome communities. *Molecular Systems Biology*, 14(6), June 2018.

[205] Jing Yang, Ji Pu, Shan Lu, Xiangning Bai, Yangfeng Wu, Dong Jin, Yanpeng Cheng, Gui Zhang, Wentao Zhu, Xuelian Luo, Ramon Rosselló-Móra, and Jianguo Xu. Species-level analysis of human gut microbiota with metataxonomics. *Frontiers in Microbiology*, 11, August 2020.

[206] Dana Gebhart, Steven R. Williams, Kimberly A. Bishop-Lilly, Gregory R. Govoni, Kristin M. Willner, Amy Butani, Shanmuga Sozhamannan, David Martin, Louis-Charles Fortier, and Dean Scholl. Novel High-Molecular-Weight, R-Type Bacteriocins of Clostridium difficile. *Journal of Bacteriology*, 194(22):6240–6247, November 2012.

[207] Selda Loase Salustiano Marques-Bastos, Marcus Lívio Varella Coelho, Ilana Nascimento de Sousa Santos, Daniela Sales Alviano Moreno, Emile Santos Barrias, Juliana França Monteiro de Mendonça, Letícia Caldas Mendonça, Carla Christine Lange, Maria Aparecida Vasconcelos de Paiva Brito, and Maria do Carmo de Freire Bastos. Effects of the natural antimicrobial peptide aureocin A53 on cells of Staphylococcus aureus and Streptococcus agalactiae involved in bovine mastitis in the excised teat model. *World journal of microbiology & biotechnology*, 39(1), January 2022.

[208] P.c. Fagundes, F.m. Farias, O.c.s. Santos, N.e.m. de Oliveira, J.a.s. da Paz,

H. Ceotto-Vigoder, D.s. Alviano, M.t.v. Romanos, and M.c.f. Bastos. The antimicrobial peptide aureocin A53 as an alternative agent for biopreservation of dairy products. *Journal of Applied Microbiology*, 121(2):435–444, 2016.

[209] Justyna Śmiałek-Bartyzel, Monika Bzowska, and Paweł Mak. Pro-inflammatory properties of aureocin A53. *Microbes and Infection*, 26(5):105365, July 2024.

[210] M. Giambiagi-Marval, M. A. Mafra, E. G. C. Penido, and M. C. F. Bastos. Distinct groups of plasmids correlated with bacteriocin production in Staphylococcus aureus. *Microbiology*, 136(8):1591–1599, 1990.

[211] Janaína dos Santos Nascimento, Marcus Lívio Varella Coelho, Hilana Ceotto, Amina Potter, Luana Rocha Fleming, Zhian Salehian, Ingolf F. Nes, and Maria do Carmo de Freire Bastos. Genes Involved in Immunity to and Secretion of Aureocin A53, an Atypical Class II Bacteriocin Produced by Staphylococcus aureus A53. *Journal of Bacteriology*, 194(4):875, February 2012.

[212] Myungsook Kim, Shin Young Yun, Yunhee Lee, Hyukmin Lee, Dongeun Yong, and Kyungwon Lee. Clinical Differences in Patients Infected with Fusobacterium and Antimicrobial Susceptibility of Fusobacterium Isolates Recovered at a Tertiary-Care Hospital in Korea. *Annals of Laboratory Medicine*, 42(2):188–195, March 2022.

[213] Eileen F. O'Shea, Paula M. O'Connor, Orla O'Sullivan, Paul D. Cotter, R. Paul Ross, and Colin Hill. Bactofencin A, a New Type of Cationic Bacteriocin with Unusual Immunity. *mBio*, 4(6):e00498–13, October 2013.

[214] Beatriz Mesa-Pereira, Paula M. O'Connor, Mary C. Rea, Paul D. Cotter, Colin Hill, and R. Paul Ross. Controlled functional expression of the bacteriocins pediocin PA-1 and bactofencin A in Escherichia coli. *Scientific Reports*, 7(1):3069, June 2017.

[215] François Bédard, Ismail Fliss, and Eric Biron. Structure–Activity Relationships of the Bacteriocin Bactofencin A and Its Interaction with the Bacterial Membrane. *ACS Infectious Diseases*, 5(2):199–207, February 2019.

[216] dltB - Teichoic acid D-alanyltransferase - Lacticaseibacillus rhamnosus (Lactobacillus rhamnosus) | UniProtKB | UniProt. https://www.uniprot.org/uniprotkb/Q7BP34/entry.

[217] Frontiers | In vitro and in vivo production and split-intein mediated ligation (SIML) of circular bacteriocins. https://www.frontiersin.org/journals/microbiology/articles/10.3389/fmicb.2022.1052686/full.

[218] Juan Borrero, Dag A. Brede, Morten Skaugen, Dzung B. Diep, Carmen Herranz, Ingolf F. Nes, Luis M. Cintas, and Pablo E. Hernández. Characterization of garvicin ML, a novel circular bacteriocin produced by lactococcus garvieae DCC43, isolated from mallard ducks (Anas platyrhynchos). *Applied and Environmental Microbiology*, 77(1):369–373, January 2011.

[219] Christina Gabrielsen, Dag A. Brede, Zhian Salehian, Ingolf F. Nes, and Dzung B. Diep. Functional genetic analysis of the GarML gene cluster in lactococcus garvieae DCC43 gives new insights into circular bacteriocin biosynthesis. *Journal of Bacteriology*, 196(5):911, March 2014.

[220] Jacques Monod. THE GROWTH OF BACTERIAL CULTURES. *Annual Review of Microbiology*, 3(Volume 3, 1949):371–394, October 1949.

[221] Micha Peleg, Maria G. Corradini, and Mark D. Normand. The logistic (Verhulst) model for sigmoid microbial growth curves revisited. *Food Research International*, 7(40):808–818, 2007.

[222] József Baranyi and Terry A. Roberts. A dynamic approach to predicting bacterial growth in food. *International Journal of Food Microbiology*, 23(3):277–294, November 1994.

[223] L. Liu, P. O'Conner, P.D. Cotter, C. Hill, and R.P. Ross. Controlling Listeria monocytogenes in Cottage cheese through heterologous production of enterocin A by Lactococcus lactis. *Journal of Applied Microbiology*, 104(4):1059–1066, April 2008.

[224] Michael Klocke, Kerstin Mundt, Frank Idler, Sabrina Jung, and Jan E. Backhausen. Heterologous expression of enterocin A, a bacteriocin from Enterococcus faecium, fused to a cellulose-binding domain in Escherichia coli results in a functional protein with inhibitory activity against Listeria. *Applied Microbiology and Biotechnology*, 67(4):532–538, June 2005.

[225] Juan Borrero, Gotthard Kunze, Juan J. Jiménez, Erik Böer, Loreto Gútiez, Carmen Herranz, Luis M. Cintas, and Pablo E. Hernández. Cloning, Production, and Functional Expression of the Bacteriocin Enterocin A, Produced by Enterococcus faecium T136, by the Yeasts Pichia pastoris, Kluyveromyces lactis, Hansenula polymorpha, and Arxula adeninivorans. *Applied and Environmental Microbiology*, 78(16):5956–5961, August 2012.

[226] Carola Elisa Heesemann Rosenkilde, Ditte Olsen Lützhøft, Ruben Vazquez-Uribe, and Morten Otto Alexander Sommer. Heterologous expression and antimicrobial potential of class II bacteriocins. *Gut Microbes*, 16(1):2369338, December 2024.

[227] Agnieszka Kaczynska, Martyna Klosinska, Kamil Janeczek, Michał Zarobkiewicz, and Andrzej Emeryk. Promising Immunomodulatory Effects of Bacterial Lysates in Allergic Diseases. *Frontiers in Immunology*, 13, June 2022.

[228] Georg Faust, Alexandra Stand, and Dirk Weuster-Botz. IPTG can replace lactose in auto-induction media to enhance protein expression in batch-cultured Escherichia coli. *Engineering life Sciences*, May 2015.

[229] Yun Kang, Mike S. Son, and Tung T. Hoang. One step engineering of T7-

expression strains for protein production. *Protein expression and purification*, 55(2):325–333, October 2007.

[230] Fei Du, Yun-Qi Liu, Ying-Shuang Xu, Zi-Jia Li, Yu-Zhou Wang, Zi-Xu Zhang, and Xiao-Man Sun. Regulating the T7 RNA polymerase expression in E. coli BL21 (DE3) to provide more host options for recombinant protein production. *Microbial Cell Factories*, 20(1):189, September 2021.

[231] Deborah A Siegele and James C Hu. Gene expression from plasmids containing the araBAD promoter at subsaturating inducer concentrations represents mixed populations. *Proceedings of the National Academy of Sciences*, 94(15), July 1997.

[232] Shen Ye Yu, Wei Peng, Wei Si, Lu Yin, Si Guo Liu, Hui Fang Liu, Hai Ling Zhao, Chun Lai Wang, Yue Hong Chang, and Yue Zhi Lin. Enhancement of bacteriolysis of Shuffled phage PhiX174 gene e. *Virology Journal*, 8(1):1–6, May 2011.

[233] Measuring the burden of hundreds of BioBricks defines an evolutionary limit on constructability in synthetic biology | Nature Communications. https://www.nature.com/articles/s41467-024-50639-9#Sec10.

[234] Mary Gearing. Plasmids 101: Inducible Promoters. https://blog.addgene.org/plasmids-101-inducible-promoters.

[235] Louise Crozier, Jacqueline Marshall, Ashleigh Holmes, Kathryn Mary Wright, Yannick Rossez, Bernhard Merget, Sonia Humphris, Ian Toth, Robert Wilson Jackson, and Nicola Jean Holden. The role of l-arabinose metabolism for Escherichia coli O157:H7 in edible plants. *Microbiology*, 167(7):001070, July 2021.

[236] W. D. Roof, S. M. Horne, K. D. Young, and R. Young. slyD, a host gene required for phi X174 lysis, is related to the FK506-binding protein family of peptidyl-prolyl cis-trans-isomerases. *Journal of Biological Chemistry*, 269(4):2902–2910, January 1994.

[237] Thomas G. Bernhardt, William D. Roof, and Ry Young. The Escherichia coli FKBP-type PPIase SlyD is required for the stabilization of the E lysis protein of bacteriophage φX174. *Molecular Microbiology*, 45(1):99–108, 2002.

[238] Shuvam Bhuyan, Mohit Yadav, Shubhra Jyoti Giri, Shuhada Begum, Saurav Das, Akash Phukan, Pratiksha Priyadarshani, Sharmilee Sarkar, Anurag Jayswal, Kristi Kabyashree, Aditya Kumar, Manabendra Mandal, and Suvendra Kumar Ray. Microliter spotting and micro-colony observation: A rapid and simple approach for counting bacterial colony forming units. *Journal of Microbiological Methods*, 207:106707, April 2023.

[239] Basic principles. http://www.qiagen.com/us/knowledge-and-support/knowledge-hub/bench-guide/protein/protein-expression-and-purification/basic-principles.

[240] Search BioNumbers - The Database of Useful Biological Numbers. https://bionumbers.hms.harvard.edu/search.aspx, January 2025.

[241] Katleen Denoncin and Jean-François Collet. Disulfide Bond Formation in the Bacterial Periplasm: Major Achievements and Challenges Ahead. *Antioxidants & Redox Signaling*, 19(1):63–71, July 2013.

[242] Lisa R. Knoke, Jannik Zimmermann, Natalie Lupilov, Jannis F. Schneider, Beyzanur Celebi, Bruce Morgan, and Lars I. Leichert. The role of glutathione in periplasmic redox homeostasis and oxidative protein folding in Escherichia coli. *Redox Biology*, 64:102800, June 2023.

[243] Daniel De Palmenaer, Patricia Siguier, and Jacques Mahillon. IS4 family goes genomic. *BMC Evolutionary Biology*, 8:18, January 2008.

[244] Korrie Pol, Marie Luise Puhlmann, and Monica Mars. Efficacy of L-arabinose in lowering glycemic and insulinemic responses: The modifying effect of starch and fat. *Foods (Basel, Switzerland)*, 11(2):157, January 2022.

[245] Alejandro Asensio-Calavia, Álvaro Ceballos-Munuera, Almudena Méndez-Pérez, Beatriz Álvarez, and Luis Ángel Fernández. A tuneable genetic switch for tight control of tac promoters in Escherichia coli boosts expression of synthetic injectisomes. *Microbial Biotechnology*, 17(1):e14328, 2024.

[246] Responsible research and innovation. https://www.ukri.org/councils/epsrc/guidance-for-applicants/what-to-include-in-your-proposal/health-technologies-impact-and-translation-toolkit/research-integrity-in-healthcare-technologies/responsible-research-and-innovation/.

[247] Richard Owen, Phil Macnaghten, and Jack Stilgoe. Framework for responsible research and innovation, January 2022.

[248] Claire Marris. The Construction of Imaginaries of the Public as a Threat to Synthetic Biology. *Science as Culture*, 24(1):83–98, January 2015.

[249] EC study on new genomic techniques - European Commission. https://food.ec.europa.eu/plants/genetically-modified-organisms/new-techniques-biotechnology/ec-study-new-genomic-techniques_en.

[250] Timothy K. Lu, Mark Mimee, Robert J. Citorik, and Karen Pepper. Engineering the Microbiome for Human Health Applications. In *The Chemistry of Microbiomes: Proceedings of a Seminar Series*. National Academies Press (US), July 2017.

[251] Jack W. Rutter, Linda Dekker, Kimberley A. Owen, and Chris P. Barnes. Microbiome engineering: Engineered live biotherapeutic products for treating human disease. *Frontiers in Bioengineering and Biotechnology*, 10:1735, September 2022.

[252] Susan Miles, Øydis Ueland, and Lynn J. Frewer. Public attitudes towards genetically-modified food. *British Food Journal*, 107(4):246–262, January 2005.

[253] Rafael Pardo, Cees Midden, and Jon D Miller. Attitudes toward biotechnology in the European Union. *Journal of Biotechnology*, 98(1):9–24, September 2002.

[254] Latifah Amin, Jamaluddin Md Jahi, and Abd Rahim Md Nor. Stakeholders' Attitude to Genetically Modified Foods and Medicine. *The Scientific World Journal*, 2013:e516742, December 2013.

[255] Ewa Woźniak-Gientka, Agata Tyczewska, and Tomasz Twardowski. Public opinion on biotechnology and genetic engineering in the European Union: Polish consumer study. *BioTechnologia*, 103(2):185–201, June 2022.

[256] Jürgen Hampel, Uwe Pfenning, and Hans Peter Peters. Attitudes towards genetic engineering. *New Genetics and Society*, 19(3):233–249, December 2000.

[257] James Anderson, Natalja Strelkowa, Guy-Bart Stan, Thomas Douglas, Julian Savulescu, Mauricio Barahona, and Antonis Papachristodoulou. Engineering and ethical perspectives in synthetic biology. *EMBO Reports*, 13(7):584–590, July 2012.

[258] Virginia Braun and Victoria Clarke. Using thematic analysis in psychology. *Qualitative Research in Psychology*, 3(2):77–101, 2006.

[259] Adam McCarthy, Claire Holland, and Philip Shapira. The Development and Testing of an Early, Rapid Sustainability Assessment Tool for Responsible Innovation in Engineering Biology, March 2024.

[260] Probiotics Industry 2024. https://www.reportlinker.com/market-report/Nutraceutical/11269/Probiotics.

[261] CHR Hansen. Consumer insights Findings from new study of consumer understanding of probiotics and takeaways for the food industry. Technical report, CHR Hansen part of Novonesis, February 2022.

[262] K. Lord, K. Ibrahim, S. Kumar, N. Rudd, A. J. Mitchell, and P. Symonds. Measuring Trust in Healthcare Professionals—A Study of Ethnically Diverse UK Cancer Patients. *Clinical Oncology*, 24(1):13–21, February 2012.

[263] Nuffield Council on Bioethics. Ideas about naturalness in public and political debates about science, technology and medicine, November 2015.

[264] Joyce Tait and David Wield. Policy support for disruptive innovation in the life sciences. *Technology Analysis & Strategic Management*, 33(3):307–319, March 2021.

[265] Michael Peel and Clive Cookson. Synthetic 'mirror' microbes pose unprecedented threat to life, scientists warn. *Financial Times*, December 2024.

[266] Robert L. Perlman. Mouse models of human disease. *Evolution, Medicine, and Public Health*, 2016(1):170–176, May 2016.

[267] Yanan Tong, Guoxiu Lu, Zhiguo Wang, Shanhu Hao, Guoxu Zhang, and Hongwu Sun. Tubeimuside I improves the efficacy of a therapeutic Fusobacterium nucleatum dendritic cell-based vaccine against colorectal cancer. *Frontiers in Immunology*, 14:1154818, May 2023.

[268] Curtis Cottam, Rhys T. White, Lauren C. Beck, Christopher J. Stewart, Scott A. Beatson, Elisabeth C. Lowe, Rhys Grinter, and James P. R. Connolly. Metabolism of L-arabinose converges with virulence regulation to promote enteric pathogen fitness. *Nature Communications*, 15(1):4462, May 2024.

[269] L. Briand, G. Marcion, A. Kriznik, J. M. Heydel, Y. Artur, C. Garrido, R. Seigneuric, and F. Neiers. A self-inducible heterologous protein expression system in Escherichia coli. *Scientific Reports*, 6(1):33037, September 2016.

[270] An engineered pill (aka lab-on-a-pill) for spatial sampling of microbiome and other contents in the gut | Tufts Office of the Vice Provost for

Research. https://viceprovost.tufts.edu/engineered-pill-aka-lab-pill-spatial-sampling-microbiome-and-other-contents-gut#.

[271] Ulrike Klier, Claudia Maletzki, Bernd Kreikemeyer, Ernst Klar, and Michael Linnebacher. Combining bacterial-immunotherapy with therapeutic antibodies: A novel therapeutic concept. *Vaccine*, 30(17):2786–2794, April 2012.

[272] Tetsuhiro Harimoto and Tal Danino. Engineering bacteria for cancer therapy. *Emerging topics in life sciences*, 3(5):623–629, November 2019.

[273] Santosh Kumar Tiwari, Katia Sutyak Noll, Veronica L. Cavera, and Michael L. Chikindas. Improved Antimicrobial Activities of Synthetic-Hybrid Bacteriocins Designed from Enterocin E50-52 and Pediocin PA-1. *Applied and Environmental Microbiology*, 81(5):1661–1667, March 2015.

[274] Silvio Peng, Roger Stephan, Jörg Hummerjohann, and Taurai Tasara. Transcriptional analysis of different stress response genes in Escherichia coli strains subjected to sodium chloride and lactic acid stress. *FEMS Microbiology Letters*, 361(2):131–137, December 2014.

[275] Kang Zhou, Lihan Zhou, Qing Lim, Ruiyang Zou, Gregory Stephanopoulos, and Heng Phon Too. Novel reference genes for quantifying transcriptional responses of Escherichia coli to protein overexpression by quantitative PCR. *BMC Molecular Biology*, 12(1):1–9, April 2011.